

**Characterization of regulatory roles of DPBF4 and
SNF4 in sugar and stress signaling in *Arabidopsis***

**Inaugural-Dissertation
zur
Erlangung des Doktorgrades
der Mathematisch-Naturwissenschaftlichen Fakultät
der Universität zu Köln**

vorgelegt von

Vijaya Shukla

aus Kanpur

KÖLN 2005

Berichterstatter: *Prof. Dr. George Coupland*
 Prof. Dr. Martin Hülskamp

Tag der mündlichen Prüfung: 11. 07. 2005

CONTENTS

I	FIGURES	I
II	ABBREVIATIONS AND SYMBOLES	IV
III	SUMMARY - ZUSAMMENFASSUNG	VII
1.	INTRODUCTION	1
1.1.	SUGAR METABOLISM, STRESS AND PLANT GROWTH CONTROL	1
1.2.	CONVERGENCE AND CROSSTALK BETWEEN ABIOTIC STRESS SIGNALING PATHWAYS	3
1.3.	DISSECTION OF DROUGHT, SALT, AND COLD SIGNALING PATHWAYS	4
1.3.1.	Signal perception	4
1.3.2.	Cold stress signaling	5
1.3.3.	Salt signaling: the SOS-SnRK3 kinase pathway	7
1.4.	ABA SIGNALING	8
1.4.1.	Regulation of ABA synthesis	8
1.4.2.	Primary signaling events and secondary messengers in ABA signaling	9
1.4.3.	Protein phosphatases and SnRK3 protein kinases in ABA signaling	13
1.4.4.	SnRK2 protein kinases and RNA-binding proteins modulating ABA signaling	14
1.4.5.	Transcription factors controlling ABA-regulated gene expression	15
1.4.5.1.	ABA signaling and seed maturation	15
1.4.5.2.	Cis-elements and transcription factors mediating ABA- responses	17
1.4.5.3.	The ABI5 family of bZIP transcription factors	17
1.4.5.4.	HD-ZIP transcription factors	19
1.5.	SUGAR SIGNALING: CROSSTALK WITH ABA AND ETHYLENE	20
1.5.1.	Sugar, ABA and ethylene modulation of seed development, germination and root growth	20
1.5.2.	ABA responses of <i>Arabidopsis</i> mutants affected in ethylene biosynthesis and signaling	21
1.5.3.	Sugar responses of ethylene and ABA biosynthesis and signaling mutants	21
1.5.4.	Glucose sensing: control by trehalose	23
1.5.5.	Glucose sensing by hexokinase	23
1.5.6.	Sensing of glucose and AMP/ATP levels by SnRK1 kinases	25
1.6.	AIMS OF THE PRESENT WORK	28
2.	MATERIALS AND METHODS	31
2.1.	MATERIALS	31
2.1.1.	Enzymes and chemicals	31
2.1.2.	Bacterial Strains	32
2.1.3.	Yeast Strain	32
2.1.4.	Plant Materials	33
2.1.5.	Plasmid constructs	33
2.1.6.	Oligonucleotides	33
2.1.6.1.	Oligonucleotides for PCR amplification of cDNA coding regions	33
2.1.6.2.	Oligonucleotides for DNA sequencing	34
2.1.6.3.	Oligonucleotides for site-directed mutagenesis of the Ost1 kinase	34
2.1.6.4.	Oligonucleotides for RT-PCR	34
2.1.6.5.	AtSNF4 primers to test alternative splicing	34
2.1.6.6.	Oligonucleotides to screen for T-DNA insertion mutants in <i>Arabidopsis</i>	34
2.1.7.	Culture media	35
2.1.7.1.	Bacterial media	35
2.1.7.2.	YPD yeast medium	35
2.1.7.3.	Plant media	35
2.1.8.	Antibiotics	36
2.1.9.	Plant hormones	36

2.1.10. Solutions	36
2.1.11. Antibodies	37
2.1.11.1. Primary antibodies	37
2.1.11.2. Secondary antibodies	37
2.1.12. Computer analyses	37
2.2. METHODS	38
2.2.1. General molecular biology methods	38
2.2.1.1. Mini-preparation of plasmid DNA from <i>E.coli</i>	38
2.2.1.2. Large scale plasmid purification from <i>E.coli</i> by CsCl gradient	38
2.2.1.3. Isolation of plasmid DNA from <i>Agrobacterium tumefaciens</i>	39
2.2.1.4. Large Scale Genomic DNA isolation from <i>Arabidopsis thaliana</i>	40
2.2.1.5. CTAB genomic DNA extraction protocol	40
2.2.2. Methods for DNA purification and quantification	41
2.2.2.1. Phenol/chloroform extraction	41
2.2.2.2. Separation of DNA by agarose gel electrophoresis	41
2.2.2.3. Purification of DNA fragments from agarose gels	41
2.2.3. Enzymatic modifications of DNA	42
2.2.3.1. Digestion with restriction enzymes	42
2.2.3.2. Phosphatase treatment of DNA	42
2.2.3.3. Generation of blunt-ended DNA fragments	42
2.2.3.4. Generation of A-Tail for blunt ended PCR fragments	42
2.2.3.5. Ligation of DNA fragments	43
2.2.4. PCR amplification	43
2.2.4.1. RT-PCR	44
2.2.5. Site-Directed Mutagenesis	44
2.2.6. Bacterial Transformation	44
2.2.6.1. Preparation of <i>E. coli</i> competent cells for transformation by heat-shock	44
2.2.6.2. Preparation and transformation of electro-competent cells	45
2.2.7. Yeast one hybrid assays	45
2.2.8. Southern DNA hybridization	46
2.2.8.1. Preparation of ³² P-labeled DNA probes	46
2.2.8.2. DNA filter hybridization with radioactively labeled DNA probes	47
2.2.8.3. DNA filter hybridization with dioxigenin-labeled DNA probes	47
2.2.9. Methods for RNA isolation from plants and cell suspension cultures	48
2.2.9.1. RNA isolation using the guanidium thiocyanate (GTC) method	48
2.2.9.2. RNA isolation using Plant RNeasy Extraction kit (Qiagen)	48
2.2.9.3. Electrophoresis of RNA in TBE agarose gel	49
2.2.9.4. Formaldehyde agarose gel electrophoresis of RNA samples	49
2.2.9.5. Northern blotting and RNA filter hybridization	49
2.2.10. Protein analytical methods	50
2.2.10.1. Preparation of crude protein extracts from plant tissues and cell suspension	50
2.2.10.2. Extraction of nuclear proteins from <i>Arabidopsis</i> cell suspension	50
2.2.10.3. Preparation of cytoplasmic protein extracts from <i>Arabidopsis</i> plant tissues and cell suspensions	51
2.2.10.4. Chromatin immunoprecipitation	51
2.2.10.5. Measurement of protein concentration by Bradford assay	52
2.2.10.6. Size separation of proteins by SDS-polyacrylamide gele electrophoresis	52
2.2.10.7. Western blotting	53
2.2.10.8. Verification of protein transfer by Ponceau staining	53
2.2.10.9. Coomassie staining	54
2.2.10.10. Colloidal Blue staining	54
2.2.10.11. Immunoblot analysis	54
2.2.10.12. Size fractionation of proteins by glycerol gradient centrifugation	54
2.2.10.13. Immunoprecipitation of proteins	54
2.2.11. Purification of recombinant proteins expressed in <i>E. coli</i>	55
2.2.11.1. Purification of 6 X histidine tagged proteins	55
2.2.11.2. In vitro protein kinase assays	55

2.2.11.3.	Protein kinase assay with SAMS peptide	56
2.2.12.	Plant growth conditions	56
2.2.12.1.	Agrobacterium-mediated plant transformation	56
2.2.12.2.	Seed sterilization and selection of transgenic and mutant plants	56
2.2.12.3.	Hormone and stress treatments	57
2.2.12.4.	Isolation of T-DNA knockout mutants	57
2.2.12.5.	Protoplast transformation and transient gene expression assays	57
2.2.12.6.	GUS histochemical assay	58
2.2.13.	Generation of epitope tagged recombinant proteins for biochemical studies	58
2.2.13.1.	Plasmids used for expression of epitope labeled proteins	58
3.	RESULTS	60
3.1.	ANALYSIS OF REGULATORY FUNCTION, EXPRESSION AND POST-TRANSLATIONAL MODIFICATION OF THE BZIP TRANSCRIPTION FACTOR DPBF4	60
3.1.1.	Identificantion of DPBF4 via yeast one hybrid screening with the G-box containing promoter region of the aspartate kinase AK1/HSD1 gene	60
3.1.2.	DPBF4 is a member of the ABI5 bZIP transcription family	62
3.1.3.	Regulation of DPBF4 expression in <i>Arabidopsis</i>	63
3.1.4.	Screening for <i>dpbf4</i> T-DNA insertion mutants in Köln T-DNA mutant collection	65
3.1.5.	Searching for <i>dpbf4</i> insertion mutations in the Salk T-DNA mutant population	67
3.1.5.1.	PCR genotyping the Salk_025758 insertion mutant line	68
3.1.5.2.	PCR genotyping the SALK_21965 insertion mutant line	68
3.1.5.3.	RT-PCR analysis of transcription of <i>dpbf4-2</i> and <i>dpbf4-3</i> mutant alleles	69
3.1.5.4.	Phenotypic characterization of <i>dpbf4</i> insertion mutants	70
3.1.6.	Epitope Tagging of DPBF4 for biochemical studies	70
3.1.6.1.	Verification of expression of epitope-tagged DPBF4 constructs in Arabidopsis cells	71
3.1.7.	DPBF4 is a nuclear protein	71
3.1.7.1.	Immunolocalization of HA-DPBF4 protein in Arabidopsis plants	72
3.1.7.2.	Transient expression of GFP-DPBF4-HA fusion protein in Arabidopsis protoplasts prepared from cell suspension	72
3.1.8.	Size fractionation of DPBF4 on a linear glycerol gradient reveals that DPBF4 undergoes dimerisation	73
3.1.9.	DPBF4 and ABI5 interact <i>in vivo</i>	74
3.1.10.	Conserved phosphorylation signature in the DPBF4 protein sequence	75
3.1.11.	Identification of a candidate kinase of DPBF4	75
3.1.11.1.	Construction of vectors for expression of DPBF4 and OST1 in <i>E. coli</i>	76
3.1.11.2.	Purification of bacterially expressed OST1-HIS and HIS-DPBF4 proteins	76
3.1.11.3.	Induction time course of expression of His-tagged DPBF4 and OST1 proteins	76
3.1.11.4.	Purification of HIS-DPBF4 and OST1-HIS fusion proteins	78
3.1.11.5.	The OST1-kinase undergoes shows autophosphorylation and phosphorylates histone H2B <i>in vitro</i>	78
3.1.12.	DPBF4 is a substrate of SnRK1 (AKIN10) and SnRK2 (Ost1) kinases <i>in vitro</i>	78
3.1.12.1.	Dose dependence of OST1 activity and DPBF4 phosphorylation	79
3.1.12.2.	Ost1 kinase phosphorylates the DPBF4-HA protein immuno-purified from Arabidopsis cells	80
3.1.13.	Analysis of OST1 and AKIN10 kinase gene expression in <i>Arabidopsis</i> .	80
3.1.14.	Identification of OST1 kinase phosphorylation sites involved necessary for kinase activity	81
3.1.14.1.	Structural analysis of the OST1 kinase	81
3.1.15.	Localization of the autophosphorylated residues of OST1 kinase by MALDI MS/MS mass spectrometry analysis	82
3.1.15.1.	Confirmation of Ser 175 as critical residue for autophosphorylation of OST1 kinase.	84
3.1.15.2.	Substitution of Ser175 to Aspartic acid (D) generates a constitutively active OST1 kinase	84
3.1.15.3.	OST1 kinase signals through Ser175 to phosphorylate DPBF4	84
3.1.15.4.	Mutation of Ser175 to aspartic acid in the OST1 kinase results in enhanced phosphorylation of DPBF4 substrate	84
3.1.15.5.	Mutation of K59 to R or deletion of catalytic domain results in a dead kinase	84

3.1.15.6.	T146 acts as an inhibitor of OST1 kinase activity	85
3.1.15.7.	The OST 1 kinase phosphorylates the SnRK1 substrate SAMS peptide	85
3.1.16.	Characterization of the regulation of <i>AK1/HSD1</i> promoter	86
3.1.16.1.	Salt and ABA activate the AK1/HSD1 promoter	86
3.1.16.2.	Transcriptional de-repression of sucrose-induced AK1/HSD1 gene in the <i>prl1</i> mutant	86
3.1.17.	Transcriptional de-repression of <i>DPBF4</i> in the <i>prl1</i> mutant	87
3.1.18.	Construction of oestradiol-inducible DPBF4 expression vectors for studying the role of DPBF4 in regulation of stress and sugar induced genes	87
3.1.18.1.	Time course of DPBF4-HA gene induction in pER8 by β -oestradiol	88
3.1.18.2.	Influence of inducible DPBF4-HA expression on the activity of ABA-regulated ADH1 gene	88
3.1.19.	Identification of DPBF4-binding sites in the AK1/HSD1 promoter using chromatin immunoprecipitation	89
3.1.19.1.	Verification of specificity of ChIP DNA by PCR	90
3.1.19.2.	Identification of DPBF4-binding sites in the AK1/HSD1 promoter	91
3.2.	FUNCTIONAL ANALYSIS OF SNRK1 ACTIVATING GAMMA-SUBUNIT SNF4	93
3.2.1.	Expression patterns of regulatory and substrate targeting subunits of SnRK1 kinases in <i>Arabidopsis</i>	93
3.2.2.	Analysis of SNF4 expression at the protein level	94
3.2.3.	Examination of alternative splicing of SNF4 transcript	94
3.2.4.	Excluding the possibility of alternative splicing at the protein level	96
3.2.4.1.	Western blot analysis of epitope tagged SNF4 overexpressing Arabidopsis cell suspension	96
3.2.5.	Isolation of <i>snf4</i> T-DNA insertion mutations.	97
3.2.5.1.	Screening for <i>snf4</i> insertion mutants in the Wisconsin mutant population	97
3.2.5.2.	Identification of a single T-DNA sub-pool (second round screening of Wisconsin T-DNA population) by Southern hybridization	98
3.2.5.3.	Structure of the T-DNA insertion in the WISCONSIN <i>snf4</i> mutant	98
3.2.5.4.	PCR analysis of segregating M3 families of the WISCONSIN <i>snf4</i> mutant	99
3.2.5.5.	Screening for <i>snf4</i> insertion mutants in the SALK and GABI-KAT collections	99
3.2.6.	Cellular localization of the SNF4 protein	100
3.2.6.1.	Transient expression of an SNF4-GFP fusion protein in a light-grown Arabidopsis cell suspension	100
3.2.6.2.	Western blot analysis of distribution of SNF4 protein in nuclear and cytoplasmic fractions prepared from dark- and light-grown cell suspensions	101
3.2.7.	Immuno-affinity purification of SNF4-HA from <i>Arabidopsis</i> cell suspension	102
3.2.7.1.	SNF4-HA immunoprecipitates an SnRK1 α subunit (either AKIN10 or AKIN11)	102
3.2.8.	SNF4 is associated with the 26S proteasome	103
3.2.8.1.	The immuno-purified SNF4-HA complex does not carry the PRL1 inhibitor of SnRK1 α kinase subunits	103
3.2.9.	Association of SNF4 with SnRK1 α -subunits and 20S proteasome is not affected by light	104
3.2.10.	Size fractionation of SNF4 protein complex by glycerol gradient centrifugation	105
3.2.10.1.	SNF4 and PRL1 are present in protein complex of similar size	105
3.2.11.	The substrate targeting AKIN β 2 subunit is associated with an SnRK1 α -subunit	106
3.2.12.	AKIN β 2 is associated with the 26S proteasome	106
3.2.13.	Transcriptional regulation of the <i>SNF4</i> gene in wild type and <i>prl1</i> mutant plants	107
3.2.14.	Assay of SNF4 protein stability	107
4.	DISCUSSION	108
4.1.	CHARACTERIZATION OF FUNCTION REGULATION AND PHOSPHORYLATION OF DPBF4	108
4.1.1.	DPBF4 binds to a G-box element within the sugar responsive enhancer of the AK1/HSD1 aspartate kinase gene	108
4.1.2.	DPBF4 knockout mutants and probable functional redundancy of DPBF4 homologs	109
4.1.3.	DPBF4 and ABI5 form heterodimers and occur in different chromatin associated protein complexes	110
4.1.4.	Phosphorylation of DPBF4 by OST1 and AKIN10	111
4.1.5.	Mapping of autophosphorylation sites in OST1	113

4.1.6. Confirmation of DPBF4 interaction with the AK1/HSD1 promoter	113
4.2. FUNCTIONAL ANALYSIS OF SNRK1 ACTIVATING GAMMA-SUBUNIT SNF4	114
4.2.1. Analysis of expression pattern and potential alternative splicing of <i>SNF4</i>	114
4.2.2. Isolation of <i>snf4</i> insertion mutant alleles	115
4.2.3. SNF4 is a nuclear protein	116
4.2.4. SNF4 in high molecular mass protein complexes	116
4.3. OUTLOOK	116
5. REFERENCES	117

I FIGURES

Figure 1.	Osmotic stress signaling pathways.....	7
Figure 2.	ABA biosynthesis pathway and enzymes involved.....	9
Figure 3.	Currently known components of early ABA signaling pathway in guard cells.....	12
Figure 4.	Promoter <i>cis</i> -elements, transcription factors and potential MAKP cascades involved in the regulation of ABA-responsive transcription.....	18
Figure 5.	Cross-talk between ABA, ethylene, glucose and AMP signaling.....	22
Figure 6.	Sugar sensing and signaling by hexokinase and AMP-activated SnRK1 kinases involves crosstalk with trehalose and G-protein coupled receptor signaling.....	24
Figure 7.	Schematic maps of epitope tagging vectors pPILY (A), pLOLA (B), pPCV812-PILY (C), and pPCV812-GIGI (D).....	59
Figure 8.	Yeast one-hybrid screen with the sugar responsive enhancer element of the <i>AK1/HSD1</i> promoter.....	61
Figure 9.	Identification of binding-site of DPBF4 in the sugar responsive enhancer domain of <i>AK1/HSD1</i> promoter.....	62
Figure 10.	Comparison of DPBF4 protein sequences to some other members of the <i>Arabidopsis</i> bZIP family.....	62
Figure 11.	RT-PCR analysis of <i>DPBF4</i> expression in various organs of <i>Arabidopsis</i>	63
Figure 12.	DPBF4 expression data in the Genevestigator microarray transcript profiling database.....	64
Figure 13.	Schematic representation of localization of T-DNA insertion in the mutant allele <i>dpbf4-1</i>	65
Figure 14.	Identification of M3 lines homozygous for the <i>dpbf4-1</i> mutant allele.....	66
Figure 15.	DIG-labeling of DPBF4 cDNA probe by PCR.....	66
Figure 16.	The <i>dpbf4-1</i> mutation does not abolish gene expression.....	67
Figure 17.	PCR genotyping the SALK_025758 mutant line and identification of the <i>dpbf4-2</i> mutant allele.....	68
Figure 18.	PCR genotyping the SALK_021965 mutant line and identification of the <i>dpbf4-3</i> mutant allele.....	69
Figure 19.	RT-PCR analysis of transcription of <i>dpbf4-2</i> and <i>dpbf4-3</i> alleles.....	70
Figure 20.	Western blot analysis of protein extracts prepared transgenic plants and cell suspensions expressing HA-DPBF4 and DPBF4-HA, respectively.....	71
Figure 21.	Detection of DPBF4-HA in cytoplasmic and nuclear protein fractions prepared from a dark-grown <i>Arabidopsis</i> Col-0 cell suspension.....	71
Figure 22.	Cellular localization of HA-DPBF4 protein in transgenic plants.....	72
Figure 23.	Transient expression of GFP-DPBF4-HA fusion protein in protoplasts.....	73
Figure 24.	Size fractionation of DPBF4-HA by glycerol gradient centrifugation.....	74
Figure 25.	Confirmation of ABI5 and DPBF4 interaction <i>in vivo</i>	74
Figure 26.	Schematic representation protein structure and predicted phosphorylation sites of DPBF4.....	75
Figure 27.	Cloning of DPBF4 and OST1 cDNAs into <i>E. coli</i> protein expression vectors.....	76
Figure 28.	Induction of HIS-DPBF4 and Ost1-HIS expression in <i>E. coli</i>	77
Figure 29.	Time course of induction of HIS-DPBF4 and OST1-HIS expression.....	77
Figure 30.	Elution profiles of purified His-DPBF4 and OST1-His proteins.....	77
Figure 31.	Purified OST1 kinase is active <i>in vitro</i>	78
Figure 32.	AKIN10 and OST1 phosphorylate DPBF4 <i>in vitro</i>	79
Figure 33.	Effect of varying dosage of OST1 and DPBF4 on substrate phosphorylation <i>in vitro</i>	79
Figure 34.	DPBF4-HA immunoprecipitated from cultured <i>Arabidopsis</i> cells is sensitive to OST1-mediated phosphorylation.....	80
Figure 35.	Expression patterns of <i>OST1</i> and <i>AKIN10</i> kinase genes in various organs of <i>Arabidopsis</i>	81
Figure 36.	Structural analysis of the OST1 kinase.....	82
Figure 37.	MALDI MS/MS identification of putative phosphopeptides.....	83
Figure 38.	The effects of mutations produced in potential phosphoresidues and the activation loop of the Ost1 kinase.....	85
Figure 39.	SAMS peptide phosphorylation by OST1.....	86
Figure 40.	PRL1 negatively controls the expression of the <i>AK1/HSD1</i> gene.....	87
Figure 41.	<i>DPBF4</i> mRNA levels are increased in the <i>prl1</i> mutant in presence of 3% sucrose.....	87
Figure 42.	Expression of DPBF4-HA mRNA upon induction with β -oestradiol under XVE system.....	88
Figure 43.	Initial testing the oestradiol inducible DPBF4-HA system and its effect on <i>ADHI</i> expression.....	89
Figure 44.	Flow-chart important quality controls of chromatin immunoprecipitation experiments.....	90
Figure 45.	PCR analysis of ChIP DNA samples.....	91
Figure 46.	ChIP PCR mapping DPBF4-HA binding sites in the <i>AK1/HSD1</i> promoter.....	92
Figure 47.	Expression analysis of SnRK1 regulatory and substrate targeting subunit gene.....	93
Figure 48.	Comparison of microarray transcript profiling data available in the Genevestigator database for SnRK1 activating and substrate targeting subunit.....	94

Figure 49.	Analysis of SNF4 protein expression in different <i>Arabidopsis</i> tissues.....	94
Figure 50.	Examination of alternative splicing of <i>Arabidopsis</i> SNF4 transcripts.....	95
Figure 51.	Analysis of stability of HA-SNF4 and SNF4-HA fusion proteins.	96
Figure 52.	Screening of the Wisconsin insertion mutant collection for T-DNA tag in the SNF4 gene.	97
Figure 53.	Identification of single pool of mutant carrying a T-DNA insertion on the SNF4 gene.	98
Figure 54.	Localization of the T-DNA insertion in the <i>snf4-1</i> (Wisconsin) mutant allele.....	98
Figure 55.	PCR genotyping of segregating M3 families for the <i>snf4-1</i> mutant allele.....	99
Figure 56.	Characterization of <i>snf4-2</i> and <i>snf4-3</i> T-DNA insertion mutant alleles.	100
Figure 57.	Determination of distribution of SNF4-HA protein in cytoplasmic and nuclear protein fractions.	101
Figure 58.	Cellular localization of the GFP-SNF4 fusion protein in protoplasts prepared from a..... light-grown <i>Arabidopsis</i> Ler cell suspension.	101
Figure 59.	In light-grown cells SNF4 is exported to the cytoplasm.	102
Figure 60.	SNF4-HA is associated with an SnRK α -subunit in vivo.....	103
Figure 61.	SNF4-HA is found in association with the 20S proteasome.	103
Figure 62.	PRL1 does not interact with SNF4.....	104
Figure 63.	Association of SNF4 with SnRK1 α and 20S proteasome is not abolished by light.	104
Figure 64.	Glycerol gradient size fractionation of SNF4 protein complexes.....	105
Figure 65.	PRL1 and SNF4 show co-fractionation on a linear glycerol gradient.	105
Figure 66.	AKIN β 2 co-immunoprecipitates with the 20S proteasome cylinder and with an SnRK1..... α -subunit.....	106
Figure 67.	Comparative RT-PCR analysis of SNF4 transcript levels in response to ABA, sucrose, glucose and sugar starvation in the <i>prl1</i> mutant and wild type.....	107
Figure 68.	Assay of HA-SNF4 protein stability under various stress treatments.	107

II ABBREVIATIONS AND SYMBOLES

A	adenine
ABA	abscisic acid
Ac	acetate
ADP	adenosine 5'-diphosphate
AMP	adenosine 5'-monophosphate
<i>A. thaliana</i>	<i>Arabidopsis thaliana</i>
ATP	adenosine 5'-triphosphate
ATPase	adenosine 5'-triphosphatase
BAC	bacterial artificial chromosome
bp	base pair
BSA	bovine serum albumin
Bq	Becquerel
C	cytosine
°C	grad Celsius
CaMV	Cauliflower Mosaic Virus
cAMP	adenosine 3',5'-cyclic-monophosphate
cDNA	complementary DNA
chr.	chromosome
CSM	<i>A. thaliana</i> Cell Suspension culture Medium
CS	<i>A. thaliana</i> Cell Suspension culture
CoA	acetyl coenzyme A
C-terminal	carboxyterminal
C-terminus	carboxyl terminus
CTAB	cetyl trimethylammonium bromide
2,4-D	2,4-Dichlorophenoxy acetic acid
DAPI	4,6-diamine-2 phenylindole dihydrochloride
dd	distilled
DEPC	diethylpyrocarbonate
DMSO	dimethyl sulfoxide
DNA	Deoxyribonucleic acid
dNTP	deoxyribonucleotide triphosphate
DTT	dithiotreitol
<i>E. coli</i>	<i>Escherichia coli</i>
EDTA	ethylenediaminetetraacetic acid
EST	expressed sequence tag
EtBr	ethidium bromide
EtOH	ethanol
G	guanine
GA	gibberellin
gm	gram
g	relative centrifugal field unit
GST	glutathione-S-transferase
GTC	guanidium thiocyanate
h	hour
HIS3	imidazole-glycerol-phosphate-dehydratase gene
IAA	indole-3-acetic acid
IGEPAL	(octylphenoxy) polyethoxyethanol
IgG	immunoglobuline G

IP	immunoprecipitation
IPTG	isopropyl- β -thiogalactoside
kb	kilobase
kDa	kilo Dalton (1,000 Da)
kV	Kilovolt
l	liter
<i>lacZ</i>	<i>E. coli</i> β -galactosidase gene
M	Mitosis
M	Molar
MDa	mega Dalton
MES	2-(N-morpholino) ethanesulfonic acid
μ g	microgram
μ l	microliter
μ M	micromolar
mA	milliampere
mg	milligram
min.	minute
ml	milliliter
mM	millimolar
mRNA	messenger RNA
Ni	nickel
nt	nucleotide
N-terminal	amino terminal
N-terminus	amino terminus
OD	optical density
P	phosphor
PAGE	polyacrylamide gel electrophoresis
POD	peroxidase
PCR	polymerase chain reaction
PEG	polyethylene glycol
pH	negative logarithm of the proton concentration
PMSF	phenylmethylsulfonyl fluoride
PVDF	polyvinylidene difluoride
RNA	ribonucleic acid
RNase	ribonuclease
RPM	revolution per minute
RT	room temperature
RT-PCR	reverse transcription PCR
<i>S. cerevisiae</i>	<i>Saccharomyces cerevisiae</i>
SDS	sodium dodecylsulfate
sec.	second
SSC	standard saline citrate
T	thymine
T	Total
TAE	Tris-acetate (40 mM); EDTA (1mM)
TCA	trichloroacetic acid
TE	Tris.HCl (10mM); EDTA (1mM)
TEMED	N,N,N',N' tetramethylenethylendiamine
Tris	Tris(hydroxymethyl) aminomethane

U	unit
Ub	ubiquitin
UTR	untranslated region
UV	ultraviolet light
V	Volt
vol.	volume
X-Gal	5-bromo-4-chloro-3-indolyl- β -D-galactopyranoside
X-Gluc	5-bromo-4-chloro-3-indolyl- β -D-glucuronic acid
wt	wild type

Aminoacids

A	Ala	Alanine
C	Cys	Cysteine
D	Asp	Aspartic acid
E	Glu	Glutamic acid
F	Phe	Phenylalanine
G	Gly	Glycine
H	His	Histidine
I	Ile	Isoleucine
K	Lys	Lysine
L	Leu	Leucine
M	Met	Methionine
N	Asn	Asparagine
P	Pro	Proline
Q	Gln	Glutamine
R	Arg	Arginine
S	Ser	Serine
T	Thr	Threonine
V	Val	Valine
W	Trp	Trptophan
Y	Tyr	Tyrosine
X		any aminoacid

III SUMMARY - ZUSAMMENFASSUNG

In höheren Pflanzen ist die Regulation von Entwicklungsprozessen und des Metabolismus fest zu einer komplexen Interaktion zwischen Hormonsignaltransduktionswegen verbunden. Viele Reaktionen die durch osmotischen Stress (Salzgehalt, Dürre und Kälte) kontrolliert werden, sind synergistisch durch das Stresshormon Abszisinäure (ABA), durch Glucose und Saccharose induziert. Der historische Stoffwechselweg der Glucose-Hemmung, der in allen Organismen vertreten ist, spielt auch eine zentrale Rolle in der Regulation der Transkription und der Wachstumsantwort in Pflanzen, obwohl dieser Stoffwechselweg die Aktivität von Genen, die an der Photosynthese beteiligt sind negativ reguliert. Grundsätzlich wirken Glucose und Saccharose durch die Stimulation der ABA-Synthese.

Die ABA-Signaltransduktion ihrerseits benötigt Elemente der Ethylene-Signaltransduktion. Innerhalb dieses Netzwerks aus Signalfunktionen, spielen die eng verwandten Proteinkinasefamilien SnRK1 und SnRK2 unterschiedliche Rollen. Während SnRK1 Enzyme eine zentrale Rolle als zelluläre Glucose und AMP Sensoren spielen, die die zelluläre Energie-Homeostase monitoren, sind ihre verwandten SnRK2 Kinasen an der Regulation zellulärer Reaktionen auf osmotische Stress-Stimuli beteiligt. Dabei bilden sie eine Verbindung zwischen frühen Signaltransduktionsereignissen wie die Generation so genannter „secondary messengers“ und der direkten Regulation der Aktivität von Transkriptionsfaktoren durch Phosphorylierung aus. In dieser Arbeit wird die Funktion und die Regulation eines bZIP-Transkriptionsfaktors, DPBF4, aus *A.thaliana* beschrieben. DPBF4 wurde als Bindungsfaktor für G-box-ähnliche, regulatorische Sequenzen im Promotor des durch Saccharose induzierten Aspartat-Kinase-Gens AK1/HSD1, welches an der Regulation der Biosynthese essentieller Aminosäuren beteiligt ist, identifiziert. DPBF4 gehört zur ABI5/DPBF/AREB/ABF bZIP Familie, die nahverwandte Transkriptionsfaktoren einschließt. Die Analyse von *dpbf4* Nullmutationen zeigt Redundanz zwischen den DPBF-Homologen aus *A.thaliana* auf. DPBF4 ist ein Substrat der SnRK2 Proteinkinase OST1 (OPEN STOMATA). Die Charakterisierung von OST1 zeigt das sich diese Kinase innerhalb ihres aktivierenden „T-loop“ autophosphoryliert und gemeinsame Substrate mit anderen SnRK1-Kinasen erkennt. Eine Analyse kritischer Aminosäurereste mittels „site-specific mutagenesis“, Punkt-mutationen, liefert eine detaillierte Einsicht in die Regulation der SnRK2-Kinaseaktivität. OST1 ist wahrscheinlich für die Stimulation der Dimerisierung und DNA-Bindung von DPBF4, welches Bestandteil verschiedener Chromatin-assoziiierter Proteinkomplexe ist, benötigt. Chromatin „crosslinking“ Experimente zeigen das DPBF4 tatsächlich spezifische cis-regulatorische Elemente im Promotor der Modelaspartokinase AK1/HSD1 besetzt.

Es stellte sich heraus, dass DPBF4 auch Substrat der SnRK1-Kinasen, deren Aktivität durch ihre SNF4 gama-Untereinheit reguliert wird, ist. Die Charakterisierung von Nullmutanten demonstriert, daß *snf4* Mutationen nicht durch männliche Gameten übertragen werden, was auf ihre essentielle Funktion hindeutet. SNF4 ist eine Kernkinaseuntereinheit, deren Kernimport als Licht reguliert erscheint. Wir zeigen das SNF4 Proteasom assoziiert ist. Die hier beschriebene Arbeit zeigt ein weites Repertoire an molekularen, genetischen und biochemischen Methoden zur Unterscheidung

von regulatorischen Elementen der Glucose und der Stress-Signaltransduktion, besonders zur Identifikation von Partnern und Regulatoren der DPBF ähnlichen bZIP-Proteine und Proteinkinasen der SnRK1 und SnRK2 Familien, auf.

In higher plants, the regulation of metabolic and developmental processes is tightly connected to a complex crosstalk between hormone signaling pathways. Many responses controlled by osmotic stress (salinity, drought and cold) stimuli are synergistically induced by the stress hormone abscisic acid and by glucose and sucrose. The ancient pathway of glucose repression, which is found in all organisms, also plays a central role in the regulation of transcription and growth responses in plants, though this pathway negatively controls the activity of genes involved in photosynthesis. Glucose and sucrose essentially signal through stimulation of ABA synthesis, whereas ABA signaling requires elements of the ethylene signaling pathway. Within this web of signaling functions, the closely related SnRK1 and SnRK2 families of protein kinases play a distinguished role. Whereas SnRK1 enzymes are key cellular glucose and AMP sensors, which monitor the cells' energy homeostasis, their relatives in the SnRK2 kinase family participate in the regulation cellular responses to osmotic stress stimuli by establishing connections between early signaling events, such as generation of secondary messengers, and direct regulation of the activity of transcription factors by phosphorylation.

In this work a study of the function and regulation of an *Arabidopsis* bZIP transcription factor, DPBF4, is described. DPBF4 was identified as a G-box binding factor, which recognizes glucose-responsive regulatory sequences in the promoter of the aspartate kinase gene *AK1/HSD1* implicated in the control of biosynthesis of essential amino acids. DPBF4 is a member of the ABI5/DPBF/AREB/ABF bZIP family, which include closely related transcription factors. Analysis of *dpbf4* knockout mutations suggests functional redundancy of *Arabidopsis* DPBF homologs. DPBF4 is a substrate of the SnRK2 protein kinase OST1 (OPEN STOMATA). Characterization of OST1 shows that this kinase is capable of autophosphorylation within its activating T-loop and recognizes common substrates with members of the SnRK1 kinase family. Mapping of critical amino acid residues by site-specific mutagenesis provides an insight into details of regulation of SnRK2 kinase activity. OST1 is probably required for stimulation of dimerization and DNA-binding of DPBF4, which was found in chromatin-associated protein complexes. Chromatin crosslinking experiments show that DPBF4 indeed occupies specific *cis*-regulatory elements in the promoter of the model *AK1/HSD1* aspartokinase gene. DPBF4 turned out to be also a substrate of SnRK1 kinases, whose activation is controlled by their SNF4 gamma subunits. Characterization of knockout mutations demonstrates that SNF4 is essential for male gametogenesis. SNF4 is a nuclear kinase subunit and its nuclear import appears to be light-regulated. The work described in this thesis offers a wide repertoire of molecular, genetic and biochemical tools for dissection of regulatory elements of glucose and stress signaling pathway, in particular for identification of partners and regulators of DPBF-like bZIP proteins and protein kinases of SnRK1 and SnRK2 families.

1. INTRODUCTION

1.1. SUGAR METABOLISM, STRESS AND PLANT GROWTH CONTROL

Plants as sessile organisms cope with various forms of biotic and abiotic stresses throughout their life. In addition to genetically determined developmental programs, their survival and lifespan in nature is largely dependent on the limits and flexibility of their inherited stress adaptation capabilities. Following a short phase of heterotrophic growth supported by the utilization of starch, lipid and other storage deposits of seed endosperm or embryonic cotyledons, developing seedlings switch to photoautotrophic growth. This genetically programmed switch to photoautotrophy is based on light-controlled chloroplast differentiation and activation of CO₂-fixation pathways in the emerging leaves that, in addition to obligatory light signal of proper quality, is primarily triggered by transient depletion of carbon (energy) supplies. As in all other eukaryotic organisms, glucose plays a central role not only as optimal energy-carrier compound in carbon metabolism, but also as central regulatory molecule in metabolic, developmental and growth signaling in plants (Smeekens, 2000). Cellular accumulation of glucose represents a metabolic growth signal in all non-photosynthetic organisms. By contrast, accumulation of glucose (as well as its metabolic precursors e.g., triose-phosphates, acetate, pyruvate, or disaccharides, such as sucrose and trehalose etc.) in actively photosynthesizing plant cells is interpreted as inhibitory signal, which results in metabolic feed-back inhibition of photosynthetic CO₂-fixation and down-regulation of transcription and transcript stability of light-stimulated genes (for review see Koch, 1996).

Glucose acts as metabolic signal triggering the repression of genes, as well as inactivation and degradation of proteins, involved in alternative carbon utilization, and thereby securing the most economic energy generation through glycolysis (and avoiding “futile” cycles in carbon metabolism; for review see e.g., Ronne, 1995; Gancedo, 1998). As glycolysis is an ancient anaerobic pathway (Kim and Dang, 1995), glucose repression in eukaryotes is coupled to negative regulation of respiration and oxidative metabolism, and inhibition of genes involved in mitochondrial and peroxisome biogenesis. The control of energy homeostasis thus also involves basic monitoring of the cells’ redox status and adenylate levels (Buchanan and Balmer, 2004; Hardie et al., 1998).

As glucose represents the ultimate end product of photosynthetic CO₂-fixation in higher plants, which negatively feed-back regulates the expression of key genes acting in photosynthesis, the maintenance of carbon-assimilation capacity of vital importance is secured by continuous removal of glucose (mostly in form of sucrose produced by the reaction of sucrose-P synthase [SPS], Lunn and MacRae, 2003) from photosynthetic cells. In general, this is achieved by two major means: i) sugar is transported from photosynthetic source tissues to other actively growing (meristems, young leaves, flowers etc.) or differentiated storage tissues (i.e., which have low, if any photosynthetic activity, e.g., roots, tubers, seeds etc.), termed collectively sink organs, and ii) sugar is incorporated transiently into starch stored in chloroplasts, which is then being degraded and converted to glucose/sucrose in the dark and transported to sink tissues (Paul and Foyer, 2001; Smith et al., 2003).

In most plant species, cells of diverse tissues and organs are connected by plasmodesmata (Lucas and Lee, 2004). Monosaccharide and disaccharide transport from photoautotrophic source to heterotrophic sink tissues thus mostly involves symplastic transport (i.e., through plasmodesmata of phloem sieve elements) mediated by various sugar transporters with specific roles in export (i.e., loading) and import (i.e., uptake; Lemoine, 2000; Williams et al., 2000). However, active transport through the apoplast (i.e., cell wall, outer membrane) plays a major role during seed development, when symplastic transport between maternal and embryonic tissues is disrupted (Patrick and Offler, 2001). Sugar transport from source to sink tissues generates a sugar gradient, which is often observable between and within actively growing and differentiated tissues of various organs (Borisjuk et al., 2002). Thus, the capacity of transport from source to sink is not only determined by the efficiency of photosynthetic and sugar export processes of source leaves, but it is also dependent on the “strength” of the sink determined by sugar uptake and utilization (i.e., which correlates with the growth-rate of non-storage sink organs). Monosaccharides are phosphorylated to corresponding sugar phosphates by e.g., hexokinase (or fructokinase, glucokinase etc.) to enter into catabolism, or starch or cellulose etc. biosynthesis. Disaccharides are split to monosaccharides either before or after their uptake to sink tissues. Depending on the mechanism of disaccharide hydrolysis, sugars may perform alternative signaling functions. Thus, in case e.g., sucrose is hydrolyzed by apoplastic invertases, the effective concentration of monosaccharide signals (glucose, fructose) is doubled extracellularly, and after uptake at the level of e.g., hexokinase (see below) and fructokinase signaling (Pego and Smeekens, 2000). Inhibition or enhancement of apoplastic cell wall invertases do not only modulate sink organ development, but also signal through the transport system by inhibiting or enhancing sugar transport of source tissues. Reduction of sink strength leads to sugar accumulation inhibiting photosynthesis in source tissues and, in more severe cases, induces sugar accumulation-related stress responses manifesting in sugar induced anthocyanin synthesis, bleaching and senescence (Roitsch and Gonzalez, 2004).

Whereas invertase action appears to be tightly coupled to glycolysis and linked to energy-providing oxidative metabolism that facilitates fast growth, cell wall biosynthesis, cell expansion and division, the hydrolysis of sucrose by sucrose synthase is more characteristic to differentiated and storage tissues. Expression of sucrose synthases (SuSys) is stimulated by low oxygen conditions e.g., in phloem sieve tube cells, which import sucrose by ATP facilitated uptake, contributing to the maintenance of sucrose gradient during plant development. From sucrose Susy produces UDP-glucose (UDPG) and fructose. UDPG is converted by UDP-glucose pyrophosphorylase (UGPase) to UTP and glucose 1-phosphate (G1P). The latter is primarily used in cell wall or callose biosynthesis (especially in response to wounding, drought or pathogenic stress), whereas UTP is spent for generation of fructose-6-P that enters the glycolysis regenerating ATP for active sucrose transport (Koch, 2004).

Although sugar transport and signaling is only one of the many means by which plant cells communicate, on this example it is easy to illustrate how environmental stress stimuli may disturb and modulate basic metabolic and growth regulation pathways of plants. Drought, salinity, cold or heat

stress all lead to cellular water deficit, termed osmotic stress. All these stress stimuli ultimately result in cessation of sugar transport and growth arrest of sink organs, and induce temporal sugar accumulation in source tissues. This leads to glucose inhibition of transcription of photosynthetic genes and parallel induction of a large set of stress-defense genes, the expression of which is positively regulated by glucose. Past analyses of regulation of various classes of genes responding to different environmental stress stimuli show that metabolic signaling through glucose repression shares numerous common regulatory targets and mechanisms with signaling pathways controlling abiotic stress responses. What is known currently about crosstalk and specific components of these pathways is reviewed below.

1.2. CONVERGENCE AND CROSSTALK BETWEEN ABIOTIC STRESS SIGNALING PATHWAYS

Despite their specific effects, frost, drought and salinity result in similar physiological changes characterized by alterations in membrane fluidity, loss of osmotic potential, generation of reactive oxygen species (ROS), and decline of photosynthetic activity. These common osmotic and oxidative stress-related changes trigger analogous, compensatory defense reactions including fast closure of leaf stomata (i.e., gas exchange cells), stimulation of compensatory water uptake, and synthesis of osmoprotective compounds, so-called osmolytes (e.g. specific sugars and sugar alcohols, such as, trehalose, sorbitol and mannitol, and amino acids and amino acid analogs, such as proline and betaine). In addition to stimulating specific sets of genes, frost, drought and salinity induce the expression of a set of osmotic and oxidative stress-regulated transcripts that code for common signaling and ROS scavenging factors, as well as osmoprotecting proteins including chaperons; antifreeze, late-embryogenesis abundant (LEA) and pathogenesis response-related (PR) proteins (for review see Zhu, 2002a; Chinnusamy et al., 2004).

Although apparently all hormones and many secondary messengers contribute to temporal and spatial regulation of stress responses during plant development, without doubt abscisic acid (ABA) is the major “stress” hormone that plays a central role in the control of abiotic (and partly also biotic) stress responses. Except for specific genes involved in cold stress responses, ABA in fact stimulates the expression of most drought and ionic stress-induced genes (for review see Shinozaki et al., 2003; Seki et al., 2003). ABA regulates many important aspects of plant development. In addition to controlling gas exchange and photosynthesis by triggering stomatal closure, ABA induces the synthesis of seed storage proteins and lipids, promotes seed desiccation tolerance and dormancy, and thereby inhibits transition from embryonic stage to germination (Leung and Giraudat, 1998). During seed germination, ABA is thought to antagonize the stimulating affect of gibberellin. Intriguingly, ABA inhibition of seed germination is alleviated by ethylene and low concentrations of glucose or sucrose suggesting a crosstalk between ABA, ethylene and sugar signaling (see for reviews Finkelstein and Gibson, 2001; Koornneef et al., 2002). Recent physiological studies indicate that ABA plays an important growth promoting role in shoots and roots by antagonizing ethylene synthesis and signaling

(Sharp and LeNoble, 2002; LeNoble et al., 2004). On the other hand, non-dormant phenotype of ethylene and ABA insensitive *ein2 abi3-4 Arabidopsis* double mutants suggests that ethylene antagonizes ABA-mediated inhibition of seed germination (Beaudoin et al., 2000). This is consistent with the observation that the *ein2* mutation results in enhanced ABA sensitivity, whereas the *ctr1* (constitutive ethylene triple response) mutation reduces ABA sensitivity of seed germination. By contrast, both *ein2* and *ctr1* mutants show ABA and ethylene insensitive root elongation phenotype demonstrating that interaction between ethylene and ABA signaling is differentially regulated in different stages of plant development. This confirms the notion that ABA signaling probably includes several components that show distinct organ and cell type specificity. ABA signaling probably represents a non-linear (i.e., branching) pathway, in which upstream components converging on ABA-specific signaling, as well as downstream components dependent on ABA signaling, may mediate responses to different environmental stress stimuli (see for review Xiong et al., 2002a).

1.3. DISSECTION OF DROUGHT, SALT, AND COLD SIGNALING PATHWAYS

Historically, dissection of stress signaling pathways started by the identification of specific gene sets that are activated or repressed by one or more stress factors and/or ABA. Following dissection of promoter regions of specific stress marker genes, various *cis*-elements were identified and showed to confer stress-specific activation of transcription when placed into artificial promoters (e.g., minimal TATA-box constructs). Subsequent studies using gel retardation, yeast one-hybrid, foot-printing and chromatin immunoprecipitation assays led to the identification of transcription factors that recognize various *cis*-elements and confer stress specific activation of transcription. Post-translational regulation of these elements by protein kinases, phosphatases and ubiquitin-mediated proteolysis is emerging to reveal important control steps in stress signaling. Forward genetic screens have identified numerous mutations that confer stress/ABA insensitivity or hypersensitivity at the level of stomata closure, germination, seedling development, root elongation, senescence etc. facilitating the genetic and molecular analysis of components of stress signaling pathways. Other genetic screens utilized luciferase gene fusions driven by specific stress regulated promoters (e.g., with defined *cis*-elements) to identify mutations that up- or down-regulate transcription induced by drought, cold or salinity. Finally, physiological studies (i.e., chiefly stomatal electrophysiology) identified several early, potentially plasma-membrane- and ER-associated components and second messengers that either act in one or more stress signaling pathways, and/or mediate ABA-response (for review see: Himmelbach et al., 2003; Yamaguchi-Shinozaki and Shinozaki, 2005).

1.3.1. Signal perception

Receptor molecules involved in primary perception of cold and osmotic (drought and salt) stress stimuli remained thus far largely unknown in higher plants. Cold stress stimulate changes in membrane fluidity and cytoskeletal organization, which ultimately leads to Ca^{2+} influx and activation of downstream events by Ca^{2+} -signaling (Plieth et al., 1999; Thomashow, 1999). However, it is unclear which Ca^{2+} -membrane channels and associated regulatory factors are involved in sensing low

temperature induced changes in membrane fluidity. In bacteria and yeast, the regulation of osmotic stress responses include canonical two-element histidine kinase receptors, which mediate by histidine to aspartate phosphotransfer the activation of response regulators, many of which interact with or function as transcription factors. In yeast, osmotic stress stimuli activate the SLN1 hybrid histidine kinase (i.e., which carries both N-terminal receiver and C-terminal kinase domains) that through the YPD1 phosphotransmitter protein transfers phosphate to an Asp residue of SSK1 response regulator and thereby activate the HOG osmosensing MAP-kinase cascade (Hohmann, 2002). The *Arabidopsis* genome encodes 11 histidine kinases, 10 A-type and 10 B-type response regulators, and 5 phosphotransmitters. One of the *Arabidopsis* hybrid histidine kinases, ATHK1, has been found to suppress the osmotic defect caused by the deficiency of yeast SLN1 (and SHO1, see Hohmann, 2002) osmosensor by activating the HOG pathway (Urao et al., 2001). Expression of ATHK1 is upregulated in response to salt and low temperature suggesting that this histidine kinase could indeed be involved in osmotic stress signaling. However, it is unknown whether ATHK1, analogously to yeast SLN1, would also lead to activation of a MAPK signaling pathway. In this respect, it is worth to note that Patharkar and Cushman (2000) found in iceplant (*Mesembryanthemum crystallinum*) a salinity and drought-induced calcium-dependent protein kinase, McCDPK1, which interacts with and phosphorylates a two-component response regulator CSP1. This suggests a possible direct link between certain Ca^{2+} /calmodulin dependent kinases and components of histidine kinase phosphorelays.

From the remaining 10 *Arabidopsis* histidine kinases ETR1 and ERS1 function as ethylene receptors along with their homologs ETR2, ERS2 and EIN4 that carry degenerate His-kinase domains. Thus far, no response regulators have been described in the ethylene signaling pathway (see below). Further members of the *Arabidopsis* two-component HIS kinase family include the cytokinin receptor CKI1 and its homolog CKI2 that lacks transmembrane domain. CRE1 is a hybrid histidine kinase and its structurally related homologs AHK2 and AHK3 probably also function as cytokinin receptors together with the response regulators ARR3, 4, 6 and 7, the expression of which is induced by cytokinin and nitrate starvation. The latter observation suggests that N-starvation is signaled by roots via cytokinin. Remarkably, response regulators ARR1 and ARR2 carry Myb-like DNA binding domains, and thus probably function as transcription factors (for review see Heyl and Schmülling, 2003; Grefen and Harter, 2004, Figure 1).

1.3.2. Cold stress signaling

Though cold stress signaling may share several upstream elements with other osmotic stress signaling pathways, the analysis of expression of low temperature regulated *COR* genes in the *Arabidopsis abi-1* and *abi2-1* mutants indicates that the regulation of these genes largely differs from those of other osmotic stress-induced genes, which are controlled by both ABA-dependent and independent signaling pathways (Xiong et al., 2002a). Promoters of cold responsive *COR* genes carry conserved drought response DRE (taCCGACAT) and CRT (C-repeat (ggCCGACAT) elements that confer transcription

activation to both drought and cold (Gilmour et al., 1997). The DRE and CRT elements were found to bind C-repeat-binding CBF or dehydration response element binding DREB1 transcription factors that belong to the ethylene response element binding/APETALA2 (EREBP/AP2) family (Liu et al., 1998; Gilmour et al., 2000). The expression of *CBF1/DRE1B*, *CBF2/DRE1C* and *CBF3/DRE1A* is cold-inducible suggesting that a transcription factor cascade is involved in cold signaling. In fact, the expression of *CBF3* gene is positively regulated by ICE1 (an inducer of CBF expression), which is a Myc-like basic helix-loop-helix (bHLH) transcription factor that binds to a MYC recognition sequence in the *CBF3* promoter, as well as by ICE homologs (Chinnusamy et al., 2003; Zarka et al., 2003). Remarkably, *CBF2* turned out to be a negative regulator of *CBF1* and *CBF3* expression (Novillo et al., 2004) and *CBF3* was shown recently to be ABA-induced through a promoter element, which differs from the canonical ABA-response (ABRE) sequence (Knight et al., 2004).

Genetic screening for upregulation of drought and cold controlled RD29A promoter-luc construct identified a mutation in the *HOS1* gene that results in high expression of osmotically regulated genes (Lee et al., 2001). *HOS1* encodes a RING-finger ubiquitin ligase that shows homology in its C-terminal domain to the IAP (inhibitor of apoptosis) class of RING finger ubiquitin E3 ligases that act as caspase inhibitors in animals. *HOS1* likely regulates the stability of CBF/DRE factors or a positive regulator of their genes (i.e. ICE1), as constitutive overexpression of *HOS1* drastically down-regulates *COR* gene expression. The DREB/CBF factors interact with several elements of chromatin remodeling complexes that include histone acetyltransferases (Stockinger et al., 2001). A histone acetyltransferase-binding partner, which corresponds the retinoblastoma RB-binding protein encoded by the flowering time regulator *FVE* gene, is a repressor of *CBF*-controlled *COR* gene expression (Kim et al., 2004a). Expression of the CBF 1, 2 and 3 genes is regulated through phytochrome B (PhyB) and the circadian clock, by a novel RNA helicase and components of an ADA2b-GCN5 transcriptional co-activator, as well as by CBL1 binding factor of SnRK3 type protein kinases (see below, Kim et al., 2002a; Gong et al., 2002; Vlachonassios et al., 2003; Albrecht et al., 2003; Fowler et al., 2005). CBF expression is negatively controlled by a novel repressor FIERY2 that carries double-stranded RNA-binding motives and a domain, which shows homology to protein phosphatases acting in dephosphorylation of the C-terminal repeat (CTD) of RNA polymerase II largest subunit (Xiong et al., 2002b). In addition, expression of DREB/CBF proteins is also regulated at the level of translation by a translation initiator factor 2 homolog, LOS1, inactivation of which inhibits RD29A-luc expression (Guo et al., 2002). Whereas CBF1, 2 and 3 participate in cold signaling, the fourth homolog CBF4 is dedicated to the control of drought signaling (Haake et al., 2002). Recent transcript profiling experiments indicate that activation of the CBF pathway of cold acclimation leads to the synthesis of special sugars and sugar alcohols through the induction of genes encoding galactinol synthase, raffinose synthase, and melibiase (Cook et al., 2004)

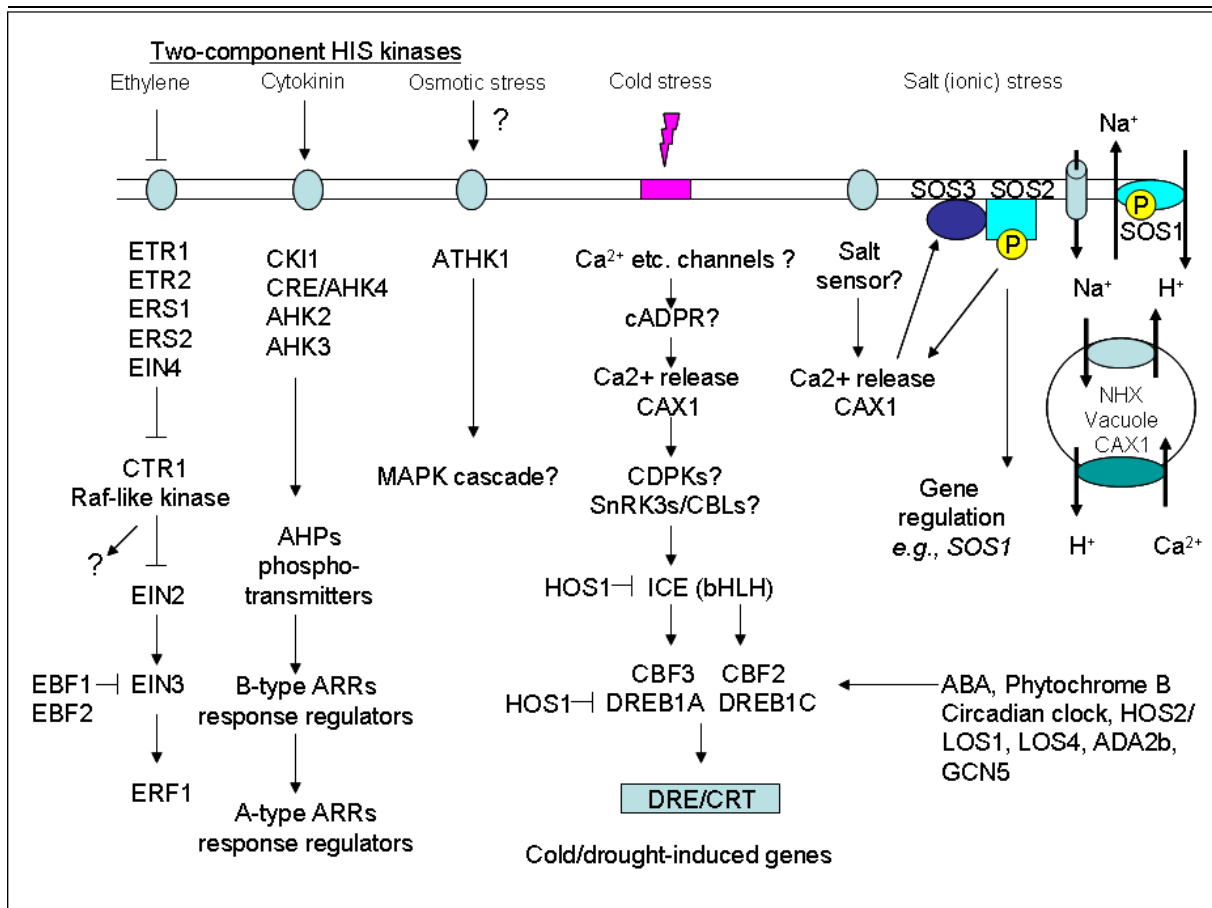


Figure 1. Osmotic stress signaling pathways.

Components of currently known elements of cold and salt stress signaling pathways are shown, their description is provided in the text. The two-component histidine kinase ATHK1 is implicated in osmotic stress signaling, but downstream elements of this pathway are not yet uncovered. For comparison, the figure shows some known elements of other two-component histidine kinase cascades.

1.3.3. Salt signaling: the SOS-SnRK3 kinase pathway

As cold stress, salt stress also results in generation of cytosolic Ca²⁺ peaks, which trigger the activation of a Ca²⁺-sensor SOS3, a myristoylated membrane-associated protein carrying Ca²⁺-binding EF-hand motives. Mutations reducing the Ca²⁺-binding capability of SOS3 results in a salt hypersensitive phenotype (Ishitani et al., 2000). SOS3 was found to interact with SOS2, a member of the Snf1-related SnRK3/CIPK (CBL-interacting kinase) kinase family, which is encoded by 25 genes in *Arabidopsis* (Hrabak et al., 2003; see also below). The C-terminal domain of SOS2/SnRK3.11 carries a FISL motif, which acts as kinase autoinhibitory domain and is required for binding of SOS3 (Guo et al., 2001). Exchange of Thr¹⁶⁸ for Asp in the T-loop of SOS2 results in a constitutively active kinase, which suppresses the salt sensitive phenotype caused by the *sos2* and *sos3* mutations (Zhu, 2002b). Genetic analysis shows that SOS2 and SOS3 function in the same pathway as SOS1, a plasmamembrane Na⁺/H⁺-antiporter, which interact with and phosphorylated by the SOS2 kinase (Shi et al., 2000; Qiu et al., 2002; Quintero et al., 2002). This data indicate that Ca²⁺-stimulated activation of SOS2, and SOS2-mediated activation of SOS1 stimulates efflux of Na⁺ from root cells exposed to salt stress. Na⁺-entry to root cells is mediated by the AtHKT1 low affinity Na⁺ transporter. The fact that the *athkt1* mutation suppresses the salt sensitive *sos3* phenotype indicates that the SOS2-SOS3

kinase probably inactivates AtHKT1 and thereby reduces the influx of Na⁺ during salt stress (Rus et al., 2001). Steady-state mRNA levels of vacuolar and tonoplast Na⁺ antiporters AtNHX1, 2 and 5, which remove Na⁺ from the cytoplasm to the vacuole, is significantly higher in the *sos* mutants suggesting that the SOS pathway controls their expression (Yokoi et al., 2002). Remarkably, SOS2 was found to phosphorylate and activate CAX1, a vacuolar H⁺/Ca²⁺-antiporter that regulates the duration and intensity of Ca²⁺-peaks. This suggests that SOS2 feed-back regulates its activation by Ca²⁺ (Cheng et al., 2004). Intriguingly, mutations of *CAX1* were found to increase the expression of DREB/CBF factors and to induce cold acclimation confirming a stimulatory role of Ca²⁺-signaling also in cold stress signaling (Catala et al., 2003).

1.4. ABA SIGNALING

1.4.1. Regulation of ABA synthesis

Drought, salt and to a certain extent cold stress result in ultimate induction of ABA synthesis (Cutler and Krochko, 1999; Taylor et al., 2000). ABA is synthesized from β -carotene, which is produced in plastids from isopentenyl pyrophosphate (IPP). Plastidic IPP is synthesized from pyruvate and glyceraldehyde-3-phosphate through 1-deoxy-D-xylulose-5-phosphate (DXP) and converted via farnesyl pyrophosphate to geranylgeranyl pyrophosphate. The latter compound is used for the synthesis of phytoene by phytoene synthase (PSY), which represents the rate-limiting step of carotene synthesis. Phytoene is converted through ζ -carotene, lycopine, and β -carotene to the xanthophyll zeaxanthin, which is the first direct precursor of ABA. Epoxidation of zeaxanthin by ZEP (zeaxanthin epoxydase) encoded by *Arabidopsis ABA1* results in two steps in the production of either 9-cis-violaxanthin or 9-cis-neoxanthin via Antheraxanthin. 9-cis-violaxanthin or 9-cis-neoxanthin are converted to xanthoxin by NCED (9-cis-epoxycarotenoid dioxygenase), which is encoded by a small gene family consisting of 9 differentially regulated genes in *Arabidopsis* (Tan et al., 2003; Figure 2). NCED represents the last plastid specific and rate-limiting step of ABA synthesis (Seo and Koshiba, 2002) upon which xanthoxin is transported to the cytoplasm by a yet undefined mechanism. Xanthoxin is converted to abscisic aldehyde by a short-chain dehydrogenase/reductase (SDR), which is encoded by *ABA2* in *Arabidopsis* (Schwartz et al., 1997). Finally, ABA aldehyde is converted to ABA by an aldehyde oxidase (AO) that requires a molybdenum cofactor (MOCO), which is absent in the *Arabidopsis* mutant *aba3* due to a defect of a MOCO sulfurylase enzyme (Bittner et al., 2001). As side pathways, ABA may also be produced by less characterized enzymes from xanthoxic acid and abscisic alcohol (Milborrow, 2001).

Recent data suggest that the very first step of carotene synthesis, including the formation of DXP can significantly affect carotene, as well as ABA levels, because DXP is required for plastid biogenesis (Guevara-Garcia et al., 2005). However, it is more likely that enzymes acting in the xanthophyll pathway limit ABA production. *ZEP/ABA1* genes are induced in roots by sugar-treatment and in response to drought, whereas all studied members of the NCED gene family respond to

drought. *ABA2* is activated by sucrose and glucose, and its mutation leads to glucose and sucrose insensitive phenotype suggesting that ABA is required for mediation of sugar/glucose repression and/or signaling (see for review Gibson, 2005). Members of the AO gene family are also stress activated, but characterization of their tissue specific regulation (except for drought induction of *AAO3*) is still incomplete. As overexpression of *NCED3* leads to ABA accumulation, it is likely that *NCEDs* control the rate-limiting step in ABA biosynthesis. Whereas many genes in ABA biosynthesis are inducible by sugar, *NCEDs* appear to be exceptions (Rolland et al., 2002a). Remarkably, except for *NCEDs*, ABA stimulates the expression of *ZEP/ABA1*, *SDR/ABA2* and *AAO3/ABA3* genes indicating the existence of a positive feed-back loop, which may play an important role in ABA signal amplification during stress. Recent data show that inactivation of *CBL9*, a gene coding for a calcineurin-B/SOS3-like Ca^{2+} -sensor protein results in ABA hypersensitivity and enhanced ABA accumulation under stress conditions (Pandey et al., 2004). This data suggests that SOS2-like SnRK3 protein kinases and/or a Ca^{2+} -stimulated SOS-like regulatory system probably participates in the regulation of genes involved in ABA synthesis.

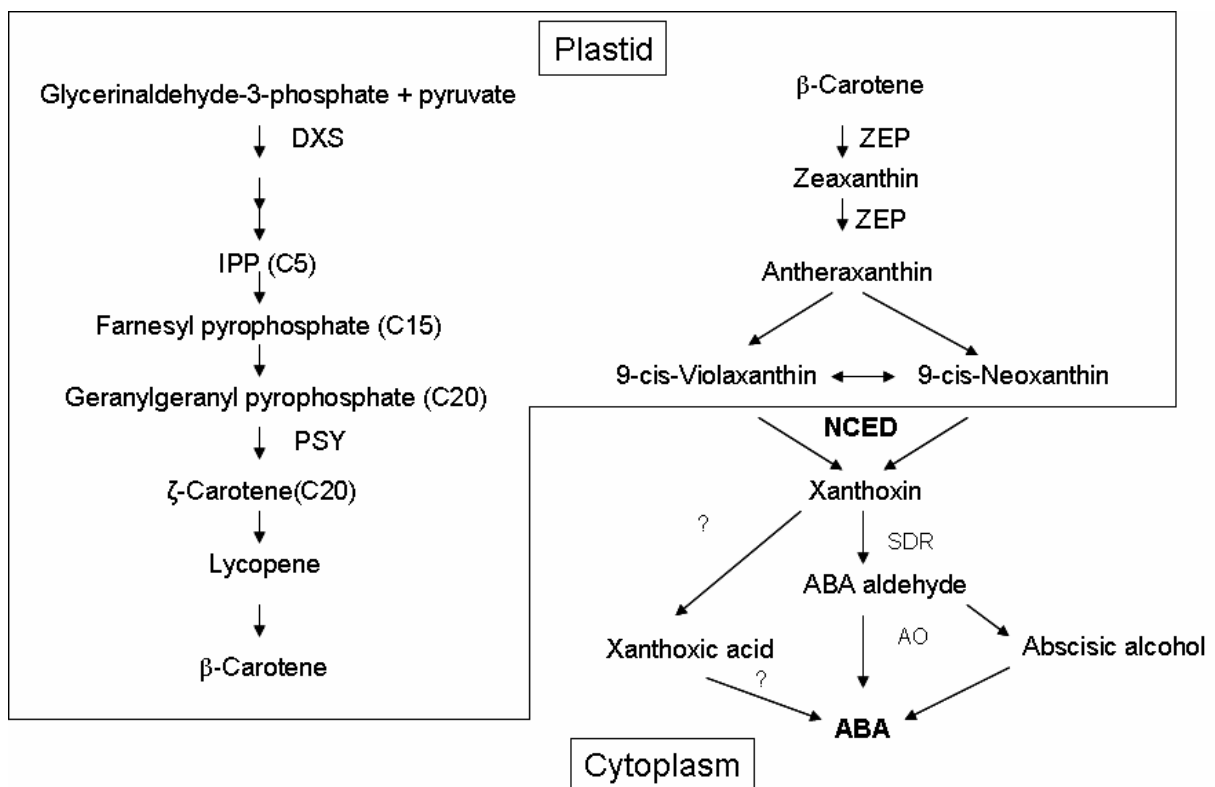


Figure 2. ABA biosynthesis pathway and enzymes involved.

Explanation of abbreviations and description of biochemical steps of ABA biosynthesis are described in the text.

1.4.2. Primary signaling events and secondary messengers in ABA signaling

Genetic and physiological studies suggest that ABA perception could involve receptors that are either associated to the plasma membrane or present in the cytoplasm (for review see Finkelstein et al., 2002; Himmelbach et al., 2003). However, no ABA receptor has been identified so far. When sensing drought or salinity, roots mediate active ABA transport to shoots initiating closure of stomata to reduce respiratory water loss. However, ABA is synthesized in most tissues, and in leaf mesophyll

cells it is stored in the chloroplasts. In response to drought, ABA is released from chloroplasts and transported to the apoplast by a yet unknown mechanisms. Activation of sugar signaling, like ABA signaling leads to decline of photosynthetic activities and activation of oxidative stress responses (Sauter et al., 2001; Schroeder et al., 2001).

Most of our current knowledge on early events in ABA and ABA-mediated osmotic stress signaling has derived from stomatal cell physiology studies. However, analysis of tissue-specific regulation of ABA biosynthesis and signaling throughout seed and plant development suggests that the order and components of signaling factors and events may considerably vary between guard cells and other cells types in shoots and roots. ABA perception in guard cells stimulates the activity of a blue-light inducible ATP-dependent proton pump and leads to plasmamembrane depolarization, transport of solutes from vacuoles to apoplast, inactivation of inward-rectifying K^+ channels, and activation of outward-rectifying K^+ -channels and anion channels involved in Cl^- and malate transport (for review see MacRobbie, 1998; Fedoroff, 2002). Proton influx and membrane depolarization leads to ATP-dependent activation of both plasmamembrane and vacuole membrane-associated Ca^{2+} transporters leading to increase of cytoplasmic Ca^{2+} concentration detected as oscillation of Ca^{2+} -peaks. Inhibitors of PP1 and PP2A protein phosphatases and ABA stimulate Ca^{2+} channel opening.

A role for GTPases in ABA signaling is suggested by that a mutation of the GPA1 α -subunit of a trimeric G-protein down-regulates ABA response. In fact, plants carrying a knockout *gpa1* allele show ABA insensitive stomatal opening, and a lack of ABA-inhibition of inward rectifying K^+ channels and anion channels (Wang et al., 2001). Recently, GPA1 was found in association with a putative seven-trans-membrane G-coupled receptor GCR1. Insertion inactivation of *GCR1* results in ABA hypersensitivity in root elongation, stomatal opening and gene transcription assays. As *gpa1* mutants display ABA insensitivity, GPA1 appears to be a negative regulator of GCR1 (Padney and Assmann, 2004). These data suggest that GCR1 is part of the putative ABA membrane receptor. Recently, it was found that sphingosine-1-phosphate (S1P), a Ca^{2+} -mobilizing secondary messenger lipid, which is an extracellular ligand of G-coupled receptors, stimulates stomatal closure in wild type plants, but not in *gpa1* mutants (for review see Worall et al., 2003). S1P is produced by sphingosine kinase (SphK), which is activated by ABA in a GPA1-dependent fashion (Coursol et al., 2003).

In addition to a trimeric G-protein, members of the Rop (Rho/Rac) GTPase family, which include 11 monomeric small G-proteins, also play various roles in ABA signaling. Mutations inactivating ROP10 result in enhanced ABA response (i.e. hypersensitivity) in seed germination, root elongation and stomatal closure assays (Zheng et al., 2002). ROP10 appears to perform overlapping functions with ROP9 in negative regulation of ABA signaling. The phenotype of *rop9, rop10* double mutant is similar to that of *eral* (enhanced response to ABA) mutant, which is impaired in the function of a protein farnesyltransferase beta-subunit (Cutler et al., 1996; Pei et al., 1998). The *eral* mutation partially suppresses ABA insensitivity of guard cells caused by the *abi1* and *abi2* mutations (see below), but appears to act downstream of ABI1 and ABI2 in the pathway stimulating Ca^{2+} release (Allen et al., 2002; Brady et al., 2003). It is hypothesized that ERA1 is probably required for

membrane localization of ROP small G-proteins and possibly also for membrane targeting of GPA1 (i.e. by farnesylation of G γ subunit).

ABA induction also leads to the generation of other lipid secondary messengers. ABA induces the expression of one of the six *Arabidopsis* PLC genes (*AtPLC1*). PLC hydrolyses phosphatidylinositol 4,5-phosphate (PIP₂) by producing two important secondary messengers, diacylglycerol and inositol 1,4,5-trisphosphate (IP₃), which may trigger Ca²⁺-release and kinase activation. Sanches and Chua (2001) showed that PLC1 is necessary, but not sufficient alone, for triggering ABA response. Production of PIP₂ is stimulated by ABA and osmotic stress, which induce the expression of phosphatidylinositol-4-phosphate 5-kinase in *Arabidopsis* (Mikami et al., 1998). PIP₃ levels are faithfully controlled by either inositol phosphate 3 kinase (generating inositol 1,3,4,5, tetraphosphate) or inositol polyphosphate 3-kinase (Ins5Pase; producing inositol 1,4-bisphosphate). As the *Arabidopsis* genome codes for 15 Ins5Pase gene, it is yet unclear which genes contribute to the control of IP₃ levels during ABA signaling and osmotic stress. Genetic screens with the drought, cold and ABA inducible RD29A-luc construct have identified the *fiery1* (*fry1*) mutation, which causes enhanced sensitivity to drought, cold salt and ABA. *FRY1* was found to encode a bifunctional enzyme, which shows Ins1Pase activity (i.e. producing e.g. Ins(3,4)P₂ from Ins(1,3,4)P₂). Whereas the *fry1* mutation confers hypersensitivity to osmotic stress and ABA, *FRY1* overexpression in yeast confers salt tolerance (Xiong et al., 2001a) suggesting that *FRY1* indeed participates in modulation of IP₃ levels.

ABA and drought induce the expression of phospholipase D genes *PLD α* and *PLD δ* , respectively, which represent two genes from 11 members of the *Arabidopsis* PLD family (for review see Finkelstein et al., 2002). PLD hydrolyses phospholipids producing phosphatidic acid (PA), another common second messenger, the synthesis of which is stimulated by drought, salt and cold in a G-protein-dependent fashion (Munnik and Musgrave, 2001). Genetic analysis revealed early on that ABA signaling is negatively regulated by two PP2C protein phosphatases ABI1 and ABI2 (Leung et al., 1998; see below). Following ABA stimulation of *PLD α 1*, phosphatidic acid was found to directly bind to ABI1 and inhibit its activity. Consistently, insertion inactivation of *PLD α 1* prevents ABA-stimulated closure of stomata (Zhang et al., 2004).

ABA signaling leads to rapid activation of the ADP-ribosyl cyclase gene, which regulates the synthesis of cyclic ADPribose (cADPR) from NAD (Sanchez et al., 2004). cADPR is a major second messenger, which stimulates Ca²⁺-release. The fact, that the dominant *abi1* mutation (see below) inhibits cADPR mediated induction of ABA-responsive genes suggest that ABI1 may control Ca²⁺-release or Ca²⁺-mediated activation of signaling (Wu et al., 2003). Pharmacological experiments show that nitric oxide (NO) produced either by nitrate reductases or a glycine decarboxylase complex selectively regulates Ca²⁺ ion channels in guard cells by promoting Ca²⁺-release (see for review Desikan et al., 2004). NO-mediated Ca²⁺ release is selectively blocked by inhibitors of guanylate cyclase (i.e., cGMP analogs) and blockers of cADPR-dependent Ca²⁺ channels (Garcia-Mata et al., 2003).

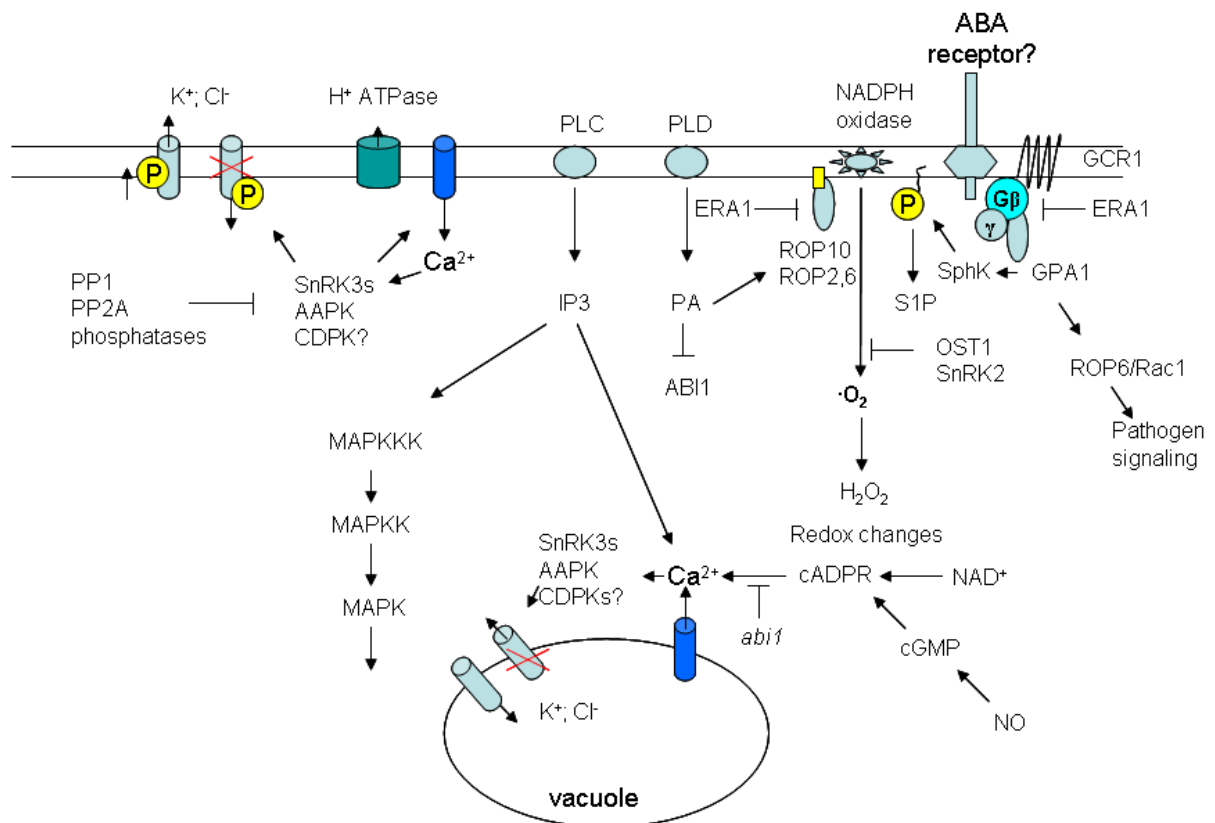


Figure 3. Currently known components of early ABA signaling pathway in guard cells.

Several components of the above depicted signaling pathways are also functional in ABA responses controlling root elongation, seed development and dormancy. This early section of ABA signaling pathway also overlaps with known elements of oxidative stress (redox), drought and salt signaling pathways. Explanation of individual functions and abbreviations is provided in the text.

ABA stimulates the production of reactive oxygen species (ROS), and accumulation of H_2O_2 by induction of catalase gene expression (Guan et al., 2000). ROS are produced by NADPH oxidases encoded by a large gene family in *Arabidopsis*. Stomatal cells express the AtRBOHD and AtRBOHF NADP oxidases, the inactivation of which (i.e. by double knockout mutations) prevents ABA-induced stomatal closure (Kwak et al., 2003). H_2O_2 is a central second messenger in many signaling pathways. In ABA signaling, H_2O_2 production following cytoplasmic alkalization stimulates Ca^{2+} release, inhibits the activity of K^+ channels and both ABI1 and ABI2 PP2C protein phosphatases (for review see Pastori and Foyer, 2002). H_2O_2 signaling has been reported to converge on the activation of a MAPK kinase cascade, the first element of which is ANP1 (MAPKKK, Kovtun et al., 2000). Nonetheless, overexpression of ANP1 does not affect the expression of osmotic stress regulated RD29A-luc marker gene (Xiong et al., 2002a).

Intriguingly, ABA-induced accumulation of H_2O_2 , and thereby stomatal closure, is inhibited by a mutation of the OST1 (*OPEN STOMATA 1*) gene, which encodes an SnRK2-type protein kinase (Mustilli et al., 2002). H_2O_2 production is also associated to the function of ROP proteins, which are activators of NADPH oxidase and controlled by H_2O_2 -induced deactivators (for review see Gu et al., 2004). Intriguingly, phosphatidic acid (PA) generated by PLD results in the induction of cell death in a ROP2-dependent fashion, but dominantly active ROP2 is not sufficient alone for cell death induction

(Park et al., 2004). ROP2, together with ROP6/Rac1 (which is also implicated in pathogenic signaling), also play a role in regulation of vesicle transport and reorganization of actin skeleton, which underlies the mechanism of stomatal closure. Disturbance of vesicle transport in the *osm1* mutant, which is impaired in the function of a syntaxin, results in a failure of ABA-stimulated stomatal closure (Zhu et al., 2002a). Components of the early ABA signaling pathway are depicted schematically in Figure 3.

1.4.3. Protein phosphatases and SnRK3 protein kinases in ABA signaling

Historically, the first ABA-signaling mutants identified in *Arabidopsis* were *abi1* and *abi2*, which defined the inhibitory functions of two closely related PP2C-type protein phosphatases (see for review Leung et al., 1998). As both *abi1* and *abi2* mutations are dominant negative, for understanding the action of these point-mutant phosphatases one needs to assume that the mutant proteins are more effective in blocking the ABA pathway (i.e., by substrate trapping) than their wild type counterparts. By contrast, mutations leading to complete inactivation of ABI1 and ABI2 cause ABA hypersensitivity (Merlot et al., 2001). In addition to *ABI1* and *ABI2*, ABA also induces the expression of *AtPP2-CA* and *AtPP2C-HA*, protein phosphatases which are involved in cold stress signaling. ABI1 and ABI2 are general regulators of ABA response, and thus they control germination, root growth and stomatal closure. ABI1 and ABI2 interact with multiple regulatory targets, including PKS3 (Protein kinase salt sensitive 3; alternative names: SnRK3.1 and CIPK15, calcineurine B-like interacting protein kinase 15) and the Ca^{2+} -sensor CBL protein ScaBP5. RNAi inhibition of PKS3 or its Ca^{2+} -sensing activator subunit ScaBP5 resulted in ABA hypersensitivity indicating that this Ca^{2+} -stimulated protein kinase acts in a negative regulatory loop controlling ABA sensitivity (Guo et al., 2002). CIPK3/SnRK3.17 and its Ca^{2+} -sensor CBL subunit were also found to negatively regulate ABA-induced gene expression (Kim et al., 2003). Ohta et al. (2003) found that the SOS2/SnRK3.11 kinase (which is required for positive control of salt tolerance) also interacts with ABI2, and precisely mapped the interacting domains in both SOS2 and ABI2. This analysis showed that the ABI1/2 interacting domain is conserved among members of the SnRK3 kinase family. Furthermore, these authors found that *abi2-1* mutation interrupts interaction with SOS2 and results in increased salt tolerance (as overexpression of SOS2; Ohta et al., 2003).

The above-described examples raise some intriguing questions about the functions of ABI1 and ABI2. If PKS3 is a negative regulator of ABA signaling, then inactivation of PKS3 by ABI1/2 would lead to enhanced ABA-signaling (as the PKS3 RNAi construct), which would ultimately define ABI1/2 as positive regulators of ABA signaling. Thus, the function of PKS3 is probably down-regulation of the signaling pathway in response to high Ca^{2+} -levels or under stress recovery (i.e. ABA desensitization). In case of SOS2, stabilization of active form of SOS2 in the *abi2-1* mutant may account for the observed increase salt tolerance phenotype. The fact that an inward rectifying K^{+} -channel AKT3 was found to interact with a related phosphatase, PP2CA (i.e., acting in cold signaling),

suggests that ABI1 and ABI2 may modulate the activity of other K⁺-channels involved in salt or ABA signaling (Vranova et al., 2001).

In addition to members of the SnRK3 family, many other kinases were described to affect ABA-regulated stomatal closure or gene expression (for review see Finkelstein et al., 2002). These include e.g. AtCDPK1, which in the heterologous barley system induces the activation of the G-box containing promoter of *RABI6* that is negatively controlled by ABI1 (for review see Chinnusamy et al., 2004). However, so far all signaling kinases were only tested in transgenic or protoplast overexpression systems using various reporter genes and the results of these studies are not yet supported by subsequent genetic analyses. One of the pathways proposed in *Arabidopsis* includes the AtMEKK1, AtMEK1/AtMKK2 and AtMPK4/AtMPK6 kinases. Expression of AtMEKK1 is induced by salt stress and this kinase activates AtMKK2 which interacts and activates AtMPK4 and AtMPK6 (Ichimura et al., 2000; Teige et al., 2004). Genetic analysis demonstrates that the *atmpk4* mutation confers jasmonate insensitivity, accumulates high amounts of salicylic acid and displays systemic acquired resistance (SAR; Petersen et al., 2000). A mutation inactivating a MPK4-interacting calmodulin binding protein phosphatase, MKP1, on the other hand, yields enhanced salt tolerance and hypersensitivity to UV-C (Ulm et al., 2002). In another cascade, ANP1 (MAPKKK) was proposed to activate AtMPK3 and AtMPK6 in response to ABA-induced oxidative stress (Kovtun et al., 2000).

1.4.4. SnRK2 protein kinases and RNA-binding proteins modulating ABA signaling

In wheat and *Vicia faba*, stomatal closure is regulated by ABA-induced kinases that represent members of the SnRK2 family. SnRK2s show a close relationship to catalytic α -subunits of plant SnRK1 kinases, which are functional orthologs of yeast Snf1 (i.e. a key regulator of glucose repression, see below) and animal AMP-activated protein kinases. However, the C-terminal regulatory domains of SnRK1 and SnRK2 kinases are completely divergent, and SnRK2 kinases do not form complexes with the activating and substrate targeting subunits of trimeric SnRK1s (Hrabak et al., 2003). The ABA-activated wheat kinase PKABA and the *Vicia* kinase AAPK are positive regulators of stomatal closure and ABA-induced gene expression. PKABA interact with and phosphorylates an ABRE (ABA-response element)-binding seed specific bZIP transcription factor, TaABF (Johnson et al., 2002). By contrast, AAPK interacts with and phosphorylates a nuclear RNA-binding protein AKIP1 in guard cells by stimulating its RNA-binding capacity and association with nuclear speckles (Li and Assmann, 2000; Li et al., 2002).

OST1 (SnRK2.6; SnRK2E), an *Arabidopsis* ortholog of AAPK and PKABA have been identified by characterization of a mutation that results in ABA-insensitivity of stomatal closure. The *ost1* mutation, however, does not effect the regulation of seed dormancy and ABA-mediated inhibition of root elongation. OST1 was shown to control the generation of H₂O₂ signal and ABA-induced transcription of the *RD22* gene (i.e., which is controlled by Myb/Myc factors, see below; Mustilli et al., 2002; Yoshida et al., 2002). Recently, Umezawa et al., (2004) reported that overexpression of the SnRK2.8/SnRK2C kinase in transgenic plants confers enhanced drought tolerance and activation of

RD29 (i.e., controlled by ABRE and CE elements) and the *DREB1/CBF3* genes. Knockout of the *SnRK2C* gene results in drought sensitive root growth. By studying stress-induction of members of *Arabidopsis* SnRK2 family, Boudsocq et al. (2004) found that 9 from 10 members are inducible by osmotic stress, whereas 5 SnRK2 enzymes are activated by salt stress, but none of the SnRK2s respond to cold stress. Surprisingly, using an affinity-purification approach, Testerink et al. (2004) identified a member of *Arabidopsis* SnRK2 family as phosphatidic acid-binding protein suggesting a link between PLD and SnRK2 signaling.

In addition to the AAPK-phosphorylated AKIP1 RNA-binding protein, downstream elements of ABA signaling seem to include several other factors involved in double-strand RNA-mediated silencing, nuclear mRNA export and splicing. A mutation in the HYL1 (HYPONASTIC LEAVES 1) locus, conferring ABA hypersensitivity in root elongation and seed germination assays, was thus found to abolish the function of a double-stranded RNA binding nuclear protein (Lu and Fedoroff, 2000). HYL plays a role in the control of microRNA accumulation and interacts with DICER RNA endonucleases mediating the cleavage of dsRNAs and generation of small inhibitory RNA molecules (Vazquez et al., 2004; Hiraguri et al., 2005). The *sad1* mutation (supersensitive to ABA and drought) result in enhanced activation of *RD29-luc* reporter and ABA hypersensitivity of stomatal closure, and inhibits activation of the ABA biosynthesis genes in response to drought (Xiong et al., 2001b). SAD1 is an Lsm5-like small nuclear ribonucleoprotein (snRNP), which appears to be involved in processing of a specific set of mRNAs. Another protein with dsRNA-binding motif is FIERY2/CPL1, an ortholog of protein phosphatases dephosphorylating the CTD-repeat of RNA polymerase II large subunit. The *fry2* mutation confers ABA-insensitivity in seed germination, but ABA-hypersensitivity in root elongation assays, and results in the activation of *DREB2/CBF3* genes (Xiong et al., 2002b). Finally, mutations affecting the CBP80/ADH1 and CBP20 subunits of CAP-binding complex involved in the regulation of nuclear mRNA export result in ABA-hypersensitive stomatal closing and greatly enhanced drought tolerance (Hugouvieux et al., 2001; Papp et al., 2004).

1.4.5. Transcription factors controlling ABA-regulated gene expression

1.4.5.1. ABA signaling and seed maturation

Within 5 to 7 day after pollination, when developing embryos are in the late torpedo stage, a peak in ABA synthesis is observable in maternal tissues signaling the onset of seed maturation process. At day 10, ABA biosynthesis declines in maternal tissues, but raises in the maturing embryos, which is essential for initiation of embryo dormancy (for review see Gubler et al., 2005). ABA-regulation of seed dormancy and expression of late-embryogenesis-abundant (LEA) genes are affected by the *Arabidopsis aba*, *abi3/vp1*, *era1*, *abi4*, *abi5*, *fus3* and *lec1* mutations (for review see Raz et al., 2001; Finkelstein et al., 2002). ABI5 is essential for regulation of the seed desiccation process and ABA-mediated inhibition of seed germination (Lopez-Molina et al., 2002).

ABI3 encodes a maize VP1-like transcription factor belonging to the B3 domain family, which binds to RY motives in the LEA gene promoters (see Figure 4). Other members of B3 DNA-binding

domain family include FUS3 and LEC1, which are required for repression of premature germination at the end of embryo development. LEC1 (LEAFY COTYLEDON 1) is required for FUS3 and ABI3-mediated stimulation of expression of seed-storage protein genes (Kagaya et al., 2005a). Genetic analysis of *abi*, *fus3* and *abi*, *lec1* double mutants indicate genetic interaction between FUS3, LEC1, ABI4 and ABI5 in ABA-mediated control of germination, gene expression during mid- and late embryogenesis, sugar metabolism, sensitivity to sugar, and etiolated growth (Brocard-Gifford et al., 2003).

LEC1 is one from the 10 HAP3b subunits of the CAAT-binding complex encoded in *Arabidopsis*, which appears to interact with FUS3, ABI3 and ABI5 (Lee et al., 2003). Expression of LEC1 and FUS3 is specifically down-regulated during germination by the PICKLE chromatin-remodelling complex, therefore *pkl* primary roots express embryonic traits (Dean Rider et al., 2003). The FUS3 and ABI3 B3-domain proteins bind to RY-box sequences conserved in seed-specific genes (Monke et al., 2004). Expression of *FUS3*, which specifies epidermal cell identity of cotyledons, negatively regulates the Myc transcription factor TTG1 (TRANSPARENT TESTA GLABRA1) in embryos. Reversal of many *fus3* traits in the *fus3*, *ttg1* double mutant suggest that part of *fus3* defects (e.g., change of cotyledon identity, premature activation of shoot and root meristems) is caused by de-repressed embryonic expression of TTG1 (Tsuchiya et al., 2004). FUS3 appears to participate in the regulation of both early and late (e.g., Myb/Myc-regulated) ABA-responsive genes (Kagaya et al., 2005b).

ABI3, 4 and 5 interact closely in ABA-regulation of seed-specific genes. Among the single *abi* mutants, *abi3* displays the most severe defects. ABI4 is an AP2-class transcription factor, which shows close similarity to the DREB/CBF family, whereas ABI5 is a bZIP factor, a member of the DPBF family (Finkelstein et al, 1998; Kim et al., 2002b; Jacoby et al., 2002; see below). A maize ortholog of ABI4 (*ZmABI4*) binds to coupling elements situated in the vicinity of bZIP/ABI5-binding ABRE elements in ABA and sugar-responsive promoters (Niu et al., 2002). *Arabidopsis* and rice ABI3s interact with ABI5/TRAB1, thus ABI5-binding to ABRE sequences may tether ABI3 to RY elements. Intriguingly, ABI4 does not seem to bind directly to either ABI3 or ABI5 (Nakamura et al., 2001; Gampala et al., 2002). The expression of both *ABI4* and *ABI5* genes is induced by glucose (Arroyo et al., 2003), to a higher levels in seeds than in vegetative tissues. Whereas *ABI4* is not inducible by ABA and stress in seedlings, *ABI5* is activated by ABA and to lower levels by stress in vegetative tissues. Nonetheless, both *ABI4* and *ABI5* are activated during transition to photoautotrophic growth during seed germination (i.e., probably due to transient increase of mobilized sugar concentrations). *ABI4* expression in seeds is lower in the *abi1-1* and *abi3-1* mutants, indicating that ABI4 acts downstream of these functions. Similarly, ABI5 is epistatic to ABI3, as ABI5 is required for expression of seed-specific *Em*-genes in the *abi3* mutant. Overexpression of ABI3, ABI4 and ABI5 results in hypersensitive growth responses to ABA, sucrose and glucose (Söderman et al., 2000; Borcard et al., 2002; Lopez-Molina et al., 2002).

1.4.5.2. *Cis-elements and transcription factors mediating ABA- responses*

The *Arabidopsis* genome encodes 75 bZIP proteins, which are classified in 11 families (Jacoby et al., 2002). bZIPs interact as dimers with G-box (ACGT) elements including ABA-response elements (ABREs). In those ABA-responsive promoters (e.g., *RD29A*), which are activated in the presence of protein synthesis inhibitor cycloheximide (i.e., and thus participate in primary ABA response), ABREs are linked to coupling elements (i.e. CE1, CE3, see for review Yamaguchi-Shinozaki and Shinozaki, 2005; Figure 4), which bind AP2-like factors, such as ABI4. In cold-induced promoters, ABREs are linked to DRE/CRT elements, which show similarity to coupling elements, but are occupied by DREB/CBF factors. In the slower induced late ABA-response promoters (e.g., *RD22*), the activation of which requires previous protein synthesis, ABA-response is generally regulated by Myb and Myc/bHLH-binding sites. In the *RD22* promoter, these sites are occupied by the AtMYC2 and AtMYB2 transcription factors (Abe et al., 2003). AtMYC2 is encoded by the *JASMONATE INSENSITIVE 1 (JAI1/JIN1)* locus, which is a positive regulator in ABA signaling, but negatively controls jasmonate and ethylene induced transcription responses (Anderson et al., 2004). On the other hand, AtMYB2 interacts directly with calmodulin, indicating a link to Ca²⁺-signaling, and plays a role in the activation of AtMYC2-regulated genes in response to salt stress and ABA (Yoo et al., 2005).

1.4.5.3. *The ABI5 family of bZIP transcription factors*

The activities of ABRE-binding bZIP factors referred to as AREBs or ABFs, are enhanced in the ABA-hypersensitive *eral* mutant, but reduced in the ABA-deficient *aba2* and ABA-insensitive *abi1* mutants. As indicated by the example of PKABA-TaBF regulation above, the activation of AREBs/ABFs require phosphorylation, potentially by ABA or other stress-regulated kinases (e.g. SnRK2s).

Phosphorylation of ABI5 was reported to correlate with ABA or H₂O₂-mediated activation of AtMAPK3 (Lu et al., 2002). Phosphorylation is required for stabilization of ABI5, which is controlled by AFP1 (ABI5-binding protein). The *afp1* mutation increases the level of ABI5 and confers ABA-hypersensitivity in seed germination assay confirming the observation that ABI5 is required for maintenance of post-embryonic growth arrest by ABA. ABI5 and AFP show co-localization with the COP1 RING E3 ubiquitin ligase suggesting its involvement in ubiquitination-dependent proteasomal degradation of ABI5 (Lopez-Molina et al., 2003). Constitutive activation of ABI5 causes growth retardation indicating that ABI5 activation may be growth-limiting in vegetative tissues (Benshimen et al., 2004). Physical interaction of ABI5 with ABI1 suggest that ABI1 may contribute to destabilization of ABI5 (Gampala et al., 2002).

DNA-binding, foot-printing and transcript profiling studies show that ABI5 binds to ABRE-elements in the promoters of clustered *Arabidopsis* seed specific genes, including the *Em* class I LEA proteins. The fact that the *abi3* mutation reduces the expression of a larger set of seed specific genes than the *abi5* mutation suggests that in addition to ABI5 other members of the ABI5 bZIP family may contribute to the regulation of ABA-responsive seed specific promoters. The *Arabidopsis*

ABI5/ABF/AREB family contains 13 members: ABF1/AtbZIP35, ABF2/AREB1/AtbZIP36, ABF3/DPBF5/AtbZIP37, ABF4/AREB2/AtbZIP38, ABI5/DPBF1/AtbZIP39, AREB3/DPBF3/AtbZIP66, GBF4/AtbZIP40, AtbZIP12/EEL1/DPBF4, AtbZIP13, AtbZIP14, AtbZIP15, AtbZIP27 and AtbZIP67/DPBF2..

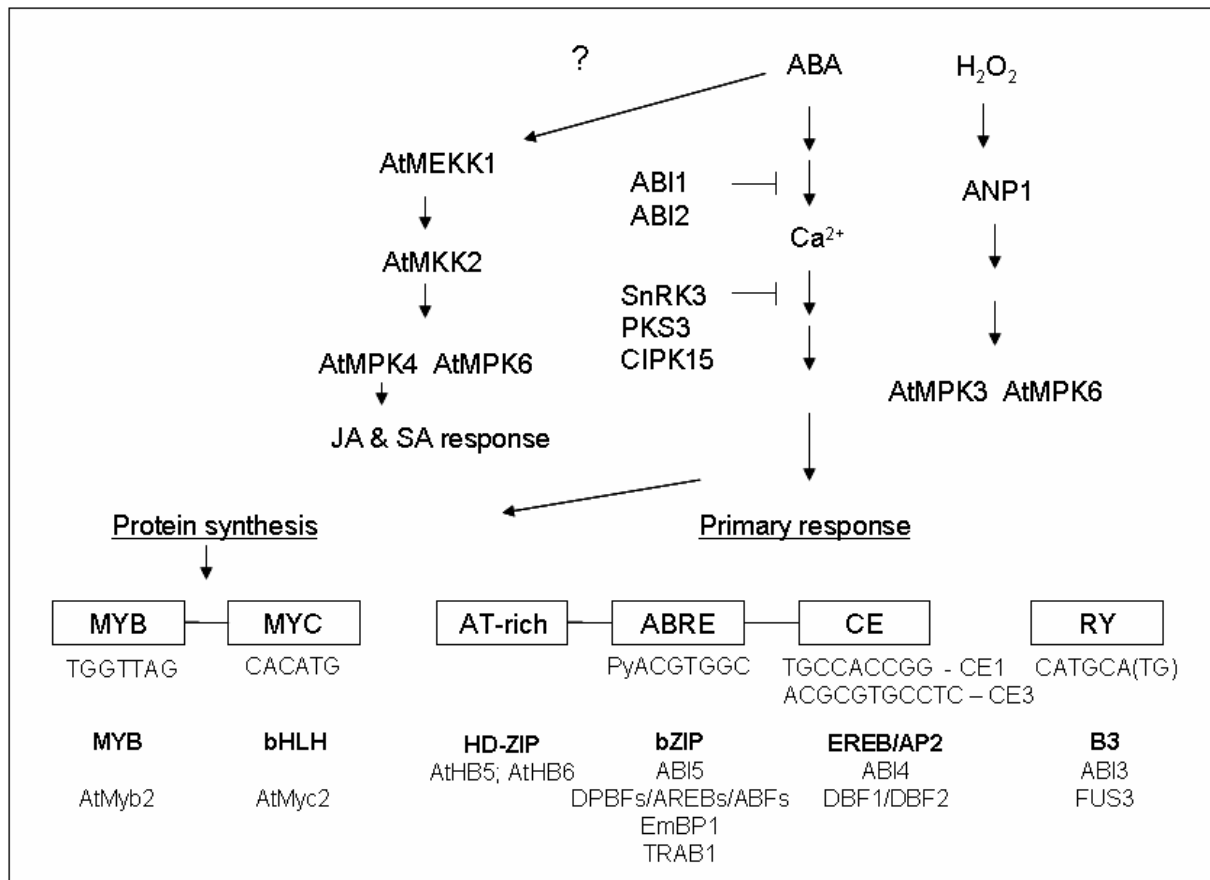


Figure 4. Promoter *cis*-elements, transcription factors and potential MAKP cascades involved in the regulation of ABA-responsive transcription.

Whereas involvement of various transcription factors, SnRK2 and SnRK3 protein kinases, and ABI1/2 protein phosphatases in ABA signaling is supported by genetic data, the connection of MAPK cascades with ABA regulation is solely suggested by kinase overexpression experiments in protoplasts. Individual elements mediating primary and late transcription responses to ABA are described in the text.

Members of the ABI5 family show differential activation in response to ABA and osmotic stress, but recognize similar *cis*-elements (Choi et al., 2000; Uno et al., 2000, Bensmihen et al., 2002, Jacoby et al., 2002). The ABI5 family has a broader consensus-binding site than other bZIP proteins as its members tolerate variability in the ACGT core of ABRE/G-box elements (Kim et al., 1997). From the ABI5 family 7 members are expressed in seeds, two of which show similar expression kinetics as ABI5. Three other genes, including *AtbZIP12/EEL1/DPBF4* show earlier expression than ABI5, which displays overlapping expression with the *Em1* storage protein gene. Three of these early seed specific bZIP genes represent orthologs of the carrot DPBF factors, which were previously found to bind ABRE-like motifs in the promoter of carrot LEA gene DC3 (Kim et al., 1997; Kim and Thomas, 1998). Analysis of heterodimerization of ABI5/DPBF1 with the *Arabidopsis* DPBF orthologs shows that except for DPBF2 (which binds only ABI5) ABI5 can equally dimerize with AREB3/DPBF3 and AtbZIP12/DPBF4 (Kim et al., 2002).

In *Arabidopsis* seeds, the *abi5* mutation reduces the expression of the late-embryogenesis-abundant *Em1* marker gene, whereas insertion inactivation of the *AtbZIP12/DPBF4* gene results in 3-4-fold enhancement of the *Em1* expression. The *atbzip12* mutation was therefore named *eel1* (enhancer of *Em1* levels; Bensmihen et al. 2002). The *eel1*, *abi5* double mutant shows similarly low *Em1* expression as the *abi5* single mutant suggesting that ABI5 is epistatic to *AtbZIP12/DPBF4/EEL1*. Therefore, it was hypothesized that *AtbZIP12/DPBF4* is a negative regulator of ABI5. Further work revealed that *AtbZIP12/DPBF4/EEL1*, *AtbZIP67/DPBF2* and *AtbZIP66/AREB3/DPBF3* show similar expression pattern during seed development, but a knock-down approach using RNAi-inhibition of all three genes failed to reveal any defect during seed maturation and further development (Bensmihen et al., 2003). In rice protoplasts, ABI3/VP1 and most ABI5-like ABFs are sufficient to induce the activation of the *Em* promoter. Whereas Ca^{2+} synergistic drugs and ABA enhance the *Em* promoter activation, PLD-inhibitors, such as 1-butanol, efficiently but incompletely inhibit ABA induction of *Em* transcription (Finkelstein et al., 2002).

Other members of the ABI5/ABF/AREB family are expressed in vegetative tissues and differentially activated by ABA and osmotic stress (Uno et al., 2000). Overexpression of ABF3/DPBF5 and ABF4/AREB2 confer ABA hypersensitivity, reduced respiration and enhanced drought tolerance (Kang et al., 2002). Remarkably, overexpression of ABF2/AREB1, which is proposed to be an essential element of glucose signaling, does not only confer tolerance to drought, but also to heat and oxidative stress (Kim et al., 2004b).

1.4.5.4. HD-ZIP transcription factors

A distinct class of ABA response regulators in seedlings is represented by the HD-ZIP family of homeodomain transcription factors. Members of the HD-ZIP family are involved in the control of root development, leaf vein-patterning, microRNA processing, auxin and cytokinin signaling, shade avoidance response, vascular differentiation and many other essential processes. AtHB6 binds to AT-rich sequences in ABA-regulated promoters and interacts directly with ABI1 (Himmelbach et al., 2002). AtHD6 shows heterodimerization with AtHB5, and its accumulation in the nucleus results in desensitization of ABA-induced stomatal closure and inhibition of seed germination (as observed for overexpression of SnRK3s and CBLs, see above). Although AtHB5 is a positive regulator of a subset of ABA-responsive genes and its expression is controlled by components of ABA-signaling, the *athb5* knockout mutants do not display any ABA- or stress-related phenotype suggesting potential functional redundancy (Johannesson et al., 2003). Promoter *cis*-regulatory elements, transcription factors and potential MAPK signaling pathways mediating ABA-regulation of transcription are depicted schematically in Figure 4.

1.5. SUGAR SIGNALING: CROSSTALK WITH ABA AND ETHYLENE

1.5.1. Sugar, ABA and ethylene modulation of seed development, germination and root growth

Loss of turgor caused by water shortage and osmotic stress is accompanied by disturbance of proper solute transport between sink and source organs and may thus cause temporal accumulation of free sugars in the transporting tissues. Lowering the power of sink (e.g., roots) by osmotic stress (i.e. inhibiting sugar uptake and growth of sink organs) ultimately increases the concentrations of free sugars at the interphase of source organs and transporting tissues. This inhibits sugar (i.e. sucrose) export from source tissues and thus leads to ultimate increase of cellular concentrations of free sugars, which ultimately lowers the rate of photosynthesis, stimulates stomatal closure and glucose repression (down-regulation of light-regulated gene expression, stimulation of starch production etc.; Paul and Foyer, 2001; Roitsch et al., 2003; Tallman, 2004). Sugars (sucrose and glucose), as osmotic stress, stimulate the transcription of several genes in ABA biosynthesis and signaling (e.g., *ZEP/ABA1*, *SDR/ABA2*, *AO/ABA3*, *ABI4*, *ABI5* etc., Cheng et al., 2002; Nambara and Marion-Poll, 2005). Whereas drought and ABA down-regulate the expression of genes involved in photosynthesis (see e.g., Oztur et al., 2002), ABA stimulates glucose uptake, sucrose and starch synthesis in sink organs (e.g., seeds; Kashem et al., 1998). ABA acts as an inhibitor of shoot and root growth of seedlings, but it counteracts ethylene-induced senescence. Though ABA does not seem to regulate the expression of *ACC* genes in *Arabidopsis* seedlings, shoots of the *aba2-1* mutant show more severe growth defects than those of the *aba-2, etr1* (ethylene resistant 1) double mutant (LeNoble et al., 2004). Ethylene and ABA, as well as high concentration of sucrose and glucose, inhibit root elongation. ABA-mediated block of root elongation is relieved by ethylene inhibitors, and ABA does not enhance the root elongation defect in the ethylene overproducing *eto1* mutant, which is ABA-insensitive. These data suggest that ethylene modulates ABA sensitivity and that ABA signaling requires functional ethylene signaling (Ghassemian et al., 2000).

In addition to stress conditions, transient increases in sugar concentrations appear to control two distinct phases of plant development: embryo maturation following arrestment of cell divisions (phases of “seed-filling”, including incorporation of sugars to storage polysaccharides) and germination (characterized by mobilization of sugars for initial heterotrophic growth, for review see Finkelstein et al., 2002). ABA stimulates sugar storage and embryo dormancy, and within a short phase of seed imbibition it can induce a reversal of sugar mobilization by effectively inhibiting the germination process. Low concentrations (30 to 90 mM) of sugars overcome the inhibition of radicle emergence by ABA, but further development and greening of seedlings remains inhibited. This stage of ABA inhibition (showing analogy to late-embryogenesis phase and characterized by accumulation of *ABI5*) can be overcome by ethylene (or gibberellin or brassinosteroid, see for review Finkelstein et al., 2002) treatment. High concentration (>300mM) of sugar causes similar germination block that can be relieved by ethylene. Recently, glucose treatment (170mM) was reported to inhibit the expression of several *ACC* (1-aminocyclopropane-1-carboxylic acid) synthase and oxidase genes that control the

synthesis of ethylene from S-adenosyl-L-methionine (Prince et al., 2004). This would suggest that down-regulation of ethylene levels (or signaling) by glucose could increase ABA sensitivity and stimulate ABA synthesis, whereas addition of ethylene would decrease sugar and ABA sensitivity through the involvement of elements of the ethylene signaling pathway (e.g., *ein2*). The antagonizing effect of ethylene (and GA) is completely light-dependent, indicating a need for functional phytochrome signaling (Finleklestein and Lynch, 2000). It is thus not surprising that during subsequent phases of germination ethylene, as well as ABA and high concentration of sugars (sucrose and glucose), cause similar inhibition of elongation growth in roots.

1.5.2. ABA responses of *Arabidopsis* mutants affected in ethylene biosynthesis and signaling

Arabidopsis encodes 4 functional ACC synthase (*ACS*) and 2 ACC oxidase (*ACO*) genes. The biosynthesis pathway is upregulated by the dominant *eto1* and *eto2*, and recessive *eto3* mutations (for review see Alonso and Ecker, 2001). *ETO2* and *ETO3* encode ACS5 and ACS9, respectively, whereas *ETO1* is a subunit of a CUL3 complex controlling ubiquitination mediated proteolysis of ACS5 (Wang et al., 2004). Ethylene binds to and inactivates the ER-associated ETR receptors that are affected by the *etr1*, *ers1*, *etr2*, *ers2* and *ein4* mutations. Inhibition of the ethylene receptors result in down-regulation of a Raf-like kinase CTR1, which is impaired in the *ctr1* mutant showing constitutive triple response and activation of ethylene signaling. Inactivation of the CTR1 kinase allows the activation of an N-RAMP-like putative ER-associated metal transporter, which when inactivated in the *ein2* mutant confers ethylene insensitivity. Activation of EIN2 leads to stimulation of expression and stabilization of the EREB transcription factor EIN3, which is a major regulator of ethylene response factor ERF involved in transcriptional activation of genes coding for ethylene-response element binding factors. The stability of EIN3 is controlled by the EBF1 and EBF2 F-box protein subunits of SCF E3 ubiquitin ligases (for review see Guo and Ecker, 2004; Figure 5).

Characterization of ABA responses of ethylene biosynthesis and signaling mutants indicates that the ethylene overproducing *eto* mutants do not show enhanced inhibition of root elongation by ABA, whereas the *ctr1* mutant is resistant to ABA inhibition of seed germination and root elongation. By contrast, the *etr1*, *ein2* and *ein3* mutants show hypersensitivity to ABA in seed germination, but are resistant to ABA in root elongation assays. In fact, *ein2* has been found to be allelic with the *era3* mutation causing enhanced response to ABA in seed germination assays (Ghassemian et al., 2000). Genetic screening for suppressors of ABA-insensitivity of *abil-1* mutant in seed germination assays led to the identification of *ctr1* as enhancer and *ein2* as suppressor of *abil* conferred ABA resistant seed germination (Beaudoin et al., 2000).

1.5.3. Sugar responses of ethylene and ABA biosynthesis and signaling mutants

By screening for mutations enhancing or alleviating sugar-induced inhibition of seed germination, root elongation and gene expression, numerous glucose and sugar insensitive (*gin*, *sis*), glucose

over/hypersensitive (*glo*), sucrose-uncoupled (*sun*), impaired sugar induction (*isi*), reduced sensitivity to sucrose induction (*rsr* and *lba*), and increased sensitivity to sucrose induction (*hba*) mutations were identified (for reviews see: Finkelstein and Gibson, 2001; Rolland et al., 2002a; Léon and Sheen, 2003; Gibson, 2000; 2004, 2005). Genetic analysis and characterization of these mutants revealed that all known *aba* mutations abolishing ABA biosynthesis result in glucose and/or sucrose insensitive phenotype in seed germination and/or root elongation assays. Thus, *aba1* is glucose/sucrose insensitive, *aba2* is allelic with *gin1/sis4*, and *aba3* is an allele of *gin5* (Figure 5). These data suggests that inhibition of seed germination and root elongation by glucose and/or sucrose may be executed through ABA signaling. From the mutations that cause ABA-insensitivity, *abi3*, *abi4/gin6* and *abi5* (but not *abi1* and *abi2*) confer also insensitivity to glucose and/or sucrose, whereas overexpression of these transcription factors result in hypersensitivity to glucose. These genes show ABA-dependent activation by glucose (for review see Léon and Sheen, 2003). From the ethylene signaling pathway all known mutations, which result in ABA-insensitivity, including *eto1* and *ctr1/gin4*, also confer glucose insensitive phenotype. On the other hand, mutations that result in ethylene resistance/insensitivity and hypersensitivity to ABA inhibition of seed germination, including *etr1*, *ein2*, *ein3*, and *ein6* result in glucose hypersensitive (*glo*) phenotype.

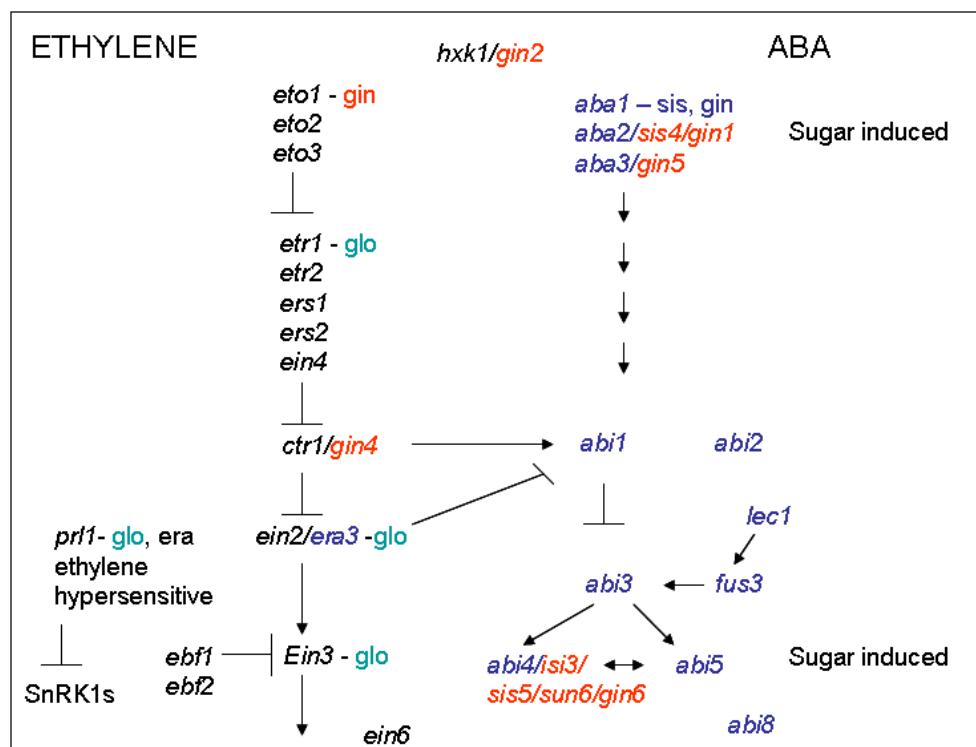


Figure 5. Cross-talk between ABA, ethylene, glucose and AMP signaling.

Components and interactions of ethylene and ABA signaling pathways are described in the text. The position of *hvk1/gin2* in the pathway is justified by the fact that *gin1/aba2* was found to be epistatic to *gin2/hvk1* (Zhu et al., 1998). Light-dependent epistatic interaction between *ein2/era3* and *prl1*, a mutation in a WD-protein inhibitor of SnRK1s has been described by Németh et al. (1998).

A clue to understand interaction between ethylene and ABA-signaling derived from the analysis of *aba2/gin1*, *etr1* and *aba2/gin1*, *ein2* double mutants, both of which display glucose insensitive *aba2* phenotype in germination assay. The *ein2/era3* mutation dramatically stimulates ABA synthesis (Ghassemian et al., 2000). Thus, at the level of signal generation glucose stimulus leads to

downregulation of ethylene and stimulation of ABA synthesis, whereas ethylene inhibits ABA synthesis. CTR1, an inhibitor of ethylene signaling, enhances ABA signaling (as *ctr1* is an enhancer of *abi1*), whereas EIN2, a positive regulator of ethylene signaling, inhibits ABA signaling/synthesis (as *ein2* is a suppressor of *abi1*). This is consistent with the observation that the *abi3*, *abi4* and *abi5* mutations are epistatic to *ein2* (for more details see Prince et al., 2003).

1.5.4. Glucose sensing: control by trehalose

As the major transported form of sugar is sucrose in most plants, cell wall invertases, and monosaccharide and disaccharide transporters are involved in developmental and metabolic control. The *Arabidopsis* genome codes for 6 cell wall invertases, 12 monosaccharide/H⁺ symporters and 9 sucrose/H⁺ co-transporters, from which SUT1/SUC2 is essential for long-distance transport (for review see Williams et al., 2000; Sherson et al., 2003; Lalonde et al., 2004). Although some of these transporters are expected to play a chief role in sensing of sucrose and glucose/fructose generated by cell wall invertases (i.e., as their yeast orthologs RGT2 and SNF3; for review Ozcan and Johnston, 1999; Rolland et al., 2000b; Holsbeeks et al., 2004), thus far no sugar transporter mutation was found to specifically abolish sugar sensing or signaling. On the other hand, a central role for an alternative system based on nutrient sensing by G-protein coupled receptors (GCPRs) is emerging from the characterization of RGS1 and GCR1 receptors (see for review: McCudden et al., 2005; Jones and Assmann, 2004). Whereas GCR1 is involved in ABA and GA signaling (see 1.4.2 and Pandey and Assmann, 2004; Chen et al., 2004), the *rgs1* mutation results in insensitivity to glucose, fructose and sucrose (Chen and Jones, 2004). RGS1 functions independently of hexokinase 1-mediated glucose phosphorylation (see below) and is probably involved in a branch of sugar and stress signaling pathway, which appears to converge on the regulation of trehalose synthesis. In yeast, trehalose-6-phosphate (T6P) controls glycolysis by stimulating the accumulation of storage polysaccharides through inhibition of hexokinase II (HXK2, for review see Eastmond et al., 2003; Gelade et al., 2003;). In *Arabidopsis*, T6P is not a hexokinase enzyme inhibitor, yet low levels of T6P cause sugar hypersensitivity. Though 11 genes code for trehalose-6-phosphate synthases (TPS) in *Arabidopsis*, mutation of *TPS1* results in lethality due to defective embryo maturation (i.e. caused by sugar and ABA hypersensitivity, Leyman et al., 2001; Eastmond et al., 2002; Schlupepmann et al., 2003, vaDijken et al., 2004).

1.5.5. Glucose sensing by hexokinase

Characterization of the *Arabidopsis gin2* glucose insensitive mutant revealed a central function of hexokinase HXK1 glucose sensing and signaling. The phenotype of *gin2* is similar to that of constitutive ethylene response mutant *ctr1*, and can be phenocopied by treatment of wild type plants with ethylene and ACC. The *aba2/gin1* mutation is epistatic to *gin2/hxk1* indicating that HXK1 signals through ABA (Jang et al., 1997). HXK1 overexpression confers glyucose hypersensitivity and results in remarkable induction of trehalose 6-phosphate synthase *TPS1* gene indicating that T6P

accumulation is *HXK1*-dependent. On the contrary, *TPS1* overexpression results in down-regulation of *HXK1* transcription suggesting a negative feed-back regulatory loop (Avonce et al., 2004). Non-metabolisable sugar analogs (i.e. 2-deoxyglucose, mannose etc.), which are recognized as substrates and phosphorylated by HXKs, efficiently inhibit seed germination and root elongation. The fact that these inhibitory effects are alleviated by the HXK-specific competitive inhibitor mannoheptulose show that HXK-mediated sugar phosphorylation is involved in growth repression stimulated by exogenous sugars (for review see: Pego et al., 1999; Rolland et al., 2002). In yeast, *HXK2* is required for glucose repression of genes involved in respiration and catabolism of carbon sources other than glucose. This HXK-controlled glucose repression pathway is counteracted by the Snf1 kinase, which stimulates de-repression of these pathways in response to glucose limitation (for review see Hardie et al., 1998; Koch et al., 2000; Rolland et al., 2002b). Glucose repression through hexokinase mediates transcriptional repression of key genes involved in photosynthesis, whereas the *gin2/hxk1* mutation results in de-repressed expression of these genes, including *CAB* (chlorophyll ab-binding protein genes), and *RBCS* (ribulose 1,5-bisphosphate carboxylase small subunit).

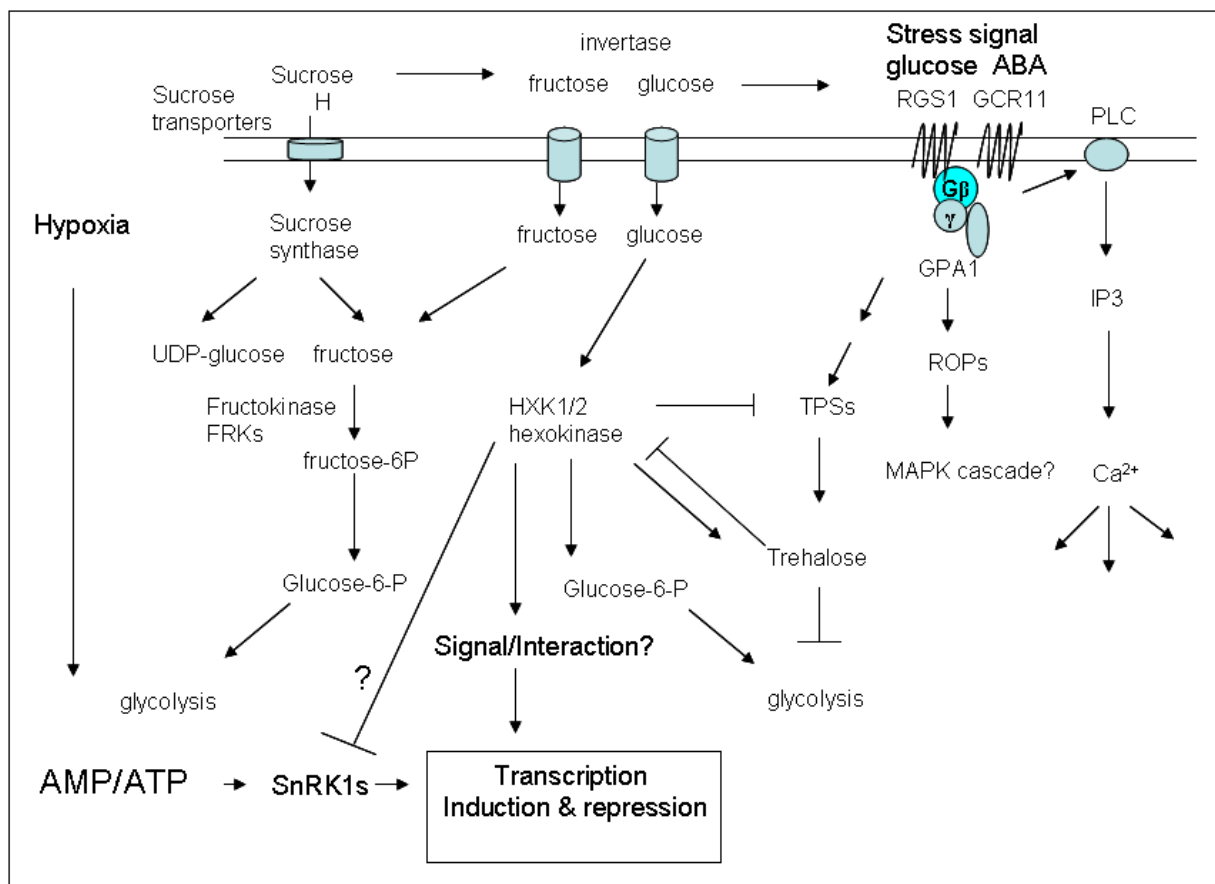


Figure 6. Sugar sensing and signaling by hexokinase and AMP-activated SnRK1 kinases involves crosstalk with trehalose and G-protein coupled receptor signaling.

Sucrose is hydrolysed by sucrose synthase, which is induced by hypoxia in sink tissues. Under respiratory conditions in growing tissues, sucrose is hydrolysed by cell wall invertases (many of which are repressed at the level of transcription by hypoxia). Cellular ratios of AMP/ATP are rapidly increased in response to hypoxia,, oxidative stress, osmotic stress etc., but also to ATP-driven transport of sucrose by sucrose/ H^+ co-transporters. Other connections between regulation of different potential components of glucose sensing and downstream signaling pathways are described in the text.

The *Arabidopsis* genome codes for 6 HXK and HXK-like genes, from which only *HXK1/GIN2* is involved in the regulation of glucose repression (Moore et al., 2003). Glucose phosphorylating activity of HXK1 is not essential for its signaling function, as HXK1 mutants showing no enzyme activity can complement the *gin2* mutation. Whereas at low light *gin2* shows growth comparable to wild type, at high light increasing the concentration of cellular glucose *gin2* displays retarded growth. Catalytically inactive HXK1 proteins can complement this growth defect to wild type by restoring repression of CAB and RBCS genes in the *gin2* mutant. This indicates that glucose phosphorylation activity is not required for negative signaling activity of HXK1. On the other hand, retarded growth of the *gin2* mutant under high light conditions suggests that an alternative glucose sensor, responding to light-stimulated photosynthetic increase of free cellular glucose levels is still functional in the *gin2* mutant. Levels of glucose 6-P and fructose 6-P do not show significant difference between wild type and *gin2* mutants. Thus, a potential involvement of glycolytic end products such as pyruvate or acetate, which have been shown to confer HXK-independent carbon catabolic/glucose repression (for review see Sheen et al., 1999; Rolland et al., 2002) may limit light intensity-dependent growth in the *gin2* mutant.

With the exception of known elements of ethylene, ABA and osmotic stress signaling (i.e., including several transcription factors), downstream component of HXK1 signaling are thus far unknown. In yeast, HXK1 is known to participate in the repression of sugar regulated promoters as a component of nuclear transcription repressor complexes (for review see Moreno and Herrero, 2002; Kin and Dang, 2005), whereas in moss a *hxx1* knockout conferring light-dependent *gin2*-like glucose insensitive phenotype identified a HXK1 enzyme, which is located in the chloroplast stroma (Olsson et al., 2003). Preliminary results indicate that HXK1 is also found in chloroplast and nuclear fractions of *Arabidopsis* cells (Rolland and Sheen, 2005).

1.5.6. Sensing of glucose and AMP/ATP levels by SnRK1 kinases

In yeast, HXK1 mediates the activation of the Reg1-Glc7 PP1 protein phosphatase, a major negative regulator of the Snf1 (sucrose non-fermenting) protein kinase, which is a prototype of eukaryotic AMP-activated kinases (Sanz et al., 2000; Hardie et al., 1998). In yeast and animals, AMPKs are required for shift from hypoxic to respiratory conditions, stimulation of ATP generation and preventing carbon flow to energy requiring biochemical pathways under stress, or temporal glucose limitation (i.e. during ATP/glucose depletion in contracting muscles, or in yeast growing on low glucose). As all eukaryotic AMPKs, the *Arabidopsis* Snf1-related SnRK1 enzymes are also trimeric kinases composed of a catalytic α (yeast Snf1p), a substrate targeting β (yeast Sip1p, Sip2p, Gal83p) and an activating γ (yeast Snf4p) subunit. The *Arabidopsis* genome encodes three α (AKIN10, AKIN11, AKIN12), two or three β (AKIN β 1, 2 and 3) and one γ (SNF4/AKIN β γ) SnRK1 subunits. AKIN10 and AKIN11, as well as SNF4, genetically complement the yeast $\Delta snf1$ and $\Delta snf4$ mutations that prevent growth on any other carbon source than glucose (i.e. because the trimeric Snf1 kinase is required for activation of genes involved in the catabolism of alternative carbon sources). This shows that AKIN10, AKIN11 and SNF4 correspond to functional orthologs of yeast Snf1 and Snf4 kinase

subunits, respectively (Bhalerao et al., 1999; Kleinow et al., 2000). As subunits of the yeast Snf1 kinase, the *Arabidopsis* SnRK1 α , β and γ subunits show glucose-dependent interaction in yeast. In yeast, the assembly and activation of Snf1 kinase is controlled by the cellular level of glucose. At high glucose levels, autoinhibitory sequences of the C-terminal Snf1 regulatory domain interact with the kinase domain and block interaction of Snf1 with Snf4. When glucose levels are low, the Snf1 α -subunit undergoes conformation change and binds Snf4 that prevents interaction of the kinase and auto-inhibitory domains of Snf1 (Jiang and Carlson, 1996). The fact that overexpression of Snf1 or its *Arabidopsis* orthologs AKIN10 and AKIN11 can suppress the $\Delta snf4$ mutation in yeast shows that though Snf4 is important for stabilization of active Snf1, it is not absolutely essential for kinase activation *in vivo* (Jiang and Carlson, 1997; Kleinow et al., 2000).

The C-terminal regulatory domain of *Arabidopsis* kinases carry some sequences which are homologous to binding sites of β and γ subunits identified within the C-terminal domains of yeast Snf1 and animal AMPK α -subunits. Within the β -subunits the kinase γ subunits recognize a γ -association sequence (ASC), whereas the kinase α -subunits bind in the vicinity of a kinase-interacting sequence (KIS-domain), which has been recently found to bind glucose moieties of glycogen (Jiang and Carlson, 1997b; Polekhina et al., 2003). Intriguingly, two classes of SNF4 cDNAs were isolated from *Arabidopsis* and maize, one corresponding to the sequence of yeast Snf4, and another longer cDNA encoding the same SNF4 protein with an N-terminal KIS domain. This long form of SNF4 was designated AKIN $\beta\gamma$. As KIS domains occur only in the β -subunits of eukaryotic AMPKs, this finding raised the possibility that in *Arabidopsis* dimeric SnRK1 α /AKIN $\beta\gamma$ complexes may exist and perform specific regulatory functions in addition to the regular trimeric SnRK1 enzymes (Lumbreras et al., 2001).

In addition to sensing and binding to glucose, members of the AMPK family bind AMP directly by their typical β -cystathionine synthase repeats and thus stimulate the phosphorylation of T-loops of kinase α -subunits (i.e., which is required for the catalytic activity) by activating protein kinases (AMPKKs). Sequences of catalytic domains (including T-loops) of *Arabidopsis* SnRK1 kinase α -subunits are remarkably similar to those carried by members of the SnRK2 family, which suggests that SnRK1 and 2 kinases may recognize similar substrates. However, a unique feature of SnRK1 α -subunits is that they carry ubiquitin-association domains (UBA) between their catalytic and regulatory domains, which suggest their possible involvement in proteolysis (Farrás et al., 2001). As yeast Snf1 and animal AMPK enzymes, plant SnRK1s do not show AMP-mediated activation *in vitro* in the absence of activating kinases (Sugden et al., 1999a). However, when purified to homogeneity the α -subunits of *Arabidopsis* SnRK1 enzymes are capable of autophosphorylation and phosphorylate the peptide and protein substrates *in vitro*. Thus, activation by upstream AMPKs is probably not necessary, but may stimulate in a signal specific fashion the activity of plant SnRK1 enzymes, which is a unique feature of plant enzymes among all eukaryotic AMPKs (Bhalerao et al., 1999).

Biochemical studies indicate that similarly to SNF1 and animal AMPKs, plant SnRK1 kinases control the activity and stability of key metabolic enzymes *in vivo*. SnRK1 kinases are thus known to

phosphorylate and inactivate 3-hydroxymethyl-3-glutaryl coenzyme A reductase (HMGR, controlling the first committed step cytoplasmic isopentenyl pathway), nitrate reductase (i.e., NO signal generator), sucrose phosphate synthase (required for sucrose synthesis to prevent glucose accumulation in photosynthetic cells), sucrose synthase (see Figure 6 and above), and fructose 2,6-bisphosphatases (Sugden et al., 1999b; Kulma et al., 2004). Glucose starvation-induced phosphorylation and subsequent degradation of these key enzymes and signaling proteins are assisted by regulatory 14-3-3 proteins and blocked by the proteasome inhibitor MG132 (Cotelle et al., 2000). The α -subunits of *Arabidopsis* SnRK1 enzymes have been identified in proteasomal complexes of SCF E3 ubiquitin ligases, in which they interact with the PAD1/ α 4 subunit of 20S proteasome cylinder and the common ASK1/SKP1 subunits of SCF complexes involved in various hormonal and light regulatory signaling pathways (Farrás et al. 2001). Nuclear localization of proteasome and SCF components suggest that some of the *Arabidopsis* SnRK1 α subunits have important nuclear functions, such as modulation of ubiquitination and degradation of transcription factors. In the ethylene signaling pathway, for example, the stability of EIN3 transcription factor is controlled by two F-box proteins, EBF1 and EBF2, the inactivation of both of which results in ethylene hypersensitivity (i.e. similarly to EIN3 overexpression, which leads to ethylene hypersensitivity, but glucose insensitivity; see Potuschak et al., 2003). Glucose stimulates ubiquitination proteasomal degradation of EIN through HXK1 signaling (Yanagisawa et al., 2003), which raises the question about possible involvement of proteasome-associated SnRK1s in this process.

Involvement of SnRK1 kinases as master regulators in plant glucose, stress and hormone signaling is indicated by the characterization of the *prl1* (*PLEITROPIC REGULATORY LOCUS 1*) mutant (Németh et al., 1998). PRL1 is a nuclear regulatory WD-protein, which interacts with and inhibits the kinase activities of *Arabidopsis* SnRK1 α -subunits. Within the C-terminal regulatory domains of AKIN10 and AKIN11 α -subunits, the PRL1-binding site overlaps with that of the γ -activating subunit SNF4/AKIN $\beta\gamma$, as well as with the binding site of SnRK1-interacting SCF subunit ASK1/SKP1 (Bhareao et al., 1999; Farrás et al., 2001). Thus, PRL1 probably represents a negative regulator of nuclear proteasome and SCF-associated SnRK1 complexes. Whereas the yeast activating γ -subunit Snf4 is principally localized to the nucleus and enhances Snf1 activity towards nuclear substrates, including the glucose-induced Mig1 transcription repressor (for review see: Vincent et al., 2001; McCartney and Schmidt, 2001), it remains to be determined what is the role of β and γ subunits in nuclear targeting and activation of *Arabidopsis* SnRK1 kinases. Inactivation of the gene encoding the SnRK1 inhibitor PRL1 protein leads to dramatic changes in signaling and plant development, which include hypersensitivity to glucose, sucrose, ethylene, ABA, auxin and cytokinin, altered leaf morphology, ectopic root hair formation, accumulation of free glucose, fructose and sucrose in photosynthetic source leaves, sensitivity to cold etc. (see Németh et al., 1998).

In contrast to yeast and dark-grown plant tissues, the total activity of *Arabidopsis* SnRK1s is increased by sugar treatment in green photosynthetic tissues, and shoots of the *prl1* mutant show higher kinase activities than wild type (Bhalerao et al., 1999). This suggest that in addition to HXK1,

the SnRK1 enzymes also control glucose sensing and signaling. In fact, inactivation of the PRL1 inhibitor of SnRK1s results in de-repressed transcription of numerous glucose repressed genes, but also enhances the transcription of some glucose and/or H₂O₂-induced genes (Németh et al., 1998).

Recently, another clue to better understanding the function of SnRK1 kinases derived from inactivation of the *PpSnf1a* and *PpSnf1b* SnRK1 α -subunit genes in *Physcomitrella* by homologous recombination (Thelander et al., 2004). The *Ppsnf1a* Δ *Ppsnf1b* Δ double mutant is devoid of SnRK1-specific SAMS peptide kinase activity, shows premature senescence (i.e. indication for chronic activation of ethylene signaling), hypersensitivity to several plant hormones, and reduced levels of starch; and survives only under continuous high light conditions. This data indicate that plant SnRK1 enzymes are essential for proper regulation of carbon metabolism during the shift from light to dark conditions. Further understanding of the regulatory role of SnRK1 kinases may come in the future from studying their regulation in the different *gin* and *glo* mutants affecting HXK1, ethylene and ABA signaling.

1.6. AIMS OF THE PRESENT WORK

During the first two years, this work was supported by a fellowship in frame of a collaboration project supported by the Minna James Heineman Foundation between the Weizmann Institute (Rehovot, Israel) and the Max-Planck Institute for Plant Breeding Research (Cologne). Major aim of the project was the identification of regulatory factors that control the biosynthesis of essential amino acids lysine, threonine and proline in higher plants. Preliminary studies demonstrated the importance of aspartate kinase (ASK) enzyme in the control of lysine and threonine biosynthesis, as well as showed that the Δ 1-pyrroline-5-carboxylate synthase (P5CS1) enzyme controls the rate-limiting step of proline biosynthesis. Research goals of the collaborative project stemmed from the recognition that the activity of genes that code for the ASK and P5CS enzymes is regulated by signaling pathways that control plant responses to glucose, ABA and osmotic stress stimuli. The research group of Prof. Gad Galili at the Weizmann Institute found that a bifunctional aspartokinase-homoserine dehydrogenase (ASK/HSD) enzyme controls the utilization of aspartate via aspartyl phosphate and aspartate semialdehyde in the lysine and threonine biosynthesis pathways (Tzchori et al., 1996; Tang et al., 1997). The same group has demonstrated that transcription of the *ASK1/HSD1* gene is specifically induced by sucrose and inhibited by phosphate in tobacco, as well as in the model plant *Arabidopsis thaliana*. Further analysis indicated that regulatory DNA sequences controlling the activation of the *ASK1* gene by sucrose are localized between positions -193 and -222 upstream of the translation start codon and carry a consensus sequence for potential binding of a transcription factor of bZIP/GCN4 family (Zhu-Shimoni and Galili, 1998). This work also showed that the ASK1 gene is positively regulated by sugars and not by nitrogen compounds (i.e., which would counteract glucose repression, for review of interactions between carbon and nitrogen regulation see Coruzzi and Zhu, 2001). These observations have been confirmed by our preliminary studies, which indicated that the expression of *ASK1* and *P5CS1* genes, as several other ABA and glucose responsive genes in de-repressed in the

prll mutant, which is deficient in a nuclear inhibitor of SnRK1 kinases (Németh et al., 1998; Bhalerao et al., 1999). Furthermore, a mutation in the G-boxII/bZIP binding-site within the ADH promoter (Dolferus et al. 1994; Lu et al., 1996) was demonstrated to alleviate the differences observed in ADH gene expression between *prll* and wild-type plants by defining a common promoter upstream element required for negative regulation of transcription by PRL1 (Németh et al., 1998). This suggested that PRL1 transcriptional regulation converges on ABRE/G-box *cis*-elements containing ABA and stress induced promoters. In addition, identification of 14-3-3 protein interactions with G-box binding transcription factors and SnRK1 substrates by other laboratories (Lu et al., 1992; Igarashi et al., 2001; Eckhardt, 2001; Comparot et al., 2003) suggested that members of the SnRK family (either SnRK1 or SnRK2 kinases) may be involved in regulation of ABRE/G-box controlled ASK1 promoter. To reach the research goals of the Minna James Heineman project, I initiated the following experiments:

- A yeast one-hybrid assay with an *Arabidopsis* cell suspension cDNA expression library was used to screen for transcription factors binding to the G-box containing *cis*-regulatory domain of *ASK1* promoter, which lead to the identification of DPBF4/AtbZIP12/EEL1.
- To provide a basis for further genetic studies of DPBF4, PCR screens were performed to identify T-DNA insertion mutations in the *DPBF4* gene.
- For biochemical characterization, immunolocalization and identification of interacting partners of DPBF4, transgenic plants overexpressing an epitope tagged form of DPBF4 constitutively or in an oestradiol-inducible fashion were generated.
- To study temporal and spatial regulation of *DPBF4* gene expression, *DPBF4* promoter- GUS fusion constructs were analysed in transgenic plants and the expression of *DPBF4* was monitored by RT PCR analysis.
- To study the effects of DPBF4 expression on the regulation of sugar, ABA and osmotic stress controlled promoters, a GUS-based reporter gene system was used in combination with GUS histochemical assays and RT PCR analysis of transcript levels.
- To identify the DNA-binding sites of DPBF4 in stress and ABA-induced promoters, chromatin immuno-precipitation experiments were performed.
- To study potential phosphorylation of DPBF4, *in vitro* phosphorylation assays were performed with purified OST1/SnRK2.6 and SnRK1 and one of the kinase α -subunit AKIN10.
- To map the autophosphorylation sites in these kinase and their phosphorylation motives in DPBF4, MALDI Q-TOF mass spectrometry analyses were performed in collaboration with Dr. Jürgen Schmidt and Dr. Thomas Colby (MPIZ, Cologne).
- To confirm the results of mass spectrometry analyses, sequence alterations were introduced in the T-loop and ATP-binding domains of OST1 by site-specific mutagenesis.
- To facilitate cataloguing the genes controlled by DPBF4, an oestradiol-inducible DPBF4 epitope-labeled DPBF4 construct was introduced into transgenic plants, which were screened for chemically inducible activation of DPBF4 at various developmental stages providing RNA samples for further transcription profiling experiments.

After termination of the Minna James Heinemann collaboration project, this work was supported by fellowship for foreign students by the Max-Planck Society. The work in the second part of the Ph.D. project focused in the functional analysis of SNF4 γ -activating subunits of SnRK1 kinases. Previous work showed that PRL1 and SNF4 recognize a similar domain in the C-terminal regulatory region of SnRK1 catalytic α -subunits AKIN10 and AKIN11 (and this predicted that SNF4 will bind to highly homologous sequences also in the seed-specifically expressed AKIN12 kinase subunit; Bhalerao et al., 1999). Kleinow et al. (2000) and Lumbreras et al. (2001) have identified two different cDNAs, one of which encoded a longer form of SNF4 that carried an N-terminal KIS domain. This longer form of SNF4 has been designated AKIN $\beta\gamma$. As KIS domain is only present in the β -subunits of eukaryotic SnRK1 enzymes, this observation suggested that plants may employ specific SnRK1 enzymes, which may only carry SnRK1 α and AKIN $\beta\gamma$ subunits. On the other hand, the detection of short and long forms of cDNAs suggested that differential splicing could control the expression of SNF4 and AKIN $\beta\gamma$ isoforms. Previous work showed that inactivation of the PRL1 inhibitor of SnRK1 enzymes results in hypersensitivity to glucose, sucrose and ABA. This raised the question whether inactivation of the *SNF4* gene of kinase activating γ -subunit would lead to glucose, sucrose and ABA hypersensitivity or to lethality, indicating essential functions of SnRK1 enzymes in plants. To clarify these questions, I initiated the following experiments:

- To characterize the function of the SnRK1 γ -activating subunit by genetic means, PCR screens were performed to identify T-DNA insertion mutations in the *SNF4* gene.
- To examine whether indeed alternative splicing is involved in the generation of SNF4 and AKIN $\beta\gamma$ isoforms of the SnRK1 γ -activating subunit, RT PCR-based transcript mapping was performed.
- For further biochemical characterization of SNF4-containing SnRK1 protein kinase complexes, epitope tagged forms of SNF4 and AKIN $\beta\gamma$ were generated, expressed in transgenic plants and cell cultures and used for immunopurification of SNF4 complexes and detection of SNF4-binding SnRK1 α and β subunits.
- Finally, to determine cellular localization of SNF4, transgenic plants and cells expressing SNF4-GFP fusions were produced, and regulation of SNF4 localization in dark and light was studied.

2. MATERIALS AND METHODS

2.1. MATERIALS

2.1.1. Enzymes and chemicals

Affinity Research Products Limited, UK: Amersham Pharmacia Biotech, Freiburg:	Antibodies γ^{32} -dATP (370 MBq/ml) ECL blotting detection reagents Gradient mixer Hybond N membrane Hyperfilm ECL Sephadex G-50
Baker chemicals, Deventer/Holland: Bio 101: Biomol GmbH, Ilveyheim; Germany:	Ethanol Gene Clean kit Cesium Chloride X-Gal(5-Bromo-4-Chloro-3-Indolyl-1- β -D-Galactopyranoside)
Bio-Rad, München, Germany:	Bradford Reagent Pre-stained SDS-PAGE Standards
Boehringer Mannheim, Germany:	Alkaline Phosphatase DNA-Polymerase I (Klenow-Fragment) Hygromycin B Restriction endonucleases RNase A T4 DNA ligase Taq DNA Polymerase
Calbiochem Corporation, Germany:	Ethidium bromide Miracloth
Clontech, Palo Alto; USA: Difco Laboratories, Detroit, USA:	Salmon sperm carrier-DNA Bacto-agar Bacto-peptone Bacto-tryptone Yeast Extract Yeast-Nitrogen-Base without amino acids
Duchefa, the Netherlands:	Carbenicillin MS basal medium with vitamins Phytoagar
Eppendorf, Germany:	Single use pipette tips Single use reaction tubes
Eastman Kodak Company, USA: Fluka, Switzerland:	Kodak X-Omat AR-5 Film ATP Formamide Leupeptine hemisulphate Pepstatin A
FMC, USA: Gibco BRL, Germany:	Seakem GTG Agarose 1kb molecular mass marker Pfx DNA polymerase Restriction edonucleases Superscript II RNase H Reverse Transcriptase Taq DNA Polymerase
Greiner, Frickenhausen, Germany: Millipore, USA:	Petri dishes Filter system apparatus Immobilon TM -P (PVDF membrane) sterile filter

New England Biolabs:	DNA polymerase I (Klenow fragment) Restriction Endonucleases
PE Biosystem:	Acetonitrile
Promega; USA:	pGEM-T vector kit
Qiagen, Germany:	Qiaprep Spin Miniprep kit Qiaquick, PCR product purification kit RNeasy Plant RNA extraction kit Ni-NTA matrices
Riedel de Haen, German:	Isopropanol
Roche	protease inhibitor cocktail (No. 11330800)
Roth, Germany:	40% Acrylamide/Bis-acrylamide 29:1 Phenol
Sartorius:	Minisart 0.22µm and 0.45µm
Serva, GmH & Co., Germany:	Ponceau S solution SDS
Sigma-Chem. Corporation, St. Louis, USA:	Ammoniumpersulfate Antibiotics (Ampicillin, Kanamycin, Rifampicin) Bromophenol Blue BSA Coomassie-Brilliant-blue R250 CTAB (Cetyl-trimethylammonium bromide) DEPC (Diethylpyrocarbonate) DTT (Dithiothreitol) IPTG (Isopropyl β-D-thiogalactoside) L-amino acids Lithium acetate MOPS (3-N-morpholinopropane sulphonic acid) MS-Basal salts mixture PEG (Polyethylene glycol) 4000, PEG 8000 Phenol for RNA and DNA PMSF (Phenylmethylsulphonyl fluoride) PVP-40 (Polyvinyl pyrrolidone-40) β-mercaptoethanol TEMED TritonX-100
Takara Schuzo, Japan:	LA Taq DNA Polymerase
Whatmann, Maidstone, USA:	3MM paper

2.1.2. Bacterial Strains

<u><i>E.coli</i></u>	<u>Genotype</u>
BL21 (DE3)	pLysS F ⁻ <i>ompT hsdS_B (r_B⁻ m_B⁻) gal dcm met</i> (DE3) pLysS (CmR)
BMH 71-18 mutS	<i>thi, supE, Δ (lac-proAB), [mutS::Tn10][F' proAB, lacI^q ZΔM15]</i>
DH5α	F ⁻ φ80 <i>lacZΔM15Δ (lacZYA-argF) U169 recA 1 endA1 hsdR17 (r_k⁻, m_k⁺) pho A sup E44 thi-1 gyrA96 relA 1 λ⁻</i>

Agrobacterium tumefaciens

GV3101::pMP90RK C58C1, *rif, pMP90 (pTiC58ΔT-DNA), Gm^r Km^r* (Koncz and Schell, 1986)

2.1.3. Yeast Strain

YM4271 MATa, *ura3-52, his3-200, ade2-101, lys2-801, leu2-3, 112, trp1-901, tyr1-501, gal4-Δ512, gal80-Δ538, ade5::hisG* (Liu *et al.*, 1993; Wilson *et al.*, 1991).

2.1.4. Plant Materials

Arabidopsis thaliana, ecotype Columbia, Wild type

Arabidopsis thaliana, *pr11* mutant (Németh et al., 1998)

Arabidopsis thaliana, cell suspension culture, ecotype Columbia

Arabidopsis thaliana, UFO-HA overexpressing cell suspension (from Gergely Molnár, MPIZ)

2.1.5. Plasmid constructs

pBluescript II SK	Stratagene, La Jolla/USA
pGEM-T	Promega, Mannheim
pGEM-T AtSNF4	Kleinow (2000)
pPCV812	Koncz et al., (1994)
pPILY	Ferrando et al. (2000a)
pLOLA	Ferrando et al. (2000b)
pLOLA-ABI5-cMYC	Shai Ufaz (unpublished)
pMESHI	Ferrando et al. (2000b)
pMENCHU	Ferrando et al. (2000a)
pPCV812-HA-GUS	Ferrando et al. (2000a)
pRSETc	Invitrogen
PET-TRX	Bhalerao et al. (1999)
XVE-pER8	Zhuo et al. (2000)
PET-AKIN10-TRX	Bhalerao et al. (1999)
PET-DPBF4-TRX	This work
PET-OST1-TRX	This work
pPILY-DPBF4	This work
pPILY-AtSNF4-HA	This work
pPILY-OST1	This work
pLOLA-DPBF4	This work
pLOLA-OST1	This work
pPCV812-Menchu-DPBF4	This work
pPCV812-Gigi-DPBF4	This work
pPCV812-DPBF4-GUS	This work
pPCV812-AtSNF4-HA	This work
pCAT-GFP-AtSNF4	This work
pCAT-GFP-DPBF4-HA	This work
PER8-DPBF4-cMYC	This work

2.1.6. Oligonucleotides

2.1.6.1. Oligonucleotides for PCR amplification of cDNA coding regions

AtSNF4-5'	5-CATACCATGGCCATGTTTGGTTCTACATTGGATAGC-3'
AtSNF4-3'	3-TGCCCATGGAAGACCGAGCAGGAATTGGAA-3'
DPBF4-5'	5'-ACCCGGGATCCTTATGGGTTCTATTAGAGGAAACATTGA-3'
DPBF4-3'	5'-ACCCGGGAATTCTCAGAGAGAAGCAGAGTTTGT-3'
OST1- <i>Xba</i> I-3'	5'-CATTCTAGACATTGCGTACACAAT-3'
OST1- <i>Nco</i> I-5'	5'-CATACCATGGATCGACCAGCAGTGAGT-3'
OST- <i>Eco</i> RI-3	5'-CAGAATTCAGTAGCGGAGAGATTGTGTACGCA-3'
OST- <i>Bam</i> HI-5' 5'	5'-CATTGGATCCGAATGGATCGACCAGCAGTGAGT-3'
TRX-OST- <i>Eco</i> RI-3'	5'-GGAATTCGCATTGCGTACACAATCTC-3'
TRX-OST- <i>Bam</i> HI-5	5'-CGGGATCCCATGGATCGACCAGCAG-3'

2.1.6.2. Oligonucleotides for DNA sequencing

OST-Seq-5'	5'-CATCGAGCGAATCTGCAATGCAGGC-3'
OST-Seq-3'	5'-GCCTGCATTGCAGATTCGCT'CGATG-3'
DPBF4-5'	5'-ACCCGTCTAGTGTAAATACCCGCAGCT-3'

2.1.6.3. Oligonucleotides for site-directed mutagenesis of the *Ost1* kinase

T146A-1	5'-GCTCGAGAATGCGTTATTAGATGGT-3'
S175D-2	5'-AGGAGTTCCAACATCTGATTTTGGTTGCG-3'
S175A-1	5'-CGCAACCAAAAGCAACTGTTGGAA-3'
T176D-1	5'-CAACCAAAATCAGATGTTGGAACCTCCTGC-3'
PET201T	5'-CGAGCTCCGTCGACAAGCTTtGGCCGtACTCGAGCAC-3'
(Selection primer)	5'-CACCACCACCACCCTGAGAT-3'

2.1.6.4. Oligonucleotides for RT-PCR

DPBF4-RT-5	5'-CATAAGCAGCCTACACTCGGTGAA-3'
DPBF4-RT-3	5'-TCTGGTGGTGGTTCACCTGGTAGGA-3'
AK-RT-5	5'-CATGACTCTGAGAGGAAGTTGGTGGT-3'
AK-RT-3	5'-AGCACTCATTATAGCTGCAGAGATG-3'
SNF4-F	5'-GGCTGCCCTACTGTTTTTCA-3'
SNF4-R	5'-TCCAACAATTGGCCTTTTC-3'
Ost1-F	5'-TTTGCCGATTATGCACGATA-3'
Ost1-R	5'-TCGCTCGAAAAGTTCTC-3'
AK-HSD-F	5'-GGTCATGCAACCGAATCTTT-3'
AK-HSD-R	5'-CGTTGGAATGTTCTGTGGTG-3'
ADH-F	5'-CATGAAGCTGGAGGGATTGT-3'
ADH-R	5'-TCCTAGAAGCACCAGCGATT-3'
P5CS1-F	5'-GAGAGGGGGTATGACTGCAA-3'
P5CS1-R	5'-CCATCTGCCACCTCTGTTTT-3'
AKIN10-F	5'-TGGTTCCTTTGGTAGGGTGA-3'
AKIN10-R	5'-CACACCACAGCTCCAGACAT-3'
AKIN11-F	5'-AATTGGGTCTTTTGGGAAGG-3'
AKIN11-R	5'-GGCTTCCACAACCTCGTCTTT-3'

2.1.6.5. *AtSNF4* primers to test alternative splicing

EXON 1-5'	5'-TCTACATTGGATAGCAGCCGTGGAAAC-3'
INTRON 1-5'	5'-GTGCTCTGTATAGTATCTATCGGGGT-3'
EXON2-5'	5'-CATTTGCAACTTGACGCCAGGATA-3'
INTRON 2	5'-CCCTGCAGAAGCATTATGTCCTTGTA-3'
EXON3-5'	5'-TGTGGATGATGTCTTCCTGCGAAC-3'
INTRON 3-5'	5'-GCTTGATGGTTCAGGTTTCCCGAGTTG-3'
INTRON 4-5'	5'-CTGTCTTCATGTCCTATAGATTATCAGTTAA-3'
EXON13-3'	5'-CTGTGGGAGTCAAAGACCGAGCAGG-3'

2.1.6.6. Oligonucleotides to screen for T-DNA insertion mutants in *Arabidopsis*

DPBF4-5'	5'-AGTTCAAGGGTATGCTCTGTGTGGG-3'
DPBF4-3'	5'-TCAGAGAGAAGCAGAGTTTGTTCGCC-3'
AtSNF4-5'	5'-GTTTGGTTCTACATTGGATAGCAGC-3'
AtSNF4-3'	5'-AGGAATTGGAAAACATCGCTCAGT-3'
JL-202	5'-CATTTTATAATAACGCTGCGGACATCTAC 3'
SALK LB	5'-TTTGGGTGATGGTTCACGTAGTGGG-3'

2.1.7. Culture media

2.1.7.1. Bacterial media (Sambrock et al., 1989)

2.1.7.1.1. LB medium:

Bacto-Tryptone	10g/l
Bacto-Yeast Extract	5g/l
NaCl	10g/l

Adjust pH to 7.5 with NaOH. For solid media add 20g/l Bacto-Agar. Autoclave for 20 min at 120°C.

2.1.7.1.2. YEB medium:

Beef Extract	5g/l
Bacto yeast extract	1g/l
Bactopeptone	1g/l
Sucrose	5g/l

Adjust pH to 7.4 with NaOH. For solid medium add 15g/l Bacto-agar. Autoclave for 20min. and after sterilization 2ml/ of 1M MgSO₄ was added.

2.1.7.2. YPD yeast medium

Difco-peptone	20g
Yeast extract	10g

All other media were used as described in the Clontech MATCHMAKER Yeast One-Hybrid System, user manual (<http://www.clontech.com/clontech/techinfo/manuals/PDF/PT1031-1.pdf>).

2.1.7.3. Plant media

2.1.7.3.1. Arabidopsis suspension culture medium (SCM)

(Murashige and Skoog, 1962)

MS Basal Mix	4.3g/l
B5 vitamin(100X)	4ml
Sucrose	3%

Adjust pH to 5.8 with KOH, autoclave at 120°C for 20 min and then add 2,4 D to final concentration of 1mg.

2, 4-D stock solution

2mg/ml in 0.5M KOH, pH 6.7, filter sterilized.

B5 Vitamin (100X)

Nicotinic Acid	1mg/ml
Pyridoxine HCL	1g/ml
myo-Inositol	100mg/ml
Thiamine	10mg/ml

2.1.7.3.2. MSAR médium (Koncz et al., 1994)

Macroelement	25.0 ml/l
Microelement	1.0 ml/l
Fe-Na ₂ -EDTA	5.0 ml/l
CaCl ₂ .2H ₂ O	5.8 ml/l
KI	2.0 ml/l
Vitamin	2.2 ml/l
Sucrose	5g/l

pH was adjusted to 5.8 with KOH. For solid MSAR medium, 0.6 g Agar was added.

MSAR stock solutions:

Macroelements: 20 g $\text{NH}_4(\text{NO}_3)_3$, 40g KNO_3 , 7.4 g KH_2PO_4 , 5 g MgSO_4 , 3 g $(\text{NH}_3)_2\text{SO}_4$

Microelements: 6.2 g H_3BO_3 , 16.9 g $\text{MnSO}_4 \cdot 4\text{H}_2\text{O}$, 8.6 g $\text{ZnSO}_4 \cdot 7\text{H}_2\text{O}$, 250 mg Na_2MoO_4 , 50 mg $\text{CuSO}_4 \cdot 5\text{H}_2\text{O}$, 250 mg $\text{CoCl}_2 \cdot 6\text{H}_2\text{O}$

Fe- Na_2 -EDTA: 5.56 g $\text{FeSO}_4 \cdot 7\text{H}_2\text{O}$, 7.45 g Na_2 -EDTA

KI: 375 g KI

CaCl_2 : 75g $\text{CaCl}_2 \cdot 2\text{H}_2\text{O}$

2.1.8. Antibiotics

<u>Antibiotics</u>	<u>Stock solution</u>	<u>Working concentration</u>
Ampicillin	100mg/ml in ddH ₂ O	100 mg/l
Carbenicillin	50mg/ml in ddH ₂ O	100 mg/l
Claforan	100mg/ml in ddH ₂ O	300 or 500 mg/l
Chloramphenicol	25mg/ml in ethanol	25 mg/l
Rifampicin	25mg/ml in methanol	100 mg/l
Hygromycin	15mg/ml in ddH ₂ O	15 to 25 mg/l
Kanamycin	50mg/ml in dd H ₂ O	25 mg/l for bacteria; 100 mg/l for plants
Spectinomycin	50mg/ml in H ₂ O	50 mg/l
Tetracyclin	10mg/ml in H ₂ O	12.5 mg/l

All antibiotics were filter sterilized and stored at -20°C.

2.1.9. Plant hormones

2,4-D (2, 4-dichlorophenoxyacetic acid)	1mg/l in ddH ₂ O, pH 7.0
BAP (6-benzylaminopurine)	1mg/l in ddH ₂ O, pH 7.0
IBA (indole-3-butyric acid)	1mg/l in ddH ₂ O, pH 7.0

2,4-D, BAP and IBA were filter sterilized and stored at -20°C.

2.1.10. Solutions

(Pre-) Hybridization solution:	2.5mM EDTA, 1% BSA, 7% SDS, 50mM $\text{Na}_2\text{HPO}_4/\text{NaH}_2\text{PO}_4$, pH 7.0
Denaturation solution:	0.5M NaOH, 1.5M NaCl
IPTG:	100mM in ddH ₂ O, filter sterilized and stored at -20°C. Working concentration: 0.4-1 mM
DNA loading buffer for gel electrophoresis:	40% glycerol, 0.25% bromophenol blue
MOPS (10X):	0.2M [3-(N-Morpholino)-propane-acid], pH 7.0, 0.05 M sodium acetate, 0.01M EDTA
Neutralization solution:	0.5M Tris.HCl (pH 7.4), 3M NaCl
Phenol/Chloroform/Iso-amylalcohol:	mix to a ratio of 25:24:1
SSC (20X):	3M NaCl, 0.3M Sodium citrate

TAE buffer (10X):	1M Tris, 0.1M Sodium acetate, 10mM EDTA, pH 8.0
TBE buffer (10X):	1M Tris, 0.8M Boric acid, 10mM EDTA, pH 8.0
TE:	10mM Tris.HCl, 1mM EDTA, pH 8.0
THE:	50mM Tris.HCl, 20mM EDTA, pH 8.0
X-Gal:	50mg/ml in N,N-dimethylformamide (DMF) store in the dark at -200C

2.1.11. Antibodies

2.1.11.1. Primary antibodies

<u>Anti-HA:</u>	Rat monoclonal antibody (clone 3F10) raised against a peptide derived from the hemagglutinin protein of the human influenza virus (Boehringer-Roche; Dilution used 1:2000 to 1:1000).
<u>Anti-cMYC:</u>	Mouse monoclonal antibody raised against a peptide from human cMYC protein (dilution used 1:2000 to 1:1000).
<u>Anti SNF4:</u>	Rabbit polyclonal antibody raised against <i>Arabidopsis</i> AtSNF4 peptide (Kleinow, 2000; Dilution used: 1:500).
<u>Anti 20S</u>	
<u>Proteasome:</u>	Monoclonal antibody raised against the human 20S proteasome particle subunits α 1, 2, 3, 4, 5, 6 and 7 (Affinity research, UK; Dilution used 1: 1000).
<u>Anti-19S</u>	
<u>Proteasome:</u>	Polyclonal antibody raised against proteasome 19S regulatory particle subunit (Affinity research, UK; Dilution used 1:2000)
<u>Anti-SnRK:</u>	Polyclonal antibody raised against the tobacco NPK5 protein (Muranaka et al., 1994; Dilution used 1: 5000).
<u>Anti-PRL1:</u>	Polyclonal antibody raised against a PRL1 specific peptide (Németh et al., 1998; Dilution used 1:1000)

2.1.11.2. Secondary antibodies

Anti-rat IgG POD	Fab fragment (Sigma; 1:10,000).
Anti rabbit IgG POD	(Bio-Rad; dilution used 1:10,000).
Anti mouse IgG POD	(Boehringer-Roche; dilution used 1:10,000).

2.1.12. Computer analyses

Sequencing of plasmid DNA was performed using the dideoxynucleotide chain terminating method (Sanger *et al.*, 1997) and an ABI 377 DNA sequencer (Applied biosystems, Weiterstadt). The sequences were analyzed with the following computer programs:

- GCG program, Wisconsin Packet (Genetic Computer Group, Sequence Analysis Software Package, 1994).
- “Megalign”, “Edit Seq”, Primer Select”, “Map Draw” and “Protean” tools from the DNA Star software package, Lasergene, DNASTar Inc. Madison, USA
- Blast Program, Identification of DNA and Protein homology (Altschul *et al.*, 1990; Gish and States, 1993); <http://www.ncbi.nlm.nih.gov>
- Clustal W (1.81) Multiple Sequence Alignments; <http://www.embl.de>

- SMART, Sequence analysis of protein functional motives; <http://smart.embl-heidelberg.de>
- CBS Bioinformatics tools, for nucleotide sequences and amino acid sequence analysis; <http://www.cbs.dtu.dk/services>

2.2. METHODS

2.2.1. General molecular biology methods

2.2.1.1. Mini-preparation of plasmid DNA from *E.coli* (Birnboim and Doly, 1979)

A single *E. coli* colony was inoculated in 3 ml LB medium with appropriate antibiotic selection and grown o/n at 37°C on a roller at speed of 250 rpm. Small-scale plasmid isolation was done by the alkaline lysis method. 1.5 ml of o/n grown culture was centrifuged at 5000 rpm for 5min in a tabletop centrifuge, then the pellet was resuspended in 250 µl of solution 1. Resuspended cells were lysed by adding 350 µl of solution 2, and then mixed gently by inverting the centrifuge tubes 3 times and incubated at RT for 2 min. To neutralize the lysate, 350 µl of solution 3 was added and incubated on ice for 10 min. The cells were centrifuged at 13,000 rpm for 10 min to pellet the cell debris. The cleared supernatant was transferred to a fresh centrifuge tube, 0.8 volume of iso-propanol was added and then the mixture was incubated on ice for 10 min. This mixture was centrifuged at 13,000 rpm to pellet the precipitated DNA, which was washed with 75% ethanol. DNA pellet was dried at RT for 10 min and resuspended in 100 µl of H₂O. For low copy number plasmids the resulting pellet was resuspended in 50 µl of H₂O.

Solution 1: 50mM Tris.HCl (pH 8.0), 50mM glucose, 10mM EDTA

Solution 2: 200mM NaOH, 1% SDS

Solution 3: 3M NaOAc (pH 4.8) or 3M KAc (pH 6.0)

Plasmid DNA prepared by this method was used for restriction enzyme digestions to check the plasmid constructs prior transformation of electro-competent *E. coli* or *Agrobacterium* strains. For sequencing purpose, the DNA was prepared using a Qiaprep plasmid isolation kit.

2.2.1.2. Large scale plasmid purification from *E.coli* by CsCl gradient (Clewell and Helinski, 1969)

A single bacterial colony was inoculated to grow o/n in 5 ml of LB medium with appropriate antibiotics. This preculture was added to 1l of LB medium with antibiotics and grown o/n at 37°C with constant shaking at 250 rpm. Cells were pelleted by centrifugation on a Sorvall GS3-rotor at 4000 rpm for 10 min. Bacterial pellet was resuspended in 30 ml of solution1 plus 60 mg/ml of Lysozyme solution (in Tris-HCl, pH 8.0) and incubated at room temperature for 30 min. To lyse the resuspended cells, 60 ml of solution 2 was added to the mix and incubated at RT for 10 min. Finally, 45 ml of

solution 3 was added to the lysed cells and the mixture was incubated on ice for 30 min. The cell debris was removed by centrifugation at 12,000 rpm for 20 min at 4°C. The supernatant was passed through miracloth, then equal volume (100 ml) of isopropanol was added to the recovered solution and incubated at -20°C for 30 min. The precipitated DNA was pelleted by centrifugation at 12,000 rpm for 20 min. The DNA pellet was washed with 75% ethanol and dried shortly. To prepare the cesium chloride gradient, the DNA pellet was dissolved in 23.3 ml high TE. 24 g of CsCl was added to the dissolved DNA solution. Resulting solution was transferred to a quickseal Beckman (30 ml) tube and balanced with blank solution (1.55g CsCl/ml in TE). To visualize the DNA, 500 µl of a 10 mg/ml stock solution of ethidium bromide was added. These samples were centrifuged for 14 h at 45,000 rpm at 20°C in a Beckman VTi50 Rotor. After centrifugation, the super-coiled DNA was collected using a 5 ml syringe under 360nm UV light. This solution was loaded in a 5 ml Quick-Seal Beckman tube and centrifuged at 55,000 rpm on a Beckman VTi65 Rotor for 6 h. The concentrated DNA band was collected with a 2 ml syringe and was transferred into a centrifuge tube. DNA was repeatedly mixed with 20X SSC saturated with isoamyl alcohol, to remove ethidium bromide. The DNA was dialyzed against TE to remove CsCl. Dialysis was performed for 48 hrs by changing the TE solution three times. The dialyzed CsCl-free DNA was stored in small aliquots at 4 °C. Solutions 1-3 were prepared as described for small-scale plasmid isolation. The plasmid DNA obtained by this method was used to prepare vector and insert DNAs for cloning purposes or for transformation of protoplasts made from *Arabidopsis thaliana* cell suspensions.

2.2.1.3. Isolation of plasmid DNA from Agrobacterium tumefaciens

Agrobacterium culture (5 ml) was grown for 2 days with constant shaking at 28°C. Bacterial cells were pelleted and then resuspended in 150 µl of AGRO-buffer and incubated at 37°C for 1 hr. Subsequently, 260 µl of lysis buffer was added and the cell suspension was incubated on ice for 10 min, then 208 µl of neutralization solution was added and the lysate was incubated on ice for 15 min. The supernatant containing plasmid DNA was cleared by centrifugation at 12,000 rpm for 10 min and then. Phenol-chloroform extraction was performed to remove proteins and the DNA was precipitated with 2.5 vol of ethanol at -20°C. Plasmid DNA was pelleted by centrifugation at 13,000 rpm for 10 min. The DNA pellet was washed with 75% ethanol and dried for 10 min. The recovered DNA was dissolved in 50 µl of H₂O and used for either restriction enzyme digestion or transformation of *E. coli*.

AGRO-buffer: TE (10mM Tris-HC [pH 8.0], 1mM EDTA), 20 µl Proteinase K (10mg/ml),
4 µl of Sarcosyl 30%

Lysis buffer: 200mM NaOH, 1% SDS

Neutralization buffer: 3M NaOAc (pH 4.8)

2.2.1.4. Large Scale Genomic DNA isolation from *Arabidopsis thaliana* (Dellaporta et al., 1983)

A. thaliana organs or cells were collected and immediately frozen in liquid N₂ and then stored at -80°C. For DNA isolation, 10 g plant material was ground to a fine powder and incubated with 15 ml of extraction buffer plus 1 ml of 20% SDS. After 30 min incubation at 65°C, 5 ml of 5M KAc was added, and then the mixture was incubated on ice for 1 hr. The crude DNA extract was subjected to centrifugation at 8,000 rpm for 20 min at 4°C, to remove cell debris. The supernatant was filtered through miracloth and transferred to a fresh Sorvall centrifuge tube. 10 ml of isopropanol was added to the filtered supernatant and incubated at -20°C for 30min. The precipitated genomic DNA was recovered by centrifugation at 10,000 rpm for 20 min at 4°C. The DNA pellet was washed with 75% ethanol, dried shortly, and then dissolved in 4 ml of THE. To the dissolved DNA 4 g of CsCl was added and the DNA-CsCl solution was transferred into a 5 ml Beckman Quick-Seal tube and was filled up to the top with CsCl blank solution. The genomic DNA was recovered by centrifugation in a Beckman VTi-65 rotor at 55,000 rpm for 16 hrs at 20°C. The DNA was collected under 360nm UV light with a 2 ml syringe and centrifuged again for 5 h exactly the same way as described above. Ethidium bromide and CsCl removal was performed in the same way as described in 2.2.1.2. The DNA obtained by this method was used for Southern hybridizations.

Extraction buffer: 100mM Tris.HCl (pH 8.0), 500mM NaCl, 50mM EDTA,
10mM β-mercaptoethanol

2.2.1.5. CTAB genomic DNA extraction protocol (Rogers and Bendich, 1985)

This protocol was used for extraction of plant genomic DNA from small amount of plant material and is suitable for processing many samples for PCR analysis. 200 to 500mg of frozen plant material was ground in liquid N₂. To the homogenized samples 500 µl of 2X CTAB extraction buffer was added (preheated at 65°C) and the samples were incubated at 65°C for 5min. After addition of 400 µl of chloroform, the lysates were cleared by centrifugation for 5min at 13,000 rpm. The supernatant was mixed with 70 µl of 10X CTAB buffer (preheated at 65°C) and then with 400 µl of chloroform. The mix was centrifuged at 13,000rpm and then aqueous phase was transferred to a fresh centrifuge tube. 1/10 vol of CTAB precipitation buffer was added to the supernatant and the mixture was incubated on ice for 10 min to precipitate the DNA. The samples were centrifuged at 12,000 g for 10min at RT. The resulting DNA pellet was resuspended in 300 µl High-Salt TE buffer and then 0.3 µl RNase A (10 mg/ml) was added and the samples were by incubation at 37°C for 10 min. Finally, the samples were extracted with phenol-chloroform and the DNA was precipitated precipitated with EtOH by at -20°C. The DNA was collected by centrifugation at 12,000g for 15 min, washed with 70% ethanol, dried shortly and dissolved in 50µl of H₂O.

2 X CTAB buffer:	100 mM Tris.HCl (pH 8.0), 1.4 M NaCl, 20mM EDTA, 2% CTAB, 1% PVP-40000
10 X CTAB buffer:	10% CTAB, 0.7 M NaCl
CTAB Precipitation Buffer:	50 mM Tris.HCl (pH 8.0), 10 mM EDTA, 1% CTAB
High Salt TE Buffer:	100mM Tris.HCl (pH 8.0), 1.4 M NaCl, 20mM EDTA, 2% CTAB, 1% PVP 40000

2.2.2. Methods for DNA purification and quantification

2.2.2.1. Phenol/chloroform extraction (Sambrook et al., 1989)

To remove contaminating proteins from the DNA, phenol/chloroform extraction was performed. The DNA sample was mixed with equal amount of phenol saturated with TE (pH 8.0), mixed and centrifuged for 2 min at 13,000 g. The aqueous upper phase was collected. To remove any traces of phenol from aqueous phase, equal amount of cold chloroform:iso-amyl alcohol (24:1) mixture was added, mixed and centrifuged at 13,000 g. Aqueous phase containing DNA was collected and precipitated with 1/10 vol. of 3 M sodium acetate (pH 6.0) and 0.7 vol. of isopropanol for 1h at -20°C. The precipitated DNA was pelleted by centrifugation at 13,000 g. Then, the DNA pellet was washed with 75% ethanol, dried and dissolved in H₂O. This method was used to clean the PCR reactions, and restriction endonuclease digestion reactions.

2.2.2.2. Separation of DNA by agarose gel electrophoresis

DNA fragments were separated by horizontal agarose gel electrophoresis. The agarose concentration was determined by the size of desired DNA fragments analysed. Agarose gels were prepared in 1 X TAE supplemented with EtBr 25 µl/l from 10mg/ ml stock. Electrophoresis was performed at 5-10 V/cm in TAE buffer. After electrophoresis, DNA was visualized on a transilluminator under UV light (254nm). For size estimation, 1kb ladder (Gibco, BRL) was used.

TAE buffer: 40mM Tris.HCl (pH 7.8), 2mM EDTA

6 X Loading dye: 40% sucrose, 0.25% bromophenol blue

2.2.2.3. Purification of DNA fragments from agarose gels

DNA fragments were separated by electrophoresis and excised from the gel by visualization under UV light (364nm). The DNA fragments were purified by electroelution.

2.2.2.3.1. Electroelution

The excised agarose piece carrying the DNA fragment was transferred to a dialysis tube (stored in 0.5 mM EDTA) and filled with 1 X TAE buffer. Tube was clamped from both the sides to close the ends. The dialysis tube was placed into an electrophoresis tank and subjected to electrophoresis at 20-25

V/cm for 10 min. After this, the polarity of electrodes was changed to opposite and electrophoresis was continued for 2 min to release the DNA from the membrane. The electroeluted DNA was removed from the dialysis tube and subjected to phenol/chloroform extraction followed by precipitation with isopropanol.

2.2.2.3.2. DNA quantification (Sambrook et al., 1989)

DNA concentration was determined by spectrophotometry. The absorption of UV light by the ring structure of purines and pyrimidines can be used to measure the amount of DNA and RNA. An OD₂₆₀ value of 1 corresponds to 50 µg of double stranded DNA per ml of solution and 40 µg RNA/ml. In pure preparations of DNA/RNA samples the OD₂₆₀/OD₂₈₀ ratio should be between 1.8/2.0.

2.2.3. Enzymatic modifications of DNA

2.2.3.1. Digestion with restriction enzymes

Digestion of DNA with restriction endonucleases was performed according to the suppliers recommendations. Plasmid digestion was carried out for 1 to 4 h (2U of enzyme/µg of DNA). For plant genomic DNA digestion, 10 units of enzyme were used per µg of DNA and digestion was run for 12-14 hrs. First 5 units of enzymes were added to the DNA and the digestion was run for 4 h. Then, another 4 units of enzymes were added and digestion was continued o/n. The digestion was stopped by heat inactivation at 65°C for 10 min followed by phenol/chloroform extraction and ethanol precipitation.

2.2.3.2. Phosphatase treatment of DNA (Chaconas and van de Sande, 1980)

To prevent self ligation of linearised vector, the 5'-terminal phosphate groups were removed by phosphatase treatment of DNA, when vector was digested with single enzyme or blunt ligation was performed. 2 units of calf-intestinal alkaline phosphatase (CIAP) was added to 1 µg linearised DNA and incubated at 37°C for 30 min. The enzyme was heat inactivated at 65°C for 10 min, followed by phenol/chloroform extraction and ethanol precipitation of DNA.

CIAP buffer: 50mM Tris.HCl (pH 8.5), 0.1mM EDTA

2.2.3.3. Generation of blunt-ended DNA fragments (Ausubel et al., 1999)

T4 DNA polymerase was used to generate blunt ended DNA fragments for cloning. 1 unit of T4 DNA polymerase was added to per microgram of DNA and samples were incubated at 37°C for 15 min. The reaction was stopped by adding EDTA to a final concentration of 10 mM and heating to 75°C for 10 min followed by phenol/chloroform extraction and ethanol precipitation of DNA.

2.2.3.4. Generation of A-Tail for blunt ended PCR fragments

DNA fragments amplified with thermostable DNA polymerases (with proof reading activity) generate blunt ends during PCR. These PCR fragments were subjected to A-tailing, to be cloned in the pGEM-T vector (Promega). The A-tailing reaction was set up as follows:

Purified PCR fragment	3 μ l
Taq DNA polymerase buffer	1X
dATP	0.2mM
Taq DNA Polymerase	5units
Reaction volume	10 μ l

The reaction was incubated at 70°C for 30 min. The A-tailed DNA fragment was ligated using an optimum molar ratio of pGEM-T vector and insert.

2.2.3.5. Ligation of DNA fragments

Ligation of DNA fragments was performed using T4 DNA ligase. The ligase buffer used in the reaction was supplied with the enzyme by manufacturers. Usually, a molar ratio of 1:3 between vector and insert was present in the ligation mixtures. Control ligations, containing exclusively vector DNA, were performed to assess self-ligation of the vectors. Blunt end ligation and linker ligation reaction were supplemented with 1 mM ATP and 6% PEG to increase the ligation efficiency. For adaptor ligation, 1 mM ATP, 2U of T4 RNA ligase per 10 ng of DNA was added. All ligation reactions were incubated o/n at 8-12°C.

PEG 40%: (40% weight volume) polyethylene glycol 6000 or 8000 (Merck) in water. Autoclave at 120°C for 20 min. and store at 4°C.

2.2.4. PCR amplification

DNA amplification or modification of DNA ends for cloning purposes, or to check the presence or absence of a gene/cDNA, PCR was performed in a gene AMP PCR System 9600 (Perkin-Elmer). Unless otherwise specified, the reaction mix was prepared as recommended by the manufacturer (Boehringer/Roche). The reactions were performed in 50 μ l volume with following components:

10 X PCR buffer (-MgCl ₂)	5 μ l
dNTP-mix (final concentration 200 μ M)	5 μ l
DNA	1-50 ng
Oligonucleotide (10pmol/ μ l)	2 μ l
Taq-polymerase	0.5 U/ μ l

In a standard reaction, DNA was denatured at 95°C for 1 min, primer annealing was performed at 55 to 60 °C for 1 min, followed by an extension step at 72°C (Taq polymerase) or 68°C (Pfx or Takara

polymerase) for 1min., using 30 cycles ended by a final extension step for 5-10 min. The annealing temperature was specifically determined for according to the melting temperature of primer.

2.2.4.1. RT-PCR

cDNA was amplified by RT-PCR using the protocol described by the manufacturer (Gibco BRL) for the gene expression analyses, as well as for testing the expression of mutant genes carrying T-DNA tags. Total RNA was prepared using RNeasy plant RNA extraction kit. Total RNA was treated with RNase free DNase for 30 min at 37°C to eliminate genomic DNA contamination. For cDNA synthesis, 2µg of total RNA was bound to 400 picomol of oligo dT primers and incubated with Superscript II reverse transcriptase (Gibco BRL) at 42°C for 1h. The enzyme was deactivated by heating at 70°C for 15 min. For PCR amplification 1 µl aliquots from the cDNA was used as template with gene specific primers. The PCR amplified DNA fragments were resolved by agarose gel electrophoresis (1.2%) and negative images of gels were recorded with a DC120 digital camera using a Kodak Digital Science™ software.

2.2.5. Site-Directed Mutagenesis

A cDNA containing the complete open reading frame of Ost1 kinase was obtained from cDNA library of RIKEN cDNA stock centre. Substitution of either Ser or Thr with Asp or Ala within the activation loop or complete removal of catalytic domain of Ost1 kinase was achieved by using a site-directed mutagenesis kit (Clontech). *In vitro* mutagenesis reactions were performed on plasmid DNAs. Primers were annealed to the plasmid in a 1:200 molar ratio. Primary mutant DNA was selected using *NotI* enzyme (to digest the parental DNA) as a selection marker. Clontech site-directed mutagenesis kit was used to produce mutations following the manufacturer's instructions. Proper sequences of mutations and the fidelity of the rest of the cDNA in all constructs were confirmed by DNA sequencing.

2.2.6. Bacterial Transformation

2.2.6.1. Preparation of *E. coli* competent cells for transformation by heat-shock (Hanahan, 1986)

A single colony of *E. coli* DH5α was inoculated to grow bacteria o/n at 37°C in 5 ml LB medium. 3 ml of this o/n grown culture was inoculated into 300 ml of LB medium and allowed to grow at 18°C until OD₆₀₀ value is 0.5. The bacterial culture was cooled down for 30 min at 4°C, then the cells were centrifuged at 5000 g at 4°C. The recovered cell pellet was resuspended in 60 ml of RF1 buffer and incubated on ice for 30 min followed by centrifugation at 4,000 g. Cells were resuspended in 5 ml of RF2 buffer and incubated on ice for 30 min. 100µl of cells were aliquoted in Eppendorf tubes and snap frozen in liquid nitrogen. The competent cells were stored at -80°C.

RF1 buffer (pH 5.8)

(filter sterilized and stored at -20°C)

0.1M RbCl, 50mM MnCl₂, 15% glycerol, 10mM

CaCl₂·2H₂O, 30mM KOAc

RF2 Buffer (filter sterilized and stored at -20°C)	10mM RbCl, 10mM MOPS, pH 6.8, 15% glycerol, (75mM CaCl ₂ ·2H ₂ O)
---	--

All buffers, centrifuge and culture tubes used for transformation of competent cells were pre-cooled at 4°C. An aliquot of competent cells was transferred to 10 ml round bottom Falcon tubes, thawed on ice, mixed with plasmid DNA or ligation mix and incubated on ice for another 20 min. Heat shock was given at 42°C for 30 sec and then cells were incubated in ice for 30 min. Subsequently, 1 ml of LB medium was added and the cells were transferred into a 1.5 ml centrifuge tube, and incubated at 37°C for 45 min. Finally, the cells were plated on LB plates containing appropriate antibiotics.

2.2.6.2. Preparation and transformation of electro-competent cells (Dower et al., 1988)

A single colony of *E. coli* DH5 α or DH10B was inoculated in 5 ml of LB medium and to grow a starter culture o/n at 37°C with constant shaking. This 5 ml culture was inoculated into a 500 ml of LB medium, and grown at 37°C on a shaker until reaching an OD₅₉₅ value of 0.4. Subsequently, the culture was transferred into ice for 30min, then the cells were pelleted by centrifugation in prechilled 250 ml Sorvall centrifuge tubes at 4000 g at 4°C. The bacterial pellet was resuspended in 500 ml of ice cold sterile dH₂O and centrifuged again at 3,500 g. Subsequently, cells were washed twice with 250 ml dH₂O to remove salts completely. Finally, cells were resuspended in 1 ml of 10% glycerol and distributed in aliquots of 50 μ l into Eppendorf tubes and snap frozen in liquid N₂.

For transformation, an aliquote of competent cells was thawed on ice and mixed with DNA. Plasmid DNAs or ligation mixes were dialysed against water on a Millipore Filter membrane to remove salt. Cells were mixed with DNA and transferred to a chilled 0.2cm electroporation cuvette and placed in a Bio-Rad Gene Pulser. The Gene Pulser was set to 2.5kV (voltage), 25 μ F (capacitance) and 200 Ω (resistance) in order to deliver a pulse of 12.5kV/cm for 4-5 milliseconds. Immediately after the pulse, 750 μ l of LB (preheated at 37°C) was added, and cells were transferred into a centrifuge tube and shaken for 45 min at 37°C for recovery.

Agrobacterium were transformed in the same way except temperature and medium as *Agrobacteria* grows in YEB medium at 28°C.

2.2.7. Yeast one hybrid assays (performed in collaboration with Prof. Aviah Zilberstein and Shai Ufaz, Tel Aviv University, Israel)

Yeast strain YM4271 (Liu et al., 1993; Wilson et al., 1991) was used as host in one-hybrid assays. The bait construct carried a 194 bp fragment from the *AtAK1/HSD1* promoter (Zhu-Shimoni et al., 1998; located between positions -239 and -46), which was PCR amplified to clone into multiple cloning sites located upstream of the HIS3 and CYC1 minimal promoters in the vectors pHISi and pLacZi, respectively (Clontech, Palo Alto, CA). These vectors were transformed into yeast YM4271 to construct two separate reporter strains capable of growing in minimal medium lacking uracil. The HIS3 reporter strain was tested for background expression using increasing concentrations of 3-amino-

1,2,4-triazole (3-AT); a competitive inhibitor of the *HIS3* gene product. To suppress the background, 60 mM 3-AT was used for stringent selection. The *HIS3* reporter strain was transformed with a prey cDNA expression library, which was prepared from an *Arabidopsis* cell culture in the vector pACT2 (Németh et al., 1998). From 5×10^5 transformants 110 colonies growing in uracil and histidine free SD-medium with 45mM 3-AT were obtained. From these 8 transformants were capable of growing SD-medium with 60 mM 3-AT. The pACT2 clones were rescued from these clones and introduced into the reporter strain carrying the pLacZi- *AtAK/HSD1* promoter construct. The activation of *lacZ* reporter was monitored by filter lift assays (Yang et al., 1992). From the *lacZ*-expressing strain the pACT2 plasmids were rescued for sequencing of their cDNA inserts. To confirm G-box specific binding of AtDPBF4, the *AtAK/HSD1* promoter fragment was modified by Shai Ufaz using site-specific mutagenesis and changing the ACGT core sequence of the G-box/ABRE motif (ACACGTGGC) in the pLacZ-bait A, and the GACT core of GCN4 motif (CTTGACTCTA) in pLacZ-bait B. These bait constructs were subsequently tested by filter lift assays.

2.2.8. Southern DNA hybridization (Southern, 1975)

For Southern DNA filter hybridizations 10 μ g genomic DNA samples were digested with the appropriate restriction enzymes and separated in 1% TAE agarose gels. After taking a photo documenting the positions of DNA size markers, the gel was treated with 0.2N HCl for 10 min to introduce nicks in the large DNA fragments. Subsequently, the DNA fragments were denatured by soaking the gel in alkaline solution for 20 min and then the gel was neutralized by incubation in neutralization solution for 20 min. Single-stranded DNA from the gel was transferred to a nylon membrane (Hybond N, Amersham) using 20X SSC buffer by capillary transfer for 13-16 hrs. After blotting, the membrane carrying the transferred DNA was dried and cross-linked with UV light (Stratagene UV Crosslinker, 12mJ).

Denaturation solution:	1.5M NaCl, 0.5M NaOH
Neutralizing solution:	0.5M Tris.HCl (pH 7.4), 4.3M NaCl
20 X SSC	3M NaCl, 0.3M NaCitrate, pH 7.4

2.2.8.1. Preparation of ³²P-labeled DNA probes (Feinberg and Vogelstein, 1984)

Radioactively labeled DNA probes were synthesized by the random priming method (Feinberg and Vogelstein, 1984) using a Ready-prime kit from Pharmacia. About 100-300 ng DNA fragment in TE was denatured at 95°C for 5 min, snap cooled in ice for 5 min and incubated with Klenow fragment of DNA polymerase in a reaction mix containing 5 μ Ci (α -³²P) dCTP for 30 min at 37°C. The labeled DNA probes were purified using a Sephadex G50 column equilibrated with TE to remove non-incorporated nucleotides. The labeling mix was loaded onto the column and the DNA was eluted with TE by collecting 150 μ l fractions. From each fraction 1 μ l aliquot was taken for measuring the incorporated radioactivity using a scintillation counter (LS 6500 Multi-purpose Scintillation counter,

Beckman, Germany). Fractions representing the peak of labeled DNA were pooled, denatured by heating, cooled down in ice and added to the hybridization buffer (see below).

Sephadex G-50: 10g Sephadex G-50 powder autoclaved in 160 ml TE (pH 7.6)

2.2.8.2. DNA filter hybridization with radioactively labeled DNA probes

Filters carrying blotted DNA samples were incubated in prehybridization buffer for at least 4 hrs or o/n at 65°C. The prehybridization buffer was replaced with hybridization buffer (pre-heated) carrying the denatured radiolabeled probe. The hybridizations were performed o/n at 65°C with gentle shaking. Upon hybridization, the filters were washed two times with 2X SSC, 0.5%SDS at 65°C for 20 min, then the level of background was measured by a bench counter. If the background was high, the filters were washed again with 2X SSC, 0.5%SDS at 55°C until the background was reduced, and then a final washing step was performed with 0.2X SSC, 0.1% SDS for 15 min at 55°C. Filters were then placed on saran wrap in an autoradiography cassette and covered with an X-ray film for autoradiography at -70 °C.

(Pre)-hybridization buffer: 2.5 mM EDTA, 1% BSA, 7% SDS, 50 mM NaH₂PO₄/Na₂HPO₄

2.2.8.3. DNA filter hybridization with digoxigenin-labeled DNA probes

To perform non-radioactive labeling of DNA probes with digoxigenin conjugated nucleotide, a PCR DIG Probe Synthesis Kit (Roche) was used according to the manufacturer's instructions. DNA fragments were labeled by digoxigenin-11-dUTP during PCR with gene specific primers. 50µl of PCR samples, each containing 1 X DIG labeling buffer (supplemented with MgCl₂), 5µl of PCR DIG labeling mix, 100 ng DNA. Following PCR, 10 µl aliquot from each PCR labeling reaction was size-separated on a 1% agarose gel, stained with ethidium bromide (0.5 µg/ml) and visualized under a 302 nm UV transilluminator. Incorporation of digoxigenin was indicated by increase in molecular mass of digoxigenin labeled DNA fragments.

Southern DNA filters were prepared as described above and prehybridized in DIG-Easy prehybridization buffer (Roche) for 1h at 42°C. The prehybridization buffer was replaced with hybridization buffer (preheated) containing heat-denatured DIG-labeled probe and incubated o/n at 42°C with gentle shaking. The nonhybridized probe was removed by washing the filter with buffer A and then with buffer B. Subsequently, the membrane was blocked for 30 min at room temperature with blocking buffer, and then incubated at room temperature for 1 h with a peroxidase-conjugated mouse anti-digoxigenin IgG (Roche, Germany), which was diluted 1:10,000 in blocking solution. After removal of unbound antibody by washing the filter two times with buffer C for 15 min, the filter was equilibrated with detection buffer for 5min and then incubated for 5 min at RT with CSPD, which was diluted in detection buffer 1:100. CSPD is a chemiluminescent substrate for alkaline phosphates. The

filter was than placed between layers of saran wrap in an autoradiography cassette and subjected to autoradiography for 30min.

10 X blocking solution.	10%(w/v) blocking reagent (Roche) in 100 mM maleic acid, 50mM NaCl (pH 7.5)
Wash buffer A	2 X SSC, 0.1% SDS
Wash buffer B	0.1 X SSC, 0.1% SDS
Wash buffer C	100 mM maleic acid (pH-7.5), 50 mM NaCl, 0.3% Tween-20
Detection buffer	100mM Tris.HCl (pH-9.5), 100mM NaCl
CSPD working solution	CSPD stock 1:100 diluted in detection buffer

2.2.9. Methods for RNA isolation from plants and cell suspension cultures (Sambrook et al., 1989)

2.2.9.1. RNA isolation using the guanidium thiocyanate (GTC) method

Plant samples frozen in liquid nitrogen were ground to a fine powder and then 2 ml of GTC solution was added per gram of tissue and the sample was subjected to thawing in a fume hood. The extract was transferred into a 50 ml Falcon tube and shaken for 30 min at RT. Subsequently, the extract was cleared by centrifugation for 20 min at 3,500 g to remove cell debris. The cleared supernatant was loaded onto a CsCl cushion (2 ml) in a tube for Beckman SW55Ti rotor and the samples were subjected to centrifugation for 12-16 h. at 35,000 rpm at 20°C. After centrifugation. the upper phase, interphase (DNA), and CsCl cushion were removed with a pipette, tube was turned upside to remove all liquid and the bottom with the RNA pellet was cut off. The RNA pellet was dissolved in DEPC (diethyl pyrocarbonate)-treated RNase-free H₂O, using usually a volume of 300 µl per RNA pellet. The RNA sample was heated at 65°C for 10 min and then cleared by centrifugation at 12,000 g for 10min at RT. RNA was precipitated with 1/10 volume of 3M NaOAc (pH 5.2) and 2.5 volumes of ethanol at -20°C for at least 3 h at -20°C. The precipitated RNA was collected by centrifugation at 13,000 g for 10min, washed with 75% ethanol, dried and dissolved in 100 µl of DEPC-treated RNase free H₂O.

GTC Buffer:	4M guanidium thiocyanate (GTC), 25 mM Na-citrate (pH 7.0), 0.5% N lauryl-sarcosine, 0.1 M β-mercaptoethanol, pH was adjusted to 6.5 – 7.5 with HCl
CsCl cushion:	5.7M CsCl, 50 mM Tris.HCl (pH 8.0), 5 mM EDTA (pH 8.0), 5 mM Na- acetate

2.2.9.2. RNA isolation using Plant RNeasy Extraction kit (Qiagen)

For RNA isolation from small amounts of plant tissues, the RNeasy kit from Qiagen was used. Plant material was ground in small Eppendorf tubes by the help of a plastic pestle or with homogenizer. RNA extraction was performed according to the manufacturer's recommendations. With 100 mg of starting material approximately 20µg of total RNA was extracted.

2.2.9.3. Electrophoresis of RNA in TBE agarose gel

1.5% agarose gel in 1X TBE was used for RNA electrophoresis to check the quality of isolated RNAs. RNA samples were denatured at 65°C for 5min, mixed with 10 X RNA loading dye and loaded on the gel. RNA was visualized under UV transilluminator.

RNA loading dye 50% glycerol, 0.1mg/ml bromophenolblue

2.2.9.4. Formaldehyde agarose gel electrophoresis of RNA samples (Ausubel et al., 1989)

To size separate RNA samples under denaturing conditions, the RNA samples were loaded onto a 1.5% agarose gel containing 6.6% formaldehyde. To prepare the gel, the agarose was melted in DEPC-treated H₂O containing 1 X MOPS buffer, cooled down to 55°C and then 6.6% formaldehyde was added. The gel was cast in a fume hood. RNA samples (20µg) were mixed with probe buffer and heated at 65°C for 5 min and then cooled in ice. 10 X loading dye was added to the samples prior loading them on the gel.

10X MOPS: 200 mM 3-(N-morpholino)-propanosulphonic acid (MOPS), 50mM NaOAc, 10 mM EDTA (pH 8.0), adjusted to pH 7.0 with KOH

Probe buffer: 50µl 10 X MOPS, 175 µl formaldehyde, 500µl formamide, 100µl 10 X loading dye

10 X loading buffer: 0.5% bromophenol blue, 4 mM EDTA (pH 8.0), 25% Ficoll

To remove potential RNase contamination, all glassware, electrophoresis tanks, gel casting trays, combs, were incubated in 3% H₂O₂ for 3hrs. All buffers and solutions were prepared in DEPC treated H₂O and autoclaved.

2.2.9.5. Northern blotting and RNA filter hybridization

After electrophoresis of RNA samples, the formaldehyde gels were washed with sterile DEPC treated H₂O to remove formaldehyde. RNA was transferred to a nylon membrane (Hybond N) by capillary transfer with 10 X SSC o/n. After blotting, the RNA membrane was dried and cross-linked under UV light (Stratagene UV Crosslinker, 12mJ). Prehybridization, hybridization with radioactive probes, and washing conditions were the same as described under Southern hybridization in section 2.2.8.

2.2.10. Protein analytical methods

2.2.10.1. Preparation of crude protein extracts from plant tissues and cell suspension

Samples from cell suspension cultures were collected by filtration through a Millipore filtration system and frozen in liquid N₂. The frozen material was ground in liquid N₂ to a fine powder in presence of extraction buffer (1 ml/g of tissues), containing protease inhibitor cocktail and detergent(s). The sample was thawed and centrifuged at 10,000g for 10 min at 4°C. The cleared supernatant was transferred into a fresh microfuge tube and stored at -20°C. Protein concentration was measured according to Bradford (1976).

Extraction buffer: 25 mM Tris.HCl (pH 7.5), 10% glycerol, 1 mM DTT, 1 mM EDTA, 150 mM NaCl, 0.8 mM PMSF, 1% Igepal

Protease inhibitor cocktail: 1 mM benzamide, 2µg/ml pepstatin, 5µg/ml of aprotinin, leupeptine

2.2.10.2. Extraction of nuclear proteins from Arabidopsis cell suspension

Frozen plant tissues were ground in liquid N₂ to a fine powder in a prechilled mortar with pistil. Nuclear grinding buffer A (40 ml/25-40 g of tissues) was added and the sample was ground again. Homogenized thick slurry was thawed in coldroom at 4°C, filtered through two layers of Miracloth and one layer of 50µM nylon mesh. The debris was ground again with 2 ml of buffer to extract the remaining proteins. The filtration step was repeated and nuclei were pelleted from the combined filtered extract by centrifugation at 3,500 rpm for 10 min at 4°C. Supernatant was removed with a pipette, the nuclear pellet was resuspended in 40 ml wash buffer and centrifuged at 3,000 g for 10 min at 4°C again. To lyse the nuclei, 0.5ml of nuclear lysis buffer was added and then the sample was passed through a 1 ml syringe needle, and then homogenized with a douncer. The homogenized nuclear extract was cleared by centrifugation at 1000 g to remove debris and the supernatant was transferred into a 1.5 ml microfuge tube. DNase (final concentration 100µg/ml) was added to digest the DNA present in the nuclear preparation for 1 h at 4°C. Finally, the nuclear extract was cleared again by centrifugation for 10 min at 13,000 g. The crude supernatant was transferred into a new microcentrifuge tube. In case nuclear lysis was not sufficient, one loses nuclei in the pellet. As a precaution, the nuclear pellet was stored at -70°C.

Nuclear extraction buffer: 1 M Hexylene glycol, 50 mM Tris.HCl (pH 7.5), 10 mM MgCl₂, 0.2% Triton X100, 1 mM DTT, 0.8 mM PMSF, 10µl/ml plant protease inhibitor cocktail (Sigma)

Nuclear wash buffer: 0.5 M Hexylene glycol, 50 mM Tris.HCl (pH 7.5), 10 mM MgCl₂, 0.2% Triton X100, 1 mM DTT, 0.8 mM PMSF, 10µl plant protease inhibitor cocktail (Sigma)

Nuclear lysis buffer:	10% Glycerol, 50mM Tris-HCl (pH 7.5), 10 mM MgCl ₂ , 0.5% Triton X100, 1% Igepal, 1 mM DTT, 0.8 mM PMSF, 10 µl/ml plant protease inhibitor cocktail (Sigma)
DNase:	5 mg/ml (Worthington, electrophoretically homogen)

2.2.10.3. Preparation of cytoplasmic protein extracts from Arabidopsis plant tissues and cell suspensions

Frozen plant tissues were ground to a fine powder in a prechilled mortar with pestle using liquid N₂, then cytoplasmic extraction buffer (40 ml/25-40 g of tissue) was added and the mixture was ground again. Homogenized thick slurry was thawed in coldroom at 4°C. The thawed mix was sieved through one layer of miracloth and one layer of 50µM nylon membrane. The debris was ground again with 2 ml of buffer for complete protein extraction. The filtration step was repeated and the combined supernatant was cleared by centrifugation at 13,000 g for 10 min at 4°C. The cleared protein extract was carefully pipetted off from the tubes and aliquoted for further analysis and storage at -70°C.

Protein extraction buffer:	20% glycerol, 50 mM Tris HCl (pH 7.5), 10 mM MgCl ₂ , 1 mM DTT, 0.8 mM PMSF, 10 µl/ml plant protease inhibitor cocktail (Sigma)
----------------------------	--

2.2.10.4. Chromatin immunoprecipitation

Immunoprecipitation of *in vivo* fixed chromatin fragments was performed according to Orlando and Paro (1993) and Tanaka *et al.* (1997) with some modifications. 50 g of wild type or transgenic cell suspension was treated with 2% formaldehyde (Sigma F1635, 37%) in crosslinking buffer (100 ml) for 2 to 3 hrs with constant stirring at 4°C. The formaldehyde-treated suspension was blocked with 125mM glycine in quenching buffer by washing twice, and finally snap frozen in liquid N₂. Frozen tissues were ground in 40 ml of nuclear grinding buffer, filtered through one layer of miracloth and one layer of 50 µM nylon mesh and then centrifuged at 3,500 g. The resulting crude nuclear pellet was washed twice with nuclear wash buffer and resuspended in 1 ml nuclear lysis buffer. The nuclei were sonicated five times for 30 sec using a Branson sonifier cell. Chromatin was sheared into an average size of 500bp. HA or cMYC tagged cross-linked proteins were immunoprecipitated with 50µl of HA or cMYC affinity matrices. The affinity matrix was rinsed with IP wash buffers 1 and 2. Tagged protein bound to the matrix was eluted by HA or cMYC peptide competition (using 1mg/ml peptide in "peptide"-buffer) for 1hr. One tenth of the immunoprecipitated protein sample was analyzed by Western blotting using rat or mouse monoclonal antibody to HA or cMYC as the first antibody, respectively. The remaining sample (9/10) was digested with RNase (250 µg/ml) followed by digestion with Proteinase K (500µg/ml). The samples were incubated at 65°C for 6 hrs to resolve the formaldehyde cross-linking. DNA was cleaned by phenol/chloroform extraction and precipitated with 1/10 vol 3 M Na-acetate (pH-6.0) and 2.5 vol. ethanol in the presence of 20 µg/ml glycogen at -20°C o/n. The DNA was collected by centrifugation at 13,000g for 20 min 4°C, washed with 75% ethanol

and dissolved in 20 μ l sterile water. This immunoprecipitated DNA was then either ligated with adapters (0.4 μ M) or digested with Sau3A and subjected to linker (0.4 μ M) ligation followed by PCR amplification. One half of the reaction was used for PCR. The PCR products were separated in a 2% gel in the presence of EtBr and photographed.

Crosslinking buffer:	50 mM K-phosphate (pH 7.0), 50 mM NaCl, 3% sucrose, 2% Formaldehyde
Quenching buffer:	50 mM PIPES/KOH (pH 7.0), 3% sucrose, 0.125 mM glycine, 0.1% Triton X-100, 1mM EDTA, 0.8 mM PMSF
Nuclear grinding buffer:	50 mM PIPES/KOH (pH 7.0), 1M hexylene glycol, 10 mM MgCl ₂ , 0.2% Tritox X-100, 1 mM DTT, 1 mM PMSF, 2 ml/100ml plant protease inhibitor cocktail (Sigma)
Nuclear washing buffer:	50 mM PIPES/KOH (pH 7.0), 1M hexylene glycol, 10 mM MgCl ₂ , 0.2% Triton X-100, 1 mM DTT, 0.8 mM PMSF 1ml/60ml protease inhibitor cocktail (Sigma)
Nuclear DNA lysis buffer:	50 mM HEPES pH 7.5, 150 mM KCl, 5 mM MgCl ₂ , 10 μ M ZnSO ₄ , 1.0% Triton-X-100, 0.5% Sarcosyl, 0.1% Na-deoxycholate, 0.1% Igepal, 1 mM PMSF, 10 μ g/ml protease inhibitor cocktail (Sigma)
IP wash buffer 1:	50 mM HEPES pH 7.5, 150 mM KCl, 5 mM MgCl ₂ , 10 μ M ZnSO ₄ , 1.0% Triton-X-100, 0.1% Na-deoxycholate, 0.1% Igepal, 1 mM PMSF, 2ml/100ml protease inhibitor cocktail (Sigma)
IP wash buffer 2:	50 mM HEPES pH 7.5, 150 mM KCl, 1.0% Triton-X-100, 0.1% Na-deoxycholate, 0.1% Igepal
Peptide buffer:	50 mM HEPES pH 7.5, 150 mM KCl, 1.0% Triton X-100, 0.1% Na-deoxycholate, 0.1% Igepal containing 1mg/ml HA or cMYC peptide

2.2.10.5. Measurement of protein concentration by Bradford assay (Bradford, 1976)

The Bradford assay is based on the principle that maximum absorbance for an acidic solution of Coomassie Brilliant Blue G.250 shifts from 465 nm to 595 nm when binding to protein occurs. Protein samples were diluted five folds in 50 mM Tris.HCl, 1mM EDTA buffer. 20 μ l of diluted protein was mixed with 980 μ l solution containing 200 μ l of Protein Assay Concentrated Dye and 780 μ l of dH₂O. Absorbance at 595 nm was extrapolated to a curve obtained with BSA standard.

2.2.10.6. Size separation of proteins by SDS-polyacrylamide gele electrophoresis (SDS-PAGE, Laemmli 1970)

Separation of proteins by SDS/Polyacrylamide denaturing gel electrophoresis was performed essentially as described by Laemmli (1970) with certain modifications. The electrophoresis was performed in a Boi Rad Protean III, 16cm cell apparatus. Resolving mix (pH 8.8) was prepared and poured in the casting apparatus. 200 μ l of 2-butanol was poured on the top to keep the surface linear

from being cranky. Stacking gel was poured on the top of the resolving gel and a comb with 10 or 15 slots was inserted. Samples were mixed with 5 X SDS sample loading buffer and denatured for 5 min at 95°C. Samples were cooled to RT and resolved by SDS/PAGE. Standard low molecular weight prestained protein marker from Bio Rad was used for protein size determination. SDS/PAGE electrophoresis was performed at constant 30 mA in 1 X SDS-PAGE running buffer.

Resolving gel (10%)	dH ₂ O	2.395 ml
	1.5 M Tris.HCl (pH 8.8)	1.25 ml
	40% Acrylamide/bis-acrylamide AA	1.25 ml
	10% SDS	5.0 µl
	10% APS	50 µl
	TEMED	10 µl
Stacking gel (6.6%)	dH ₂ O	1.21 ml
	0.5 M Tris.HCl (pH 6.8)	0.5 ml
	40% Acrylamide/bis-acrylamide	0.25 ml
	10% SDS	40 µl
	10% APS	40 µl
	TEMED	4 µl
Running Buffer:	192 mM glycine, 0.1% SDS, 25 mM Tris base (pH 8.3)	
5X Sample buffer:	7.5% SDS, 0.1 M DTT, 10 mM EDTA, 30% sucrose, 0.25 mg/ml bromophenol blue, 0.3 M Tris.HCl (pH 6.8)	
APS	10% ammonium persulfate	

2.2.10.7. Western blotting (Towbin et al., 1979)

Proteins separated on a SDS-PAGE gel were transferred onto PVDF membrane (Polyvinylidene difluoride membrane) for immunodetection with specific antibodies. The stacking gel was cut off from the resolving SDS-PAGE gel. The resolving gel containing proteins was equilibrated in 1 X transfer buffer for 5 min. The PVDF membrane was pre-incubated for 30 sec in methanol, washed with dH₂O for 5 min and equilibrated in 1 X transfer buffer for 5 min. Electrophoretic transfer of proteins was performed at 10 V for 2 h in a wet blot system.

Transfer buffer: 50 mM Tris base, 50 mM Boric acid

2.2.10.8. Verification of protein transfer by Ponceau staining (Hughes et al., 1988)

The efficiency of protein transfer is indicated by the intensity of the protein marker dye. PVDF membranes were stained with Ponceau S solution for 5 min and then washed with 1 X TBS Tween solution or H₂O for 5 min, by changing the solution.

Ponceau staining solution: 0.2% Ponceau S in 3% trichloroacetic acid

TBS Tween buffer: 20 mM Tris, 137 mM NaCl, 1M HCl, 0.05% Tween 20

2.2.10.9. Coomassie staining

Coomassie staining was performed to monitor the amounts of proteins. Proteins separated on a polyacrylamide gel were precipitated and stained using a fixing solution containing 1% Coomassie Brilliant Blue R250, for 30 min. The gel was washed several times with destaining solution to remove unspecifically bound Coomassie blue.

Coomassie blue staining solution: 1% Coomassie brilliant blue R250, 40% methanol, 10% acetic acid

Destaining solution: 40% methanol, 10% acetic acid

2.2.10.10. Colloidal Blue staining

Minimal amount of proteins were detected by colloidal blue staining (Invitrogen), according to manufacturers instruction.

2.2.10.11. Immunoblot analysis

Western blots were analyzed by using antibodies. The PVDF membranes carrying proteins were incubated with blocking solution for 1h at RT, than incubated with primary antibody for 2 h in the same buffer, and washed with 1 X TBS-Tween 20 (washing solution) three times for 10 min. After incubation with horseradish peroxidase conjugated secondary antibody (HRPO) for 1 h, and washing with 1 x TBS-Tween 20 3 times as described above, the antigen bands were detected using ECL (enhanced chemiluminescence) protein gel blot detection reagents, and exposing the membrane to an X-ray film (Hyperfilm).

TBS Tween buffer: 20 mM Tris, 137 mM NaCl, 1M HCl, 0.05% Tween 20

Blocking solution: 5% non-fat milk powder in TBS-Tween 20

2.2.10.12. Size fractionation of proteins by glycerol gradient centrifugation

Nuclear or cytoplasm protein extracts were loaded onto 10-40% glycerol gradients prepared by a gradient mixer and centrifuged for 16 h at 25,000 g. 300µl fractions were collected and 20µl aliquots from these were analyzed by SDS-PAGE and immunodetection. Positive fractions were dialyzed in 10% glycerol containing buffer and subjected to further immunoprecipitation, if required.

glycerol gradients: 10% or 40% glycerol, 50 mM Tris.HCl (pH 7.5), 10 mM MgCl₂, 1 mM DTT, 0.8 mM PMSF, 10µl/ml plant protease inhibitor mix (Sigma)

2.2.10.13. Immunoprecipitation of proteins

Proteins purified by ion exchange chromatography or isolated from crude nuclear extracts were incubated with protein G or Protein A Sepharose matrices for preclearing for 1h. The sample was

centrifuged at 10,000 g for 15 sec, then the supernatant was transferred into a new microcentrifuge tube. Anti-HA or anti-cMYC antibody conjugated to agarose affinity matrices was added to the precleared protein supernatant and the sample was put on a roller for 3 h. The matrix was washed three times with the binding buffer (nuclear extraction buffer or buffer used for ion exchange chromatography) supplemented with 150 mM NaCl. Proteins bound to the IgG matrix were eluted with HA or cMYC peptide (1 µg/µl) in binding buffer. To aliquots of immunoprecipitated proteins an equal volume of SDS-loading buffer was added and the samples were analyzed by SDS-PAGE and Western blotting.

2.2.11. Purification of recombinant proteins expressed in *E. coli*

2.2.11.1. Purification of 6 X histidine tagged proteins

Recombinant proteins were expressed in *E. coli* strain BL 21(De3)pLYS by growing cultures to OD₅₉₅ 0.7 at 37°C or 28°C and inducing them with 2 mM IPTG for 3-6 h. Cells were centrifuged and resuspended in lysis buffer. Subsequently, the cells were lysed by sonication. The crude protein lysates were cleared by centrifugation at 13,000 g. If foaming was produced during sonication, antifoaming agent n-octanol was added to the buffer. HIS₆-fusion proteins were bound at 4°C to Ni²⁺-NTA resin (Qiagen), which was equilibrated in lysis buffer. The resin was washed with ten times bed volume washing buffer containing 25 mM imidazole. Bound proteins were eluted with 250 mM imidazole in washing buffer. The purified proteins were dialyzed in Tris-EGTA buffer using three times buffer change.

Lysis Buffer (pH 7.5-8.0)	50 mM Tris.HCl (pH 7.5), 300 mM NaCl, 25 mM Imidazole, 10% glycerol, 2 mM β-mercaptoethanol, 0.5% Triton X-100, 20U benzonase (i.e. DNase Boehringer), 1 mM MgCl ₂ , 500 µl Protease inhibitor cocktail, 4g of bacterial pellet, lysozyme (250 µg/ml)
Washing buffer	50 mM Tris (pH 7.5), 300 mM NaCl, 25 mM imidazole, 10% glycerol, 2 mM β-mercaptoethanol, 0.5% Triton X-100
Elution buffer	50 mM Tris (pH 7.5), 300 mM NaCl, 250 mM imidazole, 10% glycerol
Dialysis Buffer	50 mM Tris.HCl (pH 7.5), 0.1 mM EGTA, 1mM PMSF

2.2.11.2. *In vitro* protein kinase assays

Protein kinase assays were performed in a total volume of 12.5 µl in 1 X kinase buffer containing 1 to 5 µCi (γ-³²P) ATP and 100 ng of purified kinase and 100 ng kinase substrate. The kinase reaction was initiated by the addition of ATP and the samples were incubated at RT for 1 h. The phosphorylation reactions were terminated by addition of 4 X SDS sample loading buffer supplemented with 100 mM EDTA. The kinase assays were analysed by resolving the samples on 12% SDS-polyacrylamide gels.

The gels were dried on Whatman 3MM filter papers in a gel dryer and exposed to X-ray film for autoradiography.

Kinase Buffer (5X) 20 mM HEPES (pH 7.5), 2.5% Triton X-100, 10 mM MnCl₂, 50 mM NaF, 25 mM β-glycerophosphate, 5 mM PMSF, 5 x plant protease inhibitor cocktail (Sigma)

2.2.11.3. Protein kinase assay with SAMS peptide

SAMS-peptide (HMRSAMSGHLVKRR) stock solution of 560 μM resulting in a final concentration of 44 μM, and 1 to 5 μCi (γ-³²P) ATP were used in the kinase assay. Kinase assay was performed exactly in same way as described above. The enzyme activities were measured after loading the samples onto P11 filters and washing by a scintillation counter as described by Sugden et al. (1999).

2.2.12. Plant growth conditions

Arabidopsis thaliana plants were grown in 7 x 7 cm plastic pots in trays at 22°C day and 18°C night temperature, 70% humidity under short days (8h light/16 h dark) for 2 weeks, then transferred under long day conditions (16 h light/8 h-dark period) under 200 to 400 μEinstein m⁻²s⁻¹ irradiance in the green house.

2.2.12.1. Agrobacterium-mediated plant transformation (Clough and Bent, 1988)

Floral dip transformations of *Arabidopsis thaliana* Col-0 wild type and T-DNA insertion mutants were performed using the *Agrobacterium* strain GV3101 (pMP90RK) carrying various binary vectors. After *Agrobacterium* infiltration, plants were covered with a plastic bag with slots for aeration, which were removed after 2 days.

2.2.12.2. Seed sterilization and selection of transgenic and mutant plants (Koncz et al., 1994)

Arabidopsis thaliana seeds were surface sterilized in Eppendorf tubes with 1 ml of 5% calcium hypochlorite containing 0.02% Triton X-100 (or 10% (v/v) sodium hypochlorite, 0.1% Triton X-100) for 15 min, pelleted by centrifugation, washed five times with 1 ml of sterile water, dried, and germinated on 0.5x MS agar plates exposed to a 16 h light/8 h dark period at 25°C as described by Koncz et al. (1994). Alternatively, seeds were soaked in 96% ethanol for 5 min. and 15 min in 25% sodium-hypochlorite bleach solution, washed four times in sterile dH₂O. After sterilization seeds were either stratified for 2 days at 4°C (if seeds were stored at RT), or were spread on the seed germination 0.5 MS medium containing appropriate antibiotics (i.e. 100 mg/m kanamycin or 15 mg/ml hygromycin or 12 mg/l sulfadiazine (4-amino-N-[2-pyrimidinyl]benzene-sulfonamide-Na) for GABI-Kat lines and 10mg/l BASTA (phosphinotricine) for WISCONSIN lines).

2.2.12.3. Hormone and stress treatments

Stress treatment were performed with two-weeks old plants. Seeds from wild type, *pr11* and various transgenic lines were germinated in solid 0.5 MS seed germination medium (Koncz et al., 1994). Seedlings were transferred into liquid MSAR seed medium containing either 3% sucrose, or 0.2 mM salicylic acid, or 100 μ M ABA or no sucrose. Different hormone/stress treatments were performed according to Németh et al. (1996).

2.2.12.4. Isolation of T-DNA knockout mutants

Arabidopsis T-DNA knockout mutant lines carrying T-DNA insertions in the *DPBF4* (At2g41070) and *SNF4* (At1g09020) genes were identified by screening the SALK, Wisconsin and GABI-KAT T-DNA mutant populations.

The Plant Biotechnology lab at the university of Wisconsin, Madison has generated a 72,960 BASTA (Glufosinate) resistant lines transformed with an activation-tag vector, pSK1015 (Weigel et al., 2000). An *AtSNF4* T-DNA knockout line was identified by screening for mutants with *AtSNF4* specific primers (see above) in combination with Wisconsin T-DNA left border primer (JL202). The SALK and GABI-KAT T-DNA populations were also screened to obtain additional T-DNA insertion mutants using standard PCR methods with T-DNA LB and RB primers in combination with *AtSNF4* specific primers.

We in the MPIZ (cologne) have generated a collection of *Arabidopsis* mutants consisting of 92,000 lines, which carry about 230,000 random insertions of the *Agrobacterium* transferred DNA (T-DNA) in their chromosomes (Rios et al., 2002). We screened our insertion mutant collection to identify *DPBF4* knockout mutant lines by a novel PCR based technology according to Rios et al. (2000). Genomic DNA was isolated from plant tissues and PCR was performed with the FISH1/LB and FISH2/RB and *DPBF4* gene specific primers.

2.2.12.5. Protoplast transformation and transient gene expression assays

Arabidopsis thaliana cell suspensions grown to logarithmic phase were subcultured and grown for two days. Cells were collected by centrifugation at 1,500g for 5 min in a 50ml Falcon tube. Supernatant was discarded and cells were resuspended in 25 ml of enzyme solution and then the volume was made up to 50 ml with B5 0.34M GM medium. The cells were shaken at RT for 4h at 6 rpm. Subsequently, the cells were collected by centrifugation for 5 min 1,500 g, the supernatant was discarded and cells were resuspended in 25 ml of B5-0.34 M GM medium and pelleted again at 800 g. The pelleted cells were resuspended in 5 ml of B5-0.28M medium. Upon centrifugation at 800 g for 5min, the floating protoplast were collected. The concentration of viable protoplasts was measured using a haemocytometer. Approximately, 1.4×10^6 protoplasts were used for each transformation experiment. The protoplast were transformed with 5 μ g of plasmid DNA in 25% PEG solution. To check the transformation efficiency, in all experiment we included a control transformation with 15 μ g of the 35S::GFP plasmid as an indicator. All constructs for overexpression of protein of interest were

prepared in a small vector (4kb), in which cDNA or gene sequences encoding epitope tagged proteins were driven by the promoter of the Cauliflower Mosaic Virus (CaMV) 35S RNA gene. After transformation, the cells were cultivated for 8 to 16 hrs at RT in B5-0.34M GM medium. Samples were examined using a haemocytometer and an UV microscope (Leica, stereomicroscope) for the presence of GFP fluorescence and assayed by Western immunoblot analysis.

B5-0.34M GM	MS powder 4.3 g/l, 30.5 g glucose, 30.5g mannitol (pH 5.5)
B5-0.28M Sucrose	MS powder 4.3g/l, B5 0.28 M sucrose (pH 5.5)
Enzyme Solution:	1% Cellulose (0.5g/50ml), 0.2% Macerozyme (Yakult), 0.1g/50ml in B5-0.34 M medium
PEG solution	25% PEG (6000) in 0.45M mannitol, 0.1M Ca (NO ₃) ₂ (pH 9.0)

2.2.12.6. GUS histochemical assay (Jefferson et al., 1987)

The activity of various promoter-GUS reporter gene construct in transgenic plants was monitored by GUS histochemical assays using 4-methyl-umbelliferyl- β -glucuronide as substrate. For Gus histochemistry, the plant material was stained overnight at 37°C in a solution containing 1mM 5-bromo-4-chloro-3-indolyl β -glucuronide (X-Gluc), 50mM sodium phosphate (pH 7.0), 0.1% Triton X-100, 10mM EDTA, 0.5 mM K₃Fe(CN)₆ and 0.5 mM K₄Fe(CN)₆. The plant material was cleared by washes in 70% and stored in 95% ethanol at RT for microscopic inspections.

2.2.13. Generation of epitope tagged recombinant proteins for biochemical studies

The DPBF4 and AtSNF4 cDNAs were labeled with the coding domain of hemagglutinin (HA) or cMYC epitopes. Specific primers were designed for amplification of cDNA to obtain fragments, which could be inserted in frame with the coding sequence of either HA and cMYC epitope tags. The PCR amplified cDNAs were cloned either directly in frame with the epitope coding sequence in the high copy E. coli cloning vectors pPILY and pLOLA (Figure 7 A, B) or in the binary vectors pPCV812-PILY and pPCV812-GIGI (Figure 8 C, D). From pPILY and pLOLA the expression cassettes were transferred into binary vectors as *NotI* fragments (see below, Ferrando et al., 2000a, b). The binary vectors carrying the cDNA expression cassettes were transformed into the *Agrobacterium* host GV3101 (pMP90RK; Koncz and Schell, 1986; Koncz et al., 1994) by electroporation. *Arabidopsis* plants and root cell suspensions were transformed by *Agrobacterium* and stable lines were produced for biochemical analysis as described by Ferrando et al. (2000 a, b).

2.2.13.1. Plasmids used for expression of epitope labeled proteins

The construct depicted below were described by Ferrando et al. (2000 a, b). *NotI* fragments from pPILY and pLOLA were moved into polylinker regions of the binary vectors pPCB812 or pPCV002 (Mathur et al. 1998; Koncz and Schell, 1986) by blunt-end ligation.

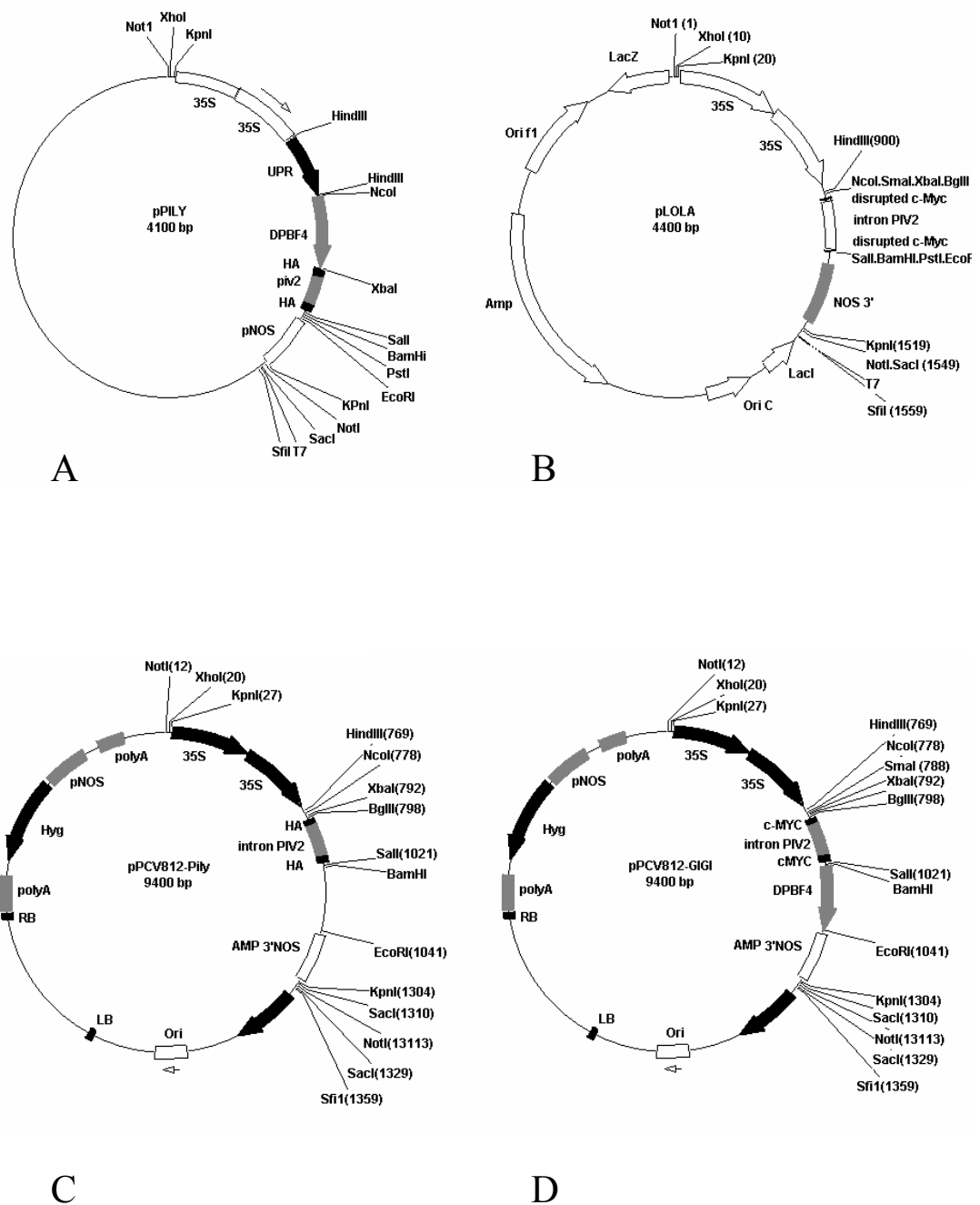


Figure 7. Schematic maps of epitope tagging vectors pPILY (A), pLOLA (B), pPCV812-PILY (C), and pPCV812-GIGI (D).

Abbreviations: pNOS – promoter of the pTiC58 Ti plasmid T-DNA-encoded nopaline synthase gene, polyA – 3' polyadenylation sequences derived from the pTiAch5 Ti plasmid T-DNA encoded octopine synthase gene; 3'-NOS – nopaline synthase polyadenylation sequences; 35S – CaMV 35S promoter; c-Myc and HA – cMYC and hemagglutinin epitope coding sequences (see Ferrando et al., 2000 a, b).

3. RESULTS

3.1. ANALYSIS OF REGULATORY FUNCTION, EXPRESSION AND POST-TRANSLATIONAL MODIFICATION OF THE bZIP TRANSCRIPTION FACTOR DPBF4

3.1.1. Identification of DPBF4 via yeast one hybrid screening with the G-box containing promoter region of the aspartate kinase AK1/HSD1 gene

A primary goal of this Ph.D was to identify regulatory factors that control the expression of the AK1/HSD1 aspartate kinase gene that is involved in the regulation of the biosynthesis of essential amino acids lysine, threonine and proline. As the G-box/ABRE-like promoter element responding to sugar-regulation in the promoter of AK1/HSD1 gene (Zhu-Shimoni and Galili., 1998) showed close similarity to the G-box/ABRE motif of the well-characterized promoter of alcohol dehydrogenase *ADHI* gene (Dolferous *et al.*, 1996), we performed parallel studies using wild type and modified derivatives of the *ADHI* promoter. Previous analysis of the *AK1/HSD1* and *ADHI* promoter thus provided a basis for initiation of a genetic screen in the so-called yeast one-hybrid system with the aim to identify transcription factors that bind to the putative *AK1/HSD1* sugar-response element and control transcription in a glucose-regulated fashion in yeast. This experiment was performed in close collaboration with Dr. Aviah Zilberstein and Shai Ufaz in the frame of a Minna James Heineman Foundation supported joined project. The yeast one-hybrid screen described below was performed by Shai Ufaz.

In the promoter of the *AK1/HSD1* gene previous deletion analysis has identified a region of 196 bp (between positions -238 and -42 upstream the transcription start site) that proved to be sufficient for transcriptional activation of a GUS reporter gene by sucrose and phosphate in transgenic tobacco plants (Zhu-Shimoni and Galili, 1998). In order to screen for transcription factors binding to this *AK1/HSD1* promoter region, we have constructed two yeast reporter strains by introducing the 196 bp promoter fragment upstream of the HIS3 and CYC1 minimal promoters driving the expression of HIS3 and lacZ reporter genes, respectively. Using a cDNA library prepared from *Arabidopsis* cell suspension in the vector pACT2, cDNA-encoded proteins were expressed in fusion with the Gal4-activation domain in the HIS3 reporter strain. To screen for binding of transcription factors to the *AK1/HSD1* promoter sequence, leading to the activation of the HIS3 reporter, 5×10^5 transformants were plated onto SD-plates containing 45 mM 3-AT, which resulted in 100 clones. Subsequent stringent selection in SD-medium containing 60mM 3-AT reduced the number of candidate clones to eight. The pACT2 vectors were rescued from the HIS3 reporter strain and their trans-activation capability was further tested in the lacZ reporter strain by filter lift assays, which identified only two clones displaying blue staining on filters containing X-Gal. Sequencing the pACT2 inserts rescued from these clones, identified two cDNA sequences, both of which carried coding region of the DPBF4 transcription factor (At2g41070; Kim *et al.*, 2002b). AtDPBF4 (named alternatively as EEL1 and AtbZIP12; Bensmihen *et al.*, 2002, Jakoby *et al.*, 2002) belongs to a family of transcription factors that

interact with promoters of Late Embryogenesis Abundant (LEA) genes and confer seed specific and ABA-induced transcription of several genes, including AtEm1 and AtEm6 (Brocard et al., 2002; Bensmihen et al., 2002).

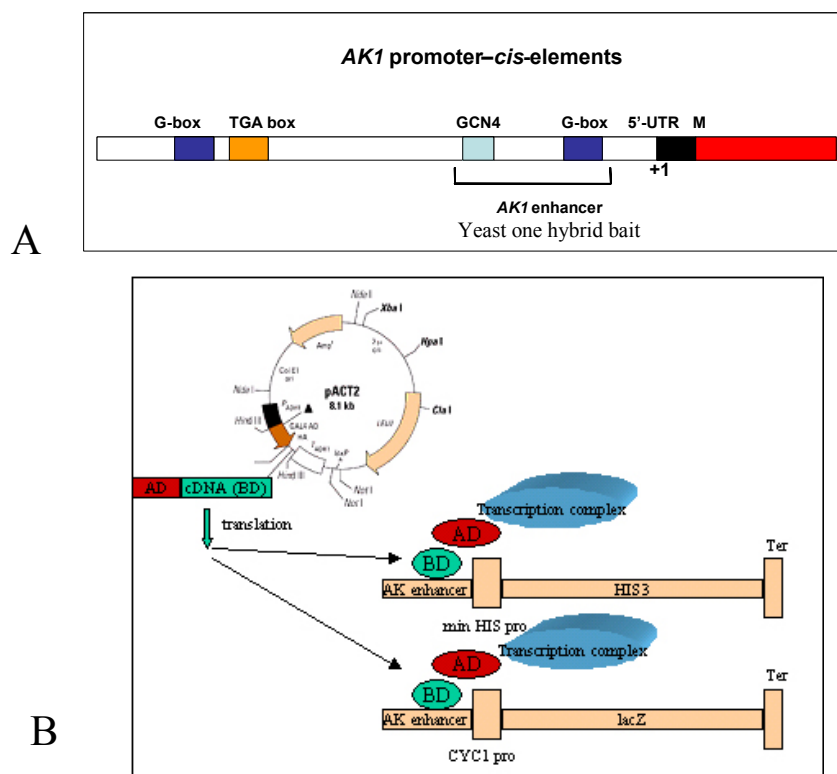


Figure 8. Yeast one-hybrid screen with the sugar responsive enhancer element of the *AK1/HSD1* promoter.

(A): The sugar responsive element identified by Zhu-Shimoni and Galili (1998) contains two slightly different G-box elements designated as GCN4 and G-box. (B) This enhancer region has been cloned into Matchmaker (Clontech) one-hybrid bait vectors upstream of yeast minimal promoters driving the expression of *HIS3* and *LacZ* reported genes. Yeast strain carrying the *AK1/HSD1* enhancer controlled *HIS3* reporter was transformed with a cDNA expression library made in pACT2, in which the cDNA encoded protein sequences are fused to an N-terminal transcription activation domain AD. cDNA encoded proteins that carry a DNA-binding domain BD, which recognizes the *AK1/HSD1* promoter elements, fused to the N-terminal AD domain will activate the transcription of the *HIS3* reporter gene in yeast. 3-AT selection was used for identification of *HIS3* expressing yeast transformants.

The 196 bp enhancer sequence of the *AK1/HSD1* gene, which was used as bait in the one-hybrid screen, contained two potential DPBF4-binding sites represented by GCN4 and G-box consensus sequences. The G-box motif carried identical sequences with a G-box/ABRE motif, which was demonstrated to bind DPBF4 *in vivo* (Kim et al., 2002). To test which motif was recognized by DPBF4 one-hybrid assays, Shai Ufaz modified these sequences separately by site-specific mutagenesis. The G-box motif 5'-ACACGTGG-3' was modified to 5'-ACCATGGG-3', whereas the GCN4 motif 5'-TTGACTCTA-3' was mutated to 5'-TTCTAGATA-3'. The resulting bait plasmids, pLacZ-GCN4 and pLacZ-G-box, were introduced into a yeast strain, which expressed DPBF4 in fusion with the Gal4-activation domain from pACT2-DPBF4. Whereas destruction of the GCN4 motif did not affect the trans-activation of the *lacZ* reporter gene, modification of the G-box consensus

abolished X-gal staining of colonies in filter lift assays indicating a lack of interaction between AtDPBF4 and the G-box mutant promoter bait (Figure 9).

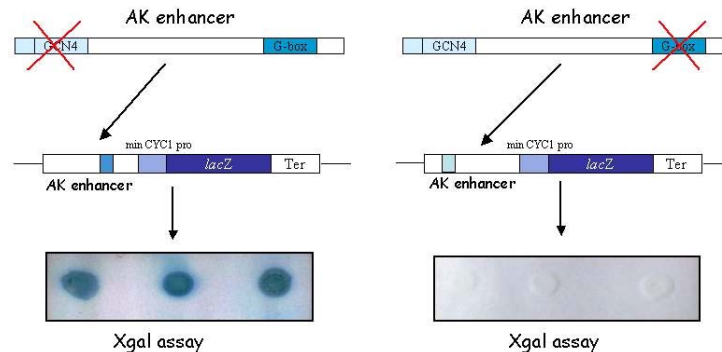


Figure 9. Identification of binding-site of DPBF4 in the sugar responsive enhancer domain of *AK1/HSD1* promoter.

The core AGCT and GCAT motives of G-box and GCN4 binding sites were altered by site specific mutagenesis in the enhancer domain of *AK1/HSD1*, which was cloned upstream of a yeast *CYC1* minimal promoter in yeast one-hybrid vectors carrying a *lacZ* reporter gene. Yeast strains harboring the pLacZ-GCN4 (with inactivated G-box) and pLacZ-G-box (with inactivated GCN4 box) were transformed with pACT2-DPBF4 and the activation of *AK1/HSD1* regulated *lacZ* reporter gene was tested using a filter lift assay.

3.1.2. DPBF4 is a member of the ABI5 bZIP transcription family

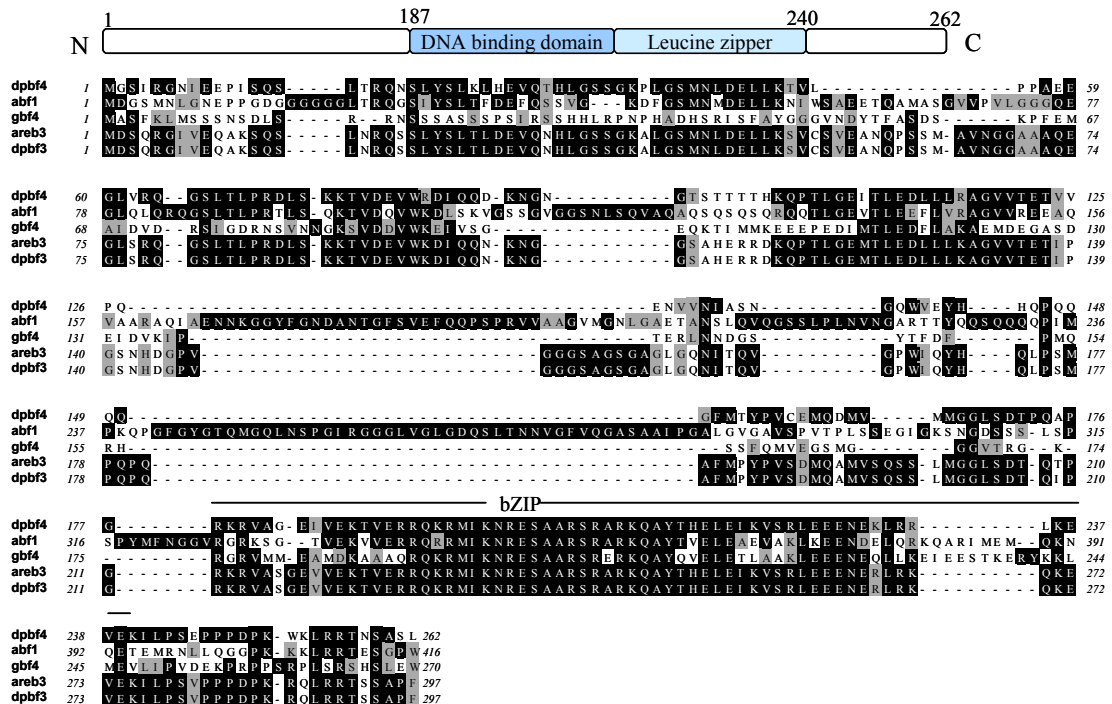


Figure 10. Comparison of DPBF4 protein sequences to some other members of the *Arabidopsis* bZIP family.

DPBF4 shares conserved C-terminal bZIP sequences with other members of the bZIP family, but carries divergent N-terminal sequences. The closest relative of DPBF4 is DPBF3, which proved to be identical with AREB3.

Nucleotide sequence analysis of cDNAs recovered in the pACT2 prey plamids confirmed the known DPBF4 amino acid sequence. DPBF4 belongs to the ABI5 family of bZIP transcription factors that bind to ABRE elements within ABA and sugar regulated promoters (for review see Yamaguchi-Shinozaki and Shinozaki, 2005). DPBF4 was originally designated as a homolog of the carrot *Dc3* Lea gene promoter binding factor-4, which carries leucine repeats near its C-terminus. This region is preceded by a basic domain. In addition to the ABI5 family, DPBF4 shows also a close structural similarity to other members of the ABF (ABRE binding factors), and GBF (G-box binding factors) families (for review see Jakoby et al., 2002; Figure 10). ABI5 and the closely related DPBF3 and DPBF4 factors are similar in their C-terminal leucine zipper domains, but carry divergent N-terminal sequences.

3.1.3. Regulation of DPBF4 expression in *Arabidopsis*

Since the DPBF4 cDNA was isolated from a cDNA library constructed from an *Arabidopsis* suspension culture, we assumed that *DPBF4* is expressed in dividing cells. (see: **footnote**) To examine the spatial expression pattern of the *DPBF4* gene, RNA was extracted from different organs of soil grown plants, two weeks old whole seedlings (grown under sterile conditions), and an *Arabidopsis* Col-0 cell suspension culture and subjected to semi-quantitative RT-PCR analysis.

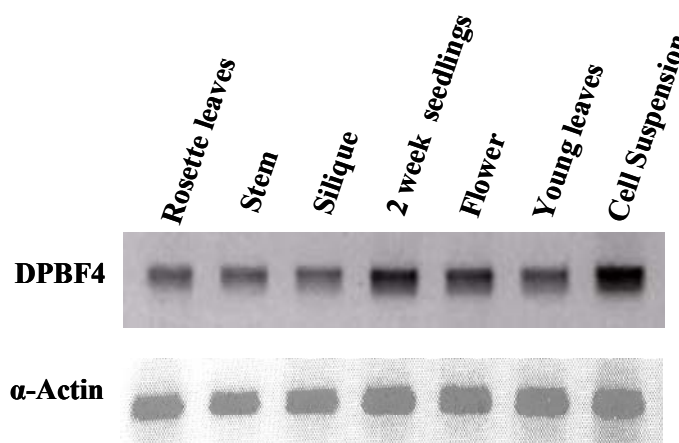


Figure 11. RT-PCR analysis of *DPBF4* expression in various organs of *Arabidopsis*.

Total RNA was prepared from different tissues of plants and subjected to RT PCR using DPBF4 gene specific primers. DPBF4 is expressed in different organs of plants and seedlings, and cultured cells of *Arabidopsis*: (1) rosette leaves, (2) stem, (3) silique, (4) in vitro cultured 2 week old plants, (5) flower, (6) young leaf, (7) cell suspension.

The specificity of the *DPBF4* oligonucleotides was determined by making a Blast search (Altschul et al., 1990) against whole *Arabidopsis* genome and taking those regions of the DPBF4 cDNA, which

Footnote: This was the timepoint of my entry into the project, and from this point on all experiments described below were performed by myself in the MPIZ (Cologne).

show the highest divergence in comparison to other bZIP sequences. α -actin primers were used as internal controls. The RT-PCR analysis revealed that *DPBF4* expression is significantly higher in actively dividing cultured cells as compared to rosette leaves, stems, siliques, leaves of 2 weeks old seedlings, and flowers and young leaves of 3 weeks old soil grown plants (Figure 11). Our RT-PCR data thus clearly showed that *DPBF4/EEL1* is not only expressed during early developmental stages in seeds, but is also active at a relatively high level in several vegetative plant organs, and particularly in actively dividing cells. Therefore, our data contradict with a previous report by Bensmihen *et al.* (2003), who claimed that *DPBF4* is expressed only in a short window of seed germination period. Inspection of combined microarray transcript profiling data in the Genevestigator database (<https://www.genevestigator.ethz.ch>) indicated that *DPBF4* was found in various experiments to be expressed in actively dividing cultured cells and calli, as well as in inflorescence, roots, and siliques, in addition to seeds. To confirm these data, we repeated our RT-PCR experiments with three sets of independently isolated RNA samples, but we found no deviation from the results displayed in Figure 11. Therefore, our data suggest that *DPBF4* is expressed in dividing vascular tissues of leaves, stems, roots and inflorescence (i.e. probably in response to sugar because *DPBF4* expression is upregulated by sugar in the sucrose and glucose hypersensitive *pr11* mutant) as in dividing cells of calli and cell cultures.

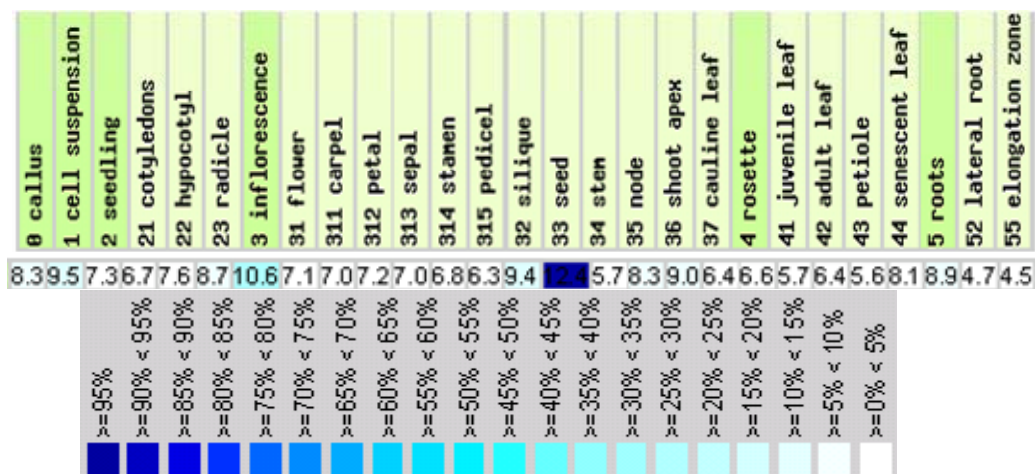


Figure 12. *DPBF4* expression data in the Genevestigator microarray transcript profiling database.

According to Genevestigator, expression of *DPBF4* is indeed high in seeds (100%), but well detectable in several other organs.

In order to study the activity pattern of the promoter of *DPBF4* gene, I have PCR amplified 5'-regulatory sequences of *DPBF4* extending 2kb upstream from the ATG codon and, after confirmation of error-free PCR-amplification by sequencing, cloned the promoter region upstream of a promoterless β -glucuronidase (*GUS*) gene in the promoter test vector pPCV812 (Koncz *et al.*, 1994). Following transformation, the T2 progeny of 10 independent transgenic plants was examined by germination of seedlings on 0.5 MS medium containing either 0.5% or 3% sucrose by performing histochemical *GUS* staining of seedlings 3, 4 and 10 days after germination. In other experiments, 10 days old seedlings were transferred to 3% sucrose-containing medium for 24 hours followed by histochemical *GUS* staining. Discouragingly, however, none of the plants displayed any *GUS* expression under the

conditions tested. RT-PCR analysis of the promoter-GUS constructs revealed no GUS mRNA in these seedlings, but indicated normal expression of the endogenous wild type *DPBF4* gene. Thus, the data indicated that sequences located 3'-downstream of the ATG start codon are essential for detectable expression of the *DPBF4* gene in plant tissues (data not shown).

3.1.4. Screening for *dpbf4* T-DNA insertion mutants in Köln T-DNA mutant collection

For systematic functional analysis of *DPBF4*, we have screened a T-DNA insertion mutant collection, which was established by our group (including my participation, see Ríos et al., 2002) in Cologne. Using a novel PCR-based screening approach, I have identified a pool of mutant seeds, which carried a T-DNA insertion in the 5'-UTR of *DPBF4*. Subsequently, DNA templates were prepared from this pool of 100 mutant plants and arranged in a 10 x 10 array. A second turn of PCR screen performed with pooled DNA templates of 10 rows and 10 columns of this array lead to the identification of a single plant line, which carried a T-DNA insertion in heterozygous stage in the 5'-UTR sequence of *DPBF4*. Nucleotide sequencing of PCR-amplified T-DNA-plant DNA insert junctions from this line showed that the insertion was localized in the 5' untranslated leader sequence of *DPBF4* at nucleotide nucleotide position -513 upstream of the ATG codon (i.e. -119 nucleotides upstream of the predicted 5'-end of *DPBF4* mRNA). This mutant allele was designated *dpbf4-1*.

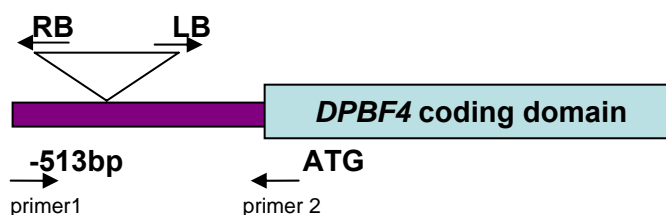


Figure 13. Schematic representation of localization of T-DNA insertion in the mutant allele *dpbf4-1*.

Sequencing of PCR-amplified left (LB) and right (RB) border junctions in the *dpbf4-1* allele revealed that the T-DNA insertion was located 513bp upstream of the ATG codon.

In order to select for lines carrying the *dpbf4-1* mutant allele in homozygous form, M3 seedlings were grown on selective medium containing hygromycin. From seedlings, which expressed the T-DNA encoded selectable hygromycin resistance gene and thus grew on the selective plates, genomic DNA was prepared and analysed by PCR. To detect the mutant allele, gene specific primers (Figure 13, primers 1 and 2) were designed to 5' and 3' positions of the *DPBF4* 5'-UTR sequences flanking the insertion. As control, the left border junction of T-DNA tags was detected in each line with a combination of primer 2 with the T-DNA specific LB (FISH1, see Materials and methods and Ríos et al., 2000) primer (Figure 14).

To confirm homozygosity of the *dpbf4-1* allele, a Southern DNA hybridization analysis was performed. Genomic DNA was prepared from wild type and *dpbf4-1* seedlings, digested with EcoRI, size separated by electrophoresis in a 0.8% agarose gel and blotted onto a nylon membrane. The

Southern filter was hybridized with a DIG-labeled *DPBF4* cDNA probe, which showed a typical shift in size upon labeling with DIG-UTP (Figure 15).

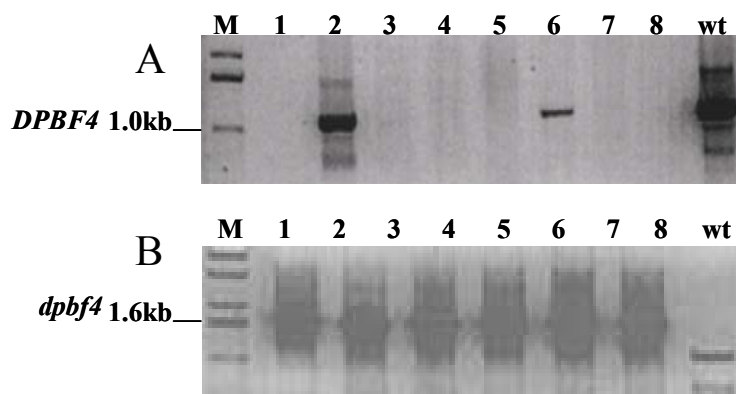


Figure 14. Identification of M3 lines homozygous for the *dpbf4-1* mutant allele.

(A) PCR was performed with primers 1 and 2 (located 5'-upstream and 3'-downstream of the position of T-DNA tag) using genomic DNA templates prepared from individual insertion lines. 1.0 kb is the predicted size of PCR product in wild type plants. The PCR results thus shows that except line no. 2 and 6 all other lines were homozygous for the *dpbf4-1* allele. (B) PCR amplification of the left border junction of T-DNA insertion in the segregating *dpbf4-1* lines. The PCR was performed with the T-DNA LB primer and gene specific primer 2 providing a product of 1.6 kb.

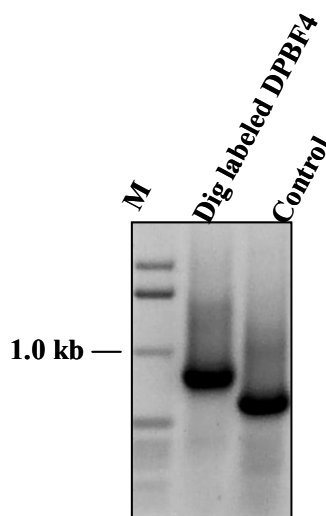


Figure 15. DIG-labeling of DPBF4 cDNA probe by PCR.

A DPBF4 cDNA fragment of 800bp was labeled with a DIG-labeling kit (Roche, Germany) using PCR. Incorporation of DIG-conjugated UTP into the probe results in a shift of size as compared to the unlabelled control DNA fragment.

Southern hybridization analysis of DNAs prepared from the segregating M3 lines, as the PCR analysis, identified plants carrying the *dpbf4-1* allele in either homozygous and heterozygous form (Figure 16A).

To determine how the insertion of the T-DNA tag in the 5'-UTR affected the expression of the *DPBF4* gene, we performed a comparative northern RNA hybridization analysis of homozygous and heterozygous *dpbf4-1* mutants and wild type control plants. Total RNA was prepared from individual lines of DPBF4 T-DNA insertion mutant identified as homozygous and heterozygous lines by

Southern hybridization. RT-PCR was performed with equal amount of RNA samples (10 μ g) using *DPBF4* cDNA specific 5' and 3' primers (Figure 16B).

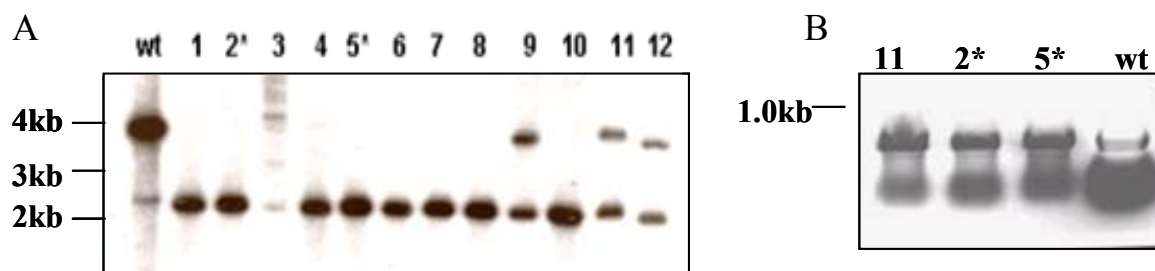


Figure 16. The *dpbf4-1* mutation does not abolish gene expression.

(A) Southern analysis of genomic DNAs prepared from individual M3 plants carrying the *dpbf4-1* mutation. Genomic DNA was digested with *EcoRI* and probed with a DIG-labeled *DPBF4* cDNA probe. Lanes 9, 11 and 12 were heterozygous for the insertion, whereas all other lines carried the *dpbf4-1* allele in homozygous form. (B) RT-PCR amplification of *DPBF4* transcript from homozygous lines 2 and 5 (*dpbf4-1/dpbf4-1*) and heterozygous line 11 (*dpbf4-1/+*), as compared to wild type. Amplification of a segment of wild type *DPBF4* cDNA in all lines indicated that the *dpbf4-1* mutation did not abolish gene transcription.

The results of RT-PCR analysis clearly indicated that a wild type *DPBF4* transcript is equally produced in wild type, *dpbf4-1/+* and *dpbf4-1/dpbf4-1* lines indicating that the T-DNA insertion in the 5'-UTR did not prevent normal transcription of the *DPBF4* gene.

3.1.5. Searching for *dpbf4* insertion mutations in the Salk T-DNA mutant population

To search for other *dpbf4* mutant alleles, we inspected the SALK T-DNA mutant population and identified two additional T-DNA mutant alleles of *DPBF4*, which were present in the SALK_025758 and SALK_21965 lines. The online information suggested that a T-DNA tag was located in the 5' untranslated leader sequence of *DPBF4* in the SALK_025758 line, whereas the SALK_21965 line was predicted to carry a T-DNA insertion in the second exon. In order to confirm the positions of these T-DNA insertions, we have PCR genotyped the segregating M2 progeny of these SALK lines and (upon amplification with combinations of *DPBF4*-specific and T-DNA specific SALK left border (LB) or right border (RB) primers) sequenced the T-DNA-plant DNA junctions in these mutant lines.

When growing the M3 progeny, we could not follow the segregation of T-DNA encoded kanamycin resistance marker, which was silenced in these T-DNA-tagged lines. Therefore, to identify homozygous mutant lines, we prepared DNAs from individual M3 progeny and performed PCR screening using three primer combinations: i) a pair of gene specific primers positioned upstream and downstream of the *DPBF4* coding domain; ii) 5' *DPBF4* primer with both T-DNA end specific primers (independently) and iii) 3'-*DPBF4* primer with the T-DNA end specific primers in separate reactions.

3.1.5.1. PCR genotyping the *Salk_025758* insertion mutant line

To identify the T-DNA insertion position in the *Salk_025758* mutant line, 11 M3 progeny were PCR genotyped. Using combinations of the *DPBF4* 5' primer with the T-DNA right (RB) and left (LB) border primers we failed to obtain a PCR product indicating that the right end of the T-DNA insertion suffered a deletion (Figure 17A). Nonetheless, sequencing of a DNA fragment obtained by PCR amplification with the *DPBF4* 3' primer and T-DNA LB primer indicated that the T-DNA insertion was localized in the first exon, which encodes a transcribed, but not translated region of the *DPBF4* mRNA. In the the *Salk_025758* mutant, designated as the *dpbf4-2* allele, the position of the T-DNA insertion was located 347 bp upstream of the ATG codon, which defines the start of exon2 (Figure 17B)

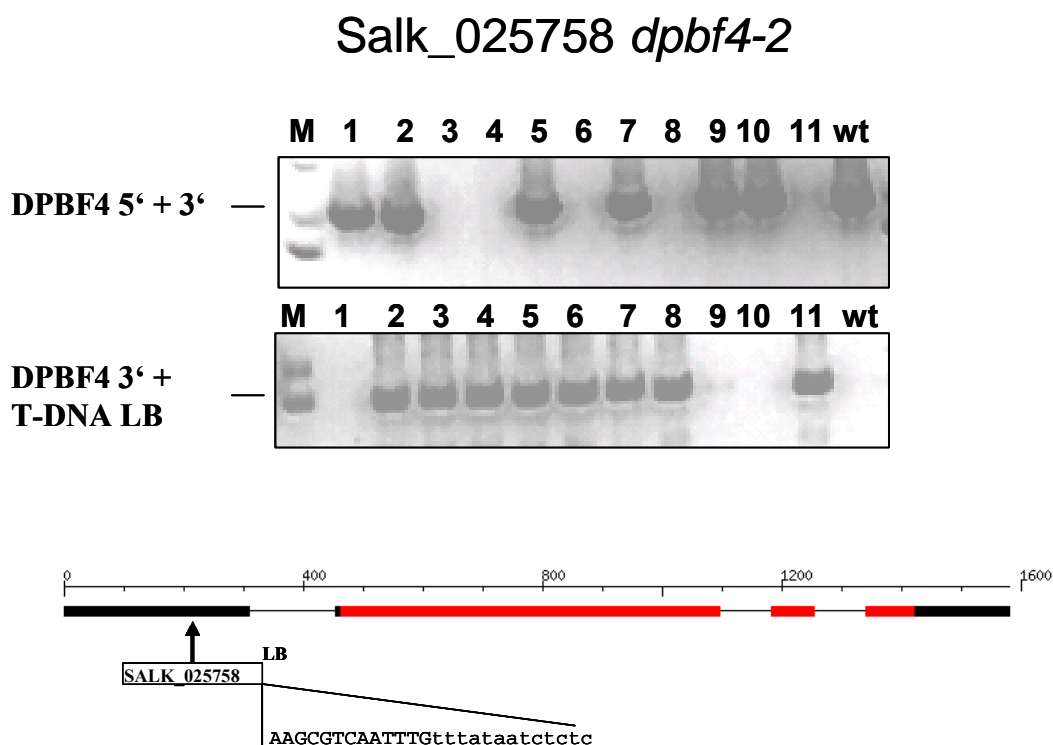


Figure 17. PCR genotyping the SALK_025758 mutant line and identification of the *dpbf4-2* mutant allele. From the SALK-025758 lines 11 M3 progeny was PCR genotyped with the *DPBF4* 5' and 3' gene specific primers and a combination of *DPBF4* 3' primer and SALK T-DNA LB primer. Neither the LB nor the RB primer of T-DNA resulted in amplification of a product with the *DPBF4* 5' primer indicating a deletion of T-DNA end facing the 5'-end of the *DPBF4* gene. The amplified T-DNA junction was sequenced indicating that the T-DNA insertion in the *dpbf4-2* allele is located in exon 1, which codes for transcribed, but nontranslated 5'-leader of *DPBF4* mRNA. The lower section of the figure shows schematic structure of *DPBF4* and the position of the insertion. In the sequence of T-DNA plant DNA junction capital letter mark T-DNA sequences, whereas letters in lower case correspond to *DPBF4* sequences. During the integration 5bp were retained from the 25bp border repeat of the T-DNA. Upstream of the left border (LB), the T-DNA carries a CaMV35S promoter, which directs transcription across the LB

3.1.5.2. PCR genotyping the SALK_21965 insertion mutant line

In case of the SALK_21965 line, 16 M3 lines were analysed by PCR genotyping (Figure 18). The results showed no amplification with the T-DNA right border RB primer, whereas the T-DNA left border primer provided a PCR product with both 5' and 3' *DPBF4*-specific primers indicating that the

the SALK_21965 line carried a head to head (LB-RB/RB-LB) inverted T-DNA repeat. Sequencing the PCR-amplified T-DNA plant DNA border junctions indicated that the T-DNA insertion was located in the second exon 283bp downstream of the ATG codon (Figure 18).

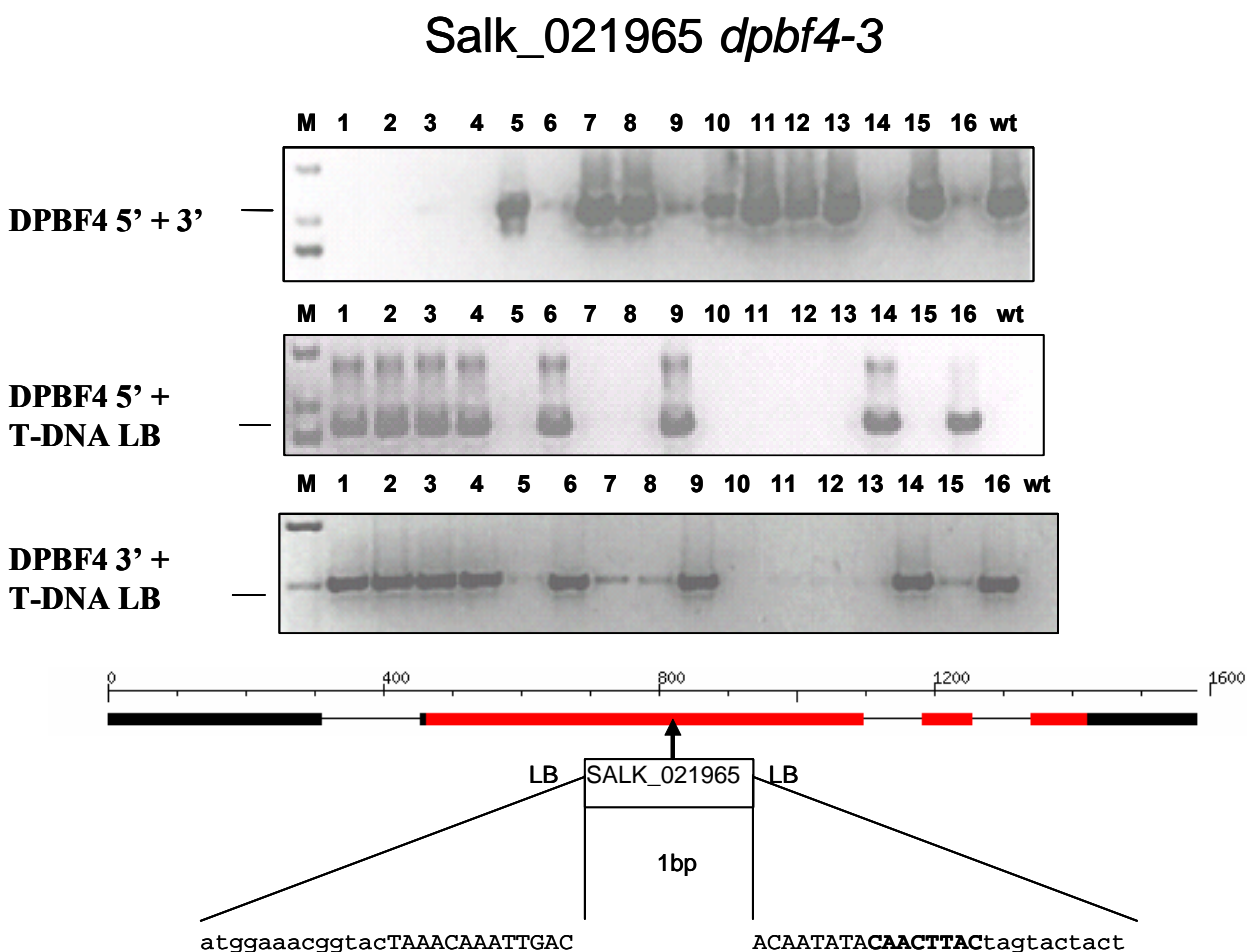


Figure 18. PCR genotyping the SALK_021965 mutant line and identification of the *dpbf4-3* mutant allele. From the SALK_021965 mutant line 16 M3 progeny was PCR genotyped using the *DPBF4* 5' and 3' primers, and combination of the T-DNA LB primer with the *DPBF4* gene specific primers. The analysis indicated that the SALK_021965 line carries an inverted (LB-RB/RB-LB) T-DNA repeat in exon2 of *DPBF4*. This mutant allele was designated *dpbf4-3*. Sequencing the T-DNA insert junctions showed that the T-DNA integration event resulted in 1bp deletion in the integration target site. At the 5' LB-border junction 5bp were retained from the 25bp LB repeat of the T-DNA. At the 3' LB border junction 17bp from the LB 25bp repeat was retained and followed by 8bp filler DNA.

3.1.5.3. RT-PCR analysis of transcription of *dpbf4-2* and *dpbf4-3* mutant alleles

To test transcription of the T-DNA insertion mutant alleles *dpbf4-2* and *dpbf4-3*, RNA was prepared from putative homozygous M3 families 6, 8 and 11 of the Salk_025758/*dbpb4-2* mutant and M3 families 1, 2, 3, 4 and 14 of the Salk_021965/*dpbf4-3* mutant for RT-PCR analysis with the *DPBF4* cDNA specific primers. The RT-PCR analysis revealed that the *dpbf4-2* mutant allele, which carries a T-DNA tag in exon 1 is normally transcribed (i.e. producing a cDNA product of 800 bp; see Figure 19), probably by the CaMV35S promoter, which is located upstream of the left T-DNA end and thus faces the insert junction with exon 1. By contrast, RT-PCR resulted in no amplified cDNA product with RNA templates from homozygous Salk_021965 lines demonstrating that the *dpbf4-3* mutation

corresponded to a genuine knockout allele. This is consistent with the sequencing results showing that in *dpbf4-3* the T-DNA insertion disrupted exon 2.

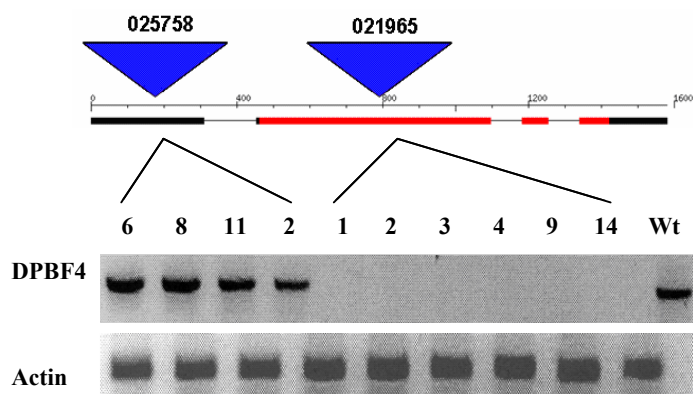


Figure 19. RT-PCR analysis of transcription of *dpbf4-2* and *dpbf4-3* alleles.

RNA samples were isolated from homozygous *dpbf4-2* and *dpbf4-3* mutant lines (see Figures 17 and 18) and used as templates in RT-PCR reactions with *DPBF4* gene specific primers. Wild type genomic DNA was used as positive control for PCR. The lower panel shows control RT-PCR reactions with the same RNA samples using actin primers.

3.1.5.4. Phenotypic characterization of *dbpf4* insertion mutants

Soil-grown plants carrying all three *dpbf4* insertion alleles showed normal development and seed set. The seeds of all the mutants germinated as wild type in the presence of 0.5% and 3% sugar, indicating that the *dpbf4-3* knockout allele had no dramatic effect on the regulation of seed development, desiccation and dormancy. These data confirmed the observations of Bensmihen et al. (2002; 2005), who concluded that DPBF4 alone is not critical for the control of seed specific functions. Further analysis of the *dpbf4-3* knockout line and its responses to various stress conditions, as well as testing changes in *dpbf4-3* vegetative tissues to ABA, sugar and other forms of osmotic stress are in progress.

3.1.6. Epitope Tagging of DPBF4 for biochemical studies

To perform biochemical studies *in vivo*, the DPBF4 coding region was fused to an intron tagged hemagglutinin (HA) epitope sequence and expressed in *Arabidopsis* cells by *Agrobacterium*-mediated transformation. The intron sequences are not processed in *Agrobacterium* preventing unwanted expression driven by plant promoters in bacteria (Ferrando *et al.*, 2000). To epitope tag DPBF4, the cDNA coding sequence was PCR amplified to generate *NcoI-XbaI* restriction sites for directional cloning and the PCR fragment was cloned in vector pPILY in frame with a C-terminal intron-tagged HA epitope (Ferrando *et al.*, 2000). The expression cassette from pPILY was moved by *NotI* into the binary vector pPCV812. The DPBF4 cDNA was also PCR amplified to generate *BamHI-EcoRI* restriction sites and cloned in frame with the intron-tagged HA epitope in the binary vector pPCV812-Menchu to create an N-terminal epitope fusion. Both constructs described above were transferred into the *Agrobacterium* host GV3101 (pMP90RK) by electroporation. *Arabidopsis* plants and cell suspension were thereafter transformed to produce transgenic plants and cell lines.

3.1.6.1. Verification of expression of epitope-tagged DPBF4 constructs in *Arabidopsis* cells

Crude protein extracts were prepared from 2X35S::HA-DPBF4 overexpressing wild type plants and 2X35S::DPBF4-HA overexpressing cell suspension. From each sample, 5 μ g of protein was resolved by SDS-PAGE and analyzed by Western blotting with anti-HA antibody. Plant lines 1, 2, 3, 5, 6 and 9 in lanes 2, 3, 4, 6, 7 and 10 showed production of the epitope tagged HA-DPBF4 protein (Figure 20A). The production of DPBF4-HA protein was similarly tested in a stably transformed *Arabidopsis* Col-0 cell suspension, as in transgenic plants, CaMV35S promoter driven expression of the epitope tagged construct conferred production of DPBF4-HA protein at a significantly high level in cultured cells.

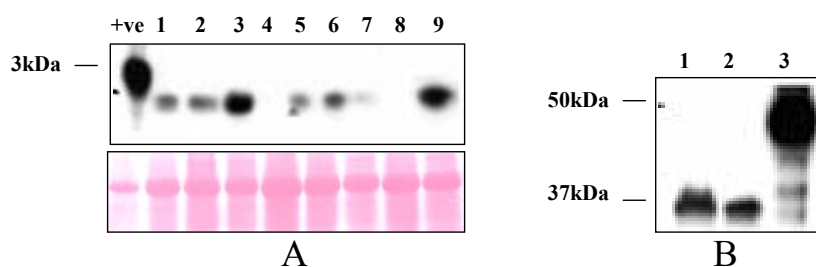


Figure 20. Western blot analysis of protein extracts prepared transgenic plants and cell suspensions expressing HA-DPBF4 and DPBF4-HA, respectively.

(A) Protein extracts were prepared from twelve day old wild type seedlings carrying the pPCV812-HA-DPBF4 construct and size separated a 12% SDS/polyacrylamide gel. Followed by Western blotting, the HA-DPBF4 protein was detected using an anti-HA antibody. Each lane contained 5 μ g of protein. (B) Equal amount of protein extracts prepared from cell suspensions transformed with the pPCV812-DPBF4-HA construct were subjected to SDS-PAGE followed by Western blotting using a monoclonal anti-HA antibody. Lane 1 and 2 contain proteins from different cell suspension lines. Lane 3 is positive control (i.e., the HA-PAM1 histone arginine methylase protein (fig.A) and HA-SNF4 protein (B) for testing the specificity of anti-HA antibody.

3.1.7. DPBF4 is a nuclear protein

To determine the intracellular localization of DPBF4, the pPCV812-HA-DPBF4 expression construct was transformed in both dark-grown *Arabidopsis* Col-0 and light-grown *Arabidopsis* Ler cell suspensions as light conditions may modify cellular localization of bZIP proteins.

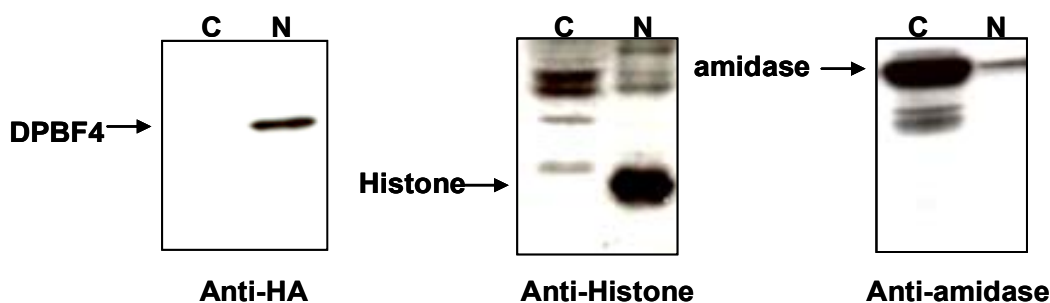


Figure 21. Detection of DPBF4-HA in cytoplasmic and nuclear protein fractions prepared from a dark-grown *Arabidopsis* Col-0 cell suspension.

Nuclear (N) and cytoplasmic (C) protein fractions were prepared from 20g cell suspension expressing DPBF4-HA and analysed by Western blotting using i) anti-HA, ii) anti-histone H2A and iii) anti-amidase AtAM1 antibodies.

Nuclear protein extracts prepared from the HA-DPBF4 expressing cells separated by 12% SDS/PAGE electrophoresis followed by western blot analysis with anti-HA antibody to monitor nuclear presence of the DPBF4-HA recombinant protein. An anti-histone H2A antibody was used as control for nuclear proteins, whereas cytoplasmic protein contamination was monitored by an anti-amidase ATAM1 antibody (i.e., over 95% of ATAM1 is localized in the cytoplasm, unpublished, Koncz lab, MPI). Results of the western blotting showed that DPBF4 was consistently localized in the nucleus and this localization was not affected by dark or light (Figure 21, the data obtained with the light-grown cell suspension are not shown)

3.1.7.1. Immunolocalization of HA-DPBF4 protein in Arabidopsis plants

Cellular localization studies using indirect immunofluorescence microscopy were performed in collaboration with Dr. Jan Jásik from our laboratory. The approach used for immunolocalization of HA and c-Myc epitope tagged proteins, including tissue fixation and the application of primary and secondary antibodies has been extensively described from our laboratory by Ferrando et al., (2000b) and Farrás et al. (2001). Transgenic plant lines expressing HA-DPBF4 were sectioned and embedded as described by Farrás et al. (2001) to examine the cellular localization of DPBF4 protein. The HA-DPBF4 fusion protein was exclusively detected in the nuclei of guard cells, epidermal cells and leaves (Figure 22).

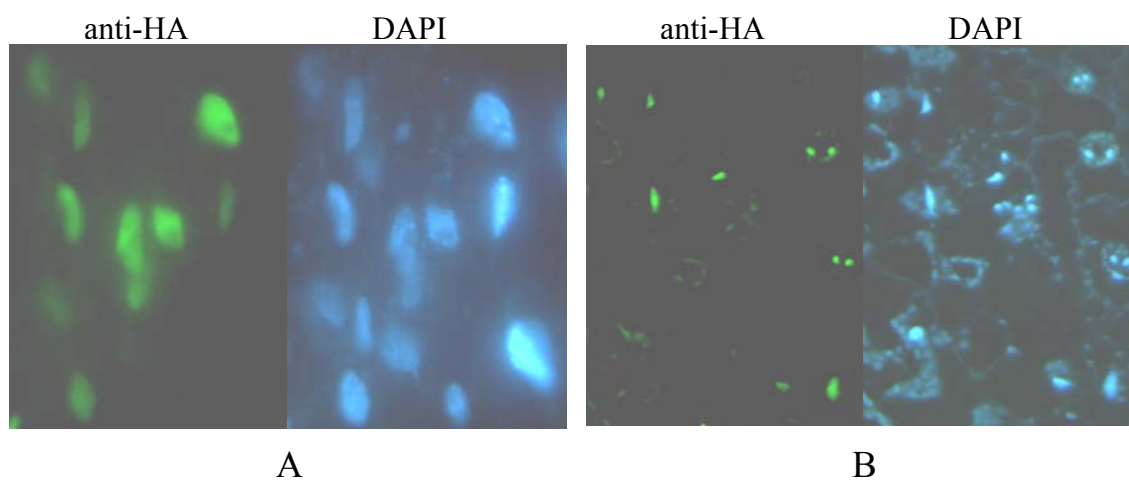


Figure 22. Cellular localization of HA-DPBF4 protein in transgenic plants

Five days old HA-DPBF4 overexpressing plants were used for subcellular localization studies. (A) Longitudinal section of a root and (B) shoot epidermis was stained with the fluorescent DNA dye DAPI, as well as incubated with a mouse monoclonal anti-HA antibody and visualized by a fluoresceine labeled anti-mouse IgG. The HA-DPBF4 signal was exclusively detected in the nuclei of cells.

3.1.7.2. Transient expression of GFP-DPBF4-HA fusion protein in Arabidopsis protoplasts prepared from cell suspension

Protoplast transformation is a very efficient method for transient expression studies of proteins (see e.g., Yanagisawa et al., 2003). To obtain a construct for GFP-DPBF4 fusion protein expression, the

coding sequence of DPBF4-HA was moved by *Xba*I to plasmid pCAT-GFP to generate an in frame fusion with the GFP coding domain under the control of a 2X CaMV35S promoter. The pCAT-GFP-DPBF4-HA construct was then transformed into protoplasts prepared from dark-grown *Arabidopsis* Col-0 cell suspension. As in the indirect immunolocalization studies, inspection of GFP fluorescence in protoplasts indicated that the GFP-DPBF4-HA protein was localized in protoplast nuclei (Figure 23).

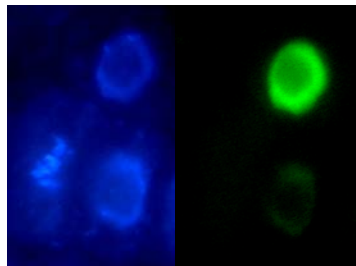


Figure 23. Transient expression of GFP-DPBF4-HA fusion protein in protoplasts.

Protoplasts were transformed with the pCAT-GFP-DPBF4-HA expression vector and upon 12 h time of transient expression have been inspected under a fluorescence microscope..

3.1.8. Size fractionation of DPBF4 on a linear glycerol gradient reveals that DPBF4 undergoes dimerisation

Nuclear extract was prepared from 20g of seven days old DPBF4-HA overexpressing cell suspension. The nuclear protein extract was loaded on a linear 10%-40% glycerol gradient to fractionate protein complexes. The gradient was centrifuged for 16 hrs in ultracentrifuge-LB30 (SW40 Ti rotor) at 30,000rpm at 4°C. After centrifugation, equal amounts of gradient fractions were collected for analysis of DPBF4 containing protein complexes by Western blotting. DPBF4-HA was detected predominantly in lower molecular weight fractions 3, 4 and 5 corresponding to a molecular mass of 60-75kDa, otherwise most of the protein accumulated in the glycerol gradient pellet suggesting that DPBF4-HA is part of large protein complex(es). The glycerol gradient pellet contains nuclear matrix and insoluble fractions. A second experiment was performed with a larger amount of the glycerol gradient fractions and a longer ECL exposure was made. The results from this experiment showed that DPBF4 is indeed distributed in high molecular mass fractions 27, 28 (over 700kDa), as well as in lower molecular fractions 4, 5 and 6 (70kDa) and in the insolubilised nuclear pellet. Lower molecular weight peak fractions corresponding to a size range of 60-75kDa is consistent with homodimerization of DPBF4 (~28.8kDa) or an interaction with a protein of similar size molecule. The presence of DPBF4 in higher molecular weight fractions (600-700kDa) suggests that DPBF4 is associated with other chromatin-bound complexes. This result raised the possibility that DPBF4 could control gene expression by having an association with the nuclear matrix, and that it may exist in different protein complexes by forming homo- or heterodimers. Lopez- Molina et al. (2003) performed size fractionation of ABI5 on a higher resolution 5 to 25% glycerol gradient and showed that ABI5 is found in a complex of 100-300 kDa. The molecular mass of fractions described by Lopez-Molina et al. (2003) thus perfectly overlap with our data concerning the mass of DPBF4 fractions, suggesting that DPBF4 monomer might dimerize with ABI5 monomer.

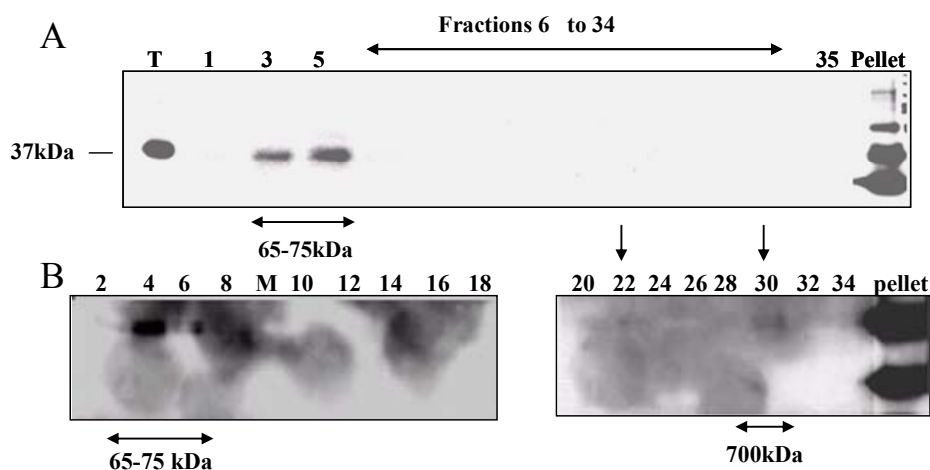


Figure 24. Size fractionation of DPBF4-HA by glycerol gradient centrifugation.

(A) Nuclear extract was prepared from DPBF4-HA expressing cell suspension and resolved on a 10-40% linear glycerol gradient. 300 μ l of fractions were collected and equal amounts of proteins were size fractionated by 12% SDS/PAGE followed by immunoblot analysis with a monoclonal anti-HA antibody. (B) Increasing the amount of protein sample input on the 12% SDS/PAGE revealed the presence of DPBF4-HA in high molecular mass complexes. The blots were subjected to visualization with 10X ECL Plus.

3.1.9. DPBF4 and ABI5 interact *in vivo*

It has been demonstrated using *in vitro* electrophoretic mobility shift assays (EMSA) that DPBF4 and ABI5 heterodimerize with each other and compete for binding on the same ABRE sequence on the AtEm1 promoter (Bensmihen et al., 2002). This fact prompted our investigation of whether DPBF4 and ABI5 can also interact *in vivo*. DPBF4-HA overexpressing stable cell suspension culture was transformed with a ABI5-cMYC expression construct and subjected to biochemical studies. As we showed for DPBF4, ABI5 is known to display constitutive nuclear localization (Lopez-Molina et al., 2003).

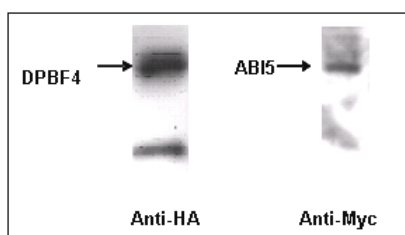


Figure 25. Confirmation of ABI5 and DPBF4 interaction *in vivo*.

(A) Nuclear protein extract from a DPBF4-HA and ABI5-cMYC coexpressing *Arabidopsis* cell suspension was immunoprecipitated using a Sepharose matrix-coupled antibody recognizing the HA epitope of DPBF4-HA protein. The matrix-bound proteins were eluted with HA peptide and analysed by Western blotting with anti-HA antibody (i.e., to detect the IP specificity) and anti-cMYC antibody to detect co-immunoprecipitated ABI5.

Co-immunoprecipitation experiments using nuclear protein extracts prepared from DPBF4-HA and ABI5-cMYC coexpressing *Arabidopsis* cell suspension showed that antibody directed against the HA-epitope of DPBF4-HA protein was able to co-immunoprecipitate ABI5-cMYC indicating that DPBF4 and ABI5 are indeed associated with each other in actively dividing cultured cells (Figure 25).

3.1.10. Conserved phosphorylation signature in the DPBF4 protein sequence

Sequence comparison and examination of the DPBF4 amino acid (AF334209) sequence using the NetPhos 2.0 and PlantP online softwares (<http://www.cbs.dtu.dk/services/NetPhos>; <http://plantsp.genomics.purdue.edu>) revealed that DPBF4 amino acid sequence has potential consensus phosphorylation recognition motives for Ca²⁺-dependent protein kinase, protein kinase C, cGMP-dependent protein kinase or casein kinase II (Bensmihen et al., 2002). Our investigation for the presence of phosphoresidue signatures in DPBF4 amino acid sequence identified a SnRK2 recognition motif in domain II and two SnRK1 recognition motifs present in domain I and domain II. The predicted sequence motif recognized by SnRK2 to some extent resembles the consensus sequence for substrates of SNF1/AMPK protein kinases (Dale et al., 1995). Therefore, the DPBF4 protein could also be potentially a substrate of SnRK1 kinases, the closest AMPK/SNF1 homologues from plants.

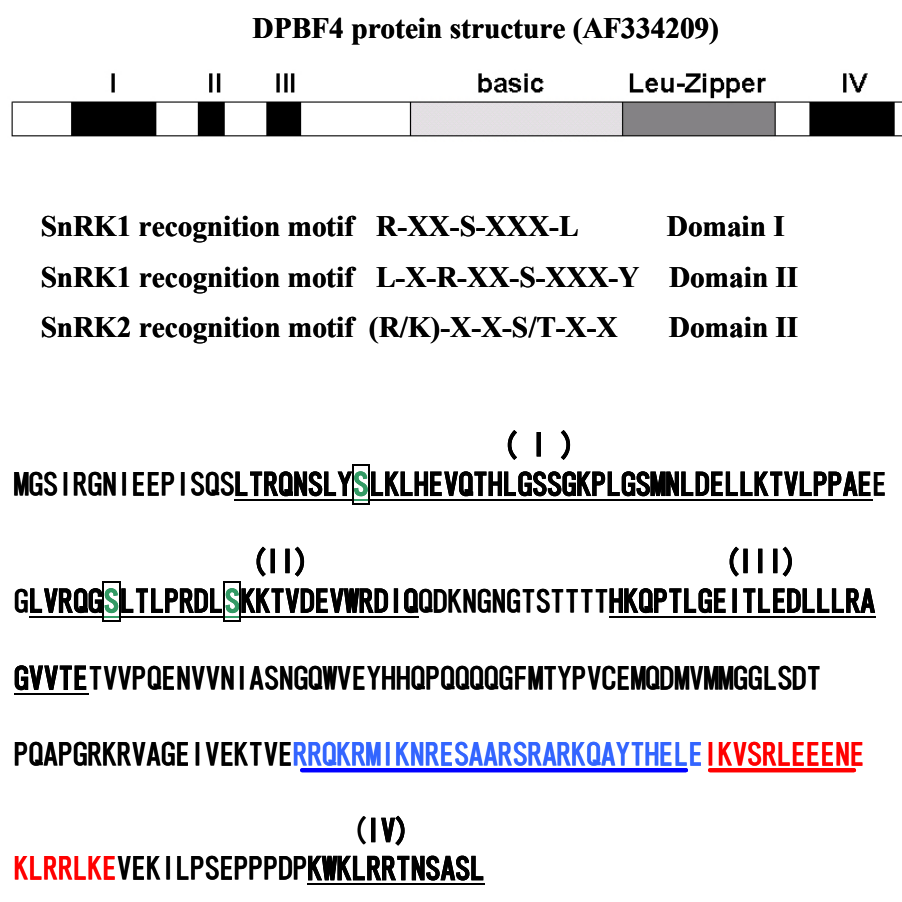


Figure 26. Schematic representation protein structure and predicted phosphorylation sites of DPBF4.

The structure of DPBF4 is shown schematically at top, where the conserved regions I to III and the bZIP domains are indicated with black and grey boxes, respectively. Consensus phospho-serine residues (S) are boxed and colored green. Conserved domains of the bZIP family are marked by bold letter and underlined, the basic domain is shown in blue, and the leucine zipper domain is indicated by red letters

3.1.11. Identification of a candidate kinase of DPBF4

Members of the SnRK2 family are known to be involved in stress and ABA signal transduction pathways (for review see Rolland et al., 2002a; Himmelbach et al., 2003). *Arabidopsis* OST1/SRK2E/SnRK2.6, a member of the SnRK2 family controls generation of H₂O₂, stomatal closure and ABA-regulated gene expression (Li and Assmann, 2000; Mustilli et al., 2002). SnRK2/OST1 was

used as a candidate SnRK type2 kinase and AKIN10 as candidate SnRK1 kinase for testing phosphorylation of DPBF4 in our experiments.

3.1.11.1. Construction of vectors for expression of DPBF4 and OST1 in *E. coli*

To generate recombinant protein that carry an N-terminal polyhistidine tags, the DPBF4 cDNA flanked by *Bam*HI-*Eco*RI restriction sites was excised from vector pGIGI-HA-DPBF4 and cloned in-frame in the vector pRSetC (Invitrogen). Vector pRSetC contains a bacterial expression cassette under the control of T7 promoter. A full-length cDNA encoding the OST1 kinase (At4g33950) was obtained from the RIKEN cDNA stock collection (Japan). The OST1 cDNA was PCR amplified with specific primers to generate *Bam*HI-*Eco*RI restriction sites. This fragment was cloned into vector pET201 (gift from László Bakó) to generate a polyhistidine tag at the C-terminus (Fig. B.) GST-AKIN10 (SnRK1 α) protein was obtained from our laboratory's stocks (Bhalerao et al., 1999; a gift of Mihály Horváth). All cDNA constructs in expression vectors were verified by sequencing.

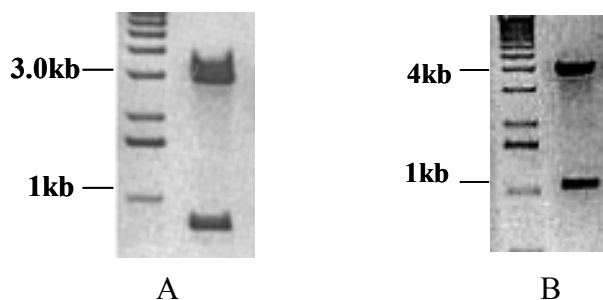


Figure 27. Cloning of DPBF4 and OST1 cDNAs into *E. coli* protein expression vectors.

(A) Restriction digestion of DPBF4-pRSET clone with *Bam*HI-*Eco*RI. The expected 800 bp insert (DPBF4) fell out the vector MCS (pRSET-3kb). (B) Restriction digestion of TRX-OST1-His with *Bam*HI-*Eco*RI revealed the right size of cDNA fragment in the correct frame confirmed by sequencing.

3.1.11.2. Purification of bacterially expressed OST1-HIS and HIS-DPBF4 proteins

OST1-HIS and HIS-DPBF4 plasmids were transformed into BL21(DE3) pLYS expression strain (see Materials) and the transformants were induced with IPTG at different temperatures. DPBF4 was induced at 28°C, while OST1 was induced at 37°C. Crude bacterial protein lysates were analyzed using a 12% SDS-PAGE. Figure 28 shows that a protein of 37kDa was induced with IPTG in the culture containing HIS-DPBF4 (lane 2), whereas no 37kDa band was observed in the control lane containing uninduced bacterial lysate. A protein of 60 kDa was induced in the culture containing the OST1-HIS expression vector.

3.1.11.3. Induction time course of expression of His-tagged DPBF4 and OST1 proteins

In order to optimize the yield of fusion proteins, a brief study of time course kinetics of IPTG-mediated induction was performed. Cultures were grown to logarithmic phase and then induced with IPTG for different time periods of 0, 2, 4, 6 and 8 hours. After harvesting, total protein extracts were analyzed by SDS-PAGE. Results of these experiments show that the synthesis of the HIS-DPBF4

reaches an optimal level after 8 h of IPTG induction while it takes only 4 h in the case of the OST1 kinase. Therefore, for all subsequent experiments, bacterial cultures were induced for 8 h for DPBF4 and 4h for OST1 purification.

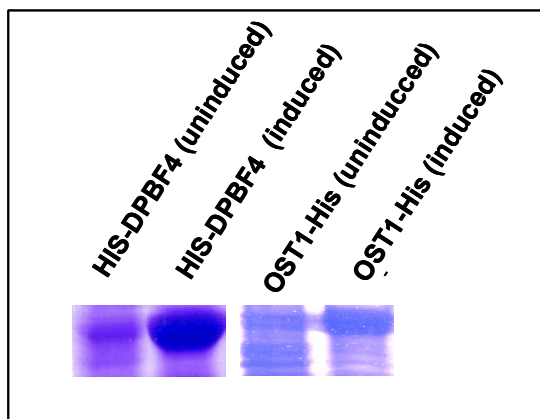


Figure 28. Induction of HIS-DPBF4 and Ost1-HIS expression in *E. coli*.

His-tagged DPBF4 (37 kDa) and Ost1 (40kDa, but migrates at 60kDa) proteins were induced with IPTG and crude bacterial protein lysates were separated 12% SDS-PAGE and stained with Coomassie Brilliant Blue. (A) Lane 2 indicates the presence of His-DPBF4 fusion protein that is absent in lane 1 (control) (B) Induced OST1-HIS is loaded in lane 2 and uninduced culture was loaded in lane 1.

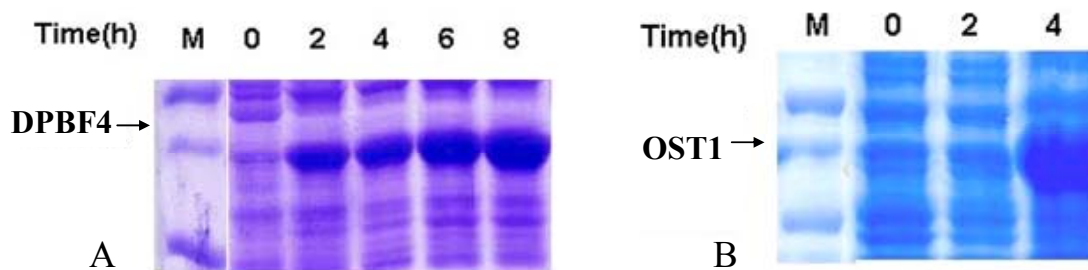


Figure 29. Time course of induction of HIS-DPBF4 and OST1-HIS expression.

Cells carrying recombinant plasmids were grown at 37°C (for Ost1) and 28°C (for DPBF4) and induced with 2 mM IPTG for different time intervals as indicated. Crude bacterial protein lysates were denatured in SDS Lammeli loading buffer and resolved by 12% SDS-PAGE electrophoresis followed by Coomassie blue staining. M, Molecular mass marker. (A) and (B) indicate the time course induction of HIS-DPBF4 and OST1-HIS expression, respectively.

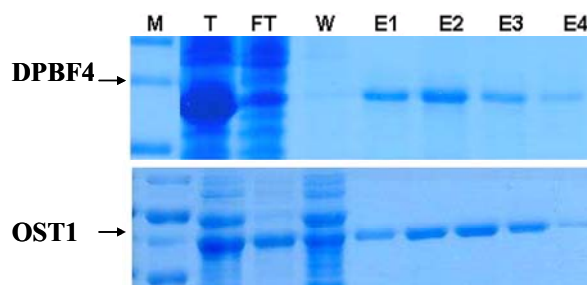


Figure 30. Elution profiles of purified His-DPBF4 and OST1-His proteins.

Proteins were purified by Ni-NTA affinity chromatography. Bound proteins were eluted with 250 mM imidazole. M - low molecular mass marker, T - total, FT - flow through, W - wash, E1 to E4 - eluted fractions containing purified proteins.

3.1.11.4. Purification of HIS-DPBF4 and OST1-HIS fusion proteins

The His-DPBF4 and OST1-His proteins were purified using Ni-NTA affinity chromatography. Fractions were collected and analyzed for protein elution pattern with 250 mM imidazole. The protein elution profiles showed that purified proteins were eluted in fractions 1 to 3 for both HIS-DPBF4 and OST1-HIS proteins (Figure 30).

3.1.11.5. The OST1-kinase undergoes autophosphorylation and phosphorylates histone H2B *in vitro*

The purified OST1-HIS kinase migrated at higher molecular mass than was expected in SDS-PAGE. Our phosphorylation assays show that OST1-HIS shows optimum level of kinase activity with histone H1A and H2B substrates. Results from other laboratories show that several protein kinases belonging to the SnRK2 subfamily (i.e., SPK-3, SPK-4, PKABA1, AAPK) including OST1 are inactive when expressed in *E. coli* as recombinant proteins (Yoon et al., 1997; Li et al., 2000; Mustilli et al., 2002; Hrabak et al., 2003). In the case of AAPK and OST1, the authors claimed that both kinases require the ABA signaling cascade for activation. Our result shows that kinase purified from bacteria undergoes self-phosphorylation and is able to phosphorylate H1A and H2B, which are routinely used as substrates for assaying the activity of different protein kinases.

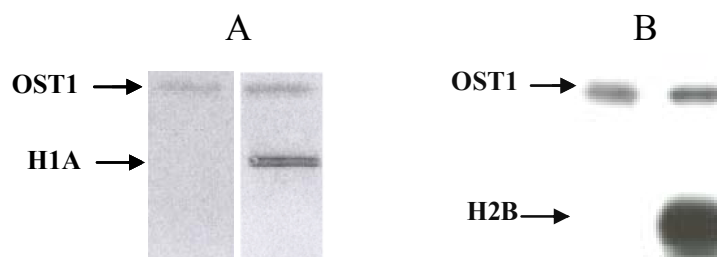


Figure 31. Purified OST1 kinase is active *in vitro*.

(A) Histone 1A (H1A) and (B) Histone 2B (H2B) were used as a substrates in OST1 kinase phosphorylation assays. The reactions contained 100 ng OST1 kinase, 100 ng histone substrates and 5 μ Ci (γ - 32 P)ATP. The gels were exposed for different time to X-ray films.

3.1.12. DPBF4 is a substrate of SnRK1 (AKIN10) and SnRK2 (Ost1) kinases *in vitro*

To investigate whether DPBF4 is phosphorylated by protein kinases AKIN10 and OST1 *in vitro*, purified HIS-DPBF4 was subjected to *in vitro* phosphorylation with purified kinases OST1-HIS and GST-AKIN10 in kinase assays containing [γ - 32 P]. GST-AKIN10 and OST1-HIS phosphorylated the HIS-DPBF4 substrate. In the same experiments, both OST1-HIS and GST-AKIN10 kinases were found to possess autophosphorylating activity (Figure 32). This result confirmed our predictions based on amino acid sequence analysis (3.1.10) that suggested DPBF4 is probably phosphorylated by SnRK1 and SnRK2 protein kinases.

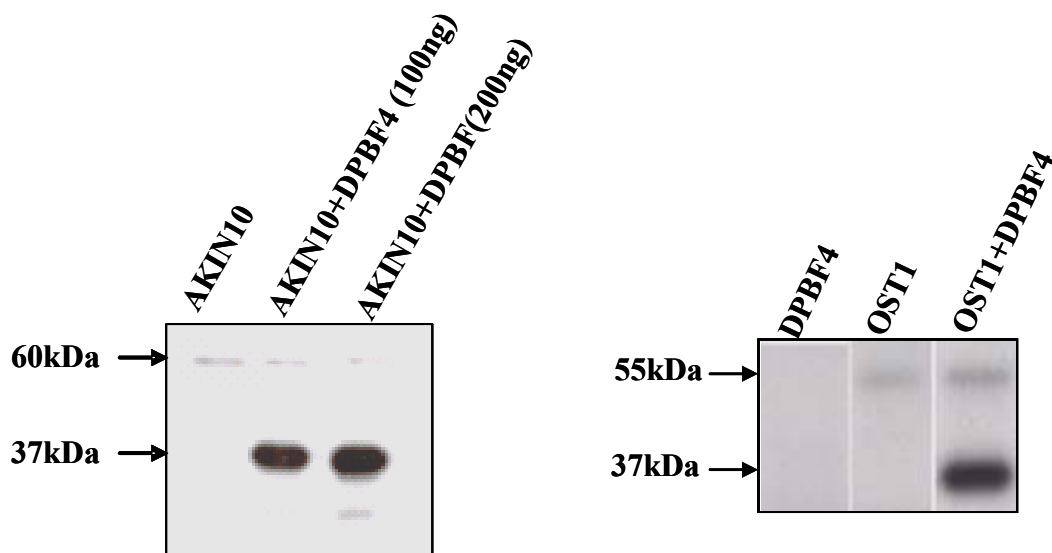


Figure 32. AKIN10 and OST1 phosphorylate DPBF4 *in vitro*.

Bacterially expressed HIS-DPBF4 was used as a substrate in kinase assays *in vitro*. (A) lane 1, GST-AKIN10 (75kDa) shows autophosphorylation; lane 2 (GST-AKIN10 + 100ng DPBF4) HIS-DPBF4 is phosphorylated; lane 3, (GST-AKIN10 + 200ng HIS-DPBF4). (B) Lane 1, HIS-DPBF4 alone; lane 2, OST1-HIS kinase (100ng) shows autophosphorylation, lane 3, OST1-HIS and HIS-DPBF4 (each 100ng), HIS-DPBF4 is phosphorylated.

3.1.12.1. Dose dependence of OST1 activity and DPBF4 phosphorylation

To understand better the involvement of OST1 kinase in DPBF4 phosphorylation, the dose dependence of OST1 kinase activity and DPBF4 phosphorylation was evaluated by varying doses of the OST1-HIS kinase (100-500ng) while keeping the substrate (HIS-DPBF4) concentration constant (100ng). As indicated in (Figure 33A), phosphorylation of the substrate was increased with increasing concentrations of OST1-HIS. To determine the effect of substrate dosage, the concentration of HIS-DPBF4 substrate was linearly increased (100-500ng) and the kinase concentration was kept constant (100ng). As anticipated, varying the concentration of HIS-DPBF4 conferred dose-dependent phosphorylation (Figure 32B). These experiments confirm that DPBF4 is a specific substrate of the OST1 kinase.

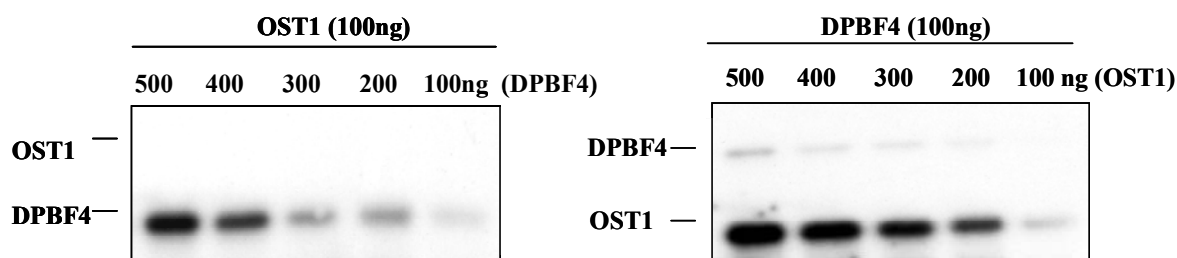


Figure 33. Effect of varying dosage of OST1 and DPBF4 on substrate phosphorylation *in vitro*.

(A) Substrate specificity was analyzed using increasing amounts of DPBF4 in *in vitro* kinase assays with [γ - 32 P] followed by analysis of phosphorylated proteins on 12% SDS-PAGE. (B) Dosage-dependent changes in OST1 kinase activity while maintaining a constant concentration of DPBF4.

3.1.12.2. *Ost1* kinase phosphorylates the DPBF4-HA protein immuno-purified from *Arabidopsis* cells

To examine the *in vivo* phosphorylation status of DPBF4, we tested the presence of phosphorylated amino acids in immunoprecipitated DPBF4 from *Arabidopsis* cell suspension. An immunoprecipitation experiment was performed using nuclear extract prepared from DPBF4-HA expressing cell suspension followed by Western blot analysis with anti-HA antibody. Equal amounts of DPBF4-HA immunoprecipitates were incubated with (γ - 32 P) ATP with and without OST1-HIS kinase. Immunoprecipitated DPBF4-HA did not show any "auto"-phosphorylation activity alone. However, when OST1 kinase was added to the immunoprecipitate, a signal appeared at the expected DPBF4-HA molecular mass (37 kDa) indicating that the OST1 kinase specifically phosphorylates DPBF4-HA. This experiment also suggested that DPBF4-HA can undergo phosphorylation in response to a certain signaling mechanism, as the bulk of immunoprecipitated DPBF4-HA appeared to be incompletely phosphorylated at the OST1-specific site *in vivo*.

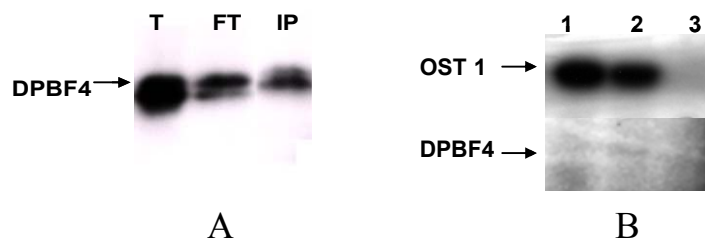


Figure 34. DPBF4-HA immunoprecipitated from cultured *Arabidopsis* cells is sensitive to OST1-mediated phosphorylation.

A) Total nuclear protein extract (T) from DPBF4-HA expressing cell suspension was immuno-affinity purified via its HA epitope and subjected to quality control by Western blot analysis with anti-HA antibody. T – total crude nuclear protein extract; FT - flow through; IP – immunoprecipitated DPBF4-HA eluted after elution with HA peptide. (B) Immunoprecipitated DPBF4-HA was incubated with [γ - 32 P] ATP in presence (2) and absence (3) of OST1-HIS kinase. (1) Autophosphorylation of OST1-HIS kinase in the absence of immunoprecipitated proteins.

3.1.13. Analysis of OST1 and AKIN10 kinase gene expression in *Arabidopsis*.

To examine the steady state mRNA expression levels of the OST1 and AKIN10 genes, RNA was extracted from different organs of soil grown plants, two weeks old whole seedlings (grown under sterile conditions on 0.5MS with 0.5% sucrose), and cell suspension culture of *Arabidopsis thaliana* Col-0 and subjected to semi-quantitative RT-PCR analysis using *OST1* and *AKIN10* gene specific primers. α -Actin primers were used as internal control. The RT-PCR analysis revealed that *OST1* is expressed almost at equal levels in all of the organs tested at the level of transcription. Expression of *AKIN10* is comparatively higher in actively dividing cells, and in two-weeks old seedlings grown *in vitro*.

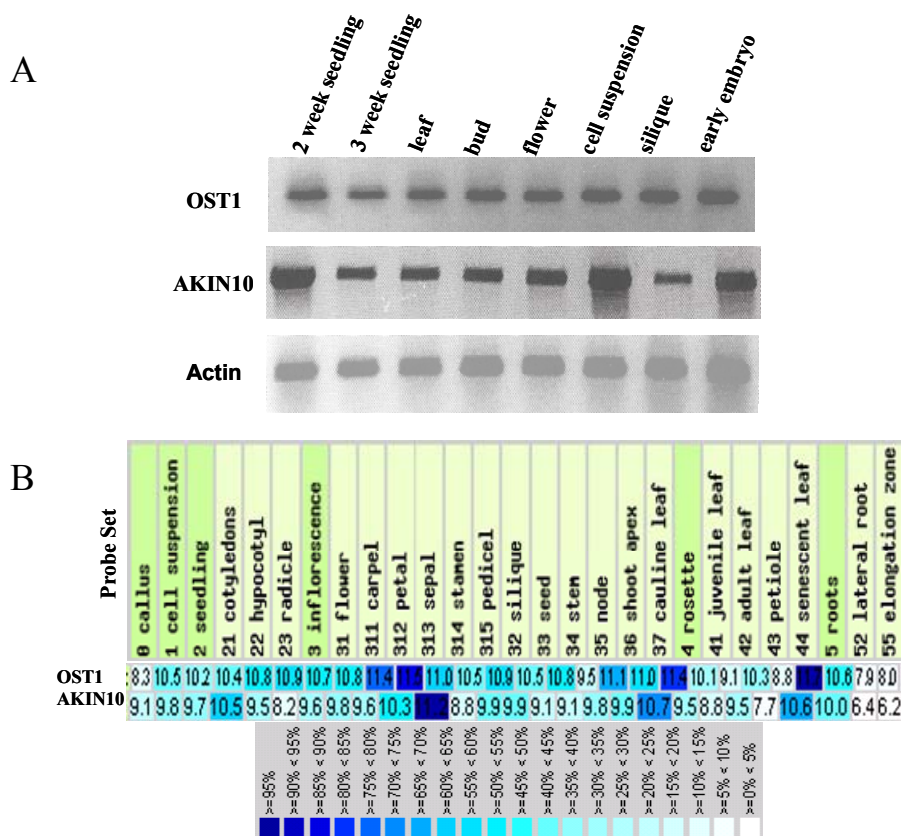


Figure 35. Expression patterns of *OST1* and *AKIN10* kinase genes in various organs of *Arabidopsis*.

(A) *OST1* kinase is expressed in different organs of plants, young seedlings and cultured cells of *Arabidopsis thaliana*. (B) Expression levels of *AKIN10* and *OST1* kinases genes according to microarray data displayed in the Genevestigator database. In general, the Genevestigator expression profiles for *OST1* and *AKIN10* suggest that both genes are expressed at low levels in most plant organs.

3.1.14. Identification of *OST1* kinase phosphorylation sites involved necessary for kinase activity

3.1.14.1. Structural analysis of the *OST1* kinase

In order to address the regulation of DPBF4 by *OST1* kinase phosphorylation, the *OST1* kinase structure was analyzed. The PREDIKIN program was used for the prediction of conserved kinase domains of SnRK2 (*OST1*) and SnRK1 (*AKIN10*). The computer prediction results suggested that both kinases have highly similar catalytic domains but they diverge in their regulatory domains as previously reported (Halford and Hardie, 1998). *OST1* contains an ATP-binding region composed of 27 to 50 amino acids and a Ser/Threonine kinase signature between amino acids 136 to 148. The Ser/Thr kinase activation loop (is bigger) phospho-receptors are present at positions 177 to 179 (Figure 36). To characterize essential residues of *OST1*, which may influence its kinase activity, site directed mutagenesis was performed using the *OST1* cDNA.

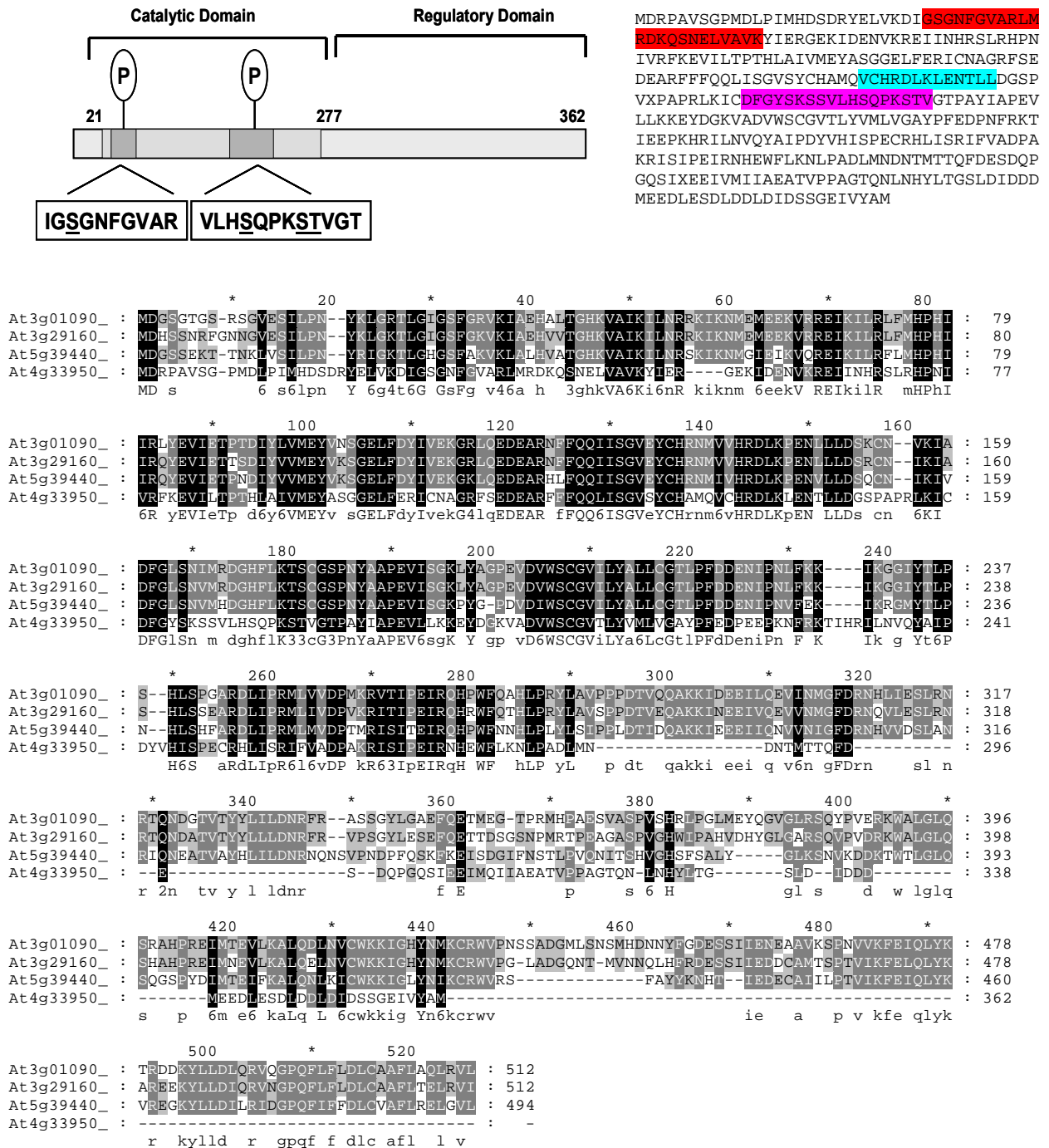


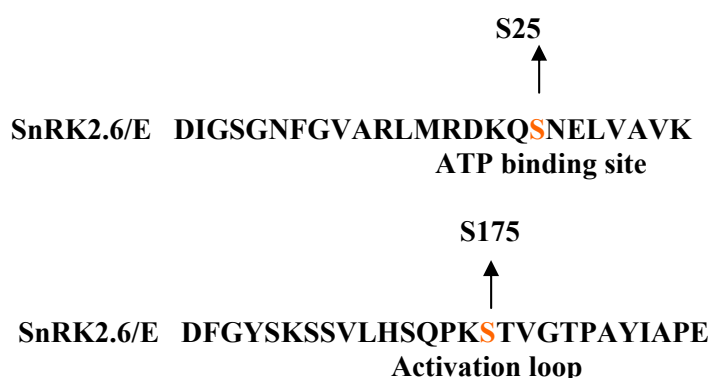
Figure 36. Structural analysis of the OST1 kinase.

(A) The OST1 kinase contains a catalytic domain and a regulatory domain. There are two major conserved protein kinase domains, one for binding ATP and the other for transferring the γ -P targeted substrates (B) Amino acid sequence of the OST1 kinase. Letters marked with red contain the ATP-binding site, the conserved protein kinase domain is shown in blue, and the activation T-loop is marked in magenta (in progressive order). (C) Amino acid alignment of SnRK1 AKIN10 (At3g01090), AKIN11 (At3g29160), AKIN12 (At5g39440) and SnRK2 OST1 (At4g33950) kinases. SnRK1 and SnRK2.6/OST1 kinases have highly similar catalytic and divergent regulatory domains.

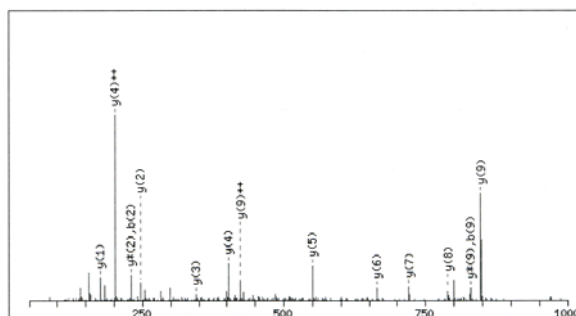
3.1.15. Localization of the autophosphorylated residues of OST1 kinase by MALDI MS/MS mass spectrometry analysis

To identify the OST1 autophosphorylation sites, the OST1-HIS recombinant protein was subjected to MALDI MS/MS analysis after autophosphorylation of the kinase using non-radiolabelled ATP. The

autophosphorylated kinase was isolated from SDS-PAGE, subjected to trypsin digestion and analysed by MS/MS (mass spectrometry) by Dr. Jürgen Schmidt. Based in the MS/MS phosphopeptide predictions, the candidate phosphopeptides were subjected to degradation using MALDI Q-TOF by Dr. Thomas Colby. Peptide sequences obtained by Q-TOF degradation confirmed the MS/MS predictions and precisely identified the positions of two phosphorylated serine residues. One of these serine residues corresponded to a canonical site, Ser-175 in the T-loop, the phosphorylation of which is essential for activation of SnRK2 kinases. Intriguingly, in SnRK1 kinases this threonine residue is found in the corresponding position and this Thr175 residue in the T-loop is phosphorylated by upstream AMPK-activating kinases (AMPKKs) leading to stimulation of AMP-activated kinases in response to stress (see for review Carling, 2004). The other autophosphorylated serine position corresponded to Ser25 in the ATP-binding domain of the OST1 kinase (Figure 37).



DIGSGNFGVAR – ATP-binding motif



STVGTPAYIAPEVLLK – Activation T-loop

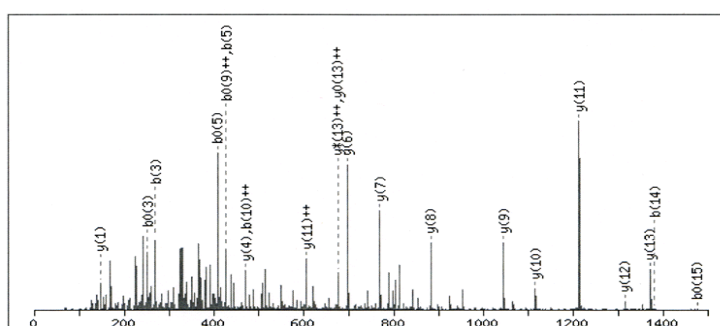


Figure 37. MALDI MS/MS identification of putative phosphopeptides.

MS/MS analysis was performed in reverse (positive) mode to search for peptides, the molecular mass shows 90Da difference in comparison to the predicted mass of unphosphorylated peptides. The candidate phosphopeptides were subjected to MALDI Q-TOF degradation to precisely localize the positions of phosphorylated serine residues.

3.1.15.1. Confirmation of Ser 175 as critical residue for autophosphorylation of OST1 kinase.

By analogy to SnRK1 kinases, attention was drawn to the highly homologous phosphorylation motif in the activation loop of OST1 kinase at Ser 175. Therefore, Ser175 was mutated to Ala to destroy the phosphorylation site by site specific mutagenesis. As indicated in Figure 38A lane 5, the S175A substitution significantly reduced autophosphorylation of the OST1 kinase in *in vitro*.

3.1.15.2. Substitution of Ser175 to Aspartic acid (D) generates a constitutively active OST1 kinase

To further investigate the role of Ser175 in autophosphorylation of the OST1 kinase, we mutated Ser 175 to aspartic acid. Substitution of Ser to Asp at position 175 in the OST1 kinase markedly enhanced its autophosphorylation (Figure 38A, lane 6). This result is in agreement with the requirement for T-loop in the kinase activation and demonstrates that aspartate substitution at codon 175 mimics a phosphate group and constitutively activates the OST1 kinase.

3.1.15.3. OST1 kinase signals through Ser175 to phosphorylate DPBF4

The effects of introduced mutations were examined on DPBF4 phosphorylation. Assuming that the phosphorylation of OST1 kinase on Ser175 is necessary for DPBF4 phosphorylation by OST1, it was anticipated that the Ser to Ala substitution would be defective in this event. Kinase assays revealed that only a very weak phosphorylation of DPBF4 substrate was catalysed by the Ser175Ala mutant of OST1 kinase in comparison to wild type OST1, consistent with the reduction in autophosphorylation activity of OST1-S175A. These results suggested that the OST1 kinase mainly signals through Ser175 to phosphorylate DPBF4 (Figure 38B, lane 4).

3.1.15.4. Mutation of Ser175 to aspartic acid in the OST1 kinase results in enhanced phosphorylation of DPBF4 substrate

The effect of the S175D substitution in the OST1 kinase on its *trans*-phosphorylation activity was tested in an *in vitro* kinase assay was performed with [γ -³²P] ATP, purified OST1-HIS kinase and DPBF4 substrate. The result presented in Figure 38 B, lane 5 showed that OST1-S175D phosphorylated DPBF4 much more efficiently than wild type OST1. This result indicated that the negative charge conferred by aspartic acid mimicks phosphorylated Ser175 in the T-loop of the OST1 kinase and significantly activates OST1.

3.1.15.5. Mutation of K59 to R or deletion of catalytic domain results in a dead kinase

Lysine (K59) was mutated to arginine (R59) in the ATP-binding region to produce a dead (inactive) kinase. Inactivation of the kinase was also achieved by complete deletion of the activation loop (Figure 36; amino acids 160 to 177). Substitution K59R, or deletion of the catalytic domain therefore resulted in a complete loss of Ost1 kinase activity for autophosphorylation (Figure 38A, lanes 7 and 8) or *trans*-phosphorylation against DPBF4 (Figure 38B, lanes 6 and7), respectively.

3.1.15.6. T146 acts as an inhibitor of OST1 kinase activity

The Ost1 kinase contains a S/T protein kinase active site signature between amino acid 136-148. Mutated kinases with T146A and T146D amino acid exchanges were expressed in *E. coli* and purified. Kinase assays performed with purified OST1-T146A and OST1-T146D revealed that the activity of OST1 kinase was increased in comparison to wild type OST1 or the constitutively active mutant of OST1 S175D (Figure 38 A, lane 2). Consistently, phosphorylation of the DPBF4 was also increased (Figure 38B, lane2). Substitution of T146 to D146 displayed similar activity as wild type Ost1 (Figure 38B, lane 3). These results suggested that T146 inhibits the OST1 kinase activity and when it is converted into a neutral form, the activity of wild type OST1 is increased.

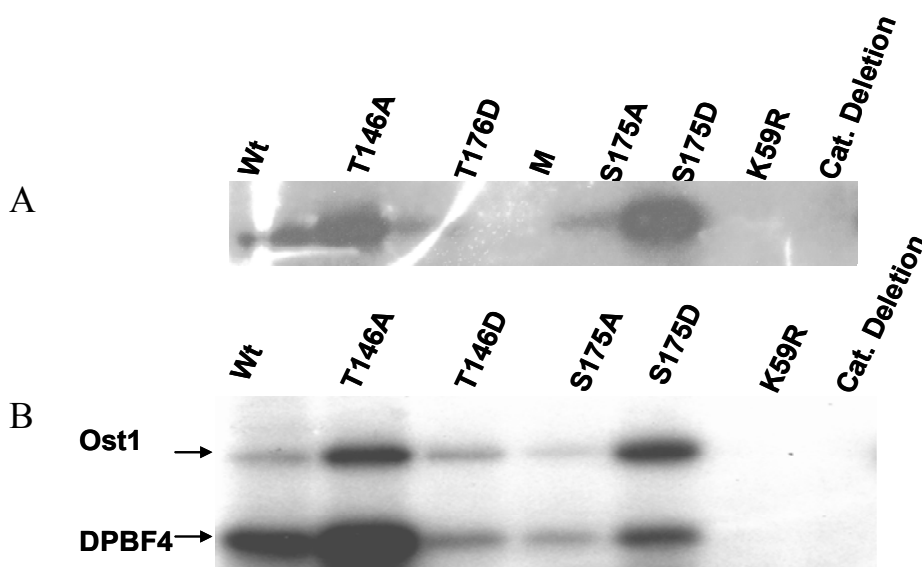


Figure 38. The effects of mutations produced in potential phosphoresidues and the activation loop of the Ost1 kinase.

Equal amounts of wild type and mutant forms of OST1 kinase were electrophoresed on a 12% polyacrylamide gel. **(A) Lane 1:** wild type Ost1 kinase shows autophosphorylation. **Lane 2:** autophosphorylation of T146A OST1 is increased in comparison to wild type. **Lane 3:** the T176D mutation does not produce any strong effect, the kinase shows weak autophosphorylation activity. **Lane 4** contains a pre-stained protein size marker. **Lane 5:** The S175A mutant kinase has very weak autophosphorylation activity. **Lane 6:** The S175D OST1 activity is significantly increased in comparison to wild type. **Lane 7** contains a dead kinase, K59R, in which the ATP-binding site has been destroyed. **Lane 8:** is a mutant form of Ost1 kinase carrying a complete deletion of the catalytic domain. **(B) Lane 1** is wild type Ost1 kinase with DPBF4, OST1 shows self- and trans-phosphorylation. **Lane 2** contains T146A kinase and DPBF4, where the autophosphorylation and trans-phosphorylation is increased in comparison to wild type. **Lane 3** contains a T146D kinase with DPBF4. **Lane 4** shows OST1 S175A and DPBF4, the kinase shows very weak self- and trans-phosphorylation activity. **Lane 6** is OST1 S175D with DPBF4, where kinase self-phosphorylation and trans-activity is strongly increased in comparison to wild type. **Lane 7** contains a dead kinase, K59R, in which the ATP binding site has been mutated. **Lane 8** contains DPBF4 and mutant form of the Ost1 kinase lacking the catalytic domain.

3.1.15.7. The OST1 kinase phosphorylates the SnRK1 substrate SAMS peptide

In order to investigate potential interaction between SnRK1 and SnRK2 kinases, a phosphorylation assay using OST1 and AKIN10 was performed. No cross-reactivity was detected between them (data not shown). In order to investigate if a SnRK1 substrate is also recognized by an SnRK2 kinase, the phosphorylation of SnRK1 substrate SAMS peptide by OST1 was examined. The SAMS peptide has been shown to be specific for the AMPK, SNF1, and SnRK1 kinases (Dale *et al.*, 1995). OST1 had effectively phosphorylated the SAMS peptide (Figure 39). (The SAMS peptide

(HMRSAMSGHLHVKRR) a synthetic peptide based on the primary site phosphorylated in rat ACC by AMPK, (Sugden et al., 1999)

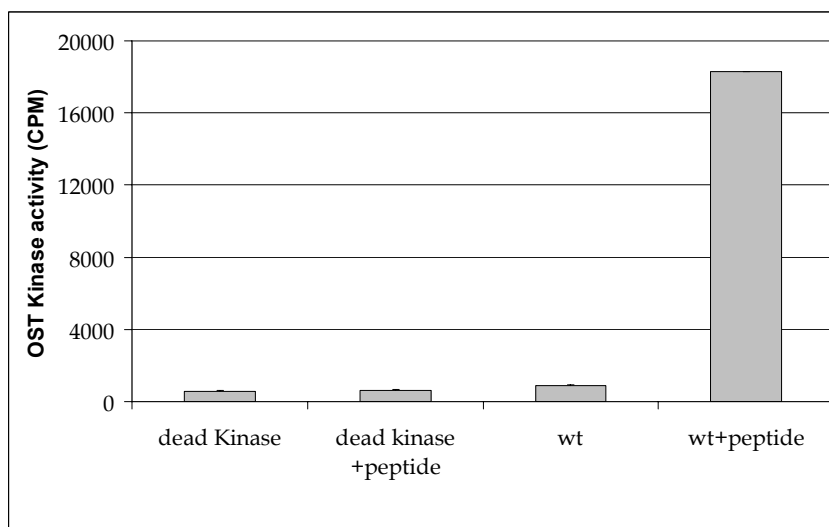


Figure 39. SAMS peptide phosphorylation by OST1

Phosphorylation of SAMS peptide (40 μ M) by wild type OST1 (100 ng) and catalytically dead kinase (K59R) was measured of γ^{32} P incorporation.

3.1.16. Characterization of the regulation of *AK1/HSD1* promoter

3.1.16.1. Salt and ABA activate the *AK1/HSD1* promoter

The observation that DPBF4 is closely related to transcription factors implicated in the regulation of gene expression by the plant hormone ABA and stress prompted the examination of whether the *Arabidopsis AK1/HSD1* promoter is activated by ABA and/or other stress stimuli. In these experiments, the induction of *AK1/HSD1* promoter by glucose and NaCl was tested using a 2kb *AK1/HSD1* promoter fusions with a β -glucuronidase (*GUS*) reporter gene (described by Zhu-Shimoni and Galili, 1998). In the same experiments, the response elements were roughly mapped using a series of promoter deletions. The results revealed that the *ASK1* promoter was induced by both glucose (300 mM) and salt (200 mM), but no change in the promoter activity was observed in response to ABA (data not shown).

3.1.16.2. Transcriptional de-repression of sucrose-induced *AK1/HSD1* gene in the *prl1* mutant

The *Pleiotropic regulatory locus 1 (PRL1)* encodes a conserved nuclear WD-protein that functions as key regulator of glucose and hormone responses in *Arabidopsis*. A T-DNA insertion in the *PRL1* gene confers hypersensitivity to glucose and sucrose. De-repression of the ABA-stimulated alcohol dehydrogenase (*ADHI*) promoter in the *prl1* mutant is controlled by a *cis*-regulatory promoter sequence that carries core bZIP-binding site (Németh *et al.*, 1998). Expression of the aspartate kinase promoter was suggested by Zhu-Shimoni and Galili (1998) who mapped a G-box containing enhanced element involved in sugar regulation of the *AK1/HSD1* gene. We tested whether the *AK1/HSD1*

promoter activity is affected in *prl1* mutant in response to different concentrations of sucrose. Plants were grown in 0.1% and 3% sucrose containing media for two weeks, then RNA samples were prepared and subjected to RT-PCR amplification using an α -actin primer as an internal standard. The transcription of *AK1/HSD1* gene was de-repressed (i.e. induced independently of sucrose-treatment) in the *prl1* mutant. In addition, the induction of *AK1/HSD1* gene by sucrose was found to be 2 to 3-fold higher in the *prl1* mutant in comparison to wild type. This experiment was performed together with Dr. Frank Breuer.

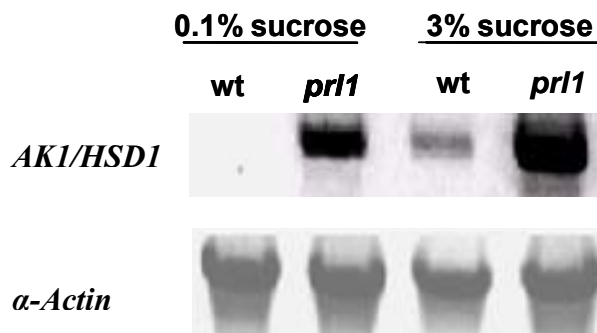


Figure 40. PRL1 negatively controls the expression of the *AK1/HSD1* gene.

Measurement of *AK1/HSD1* transcript level in wild type and *prl1* mutant seedlings grown in the presence of 0.1 and 3% sucrose in the light by semi-quantitative RT-PCR. The *AK1/HSD1* gene shows sucrose-induced transcription in wild type plants and shows de-repressed (sucrose-independent) activation in the *prl1* background.

3.1.17. Transcriptional de-repression of *DPBF4* in the *prl1* mutant

To examine the transcriptional regulation of *DPBF4* in the *prl1* mutant, wild type and *prl1* plants were grown in 3% sucrose containing medium for three weeks. Roots and shoots were harvested separately and subjected to total RNA preparation. RT-PCR analysis of the RNA prepared from shoots of *prl1* and wild type plants with *DPBF4* gene specific primers revealed that *DPBF4* expression is increased in the *prl1* mutant.

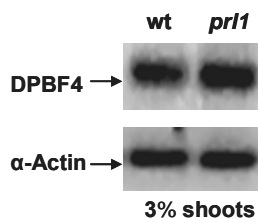


Figure 41. *DPBF4* mRNA levels are increased in the *prl1* mutant in presence of 3% sucrose.

RT-PCR was performed with *DPBF4* and control α -actin primers on RNA templates derived from shoots of wild type and *prl1* mutant plants grown in the presence of 3% sucrose for 3 weeks.

3.1.18. Construction of oestradiol-inducible *DPBF4* expression vectors for studying the role of *DPBF4* in regulation of stress and sugar induced genes

To examine the control of stress and sugar regulated genes by *DPBF4*, we used an oestrogen receptor based chemically-inducible gene expression system. For this purpose, the *DPBF4* cDNA was PCR amplified to generate *NcoI/XbaI* restriction sites and cloned in frame with the cMYC epitope coding

domain in pLOLA vector (Ferrando *et al.*, 2000). The resulting DPBF4-cMYC sequence was excised as an *NcoI-NotI* fragment and cloned by blunt-end ligation into filled in *XhoI* site of the binary vector XVE-pER8 which specifies a chemical inducible system, named XVE for *lexA-VP16-ER* (human estrogen receptor, Zhu *et al.*, 2000). The XVE activator is induced by β -oestradiol. This construct was transferred to *Agrobacterium* and to transgenic *Arabidopsis* plants by *Agrobacterium*-mediated transformation.

3.1.18.1. Time course of DPBF4-HA gene induction in pER8 by β -oestradiol

Seeds from pER8-DPBF4 (T2) transgenic plant lines were surface sterilized and plated on 0.5% sucrose seed germination medium containing hygromycin. Twenty day old plants were subjected to β -oestradiol induction (5 μ M) and samples were collected at 0, 4, 6, and 24 hours time points. Total RNA was prepared for testing the *DPBF4-cMYC* gene induction by RT-PCR using *DPBF4* gene specific primers and α -actin as internal control. This experiment resulted in the confirmation that *DPBF4* expression goes at highest peaks after 6 h of induction. However, in the lines tested so far the *DPBF4* mRNA levels increased to maximum 2-fold of non-induced levels and decreased after 6h of induction. (Figure 42). Similar results were obtained with four independent lines analysed to date.

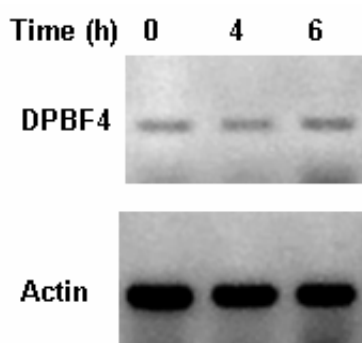


Figure 42. Expression of DPBF4-HA mRNA upon induction with β -oestradiol under XVE system

Induction of DPBF4-HA transcript levels at various time points upon induction with β -oestradiol. pER8-DPBF4-HA transgenic (T2) plant lines were germinated in hygromycin containing seed germination medium for two weeks. Plants were transferred into liquid MSAR and induced with 5 μ M β -oestradiol. Samples were collected at 0, 4, 6, 8 and 24 h and subjected to total RNA extraction followed by RT-PCR assay using DPBF4 gene specific primers. Actin primers were used as internal control. Upon 6h the induction of pER8-DPBF4-HA constructs declined.

3.1.18.2. Influence of inducible DPBF4-HA expression on the activity of ABA-regulated ADHI gene

In order to study the regulation of stress and ABA induced genes using the oestradiol-inducible construct, pER8-DPBF4-HA transgenic plant lines were grown for two weeks and then subjected to combined oestradiol and ABA treatment. The seedlings were transferred to liquid MSAR medium that contained 5 μ M β -oestradiol. 2h after the β -oestradiol induction, 100 μ M ABA was added to the medium. Samples were collected at zero point of treatment with β -oestradiol, as well as before ABA addition and 2 and 4h after ABA-induction and then subjected to total RNA preparation. RT-PCR was performed with *DPBF4* and *ADHI* gene specific primers. DPBF4 mRNA levels were induced in 2h

after β -oestradiol addition, and reached maximum levels in 4h. As ABA was added 2h later of the β -oestradiol induction, no significant change was observed in DPBF4 transcript levels because of ABA, DPBF4 expression kinetics were similar as by β -oestradiol induction (Figure 43). PCR analysis of the same cDNA templates with *ADH1* gene specific primers indicated that there was an about 2-fold increase in ADH1 transcript levels after 2h induction of DPBF4-cMYC expression with β -oestradiol, and this induced transcript level was further increased 2h after addition of ABA. To clarify whether induced DPBF4-cMYC expression would indeed positively regulate *ADH1* expression, further careful analysis is necessary with transgenic lines having better expression in XVE system.

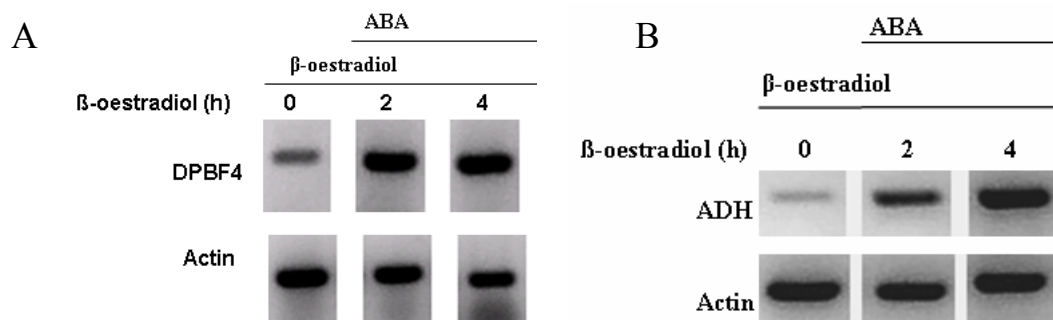


Figure 43. Initial testing the oestradiol inducible DPBF4-HA system and its effect on *ADH1* expression.

Two weeks old pER8-DPBF4-HA transgenic plants were subjected to simultaneous induction with β -oestradiol and ABA. Plants were transferred to liquid MSAR medium that contained $5\mu\text{M}$ β -oestradiol. Two hours after β -oestradiol addition, fresh MSAR medium was added that contained $5\mu\text{M}$ of β -oestradiol and $100\mu\text{M}$ of ABA. Samples were collected at various time points 0, 2, and 4 hours. Zero time samples were collected before β -oestradiol or ABA addition. Total RNA was prepared from the samples and subjected to RT-PCR analysis with (A) *DPBF4* and (B) *ADH* gene specific primers.

3.1.19. Identification of DPBF4-binding sites in the *AK1/HSD1* promoter using chromatin immunoprecipitation

To localize DPBF4-binding sites in the *AK1/HSD1* and other sugar or stress regulated promoters, we used an *in vivo* formaldehyde crosslinking technique based on immunoprecipitation of chromosomal DNA-bound DPBF4-HA protein (ChIP) and PCR amplification of potential DPBF4 target sequences. For crosslinking, 48g of seven days old *Arabidopsis* transgenic cell suspension overexpressing DPBF4-HA was collected and incubated with formaldehyde (as described in the Materials and methods). After quenching the formaldehyde, nuclear extract was prepared and subjected to shearing by sonication to an average DNA fragment size of 500 to 800 bp. The sonicated crosslinked chromatin sample was immunoprecipitated with protein-G Sepharose-immobilized monoclonal anti-HA IgG. The matrix bound DNA-protein complexes were eluted with HA peptide and then Western blot analysis was performed with anti-HA antibody to determine the quality of immunoprecipitation (Figure 44A).

As negative controls, we performed similar extraction and immunoprecipitation experiments with nuclear extracts prepared from wild type cell suspension and a transgenic cell suspension expressing an HA-tagged UFO1-HA F-box protein. UFO1 (UNUSUAL FLORAL ORGAN) is not a DNA binding protein, but a subunit of a nuclear SCF E3 ubiquitin ligase. It might bind DNA only through its transcription factors substrates. As positive control, we used an ABI5-cMYC

overexpressing cell suspension. From the UFO1-HA expressing cell suspension 90 g was collected and crosslinked prior preparation of sheared chromatin, whereas we used 65g of ABI5-cMYC and wild type cell suspensions for preparation of crosslinked chromatin samples (see Materials and methods). Chromatin from the wild type nuclei was not retained on the anti-HA and anti-cMYC IgG matrices, thus we used the flow through fraction as positive control. From the ABI5-cMYC expressing cell line, chromatin was immunoprecipitated using a monoclonal anti-cMYC IgG immobilized on protein G- Sepharose and elution with cMYC peptide.

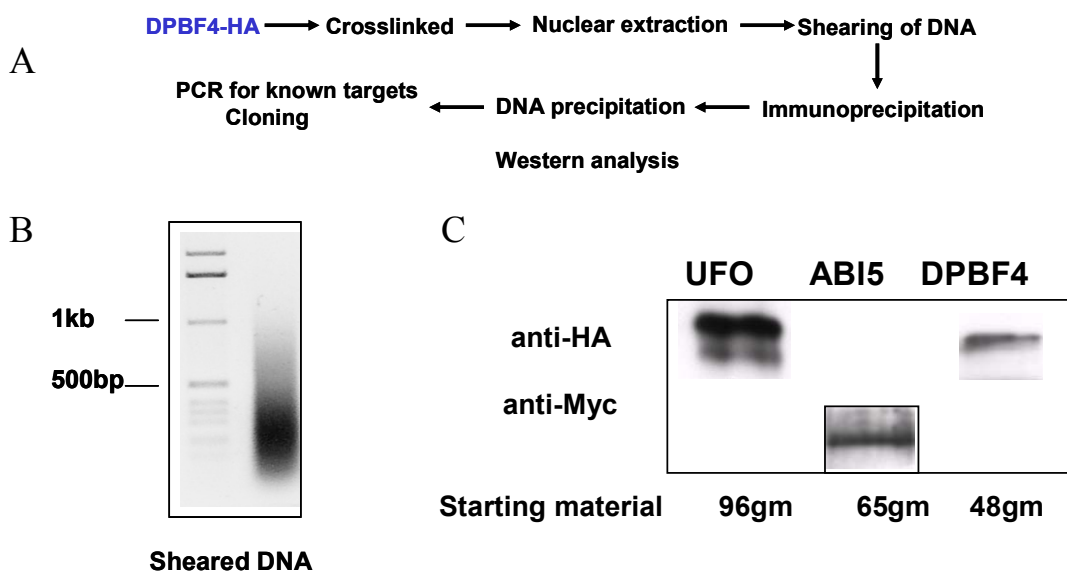


Figure 44. Flow-chart important quality controls of chromatin immunoprecipitation experiments.

(A) A flow chart depicting various steps of chromatin immunoprecipitation experiments. (B) Chromatin DNA was sheared to 500 to 800 bp of average size. (C) 65 g of wild type and ABI5-cMYC, 96g of UFO-HA and 48g of DPBF4-HA expressing cell suspension materials were used for nuclear extraction followed by shearing of chromatin and immunoprecipitation on protein G-Sepharose immobilized anti-HA or anti-cMYC IgG beads. The IgG-bound chromatin-DNA complexes were eluted with HA or cMYC peptide. 1/15 of the eluted samples was heated to resolve cross-linking and subsequently the proteins were size separated by 12% SDS-PAGE and analyzed by western blotting with anti-HA or anti-cMYC antibody.

3.1.19.1. Verification of specificity of ChIP DNA by PCR

Linear dilutions of chromatin immunoprecipitated DNA from DPBF4-HA, ABI5-cMYC, UFO1-HA and wild type samples were made and PCR (28 cycles) was performed with *AK1/HSD1* promoter primers, which flanked the promoter region that was used to fish out DPBF4 in the yeast one hybrid experiment (3.1.1; Figure 45A, B). This experiment showed that the DPBF4-HA ChIP DNA pulls down the AK1/HSD1 promoter G-box containing *cis*-element. Similar amplification of lower intensity was observed with ABI5-cMYC ChIP DNA suggesting that, as DPBF4-HA, ABI5-cMYC can also bind to the AK1/HSD1 promoter. Very faint PCR bands were also obtained with the UFO1-HA ChIP DNA, but there was no PCR product detected with the wild type control ChIP DNA (Figure 45C).

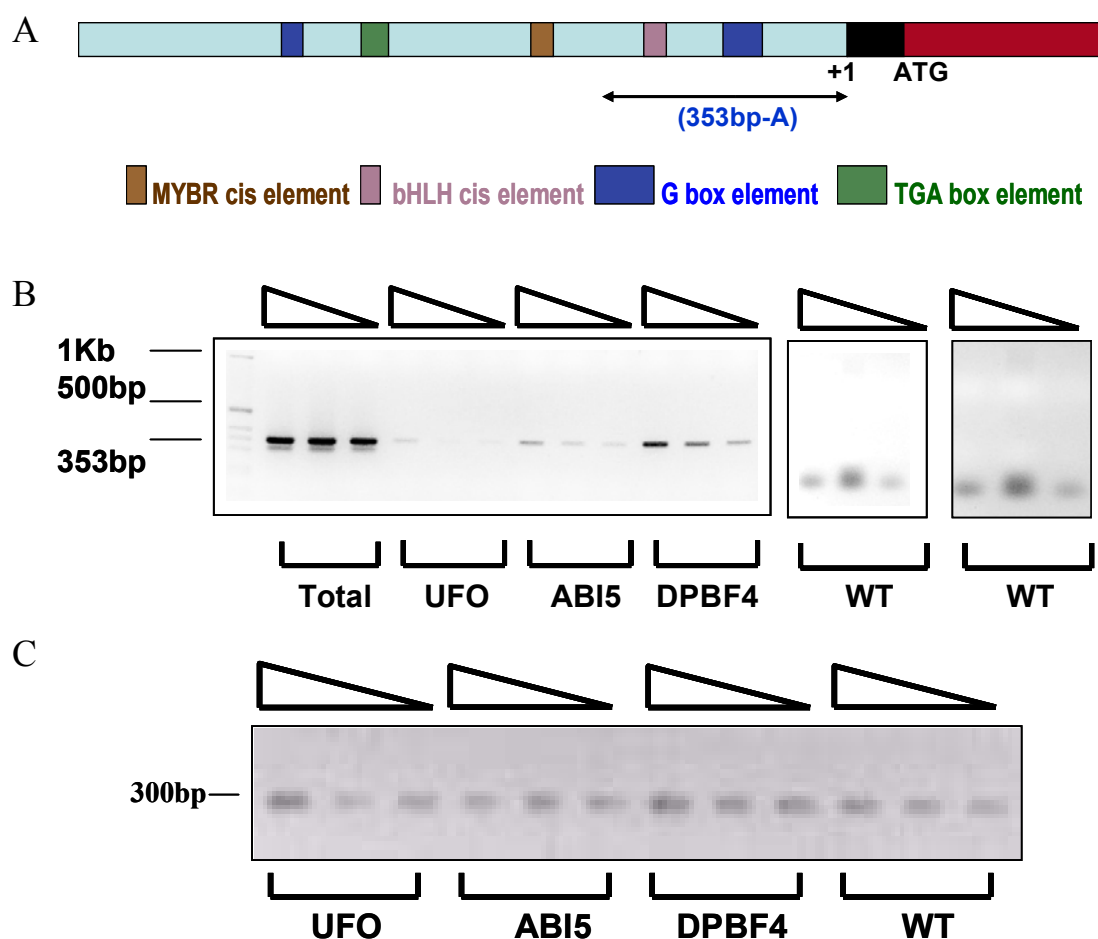


Figure 45. PCR analysis of ChIP DNA samples.

(A) Schematic representation of the *AK1/HSD1* aspartate kinase promoter. (B) ABI5-cMYC, DPBF4-HA, UFO1-HA and wild type (WT) ChIP DNAs were diluted 5, 10 and 20 times for PCR analysis. Aspartate kinase promoter primers (containing the G-box and bHLH *cis*-elements) were used for PCR amplification. (C) A control PCR was performed on ABI5-cMYC, DPBF4-HA, UFO1-HA and WT ChIP DNAs with a set of primers designed to PCR amplify (using 35 cycles) a segment of the *SNF4* gene located just upstream of the stop codon.

3.1.19.2. Identification of DPBF4-binding sites in the *AK1/HSD1* promoter

To examine the binding site of DPBF4-HA in the *AK1/HSD1* promoter, different primer pairs were designed in order to amplify all known *cis*-elements (Figure 46A). Chromatin immunoprecipitated DNA from DPBF4-HA, ABI5-cMYC and UFO1-HA cell lines was used for PCR analysis using the primer combinations shown schematically in (Figure 46.). PCR was run for 26 cycles. This experiment resulted in the amplification of *AK1/HSD1* promoter *cis*-elements, which contained the G-box and TGA-box motives. The fact that the expected G-box sequences were not found in the ChIP DNA sample with DPBF4-HA (repeated experiment) suggest that some upstream G-box-like sequence motifs, such as the TGA element may confer stronger binding of DPBF4-HA or preferentially occupied when DPBF4-HA is overexpressed in cultured cells. On the other hand, the fact that DPBF4 binds as homo- or heterodimer to DNA suggest that certain differences may occur between sequences, which are identified as transcription factor binding sites in the yeast one-hybrid system and by *in vivo* cross-linking.

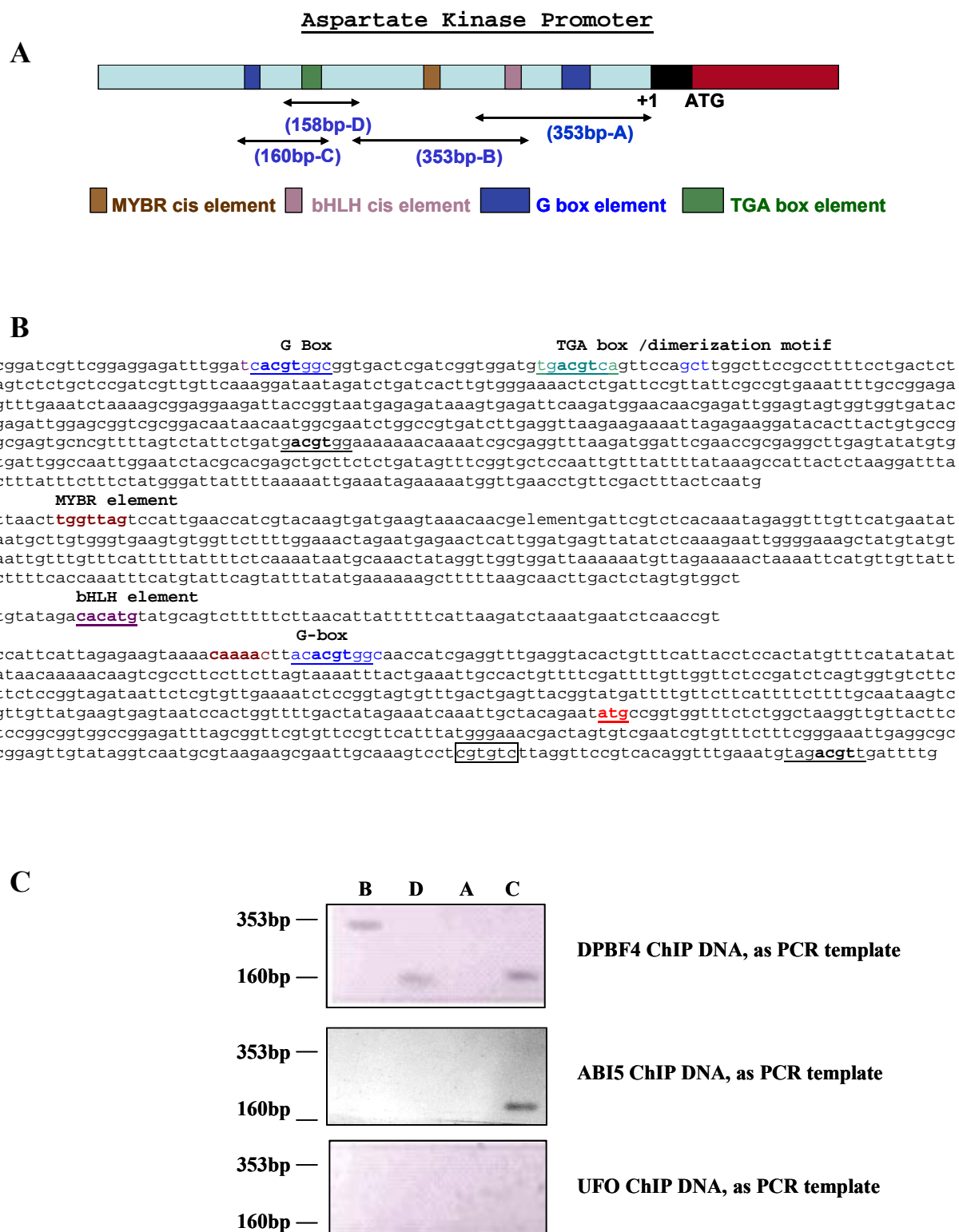


Figure 46. ChIP PCR mapping DPBF4-HA binding sites in the *AK1/HSD1* promoter.

PCR was performed with DPBF4-HA, ABI5-cMYC and UFO1-HA ChIP DNAs, in order to amplify different cis-elements present in the aspartate kinase AK1/HSD1 promoter. (A) A schematic representation of AK1/HSD1 promoter structure. Location of different sets of cis-elements is indicated by blue arrows. Each set is designated by alphabet that represents the PCR product. Sequence below the map shows the position of various cis-elements in the AK1/HSD1 promoter. (C) PCR was performed with different primer pairs in order to amplify various elements (A, B, C, D) using DPBF4-HA, ABI5-cMYC and UFO-HA ChIP DNAs as templates.

3.2. FUNCTIONAL ANALYSIS OF SnRK1 ACTIVATING GAMMA-SUBUNIT SNF4

We have initiated the characterization of the SNF4 γ -activating subunit of *Arabidopsis* SnRK1 kinases to assess whether the lack of this subunit would confer changes, which oppose to those observed in the *prll* mutant. Inactivation of the SnRK1 kinase inhibitor leads to pleiotropic alterations including hypersensitivity to sucrose and glucose, as well as to plant hormones ethylene, ABA, cytokinin and auxin. As experiments with yeast Snf1 and *Physcomitrella Ppsnf1* genes indicate that mutations affecting the catalytic subunits of Snf1/AMPK and SnRK1 kinases result in severe deficiencies allowing the organisms to survive only in the presence of glucose. However, the yeast *snf4* mutants show much milder phenotypes and their glucose requirement can be compensated by overexpression of the kinase α -subunit Snf1. Therefore, we started to characterize basic regulation and interactions of SNF4, as well as the isolation of *snf4* knockout mutants.

3.2.1. Expression patterns of regulatory and substrate targeting subunits of SnRK1 kinases in *Arabidopsis*

To examine the spatial expression pattern of the *SNF4* gene, RNA was extracted from different organs of soil grown plants, two and three weeks old whole seedlings (grown under sterile conditions), and a cell suspension culture of *Arabidopsis thaliana* and subjected to semi-quantitative RT-PCR analysis. α -Actin was used as internal control. RT PCR analysis revealed that the *SNF4* gene expression was detected in actively dividing cultured cells and two weeks old seedlings, leaves and flower buds. This data is in agreement with earlier published data (Kleinow *et al.*, 2000). *SNF4* mRNA levels were comparable to other organs also in early embryos, but it decreased significantly in siliques. The levels of steady-state mRNAs of substrate targeting subunit genes *AKIN β 1* and *AKIN β 2* are almost equal in all of tested plant organs. We also inspected the Genevestigator expression profile database for AtSNF4, AKIN β 1 and AKIN β 2. According to this database, all of these genes are expressed in all organs of plants with the highest expression levels in inflorescences and leaves (Figures 47 and 48).

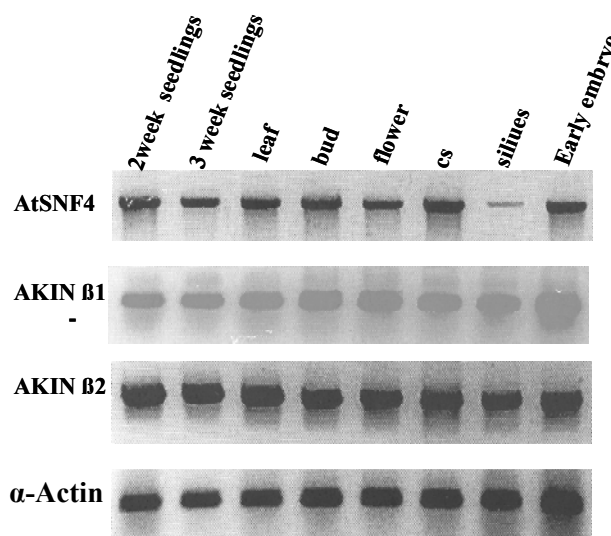


Figure 47. Expression analysis of SnRK1 regulatory and substrate targeting subunit gene. Details of the RT-PCR analysis are provided in the text.

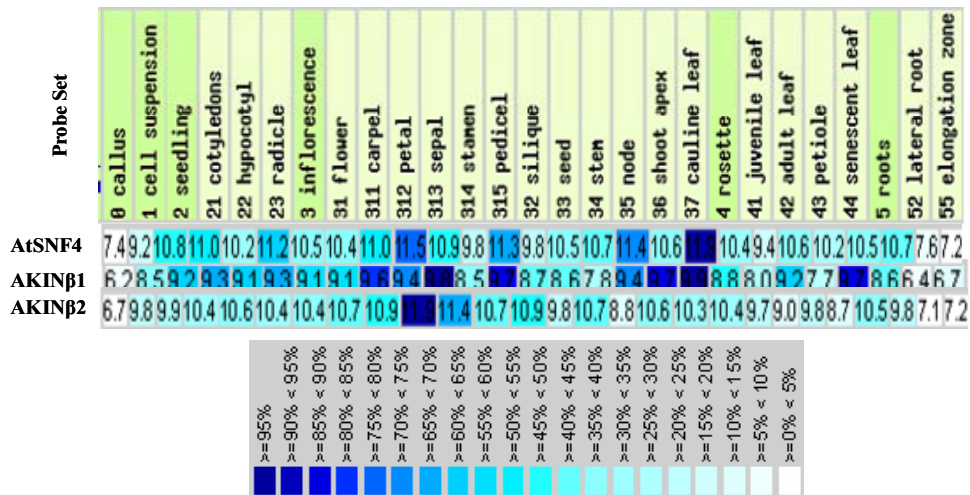


Figure 48. Comparison of microarray transcript profiling data available in the Genevestigator database for SnRK1 activating and substrate targeting subunit.

According to the Genevestigator data base *SNF4*, *AKINβ1* and *AKINβ2* are expressed in all of the plant organs except in callus and root elongation zone.

3.2.2. Analysis of SNF4 expression at the protein level

In order to investigate SNF4 expression at the protein level, crude protein extracts were prepared from leaves, flowers, roots, cell suspensions and two weeks old seedlings. An affinity- purified antibody raised against a unique SNF4 peptide (Kleinow, 2000) was used to monitor the SNF4 protein levels by western blotting. This antibody recognized a protein of 53 kDa in cell suspension, young leaves, flowers, but failed to detect SNF4 protein in roots. Control experiments using a synthetic SNF4 peptide as competitor in immunoblotting with the anti-SNF4 antibody confirmed that the protein of 53 kDa was indeed SNF4. Some non-specific proteins were however also recognized by the anti-SNF4 antibody (Figure 49).

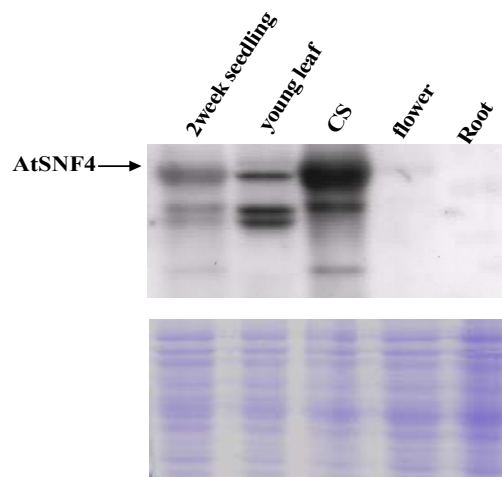


Figure 49. Analysis of SNF4 protein expression in different *Arabidopsis* tissues.

Equal amount of total protein extracts prepared from wild-type plants were loaded on a 10% SDS/polyacrylamide gel and analyzed by immunoblotting using anti-SNF4 antibody. A parallel immunoblot was prepared in order to calibrate the protein amount and stained with Coomassie blue.

3.2.3. Examination of alternative splicing of SNF4 transcript

The *AtSNF4* gene carries an N-terminal KIS (kinase interaction sequence) domain, which is fused to a C-terminal region that consists of four cystathionine β -synthase (CBS) repeats. It has been proposed

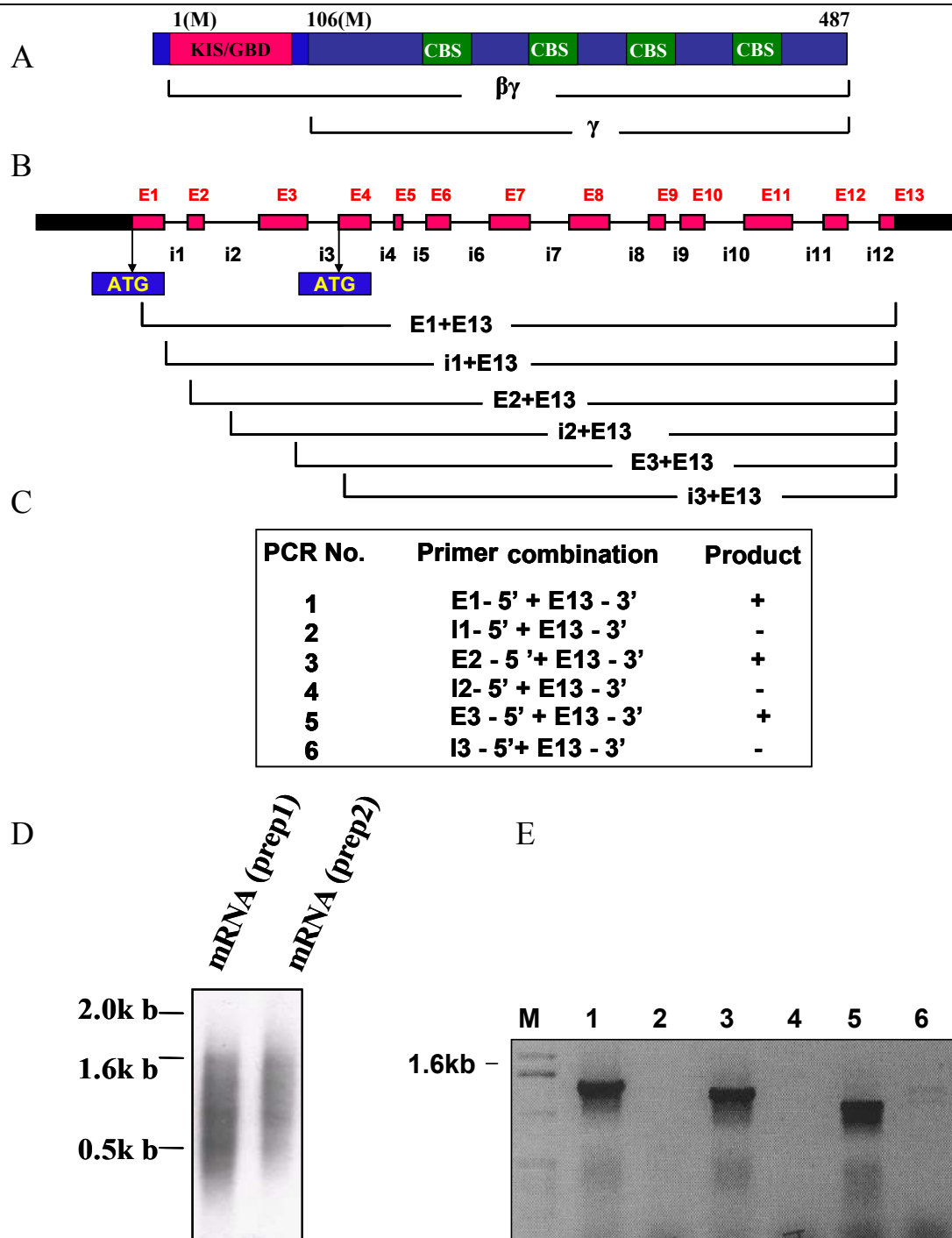


Figure 50. Examination of alternative splicing of *Arabidopsis SNF4* transcripts.

(A) Diagrammatic representation of the AtSNF4 gene. The conserved in plants long form ($\beta\gamma$) contains an N-terminal KIS domain and four CBS domains in its c-terminus, while short form (γ) contains only the CBS domains and no KIS domain (B) Intron/exon structure of the AtSNF4 gene. AtSNF4 contains 13 exons. The first three exons include the KIS domain. (C) A summary of primer combinations used in the RT-PCR analysis for alternative splicing determination and their resultant PCR product. (D) Poly-A⁺ mRNA prepared from whole plant tissues; two preparations were loaded on an 1% agarose gel. (E) RT-PCR analysis for AtSNF4 alternative splicing determination amplified with exon 1, exon 2 and exon 3 sequence as 5' primers and exon13-3' primer. No PCR product is amplified with first intron, second intron and third intron sequence used as 5' primers with exon 13-3' primer (lane 3, 4 and 6).

that the gene produces two transcripts, a short one called AtSNF γ , containing only the C β S repeats, and a long one called AtSNF $\beta\gamma$, which includes the upstream KIS reading frame. The KIS domain has been recently annotated to be actually a glycogen-binding domain (GBD) found in yeast and animals only in the substrate targeting β -subunits (Polekhina *et al.*, 2003). An AtSNF4 cDNA without the KIS domain was able to complement yeast $\Delta snf4$ mutation (Kleinow *et al.*, 2000). Two putative start codons were identified, which could correspond to the AtSNF4 $\beta\gamma$ (long) 53kDa and AtSNF4 γ (short) 43kDa forms. The published data raised the possibility that plant SNF4 might exist in two alternative isoforms, due to differential splicing of the primary transcript. To examine whether this is indeed the case, poly A⁺ RNA was prepared from whole aerial tissues of greenhouse grown plants. PolyA⁺ RNA extract was used for cDNA synthesis to produce template for RT-PCR with various combinations of *SNF4* exon and intron primers (Figure 50). None of the primer-pairs could identify any fragments, which would have confirmed alternative splicing events. This result clearly demonstrates that *SNF4* does not go under alternative splicing at transcriptional level and therefore only a single form of SNF4 transcript exists, which encodes AKIN $\beta\gamma$ with the N-terminal KIS domain.

3.2.4. Excluding the possibility of alternative splicing at the protein level

To confirm the absence of protein product produced by alternative splicing, we have generated various constructs for expressing HA epitope tagged versions of the KIS-domain containing long form AKIN $\beta\gamma$. The HA-AtSNF4 was provided by T. Kleinow. To generate the SNF4-HA construct, the *SNF4* coding sequence was PCR amplified to create *Xba*I restriction sites and cloned into the binary vector pPCV812, in frame with a C-terminal intron tagged HA epitope (HiA). This construct was transferred into the *Agrobacterium* strain GV3101 (pMP90RK) by electroporation and subsequently the pPCV812-AtSNF4-HiA construct was transformed into *Arabidopsis* (Col-0) cell suspension lines.

3.2.4.1. Western blot analysis of epitope tagged SNF4 overexpressing Arabidopsis cell suspension

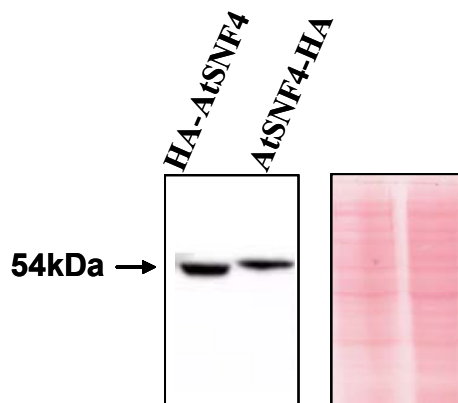


Figure 51. Analysis of stability of HA-SNF4 and SNF4-HA fusion proteins.

Crude protein extract were prepared from *Arabidopsis* cell lines expressing the HA-SNF4 and SNF4-HA proteins. Equal amounts (5 μ g) of protein samples were size separated on a 10% SDS-PAGE and analyzed by Western blot using an anti-HA antibody. Lane 1 and 2 contain the epitope tagged long form of SNF4, which were originally designated as HA-AtSNF4 $\beta\gamma$ and At-SNF4 $\beta\gamma$ -HA proteins, respectively.

Crude protein extracts were prepared from the transgenic cell lines overexpressing the N- and C-terminally HA-epitope tagged SNF4 protein and subjected to immunoblot analysis using an anti-HA antibody (Figure 51). A protein band of 53 kDa corresponding to the AKIN β γ long form of SNF4 was detected in all protein extract independently from whether they derived from cells expressing the N-terminally or C-terminally epitope labeled long SNF4 protein. The short form, SNF4 γ of 41.3 kDa was not detected on the immunoblot, confirming that no short SNF4 γ form is generated by proteolytic processing of the long form AKIN β γ . In conclusion, we showed that the *Arabidopsis* SNF4 encodes a single protein product, which is carrying an unusual N-terminal addition of a KIS domain sequence. To avoid further confusion we designated the gene product SNF4.

3.2.5. Isolation of *snf4* T-DNA insertion mutations.

To initiate functional characterization of *SNF4*, T-DNA insertion mutant screening was performed with lines derived from the SALK, GABI-KAT and Wisconsin mutant collections.

3.2.5.1. Screening for *snf4* insertion mutants in the Wisconsin mutant population

The Plant Biotechnology lab at the university of Wisconsin, Madison has generated a 72,960 BASTA (Glufosinate) resistant lines transformed with an activation-trap vector, pSK1015 (Weigel et al., 2000). Their population was arrayed in 76 x 96 well plates in groups of 10 lines. Superpools were made up of 1 or 2 DNA plate pools. DNA was isolated from both rows and columns of several plates and combined to form the "Tower" pools. Screening of 72,960 plants identified a single T-DNA insertion in the *SNF1* gene in pool no. 21 (Figure 52B) with the T-DNA LB and SNF4 gene specific 3' primers, which was detected by Southern hybridization with the *SNF4* cDNA probe. Southern hybridization of DNA amplified with SNF4 5' and T-DNA LB primers highlighted a hybridizing fragment of 7.0 kb, indicating that the insertion was far upstream of the gene as the size of the SNF4 gene is 5.0 kb.

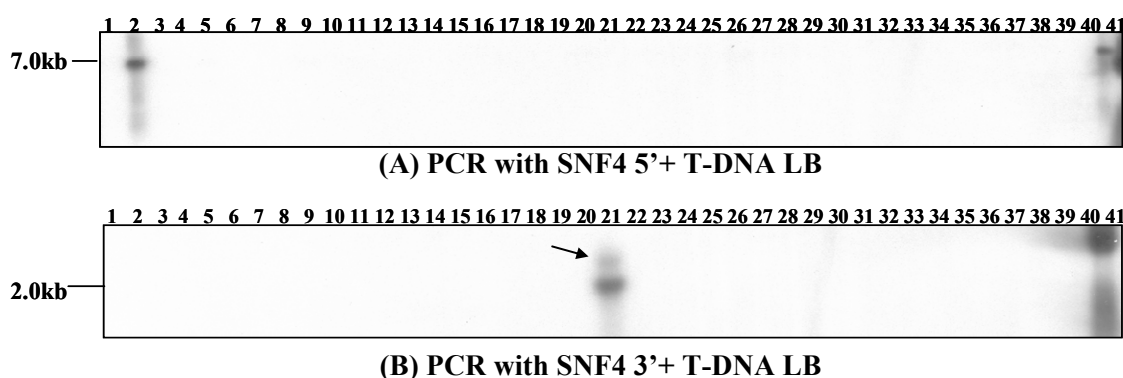


Figure 52. Screening of the Wisconsin insertion mutant collection for T-DNA tag in the *SNF4* gene.

(A) PCR amplification of DNA prepared from 40 pools with SNF4 5' and T-DNA LB primers was subjected to Southern hybridization with SNF4 cDNA probe. There was a signal of 7.0kb in pool 2. (B) Southern hybridization analysis of PCR amplified product of individual 40 pools of DNA with SNF4 3' and T-DNA LB primers. The *AtSNF4* cDNA probe detected a signal at 2.0kb in tower pool no. 21. Lane no. 41 is the super pool positive control.

3.2.5.2. Identification of a single T-DNA sub-pool (second round screening of Wisconsin T-DNA population) by Southern hybridization

The first round screening identified an insertion in super pool 21. Super pool 21 is made up of one plate pool no. 39. Second round screening was performed using 21 PCR reactions (12 columns and 10 rows) performed with *AtSNF4*-3' and T-DNA LB primers. Southern hybridization analysis identified a single pool in row 2 and column A (Figure 53 A and B). After identification of the final positive pool of 10 plants, the corresponding pool was received from Wisconsin and individual plants were analyzed to identify a single line carrying a T-DNA in the *SNF4* gene.

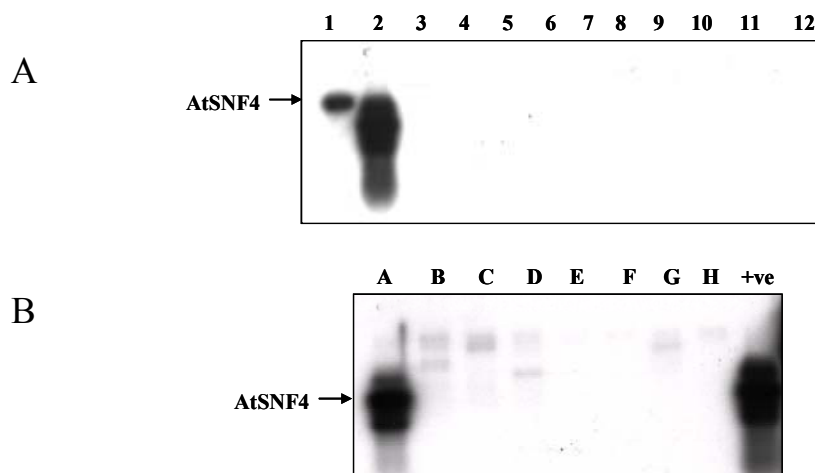


Figure 53. Identification of single pool of mutant carrying a T-DNA insertion on the *SNF4* gene.

(A) Southern hybridization analysis of DNAs amplified from 12 individual pools with *SNF4* 3' and T-DNA LB primers resulted in identification of an insertion in *SNF4* corresponding to a signal of 2.0kb in the second row (A, lane 2) and column A (B, lane 1).

3.2.5.3. Structure of the T-DNA insertion in the *WISCONSIN snf4* mutant

Genomic DNA prepared from this identified individual line was used to amplify the flanking borders to get the T-DNA junction border structure. Sequencing revealed that the T-DNA insertion is located in the 9th exon of the *SNF4* gene (Figure 54). In this *snf4-1* allele the T-DNA left border faces the 3' end of the gene. T-DNA insertion leads to a deletion of 51bp in the insertion target site.

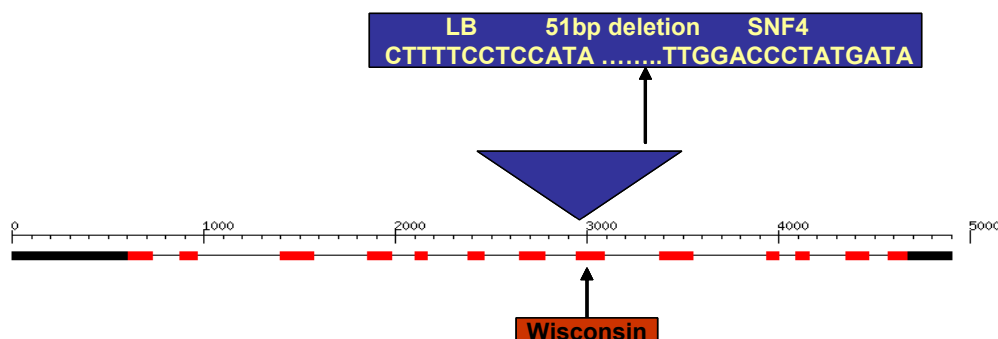


Figure 54. Localization of the T-DNA insertion in the *snf4-1* (Wisconsin) mutant allele.

Only the left T-DNA-plant DNA insert junction could be recovered by PCR amplification and was characterized by sequencing. The figure shows schematic structure of the *SNF4* gene. Exons are marked by red bars, whereas introns are indicated with black lines.

3.2.5.4. PCR analysis of segregating M3 families of the WISCONSIN *snf4* mutant

Individual M3 families derived from the WISCONSIN *snf4-1* mutant line were characterized by PCR genotyping. Individual M3 plants were grown for two to three weeks, followed by genomic DNA extraction. To screen for homozygous insertion mutant lines, primers were designed to match sequences located 5' upstream and 3' downstream of the gene. However, screening of over 30 M3 families resulted in no homozygous mutant suggesting that the mutation cause either female or male lethality. The fact that the siliques contained no aborted seeds suggested that the mutation affects male gametogenesis (Figure 55).

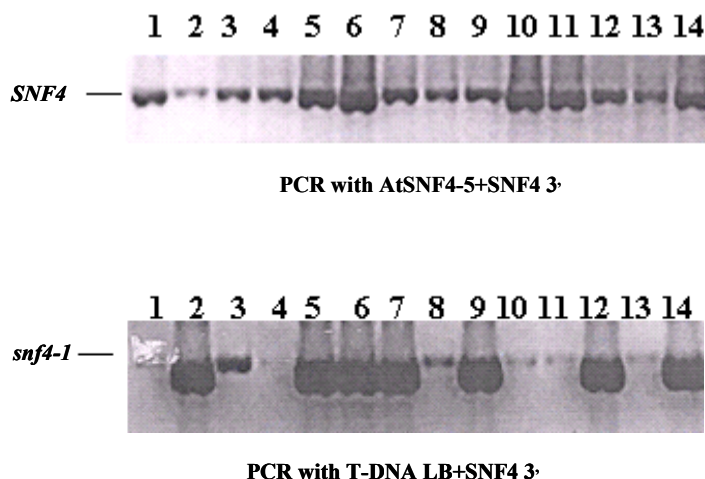


Figure 55. PCR genotyping of segregating M3 families for the *snf4-1* mutant allele.

PCR was performed on genomic DNA prepared from M3 individuals. The upper panel shows PCR performed with SNF4 gene specific primers indicating the presence of wild type allele in all lines. The lower panel shows PCR performed with the T-DNA LB and SNF4 3' primers, which indicate the presence of T-DNA tag in some M3 families (i.e., amplification of a 1.7 kb DNA fragment).

3.2.5.5. Screening for *snf4* insertion mutants in the SALK and GABI-KAT collections

In order to isolate additional *snf4* alleles, we have PCR genotyped putative T-DNA end-sequenced *snf4* mutant lines from the SALK and GABI-KAT T-DNA insertion populations in a similar way as described above. The *snf4-2* allele, which was found in the SALK collection, carries a T-DNA insertion in the 2nd intron, whereas in the *snf4-3* allele isolated from the GABI-KAT a T-DNA insertion was localized at the boundary of intron 1 and exon2. For both new alleles, both 5' and 3' junctions of T-DNA insertions were amplified and characterized by sequencing (Figure 56). Subsequently, M3 families derived by self-pollination of individual *snf4-2/+* and *snf4-3/+* lines were propagated and genotyped by PCR. As seen for the *snf4-1* allele, we failed to identify homozygous mutant lines carrying the *snf4-2* allele in the progeny of the SALK_074210 insertion line. By contrast, surprisingly we found homozygous lines for the *snf4-3* allele in the progeny of the GABI_346E09 mutant line. Inspection of the T-DNA junction sequences located just at the boundary of exon2 and intron 2 showed that the junction contained 4 potential splice-donor sites (i.e., AG) suggesting that during transcription the T-DNA sequences were probably removed from the mRNA restoring a transcript with nearly wild type reading frame. To confirm this possibility, experiments are currently

in progress. The location of T-DNA insertions and characteristics of the T-DNA-plant DNA junction sequences in the *snf4* alleles are summarized in Figure 56.

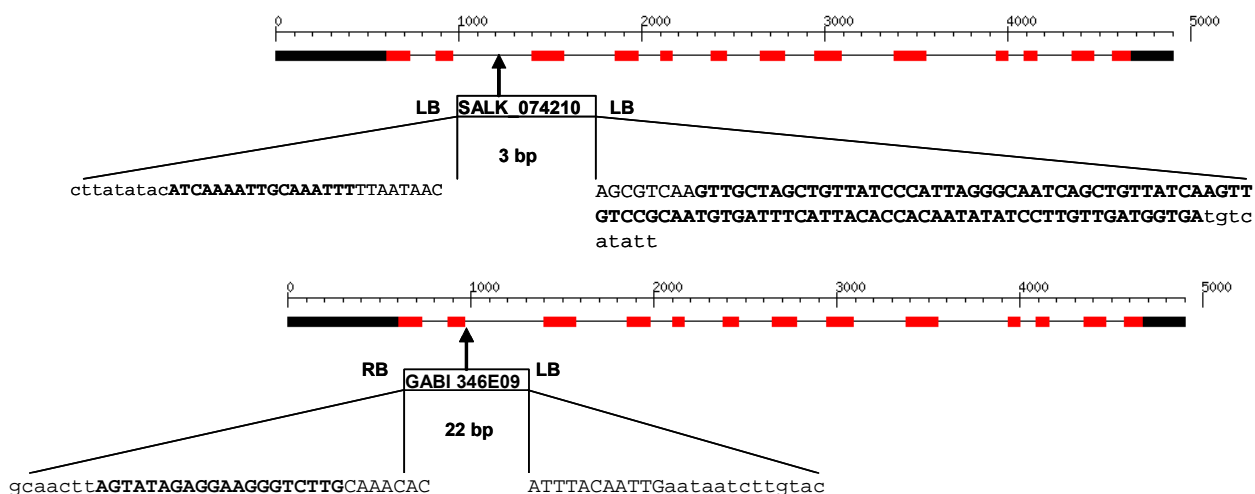


Figure 56. Characterization of *snf4-2* and *snf4-3* T-DNA insertion mutant alleles.

The positions of T-DNA insertions in the three *snf4* alleles are shown schematically. In the border sequences depicted above T-DNA sequences are printed with capital letter, whereas plant sequences are in lower case. Filler DNA sequences generated by illegitimate recombination at the T-DNA ends are labeled with bold letter. The *snf4-2* mutant allele carries a head-to-head (LB-RB/RB-LB) inverted T-DNA repeat. Below the position of insertions numbers indicate the size of target site deletions generated by the T-DNA insertion events.

3.2.6. Cellular localization of the SNF4 protein

To determine cellular localization of the SNF4 protein with biochemical fractionation assays, nuclear and cytoplasmic protein extracts were prepared from a dark-grown *Arabidopsis* cell suspension expressing the HA-epitope tagged HA-SNF4 protein. Samples from both fractions were subjected to immunoblotting with an anti-HA antibody, and the cytoplasmic contamination of nuclear protein extract was monitored by control blotting with an anti-ATAM1 amidase antibody (i.e. over 95% of the ATAM1 amidase is localized in the cytoplasm (personal communication A. Oberschall and Z. Koncz). The results of this cell fractionation experiment showed that the SNF4 protein of 53 kDa was localized in the nucleus (Figure 57).

3.2.6.1. Transient expression of an SNF4-GFP fusion protein in a light-grown *Arabidopsis* cell suspension

To visualize subcellular localization of SNF4, a protein fusion with the green fluorescent protein GFP was generated by excising the SNF4 cDNA from pPCV812-SNF4-HA (3.2.4) plasmid by *Xba*I digestion and ligated in frame with GFP coding sequences using an *Xba*I site of pCAT-GFP vector. Protoplasts were prepared from light-grown *Arabidopsis* Ler cell suspension and transformed with pCAT-GFP-SNF4. Expression and localization of the GFP-SNF4 fusion protein in the transformed protoplast were monitored by fluorescence microscopy. This experiment revealed that in protoplast prepared from light-grown cells the GFP-SNF4 protein accumulated in the nucleus, but was also present in the cytoplasm (Figure 58).

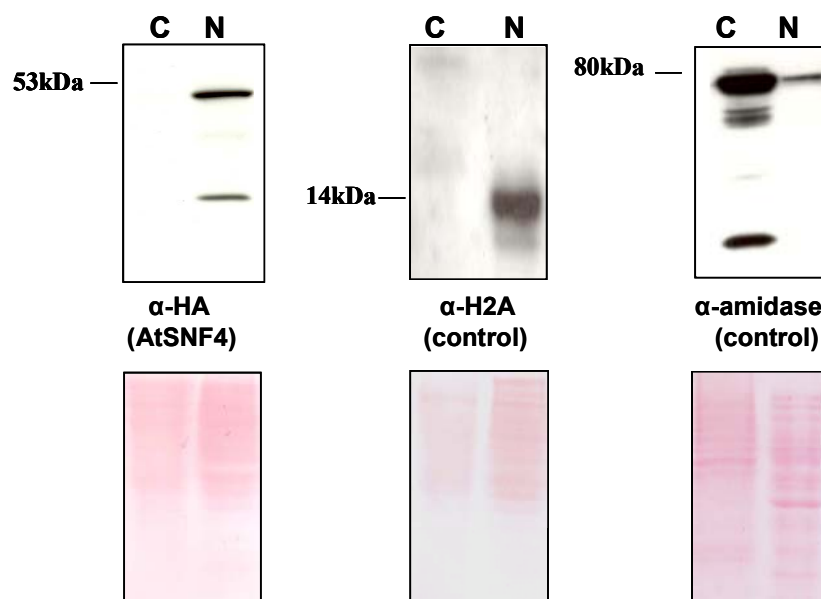


Figure 57. Determination of distribution of SNF4-HA protein in cytoplasmic and nuclear protein fractions.

Cytoplasmic and nuclear protein extracts were prepared from 10g dark grown *Arabidopsis* Col-0 cell suspension expressing SNF4-HA. Equal amounts of protein samples ($\sim 5\mu\text{g}$) were analysed by SDS-PAGE and immunoblotting with a monoclonal anti-HA antibody. As control, the protein fractions were immunoblotted with anti-histone H2A and anti-ATAM1 (α -amidase) antibodies. 'C'-cytoplasmic fraction; 'N'-nuclear fraction. The immunoblotted membranes were stained with Ponceau-S to monitor the amount of analysed proteins.

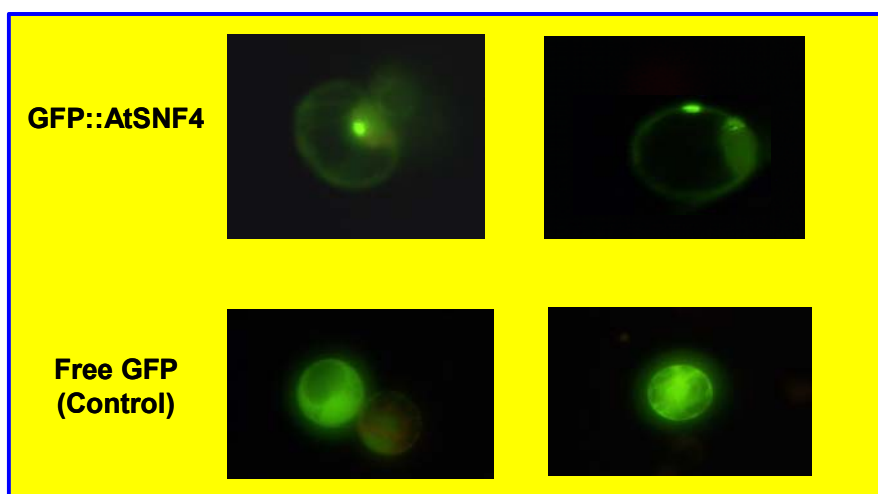


Figure 58. Cellular localization of the GFP-SNF4 fusion protein in protoplasts prepared from a light-grown *Arabidopsis* Ler cell suspension.

Protoplasts from light grown cells were transformed with $15\mu\text{g}$ of pCAT-GFP-SNF4 DNA and after 16 h the expression and localization of GFP-SNF4 fusion protein was monitored by fluorescence microscopy. Plasmid vector pCAT-GFP DNA was used as a control.

3.2.6.2. *Western blot analysis of distribution of SNF4 protein in nuclear and cytoplasmic fractions prepared from dark- and light-grown cell suspensions*

In order to examine the effect of light on the localization of SNF4 protein, cytoplasmic and nuclear extracts were prepared from light- and dark-grown *Arabidopsis* cell suspensions. The protein extracts were separated by SDS-PAGE and analyzed by immunoblotting with an anti-SNF4 antibody (unpublished, T. Kleinow). In nuclear extracts prepared from light-grown cells the SNF4 protein was

detected in the nucleus as well as in the cytoplasm, whereas SNF4 was found only in nuclear protein extract prepared from the dark-grown cell suspension (Figure 59).

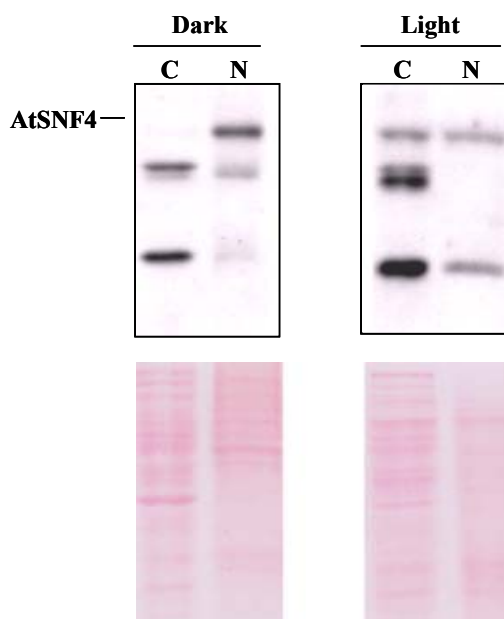


Figure 59. In light-grown cells SNF4 is exported to the cytoplasm.

Cytoplasmic and nuclear protein extracts were prepared from dark- and light-grown cell suspensions. Equal amount of proteins were loaded on 10% SDS-PAGE and immunoblotted with anti-SNF4 antibody. In dark-grown cells SNF4 was only detected in the nuclear fraction, whereas in light-grown cells it was observed to appear in the cytoplasmic protein fraction. C – cytoplasmic fraction, N – nuclear fraction. The protein filter were stained with Ponceau-S to monitor equal loading.

3.2.7. Immuno-affinity purification of SNF4-HA from *Arabidopsis* cell suspension

To isolate SNF4 in complex with other proteins, nuclear protein extract (~20 mg) was prepared from dark grown cell suspension overexpressing AtSNF4-HA and pre-cleared with protein G-Sepharose. After pre-clearing, proteins were bound to agarose beads carrying monoclonal anti-HA IgG. Followed by stringent washes, the IgG matrix-bound proteins were eluted by peptide competition using synthetic HA-peptide. The HA-peptide was also used as competitor in control immunoblotting. The results indicated that this approach is suitable for purification of sufficient amount of nuclear SNF4-HA protein (Figure 60).

3.2.7.1. SNF4-HA immunoprecipitates an SnRK1 α subunit (either AKIN10 or AKIN11)

SNF4 represents the only activating γ -subunit of SnRK1 protein kinases in *Arabidopsis*. Thus, SNF4 was predicted to show co-immunoprecipitation with SnRK1 α -subunits, which carry an SNF4-binding site in their C-terminal regulatory domains. Immunoblotting of immunoaffinity purified SNF4-HA with an anti-SnRK1 α antibody (i.e., anti-NPK5 raised against the tobacco NPK5 SnRK1 α protein, Muranaka et al., 1994; it recognized all *Arabidopsis* SnRK1 α subunits; Bhalerao et al., 1999). The data showed that SNF4-HA was indeed associated with an SnRK1 α protein *in vivo* (Figure 60).

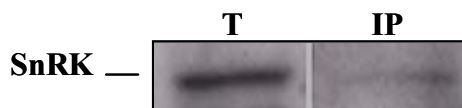


Figure 60. SNF4-HA is associated with an SnRK α -subunit in vivo.

Immunopurified SNF4-HA prepared from nuclear protein extract of a dark-grown cell suspension was resolved by 10% SDS-PAGE and immunoblotted with anti-SnRK1/ α NPK5 antibody, which detects an SnRK1 α in complex with SNF4-HA.

3.2.8. SNF4 is associated with the 26S proteasome

Our laboratory demonstrated that an α -subunit of *Arabidopsis* SnRK1 kinases is found in association with the α 4/PAD1 subunit of 20S proteasome catalytic particle (Farras *et. al.* 2001). This prompted the investigation of whether SNF4 is also associated with the 26S proteasome. To test this possibility, nuclear extract was prepared from dark-grown SNF4-HA overexpressing cell suspension in presence of 2 mM ATP (i.e., to maintain proteasome integrity) and immunoaffinity purified on Sepharose-conjugated anti-HA IgG beads after preclearing with protein G. The matrix was washed with buffer containing high salt to remove non-specifically bound proteins. The matrix-bound proteins were eluted with HA-peptide, denatured in Lammeli loading buffer, and resolved by SDS-PAGE and subjected to immunoblotting with a monoclonal antibody raised against conserved α -subunits of the 20S human proteasome (which detects several *Arabidopsis* 20S α -subunits), and with a polyclonal antibody raised against subunits of the 19S proteasome regulatory cap. In the purified SNF4-HA protein complex a 20S proteasome signal was detected, but we failed to demonstrate the presence of the 19S cap (Figure 61).

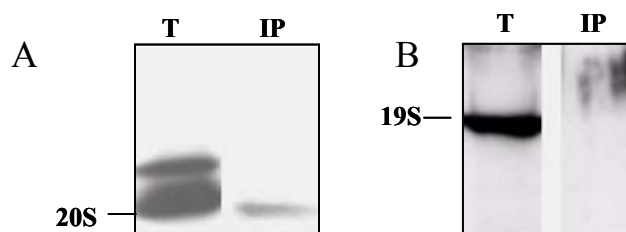


Figure 61. SNF4-HA is found in association with the 20S proteasome.

Immunoaffinity purified SNF4-HA protein complexes were resolved by 12% SDS-PAGE and immunoblotted with monoclonal anti-20S and anti-19S proteasome regulatory subunit antibodies. (A) SNF4-HA co-immunoprecipitates with α -subunits of the 20S core particle (B) anti-19S proteasome subunits are not present in the purified SNF4-HA complex.

3.2.8.1. The immuno-purified SNF4-HA complex does not carry the PRL1 inhibitor of SnRK1 α kinase subunits

In our laboratory Bhalerao *et al.* (1999) showed that the PRL1 nuclear WD-protein inhibitor of SnRK1 kinases interacts with the same C-terminal domains of *Arabidopsis* SnRK1 α -subunits AKIN10 and AKIN11, which bind the SNF4 activating γ -subunit. To investigate whether SNF4 is associated with PRL1, SNF4 was immunoaffinity purified and immunoblotted with polyclonal anti-PRL1 antibody

(Németh *et al.*, 1998). No PRL1 signal was detected, which indicated that PRL1 does not occur in complex with SNF4 (Figure 62).

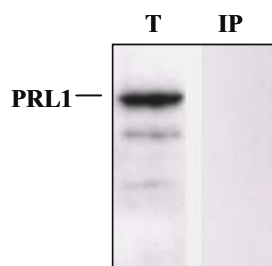


Figure 62. PRL1 does not interact with SNF4.

Immunoaffinity purified SNF4-HA protein was resolved by 10% SDS-PAGE. Western blotting with a polyclonal anti-PRL1 antibody failed to detect PRL1 in the purified SNF4-HA immunocomplex.

3.2.9. Association of SNF4 with SnRK1 α -subunits and 20S proteasome is not affected by light

Our previous experiments (3.2.6) indicated that cellular localization of SNF4 is influenced by light, and showed that SNF4 is found in protein complexes with an SnRK1 α -subunit and the 20S proteasome cylinder in nuclear protein extracts prepared from dark grown cells. To test whether association of SNF4 with these proteins is regulated by light, nuclear extract was prepared from a light grown cell suspension overexpressing SNF4-HA using HA-affinity-matrix, as described above. The HA-peptide eluted SNF4-HA protein fraction was resolved by SDS-PAGE and immunoblotted with anti-SnRK1 α , anti-PRL1, and anti-20S proteasome antibodies. The results obtained by this western blot analysis were identical with those obtained with nuclear protein extract from dark grown cells, suggesting that light probably does not abolish the association of SNF4 with SnRK1 α proteins and the 20s proteasome cylinder.

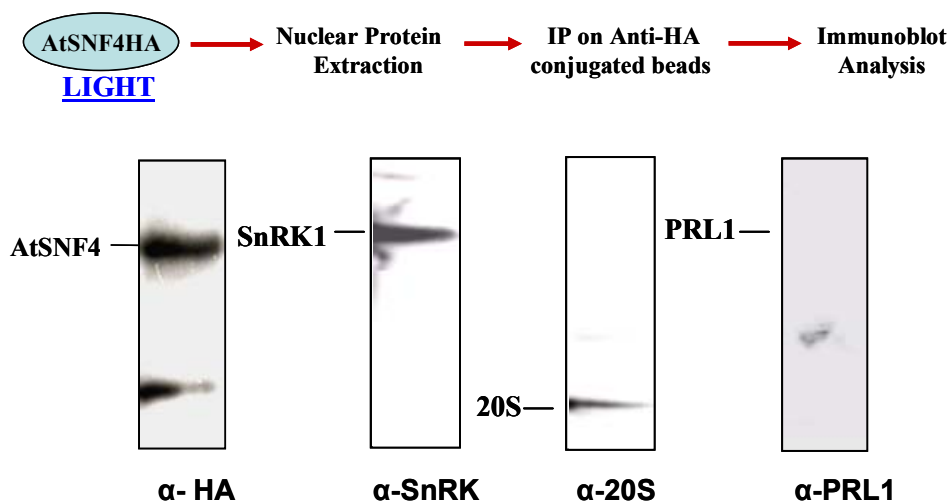


Figure 63. Association of SNF4 with SnRK1 α and 20S proteasome is not abolished by light.

Immunoaffinity purified nuclear SNF4-HA protein fraction prepared from light grown cell suspension was resolved by 10%SDS-PAGE and immunoblotted with anti-SnRK1 α , anti-PRL1 and anti-20S proteasome antibodies.

3.2.10. Size fractionation of SNF4 protein complex by glycerol gradient centrifugation

To size fractionate SNF4 protein complexes, 20g cells from dark- and light-grown cell suspensions overexpressing AtSNF4-HA were used for extraction of nuclear and cytoplasmic proteins. The extracts were loaded onto linear 10%-40% glycerol gradients to perform size fractionation of SNF4 complexes by centrifugation for 16 hrs at 30,000 rpm in a SW40Ti rotor at 4°C. After centrifugation, 300µl fractions were collected and similar aliquots from each fraction were analyzed by immunoblotting. SNF4 was detected predominantly in the higher molecular mass fractions 28-31 (~700-800kDa) of gradients prepared from dark grown cell suspensions. The predicted size of core trimeric SnRK1 complexes is about 150k Da (including the α , β and γ subunits), but this result showed that the actual size of SNF4-containing SnRK1 complex(es) is much higher (Figure 64). SNF4 was found to occur in similar size of protein complexes in nuclear extracts prepared from both light and dark grown cells (data not show).

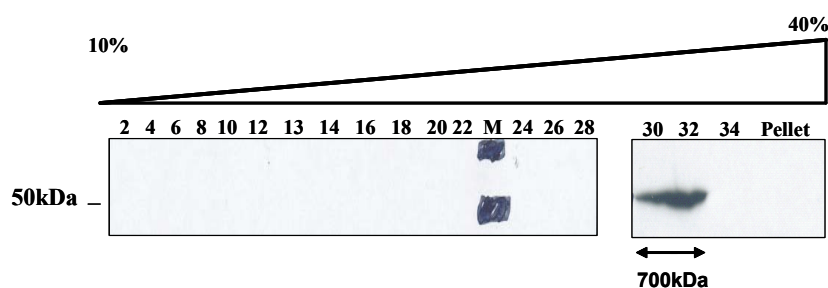


Figure 64. Glycerol gradient size fractionation of SNF4 protein complexes.

Nuclear protein extracts from SNF4-HA overexpressing dark-grown cell suspension was loaded onto a linear 10%-40% glycerol gradient to size fractionate protein complexes. After centrifugation, 300µl aliquots of gradient fractions were collected, samples of equal volumes were separated by 10% SDS-PAGE and analyzed by immunoblotting with anti-HA antibody.

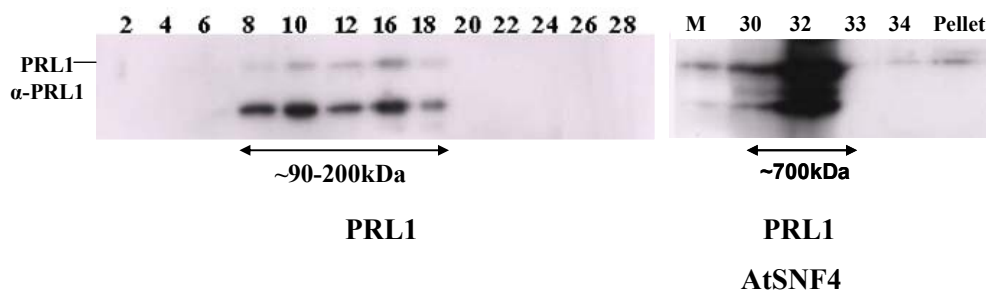


Figure 65. PRL1 and SNF4 show co-fractionation on a linear glycerol gradient.

Equal amount of SNF4-HA glycerol gradient fractions (see Figure 64) were separated by 10% SDS-PAGE and analyzed by immunoblotting with anti-PRL1 antibody. PRL1 was detected in fractions 8 to 18 as well as in fractions 30 to 32. Fractions 30 to 32 also contained AtSNF4 (Figure 64).

3.2.10.1. SNF4 and PRL1 are present in protein complex of similar size

The SNF4-HA glycerol gradient fractions were immunoblotted with anti-PRL1 antibody to detect whether SNF4 and PRL1 are present in the same fractions. The data of western blotting showed that the PRL1 protein was distributed into two complexes with a peak size of 90-200 kDa in fractions 8 to 18 and >700 kDa in fractions 30 to 32 (Figure 65). By contrast, SNF4 was only detected in fractions

30 to 32 suggesting that the size of SnRK1-PRL1 and SnRK1-SNF4 is similar. However, despite co-fractionation, SNF4-HA did not immunoprecipitate PRL1 from these glycerol gradient fractions (data not shown, personal communication A. Oberschall).

3.2.11. The substrate targeting AKIN β 2 subunit is associated with an SnRK1 α -subunit

To further investigate the organization of SnRK1 kinase complexes, an *Arabidopsis* cell suspension line overexpressing an HA epitope tagged form of one of the β -subunits, HA-AKIN β 2. A binary expression vector carrying HA-AKIN β 2 (Ferrando et al., 2000) was transferred to *Agrobacterium* followed by transformation of a light-grown *Arabidopsis* Ler cell suspension. Subsequently nuclear protein extract was prepared from the stable transgenic line and subjected to immunoaffinity purification of HA-AKIN β 2 as described above. The purified proteins were resolved by SDS-PAGE and immunoblotted with anti-SnRK1 α and anti-PRL1 antibodies. As expected, the anti-SnRK1 α antibody detected an SnRK1 α subunits in the AKIN β 2 immunocomplex confirming the observations of Ferrando et al. (2001). By contrast, the anti-PRL1 antibody failed to detect PRL1 in association with HA-AKIN β 2, indicating that, as SNF4, AKIN β 2 and PRL1 do not occur in common SnRK1 kinase complex (Figure 66).

3.2.12. AKIN β 2 is associated with the 26S proteasome

The association of AKIN β 2 with an SnRK1 α -subunit suggested that AKIN β 2 should also recruit 26S proteasome as was observed by Farrás et al. (2001) for the SnRK1 α -subunits. To examine proteasomal association of AKIN β 2, total protein extract from HA-AKIN β 2 expressing cell line was prepared and immunopurified in the presence of 2mM ATP, and then immunoblotted with anti-20S proteasome antibody. Western blot analysis detecting the 20S proteasome α -subunits in the HA-AKIN β 2 immunocomplex revealed that AKIN β 2 was indeed associated with the 20S proteasome cylinder. The HA-AKIN β 2 complex also contained a component, which cross-reacted with the anti-SnRK1 α antibody, but showed no cross-reaction with the anti-PRL1 antibody.

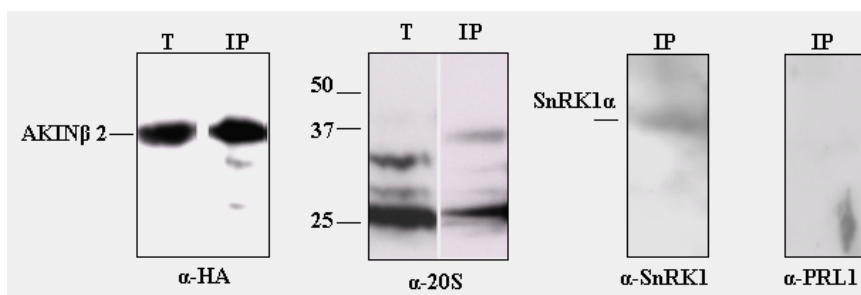


Figure 66. AKIN β 2 co-immunoprecipitates with the 20S proteasome cylinder and with an SnRK1 α -subunit.

Immunoaffinity purified HA-AKIN β 2 protein fraction was resolved by 10% SDS-PAGE and immunoblotted with anti-SnRK1 α , anti-20S proteasome, and anti-PRL1 antibodies. T – total protein extract; IP – immunoprecipitated fraction.

3.2.13. Transcriptional regulation of the *SNF4* gene in wild type and *prl1* mutant plants

To examine the transcriptional regulation of *SNF4* gene under different stress and hormonal conditions, three weeks old *Arabidopsis* (Col-0) and *prl1* mutant plants grown in sterile cultures *in vitro* were treated with either 100 μ M ABA, or 3% sucrose, or 300mM glucose and exposed to sucrose starvation (without sucrose) in liquid seed germination medium for 24h. Total RNA was prepared from treated plants and used as template in RT-PCR analyses with *SNF4* gene specific primers. Ubiquitin-10 primers were used as an internal control. RNA from untreated wild type plants served as control. Interestingly, in presence of 3% sucrose *SNF4* mRNA levels were higher in *prl1* than in wild type, whereas in the presence of 300 mM glucose *SNF4* showed higher expression in wild type than in *prl1* plants. In addition, *SNF4* transcript levels were about 2-fold lower in the *prl1* mutant than in the wild type under ABA-treatment. Current experiments address the significance of these observations, in particular in case of sucrose and glucose treatments.

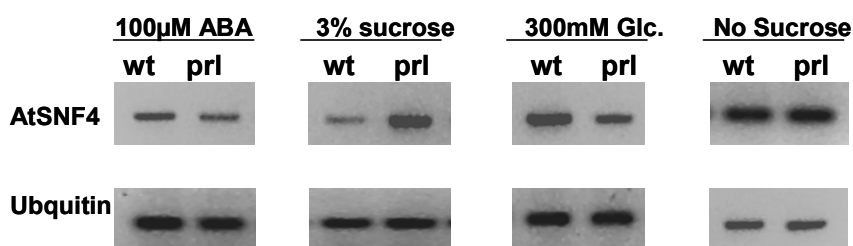


Figure 67. Comparative RT-PCR analysis of *SNF4* transcript levels in response to ABA, sucrose, glucose and sugar starvation in the *prl1* mutant and wild type.

Three weeks old plants were treated as indicated for 24 h, followed by total RNA extraction and cDNA preparation. PCR was performed using *SNF4* gene specific primers. Ubiquitin expression levels were used as loading controls.

3.2.14. Assay of *SNF4* protein stability

The results described also raised the question whether glucose/sucrose or ABA would affect the stability of the *SNF4*-HA protein. To test this, the levels of HA-*SNF4* protein were assayed in two weeks old seedlings treated with 3% sucrose, 100 μ M ABA and 600 mM Mannitol (control). This experiment indicated that HA-*SNF4* is highly stable under these stress condition.

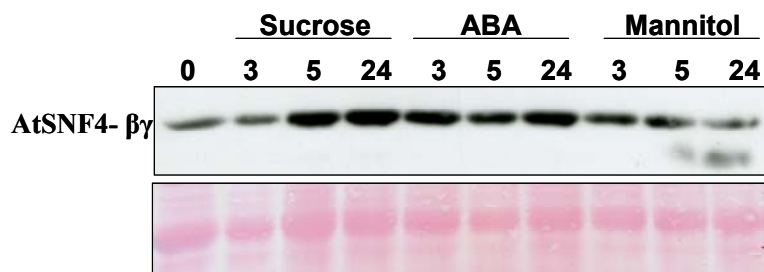


Figure 68. Assay of HA-*SNF4* protein stability under various stress treatments.

Crude protein extracts were prepared from samples collected at 3, 5 and 24 h time points from HA-*SNF4* expressing seedlings subjected to treatment with 3% sucrose, 100 μ M ABA and 600mM mannitol. Equal amount of protein was resolved by 10% SDS-PAGE electrophoresis and immunoblotted with anti-HA antibody.

4. DISCUSSION

4.1. CHARACTERIZATION OF FUNCTION REGULATION AND PHOSPHORYLATION OF DPBF4

4.1.1. DPBF4 binds to a G-box element within the sugar responsive enhancer of the AK1/HSD1 aspartate kinase gene

Using a one hybrid screen with the sugar responsive promoter element of the *AK1/HSD1* promoter Shai Ufaz and Prof. Aviah Zilberstein, with whom we worked in close collaboration in the Minna James Heinemann project, have identified a bZIP transcription factor, DPBF4. Subsequent experiments, including site-specific mutagenesis of the ABRE-like GCN4 and G-box elements in the *AK1/HSD1* enhancer revealed that DPBF4 shows specific interaction with a G-box motif in yeast, which proved to carry identical sequences as a G-box motif activated by the bZIP12/EEL1 transcription factor in the promoter of the *Em1* LEA-gene studied by Bensmihen et al. (2002).

In fact, DPBF4 is identical with bZIP12/EEL1, which has been found to negatively control the expression of the *Em1* gene during early stages of embryo development. Following 5 to 7 days after pollination, the *Em1* gene is showing increased level of transcriptional induction, which coincides with embryonic increase of ABA levels and activation of the ABI5 transcription factor. Whereas DPBF4 was defined as a negative regulator of the *Em1* promoter, Benshimen et al. (2002) found that ABI5 is a major positive regulator of *Em1* transcription. Lopez-Molina et al. (2002), on the other hand showed that ABI5 is a general regulator of ABA and sugar dependent transcription of seed specific genes during late embryogenesis and is required for proper seed maturation and desiccation (for review see Finkelstein et al., 2002; Prince et al., 2003).

However, ABI5 also plays a role during the transition phase from heterotrophic growth to photoautotrophic growth during seed germination. This phase has been shown to represent a narrow developmental window, in which germinating seeds show high sensitivity to externally provided sugars (sucrose and glucose) and ABA. The fact that overexpression of ABI5 confers hypersensitivity to both ABA and glucose in the seed germination assays, suggests that ABI5 is involved in simultaneous control of transcription in response to ABA and glucose (Lopez-Molina et al., 2002). Whether ABI5, acting for example as homodimer, is alone sufficient for activation of glucose-stimulated promoters is unknown. However, ABI5-mediated activation of ABA-induced promoters definitely requires interaction of ABI5 with the EREB/AP2 transcription factor ABI4 and most likely with the seed specific B3 family member ABI3 (Monke et al., 2004). ABI5 does not appear to be highly activated by osmotic stress, but induced by ABA in vegetative tissues. As ABI4 and ABI3 appear to act mainly during seed germination, it is unclear whether they also participate in the interaction with ABI5 in controlling the expression of ABA and sugar induced genes in vegetative source and sink organs.

The fact that DPBF4 appear to counteract ABI5-mediated activation of ABA and sugar responsive genes in seeds, does not exclude the possibility that DPBF4 and ABI5 could form heterodimers or that homodimeric forms of DPBF4 and ABI5 would control different sets of genes in

different vegetative organs during development. On this way, members of the ABI5/bZIP transcription factors family may in fact coordinate developmental responses to various stress stimuli.

Kim et al. (2002b) showed that ABI5 can form heterodimeric ABRE-binding complexes with DPBF3 and DPBF4, which indicates that combinatorial heterodimerization of ABI5/DPBF factors may also have a regulatory role *in vivo*. In fact, our data indicate that *DPBF4* is not only expressed during early stages of seed development, but is also detectable in various plant organs, especially in young seedlings, but also in the inflorescence of mature plants. These data suggest that DPBF4 does not only function in interaction with ABI5 during seed development, but probably has a regulatory role also in source and sink tissues during vegetative stage of plant development.

4.1.2. DPBF4 knockout mutants and probable functional redundancy of DPBF4 homologs

We have identified three *dpbf4* T-DNA insertion mutations, one of which, *dpbf4-3* proved to be a true knockout allele. The other alleles, *dpbf4-1* and *dpbf4-2*, show active transcription probably because the left border junctions of SALK T-DNA insertions face the 5' end of the *DPBF4* gene in these alleles. The pROK2 T-DNA (Weigel et al., 2000) used for generation of SALK insertion mutant collection carries a CaMV35S promoter-based expression cassette just upstream of and facing the left T-DNA border. It is thus not surprising that in both *dpbf4-1* and *dpbf4-2* mutants, in which the T-DNA LB-end is fused to 5'-UTR and 5'-leader sequences, the *DPBF4* gene shows active transcription, which is higher than the normal transcript levels detected in wild type plants. These mutants thus probably display 35S promoter-dependent ectopic overexpression of wild type and 5'-truncated *DPBF4* mRNAs. Nonetheless, neither the *dpbf4-1* nor the *dpbf4-2* alleles show altered seed development or stress response in our preliminary assays. Although these tests should be continued under specific stringent conditions and by testing ABA and sugar regulated gene expression, it is possible that 35S promoter driven overexpression of *DPBF4* will not confer dramatic stress-related phenotypes. This is because DPBF4 is expected to be a target for post-translational modifications, such as phosphorylation and ubiquitination, which might provide an additional control at the levels of protein stability, in addition to potential stress regulation of *DPBF4* transcription.

On the other hand, preliminary phenotypic analysis of the *dpbf4-3* mutant allele suggest that even this true knockout does not seem to result in significant defect in seed and seedling development. This data is consistent with recent results of Bensmihen et al. (2005) who found that simultaneous RNAi inhibition of AtbZIP12/DPBF4/EEL1, AtbZIP67/DPBF2 and AtbZIP66/AREB3/DPBF3 expression fails to cause observable defects in seed or seedling development. This observation would indicate that DPBF1/ABI5 performs an overlapping regulatory function with the other three DPBF bZIP factors, which show dimerization with ABI5. Nonetheless, so far no insertion mutations was identified in any available collection in *DPBF3*, which is the closest homolog of *DPBF4*. As many critical regulatory proteins are encoded by duplicated genes in *Arabidopsis* (see for review Barnes, 2002), it is possible that DPBF3 and DPBF4 perform closely similar functions. Unfortunately, in the

report of Bensmihen et al. (2005) there is no convincing evidence, which would show that the RNAi approach has indeed resulted in simultaneous and quantitative reduction of expression of all three DPBF factors in vegetative tissues. Thus, it remains open whether DPBF2, which does not dimerizes with DPBF3 and DPBF4, would perform an overlapping function with DPBF4. Finally, experiments from Kang et al. (2002) show that overexpression of ABF3/DPBF5 and ABF4/AREB2 results in ABA hypersensitivity and enhanced drought tolerance, whereas overexpression of ABF2/AREB1 confers a much wider stress and heat tolerance (Kim et al., 2004b).

Although one needs to be cautious with interpretation of transcription factor overexpression data, another line of evidence also indicates that ABF2/AREB1 also plays an important role in glucose signaling. Whereas ABF2, 3 and 4 appear to be positive regulators of osmotic stress signaling, thus far no similar functions were reported for DPBF2, 3, and 4. It is thus conceivable that these DPBF factors control the transcription regulatory functions and possibly stability of other members of the ABI5 bZIP family by heterodimerization. This would suggest a negative regulatory function for these factors, which provides a testable hypothesis e.g., by testing ABA response of DPBF overexpressing and knockout mutant lines in *abi5*, *abi4*, *ein2* etc. backgrounds.

4.1.3. DPBF4 and ABI5 form heterodimers and occur in different chromatin associated protein complexes

Our immunolocalization studies performed with both HA-epitope tagged DPBF4 and GFP-DPBF4 fusion proteins in transgenic plants and protoplasts made from cultured cells show that DPBF4 is accumulating in the nucleus and barely, if at all detectable in the cytoplasm. Nuclear import of DPBF4 appears to be independent of light signals and DPBF4 shows nuclear localization also in *Arabidopsis* cell suspensions cultured in the dark. Intact DPBF4 protein could be detected in various organs of plants and well as in actively dividing tissues in contrast to many other proteins, which show tissue specific degradation even if overproduced by CaMV35S promoter-based T-DNA vectors in transgenic plants and transformed cells.

Size fractionation of nuclear protein extracts from DPBF4-HA expressing cells on linear glycerol gradients showed that when overexpressed DPBF4-HA form dimers with a molecular mass of about 70 kDa. However, in addition to this free dimeric form, DPBF4-HA was found incorporated into higher molecular mass complexes, one of which migrated with about 700 kDa mass in glycerol gradients. However, the bulk of DPBF4 appears to be tightly associated with chromatin-bound complexes, which could not be solubilized with our mild nuclear protein extraction method.

In addition to heterodimerization of ABI5 with DPBF4 demonstrated by Bensmihen et al. (2002) *in vitro*, Lopez-Molina et al. (2002) found that ABI5 fractionates in glycerol gradients also as dimer and is present in a higher molecular mass complex of about 300 kDa. Using a cell line overexpressing both DPBF4-HA and ABI5-c-Myc, we have demonstrated that DPBF4 and ABI5 form a heterodimeric complex *in vivo*. This is intriguing, as DPBF4 is proposed to be a negative regulator of ABI5 action. In addition, ABI5 appears to undergo phosphorylation-dependent stabilization and

phosphorylation was shown to be required for activation of DNA-binding by ABI5 (Lopez-Molina et al., 2003).

The non-phosphorylated form of ABI5 was shown to interact with AFP, a ABI5 interacting protein, which is probably involved in ubiquitination and subsequent proteasomal degradation of ABI5. Our observation that DPBF4 forms *in vivo* heterodimers with ABI5 raises the question whether DPBF4 is involved in the regulation of ABI5 phosphorylation and thereby in the control of ABI5 degradation. Thus, it will be interesting to test whether ABI5 modulates DPBF4 phosphorylation and *vica versa*, and whether heterodimerization with DPBF4 would destabilize ABI5. This latter possibility would also predict that DPBF4 may interact with AFP or a similar RING finger factor, which may selectively control the stability of DPBF4.

Incorporation of overexpressed DPBF4-HA into higher molecular mass complexes provides a promising means for biochemical purification of DPBF4-associated proteins, as well as for identification of DPBF4 controlled genes using the chromatin cross-linking technology (see below). It remains to be determined whether DPBF4 occurs in common complexes e.g., with ABI4 and ABI3 or similar EREB/AP2 and B3 transcription factors, which are expressed in other organs than seeds. Given a potential involvement of EREB/AP2 factors in several other stress and hormone signaling pathways, DPBF4 may turn out to provide a link to feedback regulation of ABI5 controlled gene expression by other stimuli than ABA and sugar. Furthermore, studying the DNA-binding specificity of DPBF4-ABI5 heterodimers may also unravel some more details of bZIP-binding site recognition by various heterodimers of ABI5 transcription factor family.

Several data indicate that ABI5 may regulate the expression of other bZIP genes within the ABI5 family. Therefore, further experiments addressing the regulation of DPBF4 expression in knockout mutants and lines overexpressing various members of the ABI5 family may reveal intriguing details of regulatory crosstalks between different bZIP proteins.

4.1.4. Phosphorylation of DPBF4 by OST1 and AKIN10

In the complex introduction to this thesis, we have reviewed various aspects of signaling crosstalk between the ABA-dependent and independent ionic, cold and drought stress pathways and highlighted some evident links to thus far known elements of counter- and interacting ethylene, sugar and ABA regulatory pathways. Remarkable, SnRK2 kinases appear to be involved in most of these pathways, except cold signaling (see Boudsocq et al., 2004) and their actions appear to be closely linked to signaling through NADPH oxidase and phospholipase D (PLD). Phosphatidic acid (PA), the product of PLD was thus found to directly inhibit the activity of the PP2C protein phosphatase ABI1, which on the other hand was found to interact directly with the ABI5 bZIP transcription factor and several other HD-ZIP regulatory factors of ABA controlled genes (for review see Himmelbach et al., 2003).

Although, so far there is no available study on epistatic relationships between SnRK2 kinases and ABI1, several lines of evidence suggest that SnRK2 kinases are major regulators of bZIP transcription factors. Thus, AREB1 and AREB2 were found by Uno et al. (2000) to be phosphorylated

in their N-terminal domains by a protein kinase of 42 kDa and it is thought that similarly to ABI5 this phosphorylation is required for stimulation of AREB's DNA-binding activities.

Among the 11 members of SnRK2 kinase family OST1 appeared to perform a specific function stimulating ABA-dependent closure of stomata without affecting the inhibition of seed development and root elongation by ABA (Mustilli et al., 2002). Boudsocq et al. (2004) found that OST1 is activated by ABA and drought, whereas Mustilli et al. (2002) showed that the *ost1* mutation prevents the generation of H₂O₂ signal, which is essential for stimulation of stomatal closure. These observations would place OST1 downstream of NADPH oxidase and PLD signaling, which would be compatible with the finding of Testerink et al. (2004) that SnRK2 proteins may directly bind phosphatidic acid. On the other hand, SnRK2 kinases are supposed to act downstream in ABA signaling and phosphorylate bZIP transcription factors. However, this was thus far shown only for PKABA (Johnson et al., 2002).

Our sequence analysis of DPBF4 with several phosphorylation site prediction programmes suggested that this bZIP protein carries at least one, but possible more potential phosphorylation sites in its N-terminal domain. To test directly whether OST1 and the SnRK1 AKIN10 kinase would recognize DPBF4 as substrate, we have purified DPBF4, as well as these two kinases, to homogeneity from *E. coli*. As described previously for AKIN10 by Bhalerao et al. (1999), we found that also the SnRK2 kinase OST2 undergoes autophosphorylation *in vitro*. OST1 efficiently phosphorylated histones H1A and H2B suggesting that if imported to the nucleus OST1 may perform similar histone phosphorylation and participate in modification of the histone core by phosphorylation, i.e., leading to activation of transcription. Such a role for OST1 would be consistent with its phosphorylation activity observed with the DPBF4 bZIP transcription factors in our experiments.

Furthermore, our kinase substrate predictions suggested that SnRK2 enzymes may recognize similar substrates as the SnRK1 class of protein kinases, which include master regulators of energy balance and glucose repression. In fact, we found that the *Arabidopsis* SnRK1 kinase α -subunit, AKIN10, similarly phosphorylates DPBF4 as OST1. As these kinase undergo autophosphorylation and share very similar T-loop activation sequences, this observation raises the possibility that SnRK2 kinases may act as upstream activators (or even inhibitors) of SnRK1 enzymes or *vice versa*. How SnRK2 and SnRK1 mediated phosphorylation of DPBF4 affect the activity and stability of this bZIP transcription factor remains to be determined. However, in this respect it is interesting to note that one of the three SnRK1 kinase α -subunits have been identified in close association with the 20S cylinder of the proteasome, as well as with the common SKP1/ASK1 subunit of SCF E3 ubiquitin ligases that are involved in ethylene, jasmonate, auxin, gibberellin etc. signaling. Phosphorylation of the DPBF4 transcription factor, which is exclusively localized in the nucleus (as ABI5), by AKIN10 thus suggests that in the cytoplasm AKIN10 may control nuclear import of DPBF4 by phosphorylation or, if AKIN10 was a nuclear kinase, it may directly target DPBF4 for proteolytic degradation by its association with an SCF ubiquitin ligase and the 26S proteasome.

4.1.5. Mapping of autophosphorylation sites in OST1

Mapping the autophosphorylated residues in OST1 support our hypothesis that activation of SnRK2 (and SnRK1 kinase α -subunits) includes autophosphorylation of a critical serine (or for SnRK1 enzymes threonine) residue. MADLI MS/MS and LC/MS Q-TOF analyses show that the autophosphorylated residue corresponds to Ser175 in OST1.

Mutation of this critical residue abolishes autophosphorylation, as well as OST1-mediated phosphorylation of DPBF4. By contrast, exchanging the Ser175 residue to aspartic acid, which mimics a phosphoserine residue, increases dramatically the kinase DPBF4 phosphorylation and autophosphorylating activities. This indicates that autophosphorylation is incomplete on Ser175. As the S175D OST1 mutant will also confer resistance against OST1 inactivating kinases, the use of this dominantly active kinase form in conjunction with various stress regulated promoters has a potential biotechnological significance. As expected a K59R amino acid exchange in the ATP-binding region results in a dead kinase, which shows similarly low activity as a mutant kinase carrying a deletion in the catalytic domain. Finally, a second mutation resulting in T146A amino acid exchange leads to significant activation of OST1 indicating that threonine at this position is inhibitory for the kinase activity-

We have mentioned above that, the catalytic domains of SnRK1 and SnRK2 kinases are remarkably similar and that both SnRK1 AKIN10 and SnRK2 OST1 phosphorylate the DPBF4 bZIP transcription factor. Phosphorylation experiments performed with the SnRK1-specific SAMS peptide show that this substrate is also phosphorylated by SnRK2 enzymes. This data confirms that *Arabidopsis* SnRK1 and SnRK2 kinases share indeed common substrate specificity.

4.1.6. Confirmation of DPBF4 interaction with the AK1/HSD1 promoter

In our starting yeast one hybrid screening experiments, we have identified DPBF4 as AK1/HSD1 promoter binding factor. Subsequently, using AK1/HSD1-GUS promoter fusions we found that the aspartate kinase 1 promoter is induced by salt and glucose, but not by ABA. This observation may explain the fact why our one hybrid screening failed to identify the ABI5 transcription factor, which is also expressed in cell cultures as DPBF4. Further experiments indicated that transcription of the *AK1/HSD1* gene is de-repressed in the presence of 3% glucose in the *pr11* mutant, which is defective in the function of a nuclear SnRK1 inhibitor regulatory WD-protein (Bhalerao et al., 1999).

Our attempts to clearly define the regulatory function of DPBF4 in connection with the AK1/HSD1 promoter did not reach the expected results because chemically inducible overproduction of DPBF4 thus far resulted only in such transgenic lines that show only low levels (2-fold induction) of oestradiol-induction of DPBF4-HA. Although some preliminary data suggest that DPBF4-HA could activate the ABA, salt, cold and hypoxia responsive alcohol dehydrogenase promoter, the definition of regulatory function of DPBF4 awaits for further experiments.

As part of our complementary efforts, we have used chromatin immunoprecipitation experiments with a DPBF4-HA producing cell lines and showed that DPBF4-HA is indeed cross-

linked and immunoprecipitates the AK1/HSD1 promoter. However, mapping of the *in vivo* binding site of DPBF4-HA within the AK1/HSD1 promoter indicated that from cultured cells DPBF4-HA does not immunoprecipitate the canonical G-box element, which has been suspected to represent a sugar response element. Rather, DPBF4-HA immunoprecipitates DNA sequences that carry G-box-like TGA elements, thus further complicating the problem of the analysis of functional significance of DPBF4-G-box interaction observed in our one hybrid experiments with the AK1/HSD1 promoter.

4.2. FUNCTIONAL ANALYSIS OF SnRK1 ACTIVATING GAMMA-SUBUNIT SNF4

4.2.1. Analysis of expression pattern and potential alternative splicing of *SNF4*

Plant SnRK1 kinases belong to the family of yeast Snf1 and animal AMPK-activated protein kinases that play a central role in the regulation of carbon metabolism, energy homeostasis and transcription responses to various stress stimuli, including hypoxia (for review see Hardie et al., 1998). In yeast, the trimeric Snf1 protein kinase is linked to both hexokinase modulated glucose sensing and osmotic stress modulated HOG signaling pathways (Ronne, 1995; Rolland et al., 2002b), and essential for transcriptional reactivation of genes targeted by glucose repression. Animal AMPKs also play an important role in transcriptional regulation as they occur in transcription co-activator complexes. In addition, both yeast Snf1 and mammalian AMPKs control the activity and stability of key metabolic enzymes in the first committed or rate-limiting steps of isopentenyl, fatty acid and cholesterol biosynthesis pathways. In higher plants, members of the SnRK1 protein kinases correspond to functional orthologs of yeast Snf1 and animal AMPKs (see for review Halford and Hardie, 1998).

As their yeast and animal orthologs, the plant Snf1-related SnRK1 protein kinases are trimeric enzymes composed of catalytic/ α , substrate targeting/ β and activating/ γ subunits. The *Arabidopsis* genome codes for 3 α (AKIN10, AKIN11, and AKIN12), and 3 β (AKIN β 1, β 2 and β 3; see Gissot et al., 2004) but only one γ (SNF4) subunit. Although Bouly et al. (1999) reported the existence of another potential γ -subunit (AKIN γ), the corresponding protein was shown not to complement the yeast *Asnf4* mutation and therefore was considered not to represent a γ -subunit of plant SnRK1 enzymes.

The data available thus far show that components of plant SnRK1 kinases are not regulated by glucose and stress stimuli at the level of transcription. Although Bouly et al. (1999) reported on remarkable differences between transcriptional regulation of *AKIN β 1* and *AKIN β 2* genes, in our experiments we could not reproduce the observations suggesting that *AKIN β 1* is only expressed in light, whereas transcription of *AKIN β 2* is negatively regulated by light. However, we have observed some differences in the tissue specific regulation of the *SNF4* γ -subunit gene, which is remarkably low in siliques, especially during the stage of seed maturation, corresponding to the raise of ABA levels in embryos. In addition, we found that the levels the SNF4 γ -subunit protein show dramatic differences among source and sink organs, they are high in leaves of developing seedlings as well as in actively dividing cells, but extremely low in flowers and roots. This tissue specific pattern of availability of

SNF4 γ -subunit protein probably is an indicative also for the levels of SnRK1 kinase activities in different organs and tissues. Given the facts that SNF4 is encoded by a single gene in *Arabidopsis* and that its levels may limit the activity and functions of SnRK1 kinases, we have identified SNF4 as a critical component in regulation of the activity of SnRK1 kinases. As yeast SNF4 and animal AMPK γ -subunits, *Arabidopsis* SNF4 also carries cystathionine β -synthase (CBS) repeats, which are implicated in the binding of AMP/ATP and modulation. As in Snf1 and AMPKs, these repeat may play an important function in the activation of plant SnRK1 enzymes by upstream signaling kinases.

By complementation of the yeast *Δsnf4* mutation two different *Arabidopsis* SNF4 cDNA were identified, one encoding a yeast Snf4-like protein and another, which encoded a completely identical protein that carried extra N-terminal sequences corresponding to the KIS domain of the β -subunits. The short form was designated SNF4/ γ , whereas the long form was named AKIN $\beta\gamma$ to achieve a clear distinction (Kleinow et al., 2000; Lumbreras et al., 2001). The existence of a plant specific form of γ -subunit suggested that the regulation of plant AMPK/SnRK1 kinases could considerably differ from those of their yeast and animal counterparts and that in plants the SnRK1 α and AKIN $\beta\gamma$ subunits may form functional kinases as dimers.

We have inspected the coding sequence of the SNF4 genes and compared that to the isolated SNF4/ γ and AKIN $\beta\gamma$ cDNAs and found that these two cDNA only differ in the absence of a 5' peptide coding region, which is in frame with the ATG in the SNF4/ γ cDNA. This indicated that the SNF4 gene likely produces only one long mRNA encoding AKIN $\beta\gamma$. To exclude that the SNF4/ γ cDNA is a product of potential alternative splicing, we have performed an exon mapping RT-PCR experiment, which clearly demonstrated the lack of alternatively spliced transcripts from the SNF4 gene. To exclude also that proteolytic processing of the long AKIN $\beta\gamma$ protein would lead to the production of the short KIS-domain deficient SNF4/ γ protein, we have generated the epitope tagged versions of the long AKIN $\beta\gamma$ protein by addition of an HA epitope to either the N- or C-terminal end and expressed these proteins in transgenic plants. Examination of the size and stability of these proteins showed that they do not undergo proteolyses and their size corresponds upon translation in planta to that of AKIN $\beta\gamma$. This demonstrated that the *Arabidopsis* SNF4 gene encodes only one protein product, which carries a unique N-terminal KIS domain in fusion with the conserved core SNF4 sequence. Therefore, in our nomenclature we returned to the use of SNF4 designation of this protein.

4.2.2. Isolation of *snf4* insertion mutant alleles

To dissect the regulatory function of SNF4, we have isolated 3 *snf4* mutant alleles from different T-DNA insertion mutant collections. Segregation analysis and characterization of these alleles showed that the *snf4* mutations resulted in a 2:1 segregation. The fact that the *snf4*/+ mutant lines did not display embryo lethality in their siliques indicated that the male transmission of mutant alleles is missing, thus SNF4 is essential for the process of microsporogenesis. This observation well correlates with the data of Zhang et al. (2001) who found that antisense inhibition of a barley SnRK1 enzyme results in abnormal pollen development and male sterility. However, the plants carrying the *snf4*/+

alleles were fully fertile suggesting that the *snf4* mutation may cause a defect early on during microsporogenesis. Further detailed analysis of *snf4* mutant alleles is now in progress.

4.2.3. SNF4 is a nuclear protein

SNF4 in yeast shows exclusive nuclear localization, whereas the α and β subunits shuttle between the cytoplasm and nucleus. Elegant studies show that the β substrate targeting subunits control cellular localization of the catalytic α -subunits (for review see Schmidt and McCartney, 2000). Our cell fractionation and cellular localization studies with GFP-SNF4 fusion protein also show that SNF4 is a nuclear protein, but its nuclear export to the cytoplasm appears to be stimulated by light.

4.2.4. SNF4 in high molecular mass protein complexes

We have generated tools for biochemical purification of the SNF4 protein complexes by expression of HA-epitope tagged forms of SNF4 alone, or in combination with other SnRK1 subunits, in transgenic plants and cell cultures. In our preliminary experiments, we demonstrated that HA-SNF4 can be purified from nuclear extract and size fractionated on glycerol gradients providing a means for purification of a protein complex of over 700 kDa.

Co-immunoprecipitation studies showed that SNF4 interacts *in vivo* with AKIN β 2 and an SnRK1 α -subunit. In addition, we detected both SNF4 and AKIN β 2 together with an SnRK1 α -subunit in a complex with the 20S proteasome. These results corroborated the findings of Farrás et al. (2001) from our laboratory, which showed that SnRK1 α -subunits play a role in targeting SCF E3 ubiquitin ligases to the proteasome. In addition, our data suggest that trimeric SnRK1 kinases, carrying an α , a SNF4 and an AKIN β 2 subunit, may also form a different complex with the 20S catalytic cylinder of the proteasome. Furthermore, our biochemical studies indicate that the PRL1 nuclear kinase inhibitor WD-protein is not part of these complexes, although co-purifies on glycerol gradients with SNF4. This observation is consistent with the finding of Bhalerao et al. (1999) who showed that PRL1 bind to the same region in the C-terminal regulatory domains of SnRK1 α -subunits as the kinase activating SNF4 subunit. This implies that PRL1 and SNF4 cannot occur in common SnRK1 complexes.

4.3. OUTLOOK

The data and tools generated in this work can now be further exploited in the analysis of regulation of SnRK1 and SnRK2 protein kinases and their potential regulatory targets in the ABI5/DPBF family of bZIP transcription factors. Genetic dissection of the function of SnRK1 and SnRK2 kinases and DPBF4 is now aided by the availability of several mutant alleles of *ost1*, *dpbf4* and the SnRK1 activating subunit gene *snf4*.

5. REFERENCES

- Abe, H., Urao, T., Ito, T., Seki, M., Shinozaki, K. and Yamaguchi-Shinozaki, K. (2003) *Arabidopsis* AtMYC2 (bHLH) and AtMYB2 (MYB) function as transcriptional activators in abscisic acid signaling. *Plant Cell* 15: 63-78.
- Albrecht, V., Weinl, S., Blazevic, D., D'Angelo, C., Batistic, O., Kolukisaoglu, U., Bock, R. and Schulz B. (2003) The calcium sensor CBL1 integrates plant responses to abiotic stresses. *Plant J.* 36: 457-470.
- Allen, G. J., Murata, Y., Chu, S. P., Nafisi, M. and Schroeder, J. I. (2002) Hypersensitivity of abscisic acid-induced cytosolic calcium increases in the *Arabidopsis* farnesyltransferase mutant *era1-2*. *Plant Cell* 14:1649-1662.
- Alonso, J. M. and Ecker, J. R. (2001) The ethylene pathway: a paradigm for plant hormone signaling and interaction. *Sci STKE.* 70: RE1.
- Altschul, S.F., Gish, W., Miller, W., Myyres, E.W. and Lipman D.J. (1990) Basic local alignment search tool. *J. Mol. Biol.*, 215: 403-410.
- Anderson, J. P., Badruzaufari, E., Schenk, P. M., Manners, J. M., Desmond, O. J., Ehlert, C., Maclean, D. J., Ebert, P. R., and Kazan, K. (2004) Antagonistic interaction between abscisic acid and jasmonate-ethylene signaling pathways modulates defense gene expression and disease resistance in *Arabidopsis*. *Plant Cell* 16: 3460-3479.
- Arroyo, A., Bossi, F., Finkelstein, R. R. and Leon, P. (2003) Three genes that affect sugar sensing (abscisic acid insensitive 4, abscisic acid insensitive 5, and constitutive triple response 1) are differentially regulated by glucose in *Arabidopsis*. *Plant Physiol.* 133: 231-242.
- Ausubel, F. M., Brent, R., Kingston, R. E., Moore, D. D., Deidman, J. G., Smith, J. A. and Struhl, K. (1999) *Current protocols in molecular biology*, John Wiley & Sons, Inc.
- Avonce, N., Leyman, B., Mascorro-Gallardo, J. O., Van Dijck, P., Thevelein, J. M. and Iturriaga G. (2004) *Plant Physiol.* 136: 3649-3659.
- Barnes, S. (2002) Comparing *Arabidopsis* to other flowering plants. *Curr. Opin. Plant Biol.* 5: 128-134.
- Beaudoin, N., Serizet, C., Gosti, F. and Giraudat, J. (2000) Interactions between abscisic acid and ethylene signaling cascades. *Plant Cell* 12: 1103-1115.
- Bensmihen, S., Rippha, S., Lambert, G., Jublot, D., Pautot, V., Granier, F., Giraudat, J. and Parcy, F. (2002) The homologous ABI5 and EEL transcription factors function antagonistically to fine-tune gene expression during late embryogenesis. *Plant Cell* 14: 1391-1403.
- Bensmihen, S., To, A., Lambert, G., Kroj, T., Giraudat, J., Parcy, F. (2004) Analysis of an activated ABI5 allele using a new selection method for transgenic *Arabidopsis* seeds. *FEBS Lett.* 561: 127-131.
- Bensmihen, S., Giraudat, J. and Parcy, F. (2005) Characterization of three homologous basic leucine zipper transcription factors (bZIP) of the ABI5 family during *Arabidopsis thaliana* embryo maturation. *J. Exp. Bot.* 56: 597-603.
- Bhalerao, R. P., Salchert, K., Bakó, L., Ökrész, L., Szabados, L., Muranaka, T., Machida, Y., Schell, J. and Koncz, C. (1999) Regulatory interaction of PRL1 WD protein with *Arabidopsis* SNF1-like protein kinases. *Proc. Natl. Acad. Sci. U. S. A.* 96: 5322-5327.

- Birnboim, H.C. and Doly, J. (1979) A rapid alkaline extraction procedure for screening recombinant plasmid DNA. *Nucleic Acids Res.* 7: 1513-1523.
- Bittner, F., Oreb, M. and Mendel, R. R. (2001) ABA3 is a molybdenum cofactor sulfurase required for activation of aldehyde oxidase and xanthine dehydrogenase in *Arabidopsis thaliana*. *J Biol Chem.* 276: 40381-40384.
- Borisjuk, L., Walenta, S., Rolletschek, H., Mueller-Klieser, W., Wobus, U. and Weber, H. (2002) Spatial analysis of plant metabolism: sucrose imaging within *Vicia faba* cotyledons reveals specific developmental patterns. *Plant J.* 29: 521-530.
- Boudsocq, M., Barbier-Brygoo, H. and Lauriere, C. (2004) Identification of nine sucrose nonfermenting 1-related protein kinases 2 activated by hyperosmotic and saline stresses in *Arabidopsis thaliana*. *J. Biol. Chem.* 279: 41758-41766.
- Bouly, J. P., Gissot, L., Lessard, P., Kreis, M. and Thomas, M. (1999) *Arabidopsis thaliana* proteins related to the yeast SIP and SNF4 interact with AKINalpha1, an SNF1-like protein kinase. *Plant J.* 18: 541-550.
- Bradford, M.M. (1976) A rapid and sensitive method for the quantitation of microgram quantities of protein utilizing the principle of protein dye binding. *Anal. Biochem.* 72: 248-254.
- Brady, S. M., Sarkar, S. F., Bonetta, D. and McCourt, P. (2003) The *ABSCISIC ACID INSENSITIVE 3* (ABI3) gene is modulated by farnesylation and is involved in auxin signaling and lateral root development in *Arabidopsis*. *Plant J.* 34: 67-75.
- Brocard, I. M., Lynch, T. J. and Finkelstein, R. R. (2002) Regulation and role of the *Arabidopsis* abscisic acid-insensitive 5 gene in abscisic acid, sugar, and stress response. *Plant Physiol.* 129: 1533-1543.
- Brocard-Gifford, I. M., Lynch, T.J. and Finkelstein, R. R. (2003) Regulatory networks in seeds integrating developmental, abscisic acid, sugar, and light signaling. *Plant Physiol.* 131: 78-92.
- Buchanan, B.B. and Balmer, Y. (2004) Redox regulation: A broadening horizon. *Annu. Rev. Plant Physiol. Plant Mol. Biol.* 56: 187-220.
- Carling, D. (2004) The AMP-activated protein kinase cascade--a unifying system for energy control. *Trends Biochem. Sci.* 29: 18-24.
- Catala, R., Santos, E., Alonso, J. M., Ecker, J.R., Martinez-Zapater, J.M. and Salinas, J. (2003) Mutations in the Ca²⁺/H⁺ transporter CAX1 increase CBF/DREB1 expression and the cold-acclimation response in *Arabidopsis*. *Plant Cell* 15: 2940-2951.
- Chaconas, G. and van de Sande, J. H. (1980) 5'-³²P labeling of RNA and DNA restriction fragments. *Methods Enzymol.* 65: 75-85.
- Chen, J. G. and Jones, A. M. (2004) AtRGS1 function in *Arabidopsis thaliana*. *Methods Enzymol.* 389: 338-350.
- Chen, J. G., Pandey, S., Huang, J., Alonso, J. M., Ecker, J. R., Assmann, S. M., and Jones A. M. (2004) GCR1 can act independently of heterotrimeric G-protein in response to brassinosteroids and gibberellins in *Arabidopsis* seed germination. *Plant Physiol.* 135: 907-915.
- Cheng, W. H., Endo, A., Zhou, L., Penney, J., Chen, H. C., Arroyo, A., Leon, P., Nambara, E., Asami, T., Seo, M., Koshiba, T. and Sheen, J. (2002). A unique short-chain dehydrogenase/reductase in *Arabidopsis* glucose signaling and abscisic acid biosynthesis and functions. *Plant Cell* 14:2723-2743.

- Cheng, N. H., Pittman, J. K., Zhu, J. K. and Hirschi, K. D. (2004) The protein kinase SOS2 activates the *Arabidopsis* H⁺/Ca²⁺ antiporter CAX1 to integrate calcium transport and salt tolerance. *J Biol Chem.* 279: 2922-2926.
- Choi, H., Hong, J., Ha, J., Kang, J. and Kim, S. (2000) ABFs, a family of ABA-responsive element binding factors. *J. Biol. Chem.* 275: 1723-1730.
- Chinnusamy, V., Schumaker, K. and Zhu, J.K. (2004) Molecular genetic perspectives on cross-talk and specificity in abiotic stress signalling in plants. *J. Exp. Bot.* 55: 225-236.
- Clewell, D. B. and Helinski, D. R. (1969) Supercoiled circular DNA-protein complex in *Escherichia coli*: purification and induced conversion to an open circular DNA form. *Proc- Natl. Acad. Sci. U. S. A.* 62:1159-1166.
- Clough, S. J. and Bent, A. F. (1998) Floral dip: a simplified method for *Agrobacterium*-mediated transformation of *Arabidopsis thaliana*. *Plant J.* 16: 735-743.
- Cook, D., Fowler, S., Fiehn, O. and Thomashow, M. F. (2004) A prominent role for the CBF cold response pathway in configuring the low-temperature metabolome of *Arabidopsis*. *Proc. Natl. Acad. Sci. U. S. A.* 101: 15243-15248.
- Coruzzi, G.M. and Zhou, L. (2001) Carbon and nitrogen sensing and signaling in plants: emerging 'matrix effects'. *Curr. Opin. Plant Biol.* 4: 247-253.
- Cotelle, V., Meek, S. E., Provan, F., Milne, F. C, Morrice, N., and MacKintosh, C. (2000) 14-3-3s regulate global cleavage of their diverse binding partners in sugar-starved *Arabidopsis* cells. *EMBO J.* 19: 2869-2876.
- Comparot, S., Lingiah, G., Martin, T. (2003) Function and specificity of 14-3-3 proteins in the regulation of carbohydrate and nitrogen metabolism. *J. Exp. Bot.* 54: 595-604.
- Coursol, S., Fan, L.M., Le Stunff, H., Spiegel, S., Gilroy, S. and Assmann, S. M. (2003) Sphingolipid signalling in *Arabidopsis* guard cells involves heterotrimeric G proteins. *Nature* 423: 651-654.
- Cutler, A. J. and Krochko, J. E. (1999) Formation and breakdown of ABA. *Trends Plant Sci.* 4: 472-478.
- Cutler, S., Ghassemian, M., Bonetta, D., Cooney, S. and McCourt, P. (1996) A protein farnesyl transferase involved in abscisic acid signal transduction in *Arabidopsis*. *Science* 273:1239-1241.
- Dean Rider, S. J., Henderson, J. T., Jerome, R. E., Edenberg, H. J., Romero-Severson, J. and Ogas, J. (2003) Coordinate repression of regulators of embryonic identity by PICKLE during germination in *Arabidopsis*. *Plant J.* 35: 33-43.
- Dale, S., Wilson, W. A., Edelman, A. M. and Hardie, G. (1995) Similar substrate recognition motifs for mammalian AMP-activated protein kinase, higher plant HMG-CoA reductase kinase-A, yeast SNF1, and mammalian calmodulin-dependent protein kinase I. *FEBS Lett.* 361: 191-195.
- Dellaporta, S.L., Woods, K. and Hicks, J.B. (1983) A plant DNA miniprep: version II. *Plant Mol. Biol. Reporter* 1: 19-21.
- Desikan, R., Cheung, M. K., Bright, J., Henson, D., Hancock, J. T. and Neill, S. J. (2004) ABA, hydrogen peroxide and nitric oxide signalling in stomatal guard cells. *J. Exp. Bot.* 55: 205-212.
- Dolferus, R., Jacobs, M., Peacock, W. J. and Dennis, E. S. (1994) Differential interactions of promoter elements in stress responses of the *Arabidopsis Adh* gene. *Plant Physiol.* 105: 1075-1087.

- Dower, W. J., J. F. Miller, and C. W. 1988. High efficiency transformation of *E. coli* by high voltage electroporation. *Nucleic Acids Res.* 16: 6127-6145.
- Eastmond, P. J., van Dijken, A. J., Spielman, M., Kerr, A., Tissier, A. F., Dickinson, H. G., Jones, J. D., Smeeckens, S. C. and Graham, I. A. (2002) Trehalose-6-phosphate synthase 1, which catalyses the first step in trehalose synthesis, is essential for *Arabidopsis* embryo maturation. *Plant J.* 29: 225-235.
- Eastmond, P. J., Li, Y. and Graham, I. A. (2003) Is trehalose-6-phosphate a regulator of sugar metabolism in plants? *J. Exp. Bot.* 54: 533-547.
- Eckardt, N. A. (2001) Transcription factors dial 14-3-3 for nuclear shuttle. *Plant Cell* 13: 2385-2389.
- Farrás, R., Ferrando, A., Jasik, J., Kleinow, T., Ökrész, L., Tiburcio, A., Salchert, K., del Pozo, C., Schell, J. and Koncz, C. (2001) SKP1-SnRK protein kinase interactions mediate proteasomal binding of a plant SCF ubiquitin ligase. *EMBO J.* 20: 2742-2756.
- Fedoroff, N. V. (2002) Cross-talk in abscisic acid signaling. *Sci STKE.* 140: RE10.
- Feinberg, A.P. and Vogelstein, B. (1984) A technique for radiolabeling DNA restriction endonuclease fragments to high specific activity. *Anal. Biochem.* 132: 6-13.
- Ferrando, A., Farrás, R., Jásik, J., Schell, J. and Koncz, C. (2000a) Intron-tagged epitope: a tool for facile detection and purification of proteins expressed in *Agrobacterium*-transformed plant cells. *Plant J.* 22: 553-560.
- Ferrando, A., Koncz-Kálmán, Z., Farrás, R., Tiburcio, A., Schell, J. and Koncz, C. (2000b) Detection of in vivo protein interactions between Snf1-related kinase subunits with intron-tagged epitope-labelling in plants cells. *Nucleic Acids Res.* 29: 3685-3693.
- Finkelstein, R. R. and Lynch, T. J. (2000) Abscisic acid inhibition of radicle emergence but not seedling growth is suppressed by sugars. *Plant Physiol.* 122: 1179-1186.
- Finkelstein, R. R. and Gibson, S. I. (2001) ABA and sugar interactions regulating development: cross-talk or voices in a crowd? *Curr. Opin. Plant Biol.* 5:2 6-32.
- Finkelstein, R. R., Wang, M. L., Lynch, T. J., Rao, S. and Goodman, H. M. (1998) The *Arabidopsis* abscisic acid response locus ABI4 encodes an APETALA 2 domain protein. *Plant Cell* 10: 1043-1054.
- Finkelstein, R. R., Gampala, S. and Rock, C. D. (2002) Abscisic acid signaling in seeds and seedlings. *Plant Cell* 14 Suppl: S15-45.
- Fowler, S. G., Cook, D. and Thomashow, M. F. (2005) Low temperature induction of *Arabidopsis* CBF1, 2, and 3 is gated by the circadian clock. *Plant Physiol.* 137: 961-968.
- Gampala, S.S., Finkelstein, R. R., Sun, S. S and Rock, C. D. (2002) ABI5 interacts with abscisic acid signaling effectors in rice protoplasts. *J. Biol. Chem.* 277: 1689-1694.
- Gancedo, J. M. (1998) Yeast carbon catabolite repression. *Microbiol. Mol. Biol. Rev.* 62: 334-61.
- Garcia-Mata, C., Gay, R., Sokolovski, S., Hills, A., Lamattina, L. and Blatt, M. R. (2003) Nitric oxide regulates K⁺ and Cl⁻ channels in guard cells through a subset of abscisic acid-evoked signaling pathways. *Proc. Natl. Acad. Sci. U. S. A.* 100: 11116-11121.
- Gelade, R., Van de Velde, S., Van Dijck, P. and Thevelein, J. M. (2003) Multi-level response of the yeast genome to glucose. *Genome Biol.* 4(11): 233.

- Ghassemian, M., Nambara, E., Cutler, S., Kawaide, H., Kamiya, Y. and McCourt, P. (2000) Regulation of abscisic acid signaling by the ethylene response pathway in *Arabidopsis*. *Plant Cell* 12: 1117-1126.
- Gibson, S. I. (2000) Plant sugar-response pathways. Part of a complex regulatory web. *Plant Physiol.* 124: 1532-1539.
- Gibson, S. I. (2004) Sugar and phytohormone response pathways: navigating a signalling network. *J. Exp. Bot.* 55: 253-264.
- Gibson, S. I. (2005) Control of plant development and gene expression by sugar signaling. *Curr. Opin. Plant Biol.* 8: 93-102.
- Gilmour, S. J., Zarka, D. G., Stockinger, E. J., Salazar, M. P., Houghton, J. M. and Thomashow, M. F. (1998) Low temperature regulation of the *Arabidopsis* CBF family of AP2 transcriptional activators as an early step in cold-induced COR gene expression. *Plant J.* 16: 433-442.
- Gilmour, S.J., Sebolt, A. M., Salazar, M. P., Everard, J. D. and Thomashow, M. F. (2002) Overexpression of the *Arabidopsis* CBF3 transcriptional activator mimics multiple biochemical changes associated with cold acclimation. *Plant Physiol.* 124:1854-1865.
- Gissot, L., Polge, C., Bouly, J. P., Lemaitre, T., Kreis, M. and Thomas, M. (2005) AKINbeta3, a plant specific SnRK1 protein, is lacking domains present in yeast and mammals non-catalytic beta-subunits. *Plant Mol. Biol.* 56: 747-459.
- Gong, Z., Lee, H., Xiong, L., Jagendorf, A., Stevenson, B. and Zhu, J. K. (2002) RNA helicase-like protein as an early regulator of transcription factors for plant chilling and freezing tolerance. *Proc. Natl. Acad. Sci. U. S. A.* 99: 11507-11512.
- Grefen, C. and Harter, K. (2004) Plant two-component systems: principles, functions, complexity and cross talk. *Planta* 219:733-742.
- Gubler, F., Millar, A. A. and Jacobsen, J. V. (2005) Dormancy release, ABA and pre-harvest sprouting. *Curr. Opin. Plant Biol.* 8: 183-187.
- Guevara-Garcia, A., San Roman, C., Arroyo, A, Cortes, M. E., de la Luz Gutierrez-Nava, M. and Leon, P. (2005) Characterization of the *Arabidopsis* clb6 mutant illustrates the importance of posttranscriptional regulation of the methyl-d-erythritol 4-phosphate pathway. *Plant Cell* 17: 628-643.
- Guo, H. and Ecker, J. R. (2004) The ethylene signaling pathway: new insights. *Curr. Opin. Plant Biol.* 7: 40-49.
- Guo, Y., Halfter, U., Ishitani, M. and Zhu, J. K. (2001) Molecular characterization of functional domains in the protein kinase SOS2 that is required for plant salt tolerance. *Plant Cell* 13: 1383-1400.
- Guo, Y., Xiong, L., Song, C. P., Gong, D., Halfter, U. and Zhu, J. K. (2002) A calcium sensor and its interacting protein kinase are global regulators of abscisic acid signaling in *Arabidopsis*. *Dev Cell.* 3: 233-244.
- Haake, V., Cook, D., Riechmann, J.L., Pineda, O., Thomashow, M. F., and Zhang, J. Z. (2002) Transcription factor CBF4 is a regulator of drought adaptation in *Arabidopsis*. *Plant Physiol.* 130: 639-648.
- Halford, N. G. and Hardie, D. G. (1998) SNF1-related protein kinases: global regulators of carbon metabolism in plants? *Plant Mol. Biol.* 37: 735-748.

- Hardie, D. G; Carling, D. and Carlson, M. (1998) The AMP-activated/SNF1 protein kinase subfamily: metabolic sensors of the eukaryotic cell? *Annu. Rev. Biochem.* 67: 821–855.
- Harter K, Kudla J. Beaudoin, N., Serizet, C., Gosti, F. and Giraudat, J. (2000) Interactions between abscisic acid and ethylene signaling cascades. *Plant Cell* 12: 1103-1115.
- Heyl, A. and Schmülling, T. (2003) Cytokinin signal perception and transduction. *Curr. Opin. Plant Biol.* 6:480-488.
- Himmelbach, A., Hoffmann, T., Leube, M., Hohener, B. and Grill, E. (2002) Homeodomain protein ATHB6 is a target of the protein phosphatase ABI1 and regulates hormone responses in *Arabidopsis*. *EMBO J.* 21: 3029-3038.
- Himmelbach, A., Yang, Y. and Grill, E. (2003) Relay and control of abscisic acid signaling. *Curr. Opin. Plant Biol.* 6: 470-479.
- Hiraguri, A., Itoh, R., Kondo, N., Nomura, Y., Aizawa, D., Murai, Y., Koiwa, H., Seki, M., Shinozaki, K. and Fukuhara, T. (2005) Specific interactions between Dicer-like proteins and HYL1/DRB- family dsRNA-binding proteins in *Arabidopsis thaliana*. *Plant Mol. Biol.* 57: 173-188.
- Hohmann, S. (2002) Osmotic stress signaling and osmoadaptation in yeasts. *Microbiol. Mol. Biol. Rev.* 66: 300-372.
- Holsbeeks, I., Lagatie, O., Van Nuland, A., Van de Velde, S. and Thevelein, J. M. (2004) The eukaryotic plasma membrane as a nutrient-sensing device. *Trends Biochem. Sci.* 29: 556-564.
- Hrabak, E. M., Chan, C. W., Gribskov, M., Harper, J. F., Choi, J. H., Halford, N., Kudla, J., Luan, S., Nimmo, H. G., Sussman, M. R., Thomas, M., Walker-Simmons, K., Zhu, J. K. and Harmon, A. C. (2003) The *Arabidopsis* CDPK-SnRK superfamily of protein kinases. *Plant Physiol.* 132: 666-680.
- Hughes, J. H., Mack, K. and Hamparian, V. V. (1988) India ink staining of proteins on nylon and hydrophobic membranes. *Anal Biochem.* 173: 18-25.
- Hugouvieux, V., Kwak, J. M. and Schroeder, J. I. (2001) An mRNA cap binding protein, ABH1, modulates early abscisic acid signal transduction in *Arabidopsis*. *Cell* 106: 477-487.
- Ichimura, K., Mizoguchi, T., Yoshida, R., Yuasa, T. and Shinozaki, K. (2000) Various abiotic stresses rapidly activate *Arabidopsis* MAP kinases ATMPK4 and ATMPK6. *Plant J.* 24: 655-665.
- Igarashi, D., Ishida, S., Fukazawa, J. and Takahashi, Y. (2001) 14-3-3 proteins regulate intracellular localization of the bZIP transcriptional activator RSG. *Plant Cell* 13:2483-2497.
- Jang, J. C., Leon, P., Zhou, L. and Sheen, J. (1997) Hexokinase as a sugar sensor in higher plants. *Plant Cell* 9: 5-19.
- Jakoby, M., Weisshaar, B., Droge-Laser, W., Vicente-Carbajosa, J., Tiedemann, J., Kroj, T., Parcy, F. and bZIP Research Group. (2002) bZIP transcription factors in *Arabidopsis*. *Trends Plant Sci.* 7: 106-111.
- Jefferson, R.A. 1987. Assaying chimeric genes in plants: the GUS gene fusion system. *Plant Mol. Biol. Rep.* 5: 387-405.
- Jiang, R. and Carlson, M. (1996) Glucose regulates protein interactions within the yeast SNF1 protein kinase complex. *Genes Dev.* 10: 3105-3115.

- Jiang, R. and Carlson, M. (1997) The Snf1 protein kinase and its activating subunit, Snf4, interact with distinct domains of the Sip1/Sip2/Gal83 component in the kinase complex. *Mol. Cell. Biol.* 17: 2099-2106.
- Johannesson, H., Wang, Y., Hanson, J. and Engstrom, P. (2003) The *Arabidopsis thaliana* homeobox gene ATHB5 is a potential regulator of abscisic acid responsiveness in developing seedlings. *Plant Mol. Biol.* 51: 719-729.
- Johnson, R. R., Wagner, R. L., Verhey, S. D. and Walker-Simmons, M. K. (2002) The abscisic acid-responsive kinase PKABA1 interacts with a seed-specific abscisic acid response element-binding factor, TaABF, and phosphorylates TaABF peptide sequences. *Plant Physiol.* 130: 837-846.
- Jones, A. M. and Assmann, S. M. (2004) Plants: the latest model system for G-protein research. *EMBO Rep.* 5: 572-578.
- Kagaya, Y., Toyoshima, R., Okuda, R., Usui, H., Yamamoto, A. and Hattori, T. (2005a) LEAFY COTYLEDON1 controls seed storage protein genes through its regulation of FUSCA3 and ABSCISIC ACID INSENSITIVE3. *Plant Cell Physiol.* 46: 399-406.
- Kagaya, Y., Okuda, R., Ban, A., Toyoshima, R., Tsutsumida, K., Usui, H., Yamamoto, A. and Hattori, T. (2005b) Indirect ABA-dependent regulation of seed storage protein genes by FUSCA3 transcription factor in *Arabidopsis*. *Plant Cell Physiol.* 46: 300-311.
- Kang, J. Y., Choi, H. I., Im, M. Y. and Kim, S. Y. (2002) *Arabidopsis* basic leucine zipper proteins that mediate stress-responsive abscisic acid signaling. *Plant Cell* 14: 343-357.
- Kashem, M. A., Hori, H., Itoh, K., Hayakawa, T., Todoroki, Y., Hirai, N., Ohigashi, H. and Mitsui, T. (1998) Effects of (+)-8',8',8'-trifluoroabscisic acid on alpha-amylase expression and sugar accumulation in rice cells. *Planta* 205: 319-326.
- Kin, S. Y. and Thomas, T. L. (1998) A family of basic leucine zipper proteins bind to seed-specification elements in the carrot *Dc3* gene promoter. *J. Plant Physiol.* 152: 607-613.
- Kim, J. W. and Dang, C. V. (2005) Multifaceted roles of glycolytic enzymes. *Trends Biochem. Sci.* 30: 142-50.
- Kim, S. Y., Chung, H. J. and Thomas, T. L. (1997) Isolation of a novel class of bZIP transcription factors that interact with ABA-responsive and embryo-specification elements in the *Dc3* promoter using a modified yeast one-hybrid system. *Plant J.* 11: 1237-1251.
- Kim, H. J., Kim, Y. K., Park, J. Y. and Kim, J. (2002a) Light signalling mediated by phytochrome plays an important role in cold-induced gene expression through the C-repeat/dehydration responsive element (C/DRE) in *Arabidopsis thaliana*. *Plant J.* 29: 693-704.
- Kim, S. Y., Ma, J., Perrot, P., Li, Z. and Thomas, T. L. (2002b) *Arabidopsis* ABI5 subfamily members have distinct DNA-binding and transcriptional activities. *Plant Physiol.* 130: 688-6697.
- Kim, K. N., Cheong, Y. H., Grant, J. J., Pandey, G. K. and Luan, S. (2003) CIPK3, a calcium sensor-associated protein kinase that regulates abscisic acid and cold signal transduction in *Arabidopsis*. *Plant Cell* 15:411-423.
- Kim, H. J., Hyun, Y., Park, J. Y., Park, M. J., Park, M. K., Kim, M. D., Kim, H. J., Lee, M. H., Moon, J., Lee, I. and Kim, J. (2004a) A genetic link between cold responses and flowering time through FVE in *Arabidopsis thaliana*.
- Kim, S., Kang, J. Y., Cho, D. I., Park, J. H. and Kim, S. Y. (2004b) ABF2, an ABRE-binding bZIP factor, is an essential component of glucose signaling and its overexpression affects multiple stress tolerance. *Plant J.* 40: 75-87.

- Kleinow, T. (2000) Identifizierung und Charakterisierung von potentiellen Komponenten der Stress- und Glukose-Signaltransduktion von *A. thaliana*. Inaugural-Dissertation, Mathematisch-Naturwissenschaftlichen Fakultät der Universität zu Köln,
- Kleinow, T., Bhalerao, R., Breuer, F., Umeda, M., Salchert, K. and Koncz, C. (2000) Functional identification of an *Arabidopsis* SNF4 ortholog by screening for heterologous multicopy suppressors of *snf4* deficiency in yeast. *Plant J.* 23: 115-122.
- Knight, H., Zarka, D. G., Okamoto, H., Thomashow, M. F. and Knight, M. R. (2004) Abscisic acid induces CBF gene transcription and subsequent induction of cold-regulated genes via the CRT promoter element. *Plant Physiol.* 135:1710-1717.
- Koch, K. E. (1996) Carbohydrate-modulated gene expression in plants. *Annu. Rev. Plant Physiol. Plant Mol. Biol.* 47: 509-540.
- Koch, K. E., Ying, Z., Wu, Y. and Avigne, W. T. (2000) Multiple paths of sugar-sensing and a sugar/oxygen overlap for genes of sucrose and ethanol metabolism. *J. Exp. Bot.* 51 Spec. No: 417-427.
- Koch, K. E. (2004) Sucrose metabolism: regulatory mechanisms and pivotal roles in sugar sensing and plant development. *Curr. Opin. Plant. Biol.* 7: 235-246.
- Koncz, C., and Schell, J. (1986) The promoter of TL-DNA gene 5 controls the tissue specific expression of chimaeric genes carried by a novel type of *Agrobacterium* binary vector. *Mol. Gen. Genet.* 204: 383-396.
- Koncz, C., N. Martini, L. Szabados, M. Hroudá, A. Bachmair and J. Schell. 1994. Specialized vectors for gene tagging and expression studies. (In: *Plant Molecular Biology Manual*, eds. Gelvin, S. and B. Schilperoort B., Kluwer Academic, Dordrecht) B2: 1-22.
- Koornneef, M., Bentsink, L., and Hilhorst, H. (2002) Seed dormancy and germination. *Curr. Opin. Plant Biol.* 5: 33-36.
- Kovtun, Y., Chiu, W. L., Tena, G. and Sheen, J. (2000) Functional analysis of oxidative stress-activated mitogen-activated protein kinase cascade in plants. *Proc. Natl. Acad. Sci. U. S. A.* 97: 2940-3945.
- Kulma, A., Villadsen, D., Campbell, D. G., Meek, S. E., Harthill, J. E., Nielsen, T. H., MacKintosh, C. (2004) Phosphorylation and 14-3-3 binding of *Arabidopsis* 6-phosphofructo-2-kinase/fructose-2,6-bisphosphatase. *Plant J.* 37: 654-667.
- Kwak, J. M., Mori, I. C., Pei, Z. M., Leonhardt, N., Torres, M. A., Dangel, J. L., Bloom, R. E., Bodde, S., Jones, J. D. and Schroeder, J. I. (2003) NADPH oxidase *AtrbohD* and *AtrbohF* genes function in ROS-dependent ABA signaling in *Arabidopsis*. *EMBO J.* 22: 2623-2633.
- Laemmli U.K. (1970) Cleavage of structural proteins during assembly of the head of bacteriophage T4. *Nature* 227: 660-685.
- Lalonde, S., Wipf, D. and Frommer, W. B. (2004) Transport mechanisms for organic forms of carbon and nitrogen between source and sink. *Annu. Rev. Plant Biol.* 55: 341-372.
- Lee, H., Xiong, L., Gong, Z., Ishitani, M., Stevenson, B. and Zhu, J. K. (2001) The *Arabidopsis* HOS1 gene negatively regulates cold signal transduction and encodes a RING finger protein that displays cold-regulated nucleo-cytoplasmic partitioning. *Genes Dev.* 15: 912-924.

- Lee, H., Fischer, R. L., Goldberg, R. B. and Harada J. J. (2003) Arabidopsis LEAFY COTYLEDON1 represents a functionally specialized subunit of the CCAAT binding transcription factor. Proc. Natl. Acad. Sci. U. S. A. 100: 2152-3156.
- Lemoine, R. (2000) Sucrose transporters in plants: update on function and structure. Biochim. Biophys. Acta. 1465: 246-262.
- LeNoble M E., Spollen W. G. and Sharp, R. E. (2004) Maintenance of shoot growth by endogenous ABA: genetic assessment of the involvement of ethylene suppression. J. Exp. Bot. 55: 237-245.
- Léon, P. and Sheen, J. (2003) Sugar and hormone connections. Trends Plant Sci. 8: 110-116.
- Leung, J. and Giraudat, J. (1998) Abscisic acid signal transduction. Annu. Rev. Plant Physiol. Plant Mol. Biol. 49: 199-222.
- Leyman, B., Van Dijck, P. and Thevelein, J. M. (2001) An unexpected plethora of trehalose biosynthesis genes in *Arabidopsis thaliana*. Trends Plant Sci. 6: 510-513.
- Li, J. and Assmann, S. M. (2000) An abscisic acid-activated and calcium-independent protein kinase from guard cells of fava bean. Plant Cell 8: 2359-2368.
- Li, J., Kinoshita, T., Pandey, S., Ng, C. K., Gygi, S. P., Shimazaki, K. and Assmann, S. M. (2002) Modulation of an RNA-binding protein by abscisic-acid-activated protein kinase. Nature 418:793-797.
- Liu, J., Wilson, T.E., Milbrandt, J. and Johnston, M. (1993) Identifying DNA-binding sites and analyzing DNA-binding domains using a yeast selection system. In: Methods: A Companion to Methods in Enzymology 5: 125–137.
- Liu, Q., Kasuga, M., Sakuma, Y., Abe, H., Miura, S., Yamaguchi-Shinozaki, K. and Shinozaki, K. (1998) Two transcription factors, DREB1 and DREB2, with an EREBP/AP2 DNA binding domain separate two cellular signal transduction pathways in drought- and low-temperature-responsive gene expression, respectively, in *Arabidopsis*. Plant Cell 10:1391-1406.
- Lopez-Molina, L., Mongrand, S., McLachlin, D. T., Chait, B. T. and Chua, N. H. (2002) ABI5 acts downstream of ABI3 to execute an ABA-dependent growth arrest during germination. Plant J. 32: 317-328.
- Lopez-Molina, L., Mongrand, S., Kinoshita, N. and Chua, N. H. (2003) AFP is a novel negative regulator of ABA signaling that promotes ABI5 protein degradation. Genes Dev. 17: 410-418.
- Lu, G., DeLisle, A. J., de Vetten, N. C. and Ferl, R. J. (1992) Brain proteins in plants: an *Arabidopsis* homolog to neurotransmitter pathway activators is part of a DNA binding complex. Proc. Natl. Acad. Sci. U. S. A. 89: 11490-11494.
- Lu, G., Paul, A. L., McCarty, D. R. and Ferl, R. J. (1996) Transcription factor veracity: is GBF3 responsible for ABA-regulated expression of *Arabidopsis* Adh? Plant Cell 8: 847-857.
- Lu, C. and Fedoroff, N. (2000) A mutation in the Arabidopsis HYL1 gene encoding a dsRNA binding protein affects responses to abscisic acid, auxin, and cytokinin. Plant Cell 12: 2351-2366.
- Lu, C., Han, M. H., Guevara-Garcia, A. and Fedoroff, N. V. (2002) Mitogen-activated protein kinase signaling in postgermination arrest of development by abscisic acid. Proc. Natl. Acad. Sci. U. S. A. 99: 15812-15817.
- Lucas, W.J. and Lee, J. Y. (2004) Plasmodesmata as a supracellular control network in plants. Nat. Rev. Mol. Cell. Biol. 5: 712-726.

- Lumbreras, V., Alba, M. M., Kleinow, T., Koncz, C. and Pages, M. (2001) Domain fusion between SNF1-related kinase subunits during plant evolution. *EMBO Rep.* 2: 55-60.
- Lunn, J.E. and MacRae, E. (2003) New complexities in the synthesis of sucrose. *Curr. Opin. Plant Biol.* 6: 208-214.
- MacRobbie, E. A. (1998) Signal transduction and ion channels in guard cells. *Philos. Trans. R. Soc. Lond. B Biol. Sci.* 353: 1475-1488.
- Mathur, J., Szabados, L., Schaefer, S., Grunenberg, B., Lossow, A., Jonas-Straube, E., Schell, J., Koncz, C. and Koncz-Kálmán Z. (1998) Gene identification with sequenced T-DNA tags generated by transformation of *Arabidopsis* cell suspension. *Plant J.* 13: 707-716.
- McCartney, R. R. and Schmidt, M. C. (2001) Regulation of Snf1 kinase. Activation requires phosphorylation of threonine 210 by an upstream kinase as well as a distinct step mediated by the Snf4 subunit. *J. Biol. Chem.* 276: 36460-36466.
- McCudden, C. R., Hains, M. D., Kimple, R. J., Siderovski, D. P. and Willard, F. S. (2005) G-protein signaling: back to the future. *Cell. Mol. Life. Sci.* 62: 551-577.
- Merlot, S., Gosti, F., Guerrier, D., Vavasseur, A. and Giraudat, J. (2001) The ABI1 and ABI2 protein phosphatases 2C act in a negative feedback regulatory loop of the abscisic acid signalling pathway. *Plant J.* 25: 295-303.
- Milborrow, B. V. (2001) The pathway of biosynthesis of abscisic acid in vascular plants: a review of the present state of knowledge of ABA biosynthesis. *J Exp Bot.* 52:1145-1164.
- Mikami, K., Katagiri, T., Iuchi, S., Yamaguchi-Shinozaki, K. and Shinozaki, K. (1998) A gene encoding phosphatidylinositol-4-phosphate 5-kinase is induced by water stress and abscisic acid in *Arabidopsis thaliana*. *Plant J.* 15: 563-568.
- Monke, G., Altschmied, L., Tewes, A., Reidt, W., Mock, H. P., Baumlein, H. and Conrad, U. (2004) Seed-specific transcription factors ABI3 and FUS3: molecular interaction with DNA. *Planta* 219: 158-166.
- Moore, B., Zhou, L., Rolland, F., Hall, Q., Cheng, W. H., Liu, Y. X., Hwang, I., Jones, T. and Sheen, J. (2003) Role of the *Arabidopsis* glucose sensor HXK1 in nutrient, light, and hormonal signaling. *Science* 300: 332-336.
- Munnik, T. and Musgrave, A. (2001) Phospholipid signaling in plants: holding on to phospholipase D. *Sci STKE* 111: PE42.
- Muranaka, T., H. Banno, and Y. Machida. 1994. Characterization of tobacco protein kinase NPK5, a homolog of *Saccharomyces cerevisiae* SNF1 that constitutively activates expression of the glucose-repressible SUC2 gene for a secreted invertase of *S. cerevisiae*. *Mol. Cell Biol.* 14: 2958-2965.
- Murashige, T. and Skoog, F. (1962) A revised medium for rapid growth and bioassays with tobacco tissue cultures. *Physiol. Plant.* 15: 473-497.
- Mustilli, A.C., Merlot, S., Vavasseur, A., Fenzi, F. and Giraudat, J. (2002) *Arabidopsis* OST1 protein kinase mediates the regulation of stomatal aperture by abscisic acid and acts upstream of reactive oxygen species production. *Plant Cell* 14: 3089-3099.
- Nakamura, S., Lynch, T. J. and Finkelstein, R. R. (2001) Physical interactions between ABA response loci of *Arabidopsis*. *Plant J.* 26: 627-635.

- Nambara, E., and Marion-Poll, A. (2005) Abscisic acid biosynthesis and catabolism. *Annu. Rev. Plant Biol.* 56: 165-185.
- Németh, K., Salchert, K., Putnoky, P., Bhalerao, R., Koncz-Kálmán, Z., Stankovic-Stangeland, B., Bakó, L., Mathur, J., Ökrész, L., Stabel, S., Geigenberger, P., Stitt, M., Rédei, G. P., Schell, J. and Koncz, C. Pleiotropic control of glucose and hormone responses by PRL1, a nuclear WD protein, in *Arabidopsis*. (1998) *Genes Dev.* 12: 3059-3073.
- Niu, X., Helentjaris, T. and Bate, N. J. (2002) Maize ABI4 binds coupling element1 in abscisic acid and sugar response genes. *Plant Cell* 14: 2565-2575.
- Novillo, F., Alonso, J. M., Ecker, J. R. and Salinas, J. (2004) CBF2/DREB1C is a negative regulator of CBF1/DREB1B and CBF3/DREB1A expression and plays a central role in stress tolerance in *Arabidopsis*. *Proc. Natl. Acad. Sci. U. S. A.* 101: 3985-3990.
- Ohta, M., Guo, Y., Halfter, U. and Zhu, J. K. (2003) A novel domain in the protein kinase SOS2 mediates interaction with the protein phosphatase 2C ABI2. *Proc. Natl. Acad. Sci. U. S. A.* 100: 11771-11776.
- Olsson, T., Thelander, M. and Ronne, H. (2003) A novel type of chloroplast stromal hexokinase is the major glucose-phosphorylating enzyme in the moss *Physcomitrella patens*. *J. Biol. Chem.* 278: 44439-44447.
- Orlando, V. and Paro, R. (1993) Mapping Polycomb-repressed domains in the bithorax complex using in vivo formaldehyde cross-linked chromatin. *Cell* 75: 1187-1198.
- Ozcan, S. and Johnston, M. (1999) Function and regulation of yeast hexose transporters. *Microbiol. Mol. Biol. Rev.* 63: 554-569.
- Oztur, Z. N., Talame, V., Deyholos, M., Michalowski, C. B., Galbraith, D. W., Gozukirmizi, N., Tuberosa, R. and Bohnert, H. J. (2002) Monitoring large-scale changes in transcript abundance in drought- and salt-stressed barley. *Plant Mol. Biol.* 48: 551-573.
- Pandey, S. and Assmann, S. M. (2004) The *Arabidopsis* putative G protein-coupled receptor GCR1 interacts with the G protein alpha subunit GPA1 and regulates abscisic acid signaling. *Plant Cell* 16: 1616-1632.
- Pandey, G. K., Cheong, Y. H., Kim, K. N., Grant, J. J., Li, L., Hung, W., D'Angelo, C., Weinl, S., Kudla, J. and Luan, S. (2004) The calcium sensor calcineurin B-like 9 modulates abscisic acid sensitivity and biosynthesis in *Arabidopsis*. *Plant Cell* 16:1912-1924.
- Papp, I., Mur, L. A., Dalmaci, A., Dulai, S. and Koncz, C. (2004) A mutation in the Cap Binding Protein 20 gene confers drought tolerance to *Arabidopsis*. *Plant Mol. Biol.* 55: 679-686.
- Park, J., Gu, Y., Lee, Y., Yang, Z. and Lee, Y. (2004) Phosphatidic acid induces leaf cell death in *Arabidopsis* by activating the Rho-related small G protein GTPase-mediated pathway of reactive oxygen species generation. *Plant Physiol.* 134: 129-136.
- Pastori, G. M. and Foyer, C. H. (2002) Common components, networks, and pathways of cross-tolerance to stress. The central role of "redox" and abscisic acid-mediated controls. *Plant Physiol.* 129: 460-468.
- Patharkar, O. R. and Cushman, J. C. (2000) A stress-induced calcium-dependent protein kinase from *Mesembryanthemum crystallinum* phosphorylates a two-component pseudo-response regulator. *Plant J.* 24: 679-691.

- Patrick, J. W. and Offler, C. E. (2001) Compartmentation of transport and transfer events in developing seeds. *J. Exp. Bot.* 52: 551-564.
- Paul, M.J. and Foyer, C. H. (2001) Sink regulation of photosynthesis. *J. Exp. Bot.* 52: 1383-400.
- Pego, J. V., Weisbeek, P. J. and Smeekens, S. C. (1999) Mannose inhibits *Arabidopsis* germination via a hexokinase-mediated step. *Plant Physiol.* 119: 1017-1023.
- Pego, J. V. and Smeekens, S. C. (2000) Plant fructokinases: a sweet family get-together. *Trends Plant Sci.* 5: 531-536.
- Pei, Z. M., Ghassemian, M., Kwak, C. M., McCourt, P. and Schroeder, J. I. (1998) Role of farnesyltransferase in ABA regulation of guard cell anion channels and plant water loss. *Science* 282:287-290.
- Petersen, M., Brodersen, P., Naested, H., Andreasson, E., Lindhart, U., Johansen, B., Nielsen, H. B., Lacy, M., Austin, M. J., Parker, J. E., Sharma, S. B., Klessig, D. F., Martienssen, R., Mattsson, O., Jensen, A. B. and Mundy, J. (2000) *Arabidopsis* map kinase 4 negatively regulates systemic acquired resistance. *Cell* 103: 1111-1120.
- Plieth, C., Hansen, U. P., Knight, H. and Knight, M. R. (1999) Temperature sensing by plants: the primary characteristics of signal perception and calcium response. *Plant J.* 18:491-497.
- Polekhina, G., Gupta, A., Michell, B. J., van Denderen, B., Murthy, S., Feil, S. C., Jennings, I. G., Campbell, D. J., Witters, L. A., Parker, M. W., Kemp, B. E. and Stapleton, D. (2003) AMPK beta subunit targets metabolic stress sensing to glycogen. *Curr. Biol.* 13: 867-871.
- Potuschak, T., Lechner, E., Parmentier, Y., Yanagisawa, S., Grava, S., Koncz, C. and Genschik, P. (2003) EIN3-dependent regulation of plant ethylene hormone signaling by two *Arabidopsis* F box proteins: EBF1 and EBF2. *Cell* 115: 679-689.
- Price, J., Li, T. C., Kang, S. G., Na, J. K. and Jang, J. C. (2003) Mechanisms of glucose signaling during germination of *Arabidopsis*. *Plant Physiol.* 132: 1424-1438.
- Price, J., Laxmi, A., St Martin, S. K. and Jang, J. C. (2004) Global transcription profiling reveals multiple sugar signal transduction mechanisms in *Arabidopsis*. *Plant Cell* 16: 2128-2150.
- Qiu, Q. S., Guo, Y., Dietrich, M. A., Schumaker, K. S. and Zhu, J. K. (2002) Regulation of SOS1, a plasma membrane Na⁺/H⁺ exchanger in *Arabidopsis thaliana*, by SOS2 and SOS3. *Proc. Natl. Acad. Sci. U. S. A.* 99: 8436-8441.
- Quintero, F. J., Ohta, M., Shi, H., Zhu, J.K. and Pardo, J. M. (2002) Reconstitution in yeast of the *Arabidopsis* SOS signaling pathway for Na⁺ homeostasis. *Proc. Natl. Acad. Sci. U. S. A.* 99: 9061-9066.
- Raz, V., Bergervoet, J. H. and Koornneef, M. (2001) Sequential steps for developmental arrest in *Arabidopsis* seeds. *Development* 128: 243-252.
- Rios, G., Lossow, A., Hertel, B., Breuer, F., Schaefer, S., Broich, M., Kleinow, T., Jasik, J., Winter, J., Ferrando, A., Farras, R., Panicot, M., Henriques, R., Mariaux, J. B., Oberschall, A., Molnár, G., Berendzen, K., Shukla, V., Lafos, M., Koncz, Z., Rédei, G. P., Schell, J. and Koncz, C. (2000) Rapid identification of *Arabidopsis* insertion mutants by non-radioactive detection of T-DNA tagged genes. *Plant J.* 32: 243-253.
- Rogers, S.O. and A. J. Bendich. 1985. Extraction of DNA from milligram amounts of fresh, herbarium and mummified plant tissues. *Plant Mol. Biol.* 5: 69-76.

- Roitsch, T. and Gonzalez, M. C. (2004) Function and regulation of plant invertases: sweet sensations. *Trends Plant Sci.* 9: 606-613.
- Roitsch, T., Balibrea, M. E., Hofmann, M., Proels, R. and Sinha, A. K. (2003) Extracellular invertase: key metabolic enzyme and PR protein. *J. Exp. Bot.* 54: 513-524.
- Rolland, F., Moore, B. and Sheen, J. (2002a) Sugar sensing and signaling in plants. *Plant Cell* 14 Suppl: S185-205.
- Rolland, F., Winderickx, J. and Thevelein, J. M. (2002b) Glucose-sensing and -signalling mechanisms in yeast. *FEMS Yeast Res.* 2: 183-201.
- Rolland, F. and Sheen, J. (2005) Sugar sensing and signalling networks in plants. *Biochem. Soc. Trans.* 33: 269-271.
- Ronne, H. (1995) Glucose repression in fungi. *Trends Genet.* 11: 12-17.
- Rolland, F., Moore, B. and Sheen, J. (2002) Sugar sensing and signaling in plants. *Plant Cell* 14 Suppl:S185-205.
- Rus, A., Yokoi, S., Sharkhuu, A., Reddy, M., Lee, B. H., Matsumoto, T. K., Koiwa, H., Zhu, J. K., Bressan, R.A. and Hasegawa, P. M. (2001) AtHKT1 is a salt tolerance determinant that controls Na(+) entry into plant roots. *Proc. Natl. Acad. Sci. U. S. A.* 98: 14150-14155.
- Sambrook, J., E.F. Fritsch, and T. Maniatis. 1989. *Molecular cloning. A laboratory manual.* Cold Spring Harbor Laboratory, Cold Spring Harbor, N.Y.
- Sanchez, J.P. and Chua, N. H. (2001) *Arabidopsis* PLC1 is required for secondary responses to abscisic acid signals. *Plant Cell* 13:1143-1154.
- Sanchez, J. P., Duque, P. and Chua, N. H. (2004) ABA activates ADPR cyclase and cADPR induces a subset of ABA-responsive genes in *Arabidopsis*. *Plant J.* 38: 381-395.
- Sanger, F., Nicklen, S. and Coulson, A. R. (1977) DNA sequencing with chain-termination inhibitors. *Proc. Natl. Acad. Sci. U. S. A.* 74: 5463-5467.
- Sanz, P., Alms, G. R., Haystead, T. A. and Carlson, M. (2000) Regulatory interactions between the Reg1-Glc7 protein phosphatase and the Snf1 protein kinase. *Mol Cell. Biol.* 20: 1321-1328.
- Sauter, A., Davies, W. J. and Hartung, W. (2001) The long-distance abscisic acid signal in the droughted plant: the fate of the hormone on its way from root to shoot. *J. Exp. Bot.* 52: 1991-1997.
- Schluepmann, H., Pellny, T., van Dijken, A., Smeeckens, S. and Paul, M. (2003) Trehalose 6-phosphate is indispensable for carbohydrate utilization and growth in *Arabidopsis thaliana*. *Proc. Natl. Acad. Sci. U. S. A.* 100: 6849-6854.
- Schroeder, J. I., Allen, G. J., Hugouvieux, V., Kwak, J. M. and Waner, D. (2001) Guard cell signal transduction. *Annu. Rev. Plant Physiol. Plant Mol. Biol.* 52: 627-658.
- Schwartz, S. H., Leon-Kloosterziel, K. M., Koornneef, M. and Zeevaart, J. A. (1997) Biochemical characterization of the *aba2* and *aba3* mutants in *Arabidopsis thaliana*. *Plant Physiol.* 114: 161-166.
- Seki, M., Kamei, A., Yamaguchi-Shinozaki, K., and Shinozaki, K. (2003) Molecular responses to drought, salinity and frost: common and different paths for plant protection. *Curr. Opin. Biotechnol.* 14:194-199.

- Seo, M. and Kosiba, T. (2002) Complex regulation of ABA biosynthesis in plants. *Trends Plant Sci.* 7: 41-48.
- Sharp, R. E. and LeNoble, M. E. (2002) ABA, ethylene and the control of shoot and root growth under water stress. *J. Exp. Bot.* 53: 33-37.
- Sherson, S. M., Alford, H. L., Forbes, S. M., Wallace, G. and Smith, S. M. (2003) Roles of cell-wall invertases and monosaccharide transporters in the growth and development of *Arabidopsis*. *J. Exp. Bot.* 54: 525-531.
- Shi, H., Ishitani, M., Kim, C. and Zhu, J. K. (2000) The *Arabidopsis thaliana* salt tolerance gene SOS1 encodes a putative Na⁺/H⁺ antiporter. *Proc. Natl. Acad. Sci. U. S. A.* 97: 6896-6901.
- Shinozaki, K., Yamaguchi-Shinozaki, K., and Seki, M. (2003) Regulatory network of gene expression in the drought and cold stress responses. *Curr. Opin. Plant Biol.* 6: 410-417.
- Southern, E.M. (1975) Detection of specific sequences among DNA-fragments separated by gel electrophoresis. *J. Mol. Biol.* 98: 503-517.
- Sugden, C., Crawford, R. M., Halford, N. G. and Hardie, D. G. (1999a) Regulation of spinach SNF1-related (SnRK1) kinases by protein kinases and phosphatases is associated with phosphorylation of the T loop and is regulated by 5'-AMP. *Plant J.* 19: 433-449.
- Sugden, C., Donaghy, P. G., Halford, N. G. and Hardie, D. G. (1999b) Two SNF1-related protein kinases from spinach leaf phosphorylate and inactivate 3-hydroxy-3-methylglutaryl-coenzyme A reductase, nitrate reductase, and sucrose phosphate synthase *in vitro*. *Plant Physiol.* 120: 257-274.
- Smeekens S. (2000) Sugar-induced signal transduction in plants. *Annu. Rev. Plant Physiol. Plant. Mol. Biol.* 51: 49-81.
- Schmidt, M. C. and McCartney, R. R. (2000) β -subunits of Snf1 kinase are required for kinase function and substrate definition. *EMBO J.* 19: 4936-4943.
- Smith, A.M., Zeeman, S.C., Thorneycroft, D. and Smith, S. M. (2003) Starch mobilization in leaves. *J. Exp. Bot.* 54: 577-583.
- Söderman, E. M. , Brocard, I. M. , Lynch, T. J., Finkelstein, R. R. (2000) Regulation and function of the *Arabidopsis* ABA-insensitive4 gene in seed and abscisic acid response signaling networks. *Plant Physiol.* 124: 1752-1765.
- Stockinger, E. J. , Mao, Y., Regier, M. K, Triezenberg, S. J. and Thomashow, M. F. (2001) Transcriptional adaptor and histone acetyltransferase proteins in *Arabidopsis* and their interactions with CBF1, a transcriptional activator involved in cold-regulated gene expression. *Nucleic Acids Res.* 29: 1524-1533.
- Tallman, G. (2004) Are diurnal patterns of stomatal movement the result of alternating metabolism of endogenous guard cell ABA and accumulation of ABA delivered to the apoplast around guard cells by transpiration? *J. Exp. Bot.* 55: 1963-1976.
- Tan, B. C., Joseph, L. M., Deng, W.T., Liu, L., Li, Q. B., Cline, K., and McCarty, D. R. (2003) Molecular characterization of the *Arabidopsis* 9-cis epoxy-carotenoid dioxygenase gene family. *Plant J.* 35: 44-56.
- Tanaka, T., Knapp, D. and Nasmyth, K. (1997) Loading of an Mcm protein onto DNA replication origins is regulated by Cdc6p and CDKs. *Cell* 90: 649-660.

- Tang, G., Zhu-Shimoni, J. X., Amir, R., Zchori, I. B. and Galili, G. (1997) Cloning and expression of an *Arabidopsis thaliana* cDNA encoding a monofunctional aspartate kinase homologous to the lysine-sensitive enzyme of *Escherichia coli*. *Plant Mol. Biol.* 34: 278-293.
- Taylor, I. B., Burbidge, A. and Thompson, A. J. (2000) Control of abscisic acid synthesis. *J. Exp. Bot.* 51:1563-1574.
- Teige, M., Scheikl, E., Eulgem, T., Doczi, R., Ichimura, K., Shinozaki, K., Dangl, J. L. and Hirt, H. (2004) The MKK2 pathway mediates cold and salt stress signaling in *Arabidopsis*. *Mol Cell.* 15:141-152.
- Testerink, C., Dekker, H. L., Lim, Z. Y., Johns, M. K., Holmes, A. B., Koster, C. G., Ktistakis, N. T. and Munnik, T. (2004) Isolation and identification of phosphatidic acid targets from plants. *Plant J.* 39: 527-536.
- Thelander, M., Olsson, T. and Ronne, H. (2004) Snf1-related protein kinase 1 is needed for growth in a normal day-night light cycle. *EMBO J.* 23: 1900-1910.
- Thomashow, M. F. (1999) Plant cold acclimation: Freezing tolerance genes and regulatory mechanisms. *Annu. Rev. Plant Physiol. Plant Mol. Biol.* 50: 571-599.
- Toroser, D. and Huber, S. C. (1995) 3-Hydroxy-3-methylglutaryl-coenzyme A reductase kinase and sucrose-phosphate synthase kinase activities in cauliflower florets: Ca²⁺ dependence and substrate specificities. *Arch. Biochem. Biophys.* 355: 291-300.
- Towbin, H., Staehelin, T. and Gordon, J. (1979) Electrophoretic transfer of proteins from polyacrylamide gels to nitrocellulose sheets: procedure and some applications. *Proc. Natl. Acad. Sci. U. S. A.* 76: 4350-4354.
- Tsuchiya, Y., Nambara, E., Naito, S. and McCourt, P. (2004) The FUS3 transcription factor functions through the epidermal regulator TTG1 during embryogenesis in *Arabidopsis*. *Plant J.* 37: 73-81.
- Tzchori, B.-T. I., Perl, A. and Galili, G. (1996) Lysine and threonine metabolism are subject to the complex patterns of regulation in *Arabidopsis*. *Plant Mol. Biol.* 32: 727-734.
- Ulm, R., Ichimura, K., Mizoguchi, T., Peck, S. C., Zhu, T., Wang, X., Shinozaki, K. and Paszkowski, J. (2002) Distinct regulation of salinity and genotoxic stress responses by *Arabidopsis* MAP kinase phosphatase 1. *EMBO J.* 21: 6483-6493.
- Umezawa, T., Yoshida, R., Maruyama, K., Yamaguchi-Shinozaki, K. and Shinozaki, K. (2004) SRK2C, a SNF1-related protein kinase 2, improves drought tolerance by controlling stress-responsive gene expression in *Arabidopsis thaliana*. *Proc. Natl. Acad. Sci. U. S. A.* 101:17306-17311.
- Uno, Y., Furihata, T., Abe, H., Yoshida, R., Shinozaki, K. and Yamaguchi-Shinozaki, K. (2000) *Arabidopsis* basic leucine zipper transcription factors involved in an abscisic acid dependent signal transduction pathway under drought and high-salinity conditions. *Proc. Natl. Acad. Sci. U. S. A.* 97: 11632-11637.
- Urao, T., Yamaguchi-Shinozaki, K. and Shinozaki, K. (2001) Plant histidine kinases: an emerging picture of two-component signal transduction in hormone and environmental responses. *Sci STKE.* 109: RE18.
- Wang, K. L., Yoshida, H., Lurin, C. and Ecker, J. R. (2004) Regulation of ethylene gas biosynthesis by the *Arabidopsis* ETO1 protein. *Nature* 428: 945-950.
- Williams, L. E., Lemoine, R. and Sauer, N. (2000) Sugar transporters in higher plants - A diversity of roles and complex regulation. *Trends Plant Sci.* 5: 283-290.

- Wilson, T. E., Fahrner, T. J., Johnston, M. and Milbrandt, J. (1991) Identification of the DNA binding site for NGFI-B by genetic selection in yeast. *Science* 252: 1296–1300.
- Xiong, L., Lee, B., Ishitani, M., Lee, H., Zhang, C. and Zhu, J. K. (2001a) FIERY1 encoding an inositol polyphosphate 1-phosphatase is a negative regulator of abscisic acid and stress signaling in *Arabidopsis*. *Genes Dev.* 15: 1971-1984.
- Xiong, L., Gong, Z., Rock, C. D., Subramanian, S., Guo, Y., Xu, W., Galbraith, D. and Zhu, J. K. (2001b) Modulation of abscisic acid signal transduction and biosynthesis by an Sm-like protein in *Arabidopsis*. *Dev. Cell.* 1: 771-781.
- Xiong, L., Schumaker, K. S. and Zhu, J. K. (2002a) Cell signaling during cold, drought, and salt stress. *Plant Cell* 14 Suppl: S165-183.
- Xiong, L., Lee, H., Ishitani, M., Tanaka, Y., Stevenson, B., Koiwa, H., Bressan, R. A., Hasegawa, P. M., and Zhu, J. K. (2002b) Repression of stress-responsive genes by FIERY2, a novel transcriptional regulator in *Arabidopsis*. *Proc. Natl. Acad. Sci. U. S. A.* 99:10899-10904.
- Yamaguchi-Shinozaki, K. and Shinozaki, K. (2005) Organization of cis-acting regulatory elements in osmotic- and cold-stress-responsive promoters. *Trends Plant Sci.* 10: 88-94.
- Yanagisawa, S., Yoo, S. D. and Sheen, J. (2003) Differential regulation of EIN3 stability by glucose and ethylene signalling in plants. *Nature* 425: 521-525.
- Yang, X., Hubbard, E. J. A. and Carlson, M. (1992) A protein kinase substrate identified by the two-hybrid system. *Science* 257: 680–682.
- Yokoi, S., Quintero, F. J., Cubero, B., Ruiz, M. T., Bressan, R. A., Hasegawa, P. M., Pardo, J. M. (2002) Differential expression and function of *Arabidopsis thaliana* NHX Na⁺/H⁺ antiporters in the salt stress response. *Plant J.* 30: 529-539.
- Yoo, J. H., Park, C. Y., Kim, J. C., Heo, W. D., Cheong, M. S., Park, H. C., Kim, M. C., Moon, B. C., Choi, M. S., Kang, Y. H., Lee, J. H., Kim, H. S., Lee, S. M., Yoon, H. W., Lim, C. O., Yun, D. J., Lee, S. Y., Chung, W. S. and Cho, M. J. (2005) Direct interaction of a divergent CaM isoform and the transcription factor, MYB2, enhances salt tolerance in *Arabidopsis*. *J. Biol. Chem.* 280: 3697-3706.
- Yoon, H. W., Kim, M. C., Shin, P. G., Kim, J. S., Kim, C. Y., Lee, S. Y., Hwang, I., Bahk, J. D., Hong, J. C., Han, C. and Cho, M. J. (1997) Differential expression of two functional serine/threonine protein kinases from soybean that have an unusual acidic domain at the carboxy terminus. *Mol. Gen. Genet.* 255: 359-371.
- Yoshida, R., Hobo, T., Ichimura, K., Mizoguchi, T., Takahashi, F., Aronso, J., Ecker, J. R. and Shinozaki, K. (2002) ABA-activated SnRK2 protein kinase is required for dehydration stress signaling in *Arabidopsis*. *Plant Cell Physiol.* 43:1473-1483.
- van Dijken, A. J., Schluepmann, H. and Smeekens, S. C. (2004) *Arabidopsis* trehalose-6-phosphate synthase 1 is essential for normal vegetative growth and transition to flowering. *Plant Physiol.* 135: 969-977.
- Vazquez, F., Gascioli, V., Crete, P. and Vaucheret, H. (2004) The nuclear dsRNA binding protein HYL1 is required for microRNA accumulation and plant development, but not posttranscriptional transgene silencing. *Curr Biol.* 17;14: 346-351.
- Vincent, O., Townley, R., Kuchin, S. and Carlson, M. (2001) Subcellular localization of the Snf1 kinase is regulated by specific beta subunits and a novel glucose signaling mechanism. *Genes Dev.* 15:1104-1114.

- Vlachonasios, K. E., Thomashow, M. F. and Triezenberg, S. J. (2003) Disruption mutations of ADA2b and GCN5 transcriptional adaptor genes dramatically affect *Arabidopsis* growth, development, and gene expression. *Plant Cell* 15: 626-638.
- Vranova, E., Tahtiharju, S., Sriprang, R., Willekens, H., Heino, P., Palva, E. T., Inze, D. and Van Camp, W. (2001) The AKT3 potassium channel protein interacts with the AtPP2CA protein phosphatase 2C. *J. Exp. Bot.* 52: 181-182.
- Wang, X. Q., Ullah, H., Jones, A. M. and Assmann, S. M. (2001) G protein regulation of ion channels and abscisic acid signaling in *Arabidopsis* guard cells. *Science* 292: 2070-2072.
- Weigel, D., Ahn, J. H., Blazquez, M. A., Borevitz, J. O., Christensen, S. K., Fankhauser, C., Ferrandiz, C., Kardailsky, I., Malancharuvil, E. J., Neff, M. M., Nguyen, J. T., Sato, S., Wang, Z. Y., Xia, Y., Dixon, R. A., Harrison, M. J., Lamb, C. J., Yanofsky, M. F. and Chory, J. (2000) Activation tagging in *Arabidopsis*. *Plant Physiol.* 122:1003-1013.
- Worrall, D., Ng, C. K. and Hetherington, A. M. (2003) Sphingolipids, new players in plant signaling. *Trends Plant Sci.* 8: 317-320.
- Wu, Y., Sanchez, J. P., Lopez-Molina, L., Himmelbach, A., Grill, E. and Chua, N. H. (2003) The *abi1-1* mutation blocks ABA signaling downstream of cADPR action. *Plant J.* 34:307-315.
- Zarka, D. G., Vogel, J. T., Cook, D. and Thomashow, M. F. (2003) Cold induction of *Arabidopsis* CBF genes involves multiple ICE (inducer of CBF expression) promoter elements and a cold-regulatory circuit that is desensitized by low temperature. *Plant Physiol.* 2003 133: 910-918.
- Zhang, Y., Shewry, P.R., Jones, H., Barcelo, P., Lazzeri, P.A. and Halford, N. G. (2001) Expression of antisense SnRK1 protein kinase sequence causes abnormal pollen development and male sterility in transgenic barley. *Plant J.* 28: 431-441.
- Zhang, W., Qin, C., Zhao, J. and Wang, X. (2004) Phospholipase D alpha 1-derived phosphatidic acid interacts with ABI1 phosphatase 2C and regulates abscisic acid signaling. *Proc. Natl. Acad. Sci. U. S. A.* 101: 9508-9513.
- Zheng, Z. L., Nafisi, M., Tam, A., Li, H., Crowell, D. N., Chary, S. N., Schroeder, J. I., Shen, J. and Yang, Z. (2002) Plasma membrane-associated ROP10 small GTPase is a specific negative regulator of abscisic acid responses in *Arabidopsis*. *Plant Cell* 14: 2787-2797.
- Zhou, L., Jang, J. C., Jones, T. L. and Sheen, J. (1998) Glucose and ethylene signal transduction crosstalk revealed by an *Arabidopsis* glucose-insensitive mutant. *Proc. Natl. Acad. Sci. U. S. A.* 95: 10294-10299.
- Zhu, J. K. (2002a) Genetic analysis of plant salt tolerance using *Arabidopsis*. *Plant Physiol.* 124: 941-948.
- Zhu, J. K. (2002b) Salt and drought stress signal transduction in plants. *Annu. Rev. Plant Biol.* 53: 247-273.
- Zhu, J., Gong, Z., Zhang, C., Song, C. P., Damsz, B., Inan, G., Koiwa, H., Zhu, J. K., Hasegawa, P. M. and Bressan, R. A. (2002) OSM1/SYP61: a syntaxin protein in *Arabidopsis* controls abscisic acid-mediated and non-abscisic acid-mediated responses to abiotic stress. *Plant Cell* 14: 3009-3028.
- Zuo, J., Niu, Q. W. and Chua, N. H. (2000) An estrogen receptor-based transactivator XVE mediates highly inducible gene expression in transgenic plants. *Plant J.* 24: 265-273.

Zhu-Shimoni, J. X. and Galili, G. (1998) Expression of an *Arabidopsis* aspartate kinase/homoserine dehydrogenase gene is metabolically regulated by photosynthesis-related signals but not by nitrogenous compounds. *Plant Physiol.* 116: 1023-1028.

I am deeply indebted to my supervisor Prof. Csaba Koncz, for his valuable guidance during my research work. His invaluable criticism made my scientific pursuit more meaningful. I most sincerely extend my gratitude to Dr. Koncz for his expert guidance and constant encouragement, which enabled me to take the first steps in the field of signal transduction. It has been an unforgettable training to have worked with him. I am extremely grateful to him for his untiring support, meaningful counsel and encouragement without which this thesis would not have been possible.

I would like to thank Prof. George Coupland for his support and providing necessary facility. I would also like to thank Prof. G. Galili and A. Zilberstien for their valuable suggestions. I am also thankful to Shai Ufaz for exchanging ideas as we worked on similar projects.

My special thanks to Kenneth for always being there in the hour of need and for interesting scientific discussions, those of which, sometimes turned out to be valuable.

My sincere thanks to Marcel and Isabella for their ever willing help and moral support.

I also like to thank Dr. Zsuzsa Koncz and Dr. G. Molnar for their helpful comments on my thesis. I would like to thank Dr. J. Schmidt and Dr. T. Colby for the MALDI analysis.

I am very thankful to Prof. S. K. Sopory, Dr. Raj Bhatnagar and Dr. Shiva Reddy for their guidance and invaluable contribution into my carrier in early days.

I would like to thank Dr. F. Breuer and Dr. T. Kleinow for their initial guidance and introduction to the projects.

I thank Sabine for sacrificing her energy, Roswitha for teaching me German, Dora for being Dora, Mihaly for teaching me the theory of everything, Gabino for his affection and all the lab members.

I am grateful to my sisters for their support and encouragement at every step.

My heartfelt thanks to Zafar, my fiancé for his excellent cooperation, scientific suggestions and wonderful friendship. Without his help I won't be able to reach this point.

Last, but not the least, my indebtedness towards my parents, for their much needed support, their patience, understanding and encouragement.

Erklärung

Ich versichere, daß ich die von mir vorgelegte Dissertation selbständig angefertigt, die benutzten Quellen und Hilfsmittel vollständig angegeben und die Stellen der Arbeit - einschließlich Tabellen, Karten und Abbildungen -, die anderen Werken im Wortlaut oder dem Sinn nach entnommen sind, in jedem Einzelfall als Entlehnung kenntlich gemacht habe; daß diese Dissertation noch keiner anderen Fakultät oder Universität zur Prüfung vorgelegen hat; daß sie - abgesehen von unten angegebenen Teilpublikationen - noch nicht veröffentlicht worden ist sowie, daß ich eine solche Veröffentlichung vor Abschluß des Promotionsverfahrens nicht vornehmen werde.

Die Bestimmungen der Promotionsordnung sind mir bekannt. Die von mir vorgelegte Dissertation ist von Prof. Dr. George Coupland betreut worden.

Teilpublikationen:

Rapid identification of Arabidopsis insertion mutants by non-radioactive detection of T-DNA tagged genes

G. Rios, A. Lossow, B. Hertel, F. Breuer, S. Schaefer, M. Broich, T. Kleinow, J. Jasik, J. Winter, A. Ferrando, R. Farras, M. Panicot, R. Henriques, J.B. Mariau, A. Oberschall, G. Molnar, K. Berendzen, V. Shukla, M. Lafos, Z. Koncz, G.P. Redei, J. Schell and C. Koncz, *The Plant Journal* (2002) 32, 243–253.

Köln den 19 Mai 2005

Vijaya Shukla

Lebenslauf

Name: Vijaya Shukla
Geburtsdatum: 13. Dezember 1973, Kanpur (U.P.), India
Geschlecht: weiblich
Familienstand: ledig
Staatsangehörigkeit: indisch
Sprachkenntnisse: Englisch, Hindi

Akademische Qualifikationen:

Abschluss	Universität	Jahr	Fachrichtung
M.Sc.	Meerut Universität	2000	Botanik
B.Ed.	Kanpur Universität	1995	Chemie, Botanik
B.Sc.	Kanpur Universität	1992	Zoologie, Botanik, Chemie
Abitur	S. N. Sen Balika Vidhyalaya. Kanpur	1989	Biologie, Physik, Chemie, Hindi, Englisch,

Berufliche Qualifikationen:

Period	Position held	Institut/University
Juli 1993- Mai 1994	Lehrer	Central Academy, Higher Secondary School, Deoria, U.P.
August 1995-August 2001	Wissenschaftlicher Assistent	Plant Molecular Biology Group, ICGEB, Aruna Asaf Ali Marg, New Delhi.
August 2001- heute	MPG-Promotionsstipendium	Entwicklungsbiologie der Pflanzen, Max Planck Institut für Züchtungsforschung, Carl-von-Linné Weg 10, 50829 Köln

Publikationen:

1. Rapid identification of Arabidopsis insertion mutants by non-radioactive detection of T-DNA tagged genes. *Plant J.* 2002 Oct; (2)32:243-53

Rios G, Lossow A, Hertel B, Breuer F, Schaefer S, Broich M, Kleinow T, Jasik J, Winter J, Ferrando A, Farras R, Panicot M, Henriques R, Mariaux JB, Oberschall A, Molnar G, Berendzen K, Shukla V, Lafos M, Koncz Z, Redei GP, Schell J, Koncz C.

2. Analysis of chloroplast transformed tobacco plants with cryIIa5 under ricer *psbA* transcriptional elements reveal high level expression of Bt toxin without imposing yield penalty and stable inheritance of transplastome. *Molecular breeding* (2002).

Vanga Sive Reddy, Sadhu Leelavathi, Angamuthu Selvapandian, Rajagopal Raman, Ferraiolo Giovanni, Vijaya Shukla and Raj Kamal Bhatnagar.

Patente:

1. Co-inventor in a patent entitled “**Plastid Transformation**” filed in United Kingdom (UK Application No. 9929075.1, year 2000).
2. Co-inventor in another patent entitled “**Transplastomic Plants**” filed in United Kingdom (supplementary application filed).